SAPIENZA
UNIVERSITÀ DI ROMA

UNIVERSITÉ FRANCO ITALIENNE | UNIVERSITÀ ITALO FRANCESE

Theory of fluctuations in disordered systems

Scuola di dottorato in Fisica, Ecole Doctorale 107

Dottorato di Ricerca in Fisica – XXVI Ciclo

Candidate

Pierfrancesco Urbani
ID number 1088567

Thesis Advisors

Prof. Giorgio Parisi
Prof. Silvio Franz

A thesis submitted in partial fulfillment of the requirements
for the degree of Doctor of Philosophy in Physics

October 2013

Thesis defended on 04 February 2014
in front of a Board of Examiners composed by:

Prof. Florent Krzakala (chairman)
Prof. Jean-Philippe Bouchaud
Prof. Silvio Franz
Prof. Giorgio Parisi
Prof. Luca Leuzzi
Prof. Enzo Marinari
Prof. Victor Martin-Mayor

Theory of fluctuations in disordered systems
Ph.D. thesis. Sapienza – University of Rome

This thesis has been typeset by LaTeX and the Sapthesis class.

Author's email: pierfrancesco.u@gmail.com

A mamma e papà, sempre.

Abstract

This thesis is devoted to study various aspects of the glass transition problem. Although the problem of the glass transition dates back to at least a century ago, the modern approach based on statistical mechanics tools started more recently and many results have been obtained. However a complete and exhaustive theory of the glass transition is not established yet.

The first part of the thesis concerns the study of the theory of fluctuations at the dynamical transition for structural glass models. We have developed a field theory where the study of the dynamical fluctuations of a system that undergoes to a dynamical arrest can be carried out on the same lines of the standard theory of critical phenomena. The field theory derived has been studied at the Gaussian level and a Ginzburg Criterion has been introduced in order to see where the Gaussian results are correct. This approach is all based on the replica method and is mean field in nature in the sense that it neglects activated processes. Moreover it is developed in a completely static framework so that standard static approximation schemes can be employed to obtain quantitative results and predictions. Finally, the theory developed concerns the fluctuations only in the so called β regime of the dynamics, namely for times such that the dynamical correlation function is close to its plateau value. Within this scheme we have been able to compute in a static way the dynamical exponents that control the behavior of the dynamical correlation function.

The second part of this thesis is devoted to the study on how the dynamics in the α regime can be described using a quasi equilibrium approach. Based on a recent result on the dynamics of mean field spin glass models, we have developed the so called Boltzmann Pseudodynamics for structural glasses. We have introduced a dynamical version of the Ornstein-Zernike equations and we have shown that the dynamical equations that can be obtained closing them with the Hypernetted Chain closure give the same dynamical exponents that are computed in the first part of the thesis. This results is important from different points of view. Firstly it shows that the mode-coupling dynamics in the slow α regime can be understood using quasi equilibrium ideas; secondly it gives the opportunity to study the α regime using static approximation schemes and tools. This implies that this approach could open the way to the study of dynamical fluctuations in the α regime.

The third part of this thesis is devoted to the study of the statistical mechanics of Hard Spheres in the limit of very large dimensions. The motivations for this part of the work came from the fact that at the quantitative level, the results for the dynamical exponents presented in the first two parts of the thesis were quite bad. We expected that this came from the poor quantitative reliability of the approximations involved (namely the Hypernetted Chain approximation) so we tried to see if there is a structural glass model where we could compute the dynamical exponents without using any kind of approximation. Based on a recent result on the description of Hard Spheres in the limit of large dimensions, we have seen that the previously known phase diagram that was based on the one-step replica symmetry breaking (1RSB) scheme has to be deeply modified to take into account full replica symmetry breaking effects. In this spirit we have performed a stability calculation of the 1RSB

solution and we have shown that a Gardner transition is present. Having found an instability in the 1RSB calculation we have performed a 2RSB calculation and in the end a fullRSB calculation. In the latter framework we have written the saddle point equations and we have seen that they are closely related to the ones that can be obtained to solve the Sherrington-Kirkpatrick model that is a the simplest mean field spin glass model that displays fullRSB. Moreover we have solved numerically the equations and we have seen that the preliminary results we have obtained seems to be roughly consistent with the scaling with the pressure of the Debye-Waller that is observed at jamming. However further analytical and numerical investigations are needed to establish these results on more solid grounds. As a side result we have also computed in the same framework the dynamical exponents showing a better quantitative prediction for them.

The last part of this thesis is devoted to the study the mode-coupling dynamics in a particular case where the dynamical transition becomes continuous. In this case a correct set of predictions on the shape of the dynamical correlation function in the α regime can be obtained.

Contents

1 The glass transition **1**
- 1.1 Basic phenomenology of the glass transition . . . 2
  - 1.1.1 Fragility . . . 3
  - 1.1.2 Structural relaxation time . . . 3
  - 1.1.3 Configurational entropy and the ideal glass transition . . . 6
  - 1.1.4 Dynamical heterogeneities . . . 8
- 1.2 Dynamical approaches . . . 12
  - 1.2.1 Mode-coupling theory . . . 12
  - 1.2.2 Kinetically constrained models . . . 16
- 1.3 Static Approaches . . . 20
  - 1.3.1 Mean field theory . . . 20
  - 1.3.2 Random First Order Transition Theory . . . 30

2 Theory of fluctuations in structural glass models **37**
- 2.1 Introduction . . . 37
- 2.2 The ferromagnetic transition as a paradigm . . . 38
  - 2.2.1 Landau theory and the mean field approximation . . . 39
  - 2.2.2 Gradient expansion around the mean field solution . . . 40
  - 2.2.3 From the microscopic details to a coarse grained field theory 41
  - 2.2.4 The Ginzburg criterion . . . 42
- 2.3 Dynamical heterogeneities and replicas . . . 45
  - 2.3.1 The dynamical order parameter: two point functions . . . 46
  - 2.3.2 Fluctuations of the order parameter and four point functions 48
  - 2.3.3 The key connection between replicas and dynamics . . . 49
  - 2.3.4 The replicated free energy for structural glasses . . . 52
- 2.4 Landau expansion of the free energy around the glassy solution . . . 55
  - 2.4.1 Free energy for a uniform field . . . 55
  - 2.4.2 Computation of λ . . . 57
  - 2.4.3 The mass matrix and the zero mode . . . 59
  - 2.4.4 Analysis of the cubic terms and computation of λ . . . 62
- 2.5 Gradient expansion around the mean field uniform solution . . . 64
  - 2.5.1 Fourier transform . . . 64
  - 2.5.2 Analysis of the spectrum of the mass matrix . . . 67
- 2.6 Ginzburg criterion . . . 69
  - 2.6.1 Projection on the critical mode . . . 69
  - 2.6.2 The mapping on the φ^3 theory in random field . . . 70

2.7 Explicit calculations in the Hypernetted Chain approximation (HNC) 73
2.7.1 The saddle point equations in HNC . . . 75
2.7.2 Derivatives of the free energy . . . 76
2.7.3 The mass matrix . . . 77
2.7.4 Expression of λ . . . 78
2.7.5 Computation of μ and σ . . . 79
2.7.6 Numerical results . . . 80
2.8 Conclusions and perspectives . . . 83

3 The Boltzmann Pseudodynamic approach to long time dynamics 85
3.1 The Potential Method . . . 85
3.2 The potential method for non equilibrium states . . . 88
3.3 The Boltzmann Pseudodynamics construction . . . 93
3.3.1 The general definition . . . 94
3.3.2 Response functions . . . 95
3.3.3 Equilibrium measure . . . 96
3.4 The p-spin spherical model . . . 96
3.4.1 Equilibrium dynamics . . . 107
3.4.2 Off-equilibrium dynamics . . . 108
3.5 Boltzmann Pseudodynamics for HNC liquids . . . 109
3.5.1 The aging regime . . . 117
3.6 Perspectives . . . 119

4 Theory of dense amorphous hard spheres in high dimensions 123
4.1 The glass and jamming transition of hard spheres . . . 124
4.2 Hard Spheres in high dimensions. The replica approach . . . 129
4.3 The 1RSB phase diagram . . . 132
4.4 Inconsistencies of the 1RSB solution . . . 136
4.5 Stability of the 1RSB phase diagram: the Gardner transition . . . 137
4.5.1 The general structure of the stability matrix . . . 139
4.5.2 The entropic term . . . 140
4.5.3 The interaction term . . . 141
4.5.4 The replicon eigenvalue . . . 144
4.6 Computation of the dynamical exponents from the cubic expansion . 147
4.6.1 The entropic term . . . 148
4.6.2 The interaction term . . . 148
4.6.3 Numerical result . . . 149
4.7 Phenomenological extension to finite dimensions . . . 150
4.8 Towards the fullRSB computation: general expression for the entropy 152
4.9 The replicated entropy within the RSB construction . . . 155
4.9.1 Parametrization of hierarchical matrices . . . 155
4.9.2 Hierarchical matrices: their algebra and the entropic term . . 157
4.9.3 The computation of the interaction term . . . 160
4.9.4 Summary: 1RSB, 2RSB, kRSB and fullRSB results . . . 163
4.10 Variational equations . . . 164
4.10.1 Derivation from the kRSB solution . . . 164
4.10.2 Derivation from the full RSB solution . . . 167

4.11 Perturbative 2RSB solution around the Gardner line 169
4.11.1 Development around the 1RSB solution 169
4.11.2 The large density behavior of $\lambda(m)$ 172
4.12 The 2RSB solution in the jamming limit 175
4.12.1 2RSB equations at $m = 0$ 175
4.12.2 Asymptotic analysis at jamming for high density 176
4.13 The new 2RSB threshold 180
4.14 Numerical solution of the fullRSB equation 181
4.15 Conclusion and Perspectives 186

5 Mode-coupling dynamics for a quasi continuous transition 189
5.1 Mode-coupling theory near a continuous transition 190
5.1.1 Mode-coupling equations near an A_2 singularity 190
5.1.2 Mode-coupling equations near an A_3 singularity 192
5.1.3 α-relaxation near weakly discontinuous transitions 193
5.1.4 The aging regime 194
5.2 Phenomenological approach to fluctuations 196
5.3 Conclusions 197

6 Conclusions and Perspectives 199

A Double Counting Problem on the φ^4 theory 203

B Computation of the Jacobian $J(\hat{q})$ 205

C Stability of the 1RSB solution via the 2RSB calculation 209
C.1 The interaction part of the replicon eigenvalue 210
C.2 The entropic part of the replicon eigenvalue 215

D Riassunto 217

E Résumé 229

Chapter 1

The glass transition

The glass transition problem and the physical characterization of the disordered and amorphous states of matter are one of the most interesting challenges in physics. Even if the problem dates back on the first works of Kauzmann, Adam, Gibbs and Di Marzio, despite a huge theoretical effort, no satisfactory and systematic theory of amorphous disordered materials in finite dimension is known. In particular studying the glass transition with the standard methods of statistical mechanics is a long standing challenge.

Part of the modern comprehension of these materials is based on some schematic mean fields model whose statics and dynamics can be exactly solved. Moreover there are pure dynamical models or frameworks that have been used successfully in order to describe the physical details that are measured in experiments. However the two approaches have many problems. The mean field models suffer from the fact that they are mean field in nature: carrying mean-field analysis to the finite dimensional case is rather problematic, and a satisfactory construction has not been proposed yet although in recent years a scaling theory has been put forward. The dynamical approaches are fruitfully employed in the comparison with the experiments but some of them suffer from the fact that they rely on approximations that are not very well understood and that turn out to be mean field approximations. Moreover they do not clarify if the dynamical aspects are connected to something that can be related to equilibrium properties. One of the main problems is that these two approaches are not easy to compare because they usually focus on different kind of observables. In this thesis we will partially solve this issue.

Our scope in this chapter is to review the basic glass phenomenology. We shall choose a perspective that highlights the problems to which the present thesis contribute. Due to space limitations, we shall be sketchy in our presentation. However, reference to more paused expositions will be given. In particular the reader may like to consult some of the available reviews or books [17, 40, 59, 63, 114, 178, 145, 165]. In the end we will take the perspective of replica theory for the original part of this thesis.

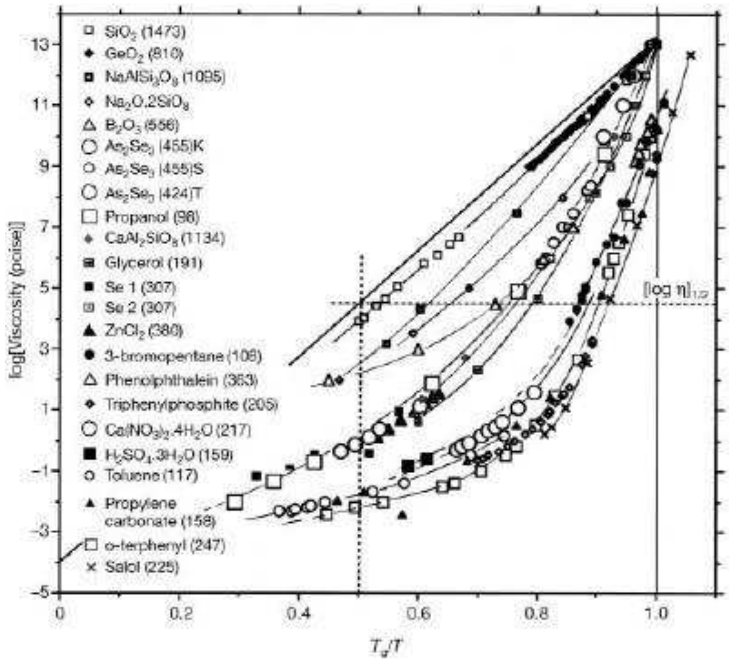

Figure 1.1. The increase of the viscosity when the temperature is lowered towards the glass transition temperature for various materials (picture taken from [6])

1.1 Basic phenomenology of the glass transition

The general behavior of liquids when the temperature is changed is described by a high temperature phase separated by a first order phase transition from the low temperature phase where they are crystalline solids. However, many liquids can be supercooled well below the melting point T_m. On decreasing the temperature, in the supercooled phase, the viscosity of the liquid starts to increase rapidly and at some point the liquid is so viscous that it does not flow anymore becoming a solid.

Let us call $\eta(T)$ the temperature dependent viscosity. We define the glass transition point as the temperature T_g at which the viscosity is

$$\eta(T_g) = 10^{13} \quad \text{Poise}$$

One of the most interesting and intriguing aspects of the supercooled phase is the increase of the viscosity when the temperature is lowered. This is very well described by the so called Angell plot of Fig. 1.1, [6, 7, 124] where $\log_{10}(\eta(T)/\text{Poise})$ is plotted against T_g/T. From this plot we clearly see the dramatic increase of the viscosity that changes of several order of magnitude when the temperature is halved. It is often found that for temperatures close to the glass transition point the behavior of the viscosity is described by the Vogel-Fulcher-Tamman (VFT) law [175, 80, 164]

$$\eta(T) = \eta_\infty \mathrm{e}^{\frac{\Delta}{T-T_0}} \tag{1.1}$$

where the constants η_∞, T_0 and Δ depend on the system but the exponential law seems robust. If $T_0 = 0$ we obtain the Arrhenius behavior.

At the structural level, if we take two snapshots of the system, one in the liquid phase and one in the glass phase, we can observe almost no qualitative difference. This reflects one of the major problems in glass physics that is the identification of a suitable order parameter at which we have to look at. However the difference between the glass phase and the crystalline phase is quite simple to understand because in the first case we have a disordered solids where particles are arranged in an amorphous way while in the latter a crystalline geometrical structure can be detected and usually can be studied by means of symmetry.

One of the way that can be used to see the difference between the crystal and the glass is by looking at the radial distribution function that tells us what is the probability to find a particle at a distance r from a reference particle

$$g(r) = \frac{1}{4\pi N r^2 \rho} \langle \sum_{i=1}^{N} \sum_{j \neq i} \delta(r - r_{ij}) \rangle \tag{1.2}$$

where r_{ij} is the distance between particle i and particle j and N and ρ are respectively the total number of particles and the density of particles. In a crystalline structure, particles are organized in the vertices of a lattice so that $g(r)$ will have many peaks that reflect the lattice points. In the glass (or liquid) phase, the absence of spatial order is such that $g(r)$ will not be peaked as for the crystalline phase, especially at large distances. This is because at short distance some local structure can always be present but in the glass this is completely lost at large distance where the system is almost uniformly disordered.

1.1.1 Fragility

An important concept that has been introduced by Angell in [5] is the one of *fragiliy* and it describes how fast the viscosity increase when the temperature is lowered near T_g. Two kind of glasses can be defined:

- Strong glasses: they do not display a very strong dependance of the viscosity on temperature and close to T_g they display Arrhenius behavior. A standard example of a strong glass is SiO_2.
- Fragile glasses: they show a very strong dependance of the viscosity on temperature and are always characterized by a VFT behavior. A typical example is *o-terphenyl* (OTP).

It is possible to introduce a *fragility index* in the following way

$$m_A = \left. \frac{\mathrm{d} \log \left[\eta(T)/\mathrm{Poise} \right]}{\mathrm{d}(T_g/T)} \right|_{T=T_g} \tag{1.3}$$

Strong glasses have $m_A \sim 17$ while fragile glasses have $m_A \sim 160$.

1.1.2 Structural relaxation time

We have said that if we look at the configurations of a glass and the ones of a liquid we are not able to find many differences being them qualitatively very close.

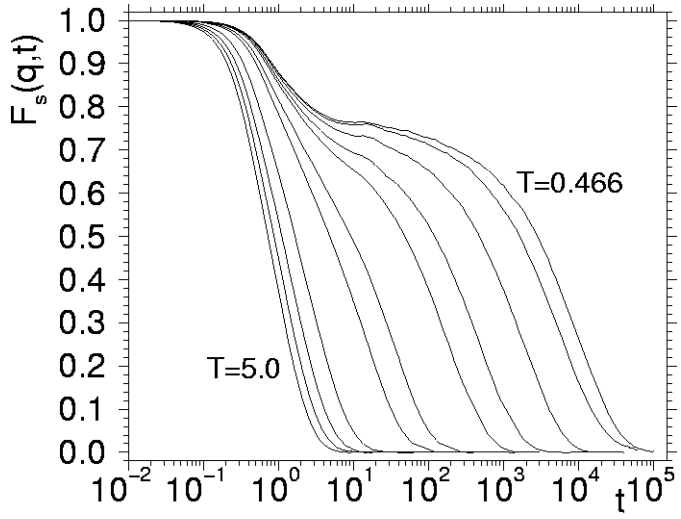

Figure 1.2. The typical behavior of $F_s(q,t)$ as a function of the temperature (picture taken from [104]) for a Lennard-Jones system. The dynamics is such that the initial configuration is an equilibrated one. The value of q chosen in the plot corresponds to the position of the maximum of $F(q,0)$. The appearance of the two steps relaxation with the development of the plateau is a typical sign of the approach to the glass transition point.

An alternative way to study this transition is by looking at the dynamics. Let us consider $\phi_i(t)$ an observable of the position at time t of the particle i. Then we can define a dynamical correlation function in the following way

$$C(t,t') = \frac{1}{N}\sum_{i=1}^{N}\langle \phi_i(t)\phi_i(t')\rangle \tag{1.4}$$

where the average is over the dynamical history. At high temperature, the typical behavior of the quantity above is such that it firstly satisfies time translational invariance (TTI) so that $C(t,t') = C(t-t')$ and moreover it is given by given by

$$C(t) = C_0 e^{-t/\tau(T)} \tag{1.5}$$

where $\tau(T)$ is the relaxation time that depends on the temperature. If we consider the special case of $\phi_i(t) = e^{-i\mathbf{q}\cdot\mathbf{r}_i(t)}$ we obtain the incoherent intermediate scattering function $F_s(q,t)$ that is the Fourier transform of the self part of the Van Hove function defined by

$$G_s(r,t) = \frac{1}{N}\sum_{j=1}^{N}\langle \delta(r - r_j(t) - r_j(0))\rangle \ . \tag{1.6}$$

The typical behavior of the above function on approaching the glass transition point is reported in Fig. 1.2. This picture is very typical for all glass-forming liquids and it shows that the glass transition is very well described at the dynamical level.

The physical meaning of Fig. 1.2 is that on approaching the glass transition, the dynamical relaxation happens in two steps. In the first one the system relaxes

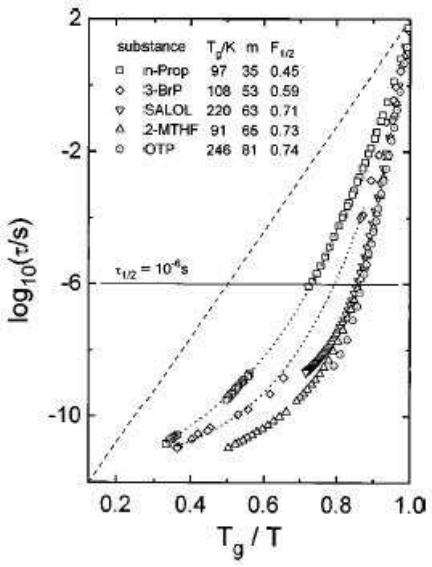

Figure 1.3. The behavior of structural relaxation time with temperature (picture taken from [148]). The straight line stands for Arrhenius behavior. The dashed lines represent data fits that have been done combining the VFT law (1.1) with the Maxwell relation $\eta = G_\infty \tau_\alpha$.

rapidly in a metastable state. This is the behavior described by the first part of the relaxation where the dynamical correlation function decays from its initial value up to the plateau value. Then the second part of the relaxation is a very slow relaxation to escape form the first metastable state encountered. If we imagine the dynamics at the particle level we could see that the first part of the relaxation describe the relaxation of the particles inside the cages that the sorounding particles make and the second part describes the structural relaxation that corresponds to a cooperative rearrangement of the particles. The first part of the relaxation is usually called the β regime while the second part is the α regime. At the glass transition temperature the length of the plateau is on human time-scales so that the structural relaxation is frozen and the system we observe is no more an equilibrated systems but a system that is fallen out of equilibrium.

The α relaxation clearly determines the structural relaxation time τ_α that is plotted in Fig. 1.3 and it is connected with the viscosity through the Maxwell relation $\eta = G_\infty \tau_\alpha$ where G_∞ is the infinite frequency shear modulus of the liquid. From the picture we clearly see that also the α relaxation time shows a VFT behavior similar to Eq. 1.1 with a divergence at $0 < T_0 < T_g$.

The two steps relaxation and the cage effect can also be seen by looking at the mean square displacement (MSD) defined by

$$\Delta(t) = \langle r^2(t) \rangle = \frac{1}{N} \sum_{i=1}^{N} \langle |r_i(t) - r_i(0)|^2 \rangle \,. \tag{1.7}$$

The typical behavior of the quantity above is reported in Fig. 1.4. At high temperature we have two regimes: a ballistic regime and a diffusive one. In the ballistic regime the particles do not fell the presence of all the other particles and their dis-

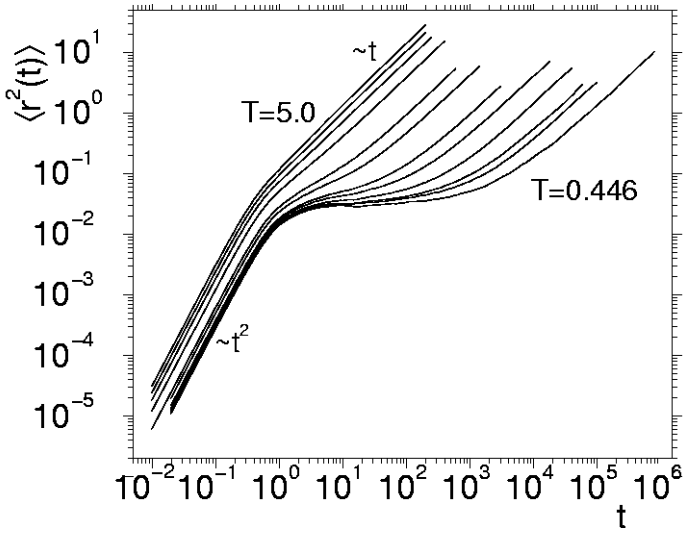

Figure 1.4. The mean square displacement as a function of time for different temperatures on approaching the glass transition point. The data are taken from [104] and are referred to a binary mixture of Lennard-Jones particles.

placement is linear in time. In the diffusive regime, the particles start to fell the presence of the other particles. Due to the collisions the displacement will be of order $\sqrt{t}$. This picture shows that when we lower the temperature, near the glass transition point, the two regime become separated by a plateau whose length increases when decreasing the temperature. The plateau is nothing but the signature of the cage effect of the particles surrounding a given particle. In fact the diffusive behavior can happen only if the particles can escape from the cages they are trapped in. This process can happen only if there is a structural rearrangement of all the particles. If we are close to the glass transition point, this structural rearrangement is frozen and particles hardly escape from the cages. The height of the plateau is nothing but the mean size of the cage.

1.1.3 Configurational entropy and the ideal glass transition

In the previous section we have seen that if we analyze the dynamics we clearly see that on approaching the glass transition temperature the dynamics develops in two steps. The first one is a relaxation inside the cages while the second one is a cooperative rearrangement of the cages. This means that we can associate to each one of these two well separated timescales two different entropies. The first one is the vibrational entropy that can be defined having frozen the structural relaxation and is denoted with $S_{vib}(T)$. The second one is related to the cooperative rearrangements. In fact one can imagine that each cage configuration identifies a metastable state and the α relaxation is just the time needed to explore the phase space of cage configurations. This means that we can define a configurational entropy $S_c(T)$ so that the total entropy of the liquid is given by

$$S_{liq}(T) = S_{vib}(T) + S_c(T) \ . \tag{1.8}$$

A way to compute the configurational (or excess) entropy S_c is to approximate

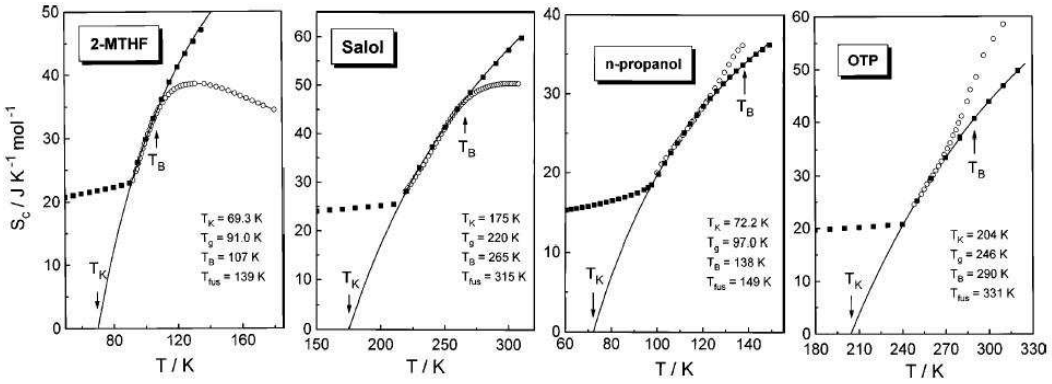

Figure 1.5. The configurational entropy $S_c(T)$ measured for four different fragile glass-forming liquids. The picture is taken form [148]. The black squares come from the calorimetric measurements while the white circles are from dielectric relaxation. At the glass transition point each system fall off equilibrium and the black line shows the extrapolation of the measurements for temperatures below the glass transition point. We clearly see that this extrapolation predicts that there is a temperature T_k at which the configurational entropy goes to zero so that the entropy of the glass becomes equal to the one of the crystal.

the vibrational entropy with the entropy of the crystal. This means that

$$S_c(T) = S_{liq}(T) - S_{cry}(T) = \Delta S_m - \int_T^{T_m} \mathrm{d}\log T' \left(C_{liz}(T) - C_{cry}(T')\right) \qquad (1.9)$$

where ΔS_m is the difference of the entropy of the liquid and the crystal at the melting point and $C(T) = T\mathrm{d}S/\mathrm{d}T$ is the specific heat.

The configurational entropy for some substances is shown in Fig. 1.5 as can be obtained from calorimetric measurements for different fragile glass-formers. On lowering the temperature we see that the configurational entropy tends to decrease up to the glass transition point where the system falls out of equilibrium and the structural relaxation is frozen. This means that for $T < T_g$ the measurements take into account only the vibrational entropy that is almost constant. However if we extrapolate the data to lower temperature we can find a temperature T_K at which the configurational entropy vanishes [94]. This means that if we were able to equilibrate the system below the glass transition point we would observe that at some point the entropy of the supercooled liquid becomes equal to the one of the crystal. This is the Kauzmann paradox. The same Kauzmann proposed a way out from this. If we assume that the free energy barrier to nucleate the crystal is of the same order of the barriers between different structures of the liquid then the structural relaxation time becomes of the same order of the nucleation time-scale. This means that we cannot think more on the liquid as in equilibrium since the structural relaxation is the same as the nucleation time-scale.

An alternative solution to this is that we can assume that if we are able to avoid crystallization[1] in such a way that it is strongly inhibited, then we cannot

[1] There is not a standard protocol to avoid the crystallization. One could for example introduce polidispersity in the system but this suffers for the problem that the system could undergo to a phase separation. A very deep and detailed discussion is given in [40].

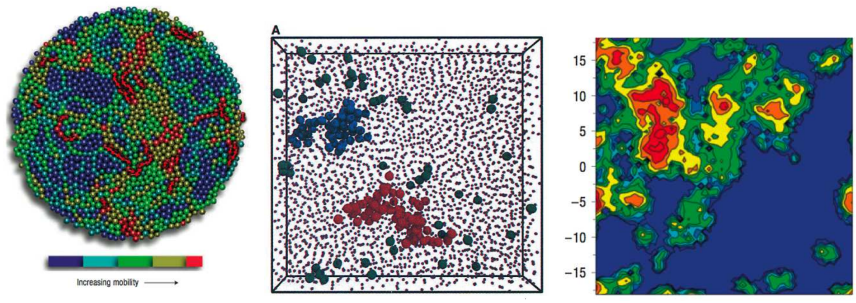

Figure 1.6. Three different examples of dynamical heterogeneities. The picture on the left is taken from [96] is a snapshot of the mobility of a granular fluid of ball bearings. The picture in the centre is taken from [176] is from a colloidal hard spheres suspension where the regions of high mobility have been colored. The picture on the right is taken from [177] and represents the a computer simulation of a two dimensional system made of repulsive disks.

think anymore to the crystalline state and we can neglect it. This means that a phase transition can take place at T_K since the number of structures in which the liquid can stay is no more exponential. Below the Kauzmann point the entropy of the liquid is given by the vibrational entropy and the specific heat has a jump downward. The system remains stuck in an *ideal* glass state. Of course this phase transition is not directly observables because the system is out of equilibrium at $T_g > T_K$. An evidence in favor of an ideal glass transition is the experimental fact that the temperature at which the viscosity seems to diverge in fragile glasses, namely T_0, coincides with the Kauzmann point $T_0 = T_K$. This means that the structural relaxation diverges at the ideal glass transition so that the structure reached at T_K is thermodynamically stable. This picture is observed also in a large class of mean field models that will be discussed in the following.

1.1.4 Dynamical heterogeneities

In recent years an improvement in the comprehension of the slowing down of the dynamics in glasses has come from the study of dynamical fluctuations [12]. In fact if we are able to follow the dynamics of a glass-forming liquid on approaching the glass transition point we can see that the dynamics becomes very heterogeneous in space. In particular the liquid becomes clustered in regions of particles with very different mobility.

The study of dynamical heterogeneities has been carried on by indirect experimental observation in molecular liquids [65, 149] and by the direct observation of single particle motion in colloids and granular media [176, 54, 96, 95]. Fig. 1.6 represents some of the results of these studies and it underlines how the different mobility regions are characterized in clusters.

Another way to analyze the heterogeneous character of the dynamics is by looking at the square displacement of a given particle. This is reported in Fig. 1.7 from which we can see that the movements of the particles are made of vibrations around a center inside the cage followed by jumps outside the cages. The jumps are widely

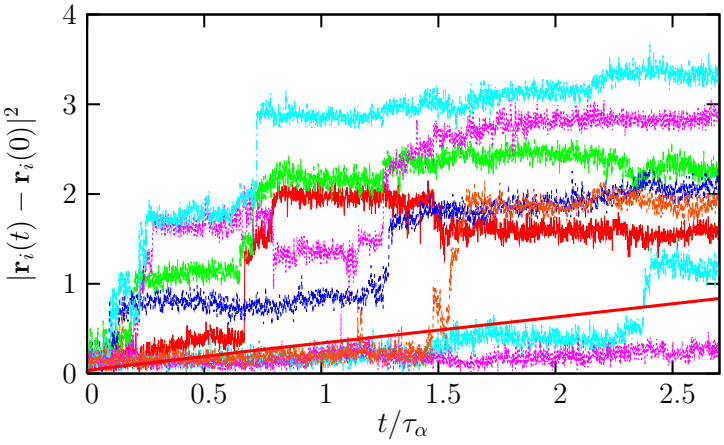

Figure 1.7. The plot shows the mean square displacement of a single tagged particle. It shows how intermittent is the relaxation with the particles that vibrate inside the cages built by the surrounding particles for a long time before relaxing cooperatively. It shows also that the cooperative rearrangement is intermittent and well localized in time. The plot is for a supercooled Lennard-Jones liquid and has been taken from [12]

distributed in time underlining again the importance of fluctuations.

The space fluctuations in the local dynamics is relevant also for the experimental observation of the violation of the Stokes-Einstein relation [89]. In the high temperature liquid there is a relation between the self-diffusion D_s and the viscosity η that is given by $D_s\eta/T = const.$ For a large particle of radius R in fluid the constant is equal to $1/(6\pi R)$. Because the self-diffusion and the viscosity can be used to estimate the relaxation time, we see that the two estimates differ only for a constant factor. In supercooled liquids, on approaching the dynamical arrest, the Stokes-Einstein relation is violated and one finds that D_s decrease not as fast as η increase close to T_g [166]. This means that $D_s\eta$ is greater than the same product in the high temperature liquid. This phenomenon is represented in Fig. 1.8. The violation of the Stokes-Einstein relations tells us that different ways to measure the relaxation times cannot agree close to T_g. A natural explanation for this is the following. The self-diffusion coefficient measures how fast a given particle can diffuse in a system and it is dominated by the presence of clusters of high mobility. Instead the viscosity is related to the mobility of each particles and this means that it is deeply affected by the immobile clusters. This means that on approaching the glass transition, the viscosity will increase faster then D_s^{-1} as it is observed.

The experimental observation of dynamical heterogeneities asks for an experimental characterization and a corresponding theoretical explanation for their aspects close to the glass transition point. One of the key point is related to the size of the clusters of different mobility. How does the size of the clusters behave when the temperature is decreased? Can we define a proper correlation length? There has been a huge experimental work to answer to these questions and the general picture that has come out is that on approaching the glass transition temperature the size of mobility clusters grows up to 5-10 molecule diameters. Of course this kind of measurement strongly depends on the way it is possible to define mobile

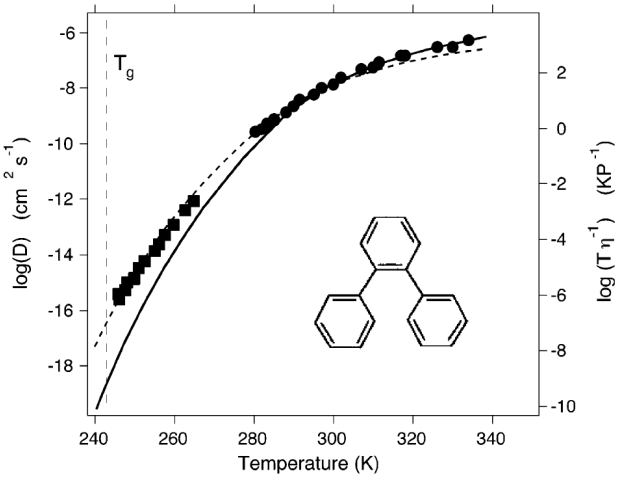

Figure 1.8. The full line represents the behavior of the viscosity with temperature while squares and dots are experimental points for the self-diffusion coefficient. At high temperature we see that the Stokes-Einstein relation is satisfied because the measurements from self-diffusion coefficients are on the viscosity line. However at low temperature this is no more true. The dashed line represents a fit with a modified Stokes-Einstein relation $D_s \sim (T/\eta)^{\zeta}$ with $\zeta = 0.82$. The plot is taken from [120] and represents data obtained for the prototypical fragile glass that is the o-terphenile.

clusters of different mobility but now an overall consensus on the results has been reached.

To define properly this problem at the theoretical level we need to go deeply in the definition of the degree of mobility we have referred to. The first thing to note is that in whatever definition of mobility we take there is an underlining observation time inside it: we can say that a particle has moved in a given distance in a certain time window t. This means that to define the mobility we need two configurations of the system at two different times. Moreover it is clear that the observation time is crucial. If the time window is too much small we do not observe nothing due to the fact that we have not waited for enough time such that particles can interact. If the time window is too much large, for example larger than the correlation time, then the system will be equilibrated and we cannot observe any fluctuations from one region to the other in the liquid. Only if we are in an intermediate region we will be able to observe heterogeneity.

Let us be more precise. We define the time dependent displacement of a given particle by

$$u_i(t) = r_i(t) - r_i(0) \tag{1.10}$$

being r_i the position of the particle i. $u_i(t)$ gives an estimate of the mobility of particle i. We define now its fluctuations from the average value

$$\delta u_i(t) = u_i(x) - \langle u_i(t) \rangle \tag{1.11}$$

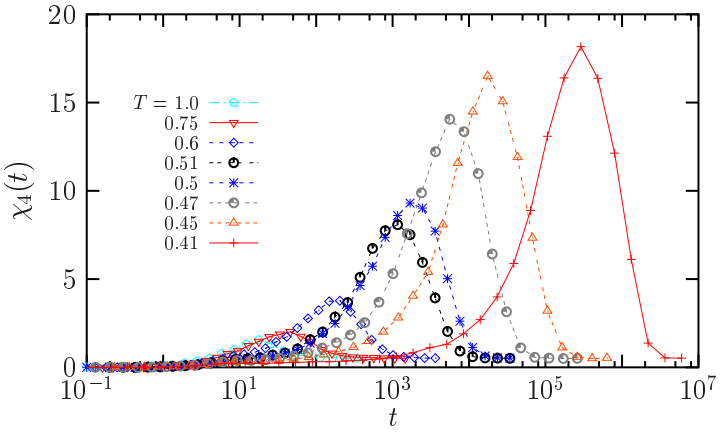

Figure 1.9. Plot of $\chi_4(t)$ as a function of time for different temperature. The plot is taken from [16] where the χ_4 has been measured from the fluctuations of the intermediate scattering function of a Lennard-Jones glass-forming liquid. From this plot we clearly see that the size of the clusters of different mobility grows when the temperature is closer and closer to the glass transition point.

from which we can define a correlation function of the mobility

$$G_u(r,t) = \frac{\langle \sum_{i,j} \delta u_i(t) \delta u_j(t) \delta(r - |r_i(t) - r_j(t)|) \rangle}{\langle \sum_{i,j} \delta(r - |r_i(t) - r_j(t)|) \rangle} \tag{1.12}$$

and the associated susceptibility

$$\chi_4(t) = \int \mathrm{d}r G_u(r,t) \tag{1.13}$$

In Fig. 1.9 there is the plot of χ_4 as measured from a molecular dynamics simulation of a Lennard-Jones liquid. At large r one expect that

$$G_u(r,t) \sim \frac{A(t)}{r^p} e^{-r/\xi_4(t)} \; ; \tag{1.14}$$

This implies that the more long ranged is G_u, namely the largest is $\xi(t)$, the higher is χ_4. Let us note here that G_u is a four point function when expressed in terms of the positions of the particles.

From the plot we can see two things. The first one is that the susceptibility does not grow monotonically. It has a maximum at a precise value of the time window used to define the mobility. Moreover, upon decreasing the temperature, the position of the peak shifts to higher value of the time window. The first fact is nothing but the signature that the time window must be properly selected in order to observe heterogeneity. If it is too short, then we observe no correlations between particles because they have not enough time to interact. If we wait too much we restore homogeneity and equilibrium in the system and we cannot observe any fluctuation of the mobility. Let us call t^* the value of the time t at which $\chi_4(t)$ has a peak. Interestingly enough it happens that t^* is of the order of the relaxation time. We can define a dynamical correlation length $\xi_d = \xi_4(t^*)$ which is the largest

correlation length at a given temperature. We can observe that ξ_d grows when the temperature is lowered on approaching the glass transition point. This means that the slowing down in glass-forming liquids is associated to genuine collective phenomenon.

Of course, there are many statistical mechanics tools that have been developed to study the behavior of fluctuations from scaling theory to the renormalization group machinery. However the application to these tools to glassy systems is very difficult because of the dynamical nature of the problem. In this thesis we will address the problem using the replica theory. A phenomenological approach to this problem has been developed in [74, 73, 72] where the problem has been deeply analyzed and an important connection with the physics of the random field Ising model has been established. We will apply this new insights in the next chapter where a first principle theory of dynamical heterogeneities in the β regime will be derived.

1.2 Dynamical approaches

In this section we review two of the most popular dynamical approaches that are used to describe theoretically the slowing down in glass-forming liquids. The first approach is the Mode-Coupling theory (MCT) that has been developed by Götze and collaborators [84] and which has been successfully employed to describe experimental results. The second approach is based on Kinetically Constrained models (KCM) [150, 81] that have been developed as first principle dynamical models of the glass transition.

1.2.1 Mode-coupling theory

In this section we will review the mode-coupling theory using the Mori-Zwanzig formalism [89, 136, 184, 104]. Consider a system of N interacting particles. At a classical level it is possible to describe the dynamical behavior through the Hamilton equations. The evolution of the phase space coordinates can be obtained with the Liouville operator. In particular, suppose that we have defined a function on the phase space, namely $O(p, q)$, which is function only of the coordinates and conjugate momenta. Then the evolution of such a quantity is solved through the equation

$$\frac{\mathrm{d}O}{\mathrm{d}t} = i\mathcal{L}O \qquad \mathcal{L} = -i\{H, \cdot\} \tag{1.15}$$

where H is the Hamiltonian of the system and $\mathcal{L}$ is the Liouville operator. The Mori-Zwanzig formalism is a powerful technique to describe in a compact way the equations satisfied by the correlation functions:

$$\langle A(t)|B(0)\rangle = \int \prod_{i=1}^{N} \mathrm{d}^D q_i \mathrm{d}^D p_i \left[\mathrm{e}^{i\mathcal{L}t} A(0)\right] B^*(0) F(q, p) \tag{1.16}$$

where $F(q, p)$ is an equilibrium measure satisfying the Liouville equation (it is invariant under the Hamiltonian flux).

Let us define a set of phase space functions $\{A_i\}_{i=1,\ldots,N}$. These variables may represent some degrees of freedom of the system under study. In the theory of glasses they stand for the density of particles and the current of particles. Define also the projector operator onto this set of functions:

$$\mathcal{P}B(t) = \sum_{i,j}^{N} A_i(0) \left[\langle A(0)|A(0)\rangle^{-1}\right]_{ij} \langle A_j(0)|B(t)\rangle \ . \tag{1.17}$$

It is straightforward to prove that $\mathcal{P}$ is a projector because $\mathcal{P}^2 = \mathcal{P}$. Moreover $\mathcal{P}A_i(0) = A_i(0)$. The evolution of the functions A_i is given by

$$\begin{aligned}\frac{\mathrm{d}A_i(t)}{\mathrm{d}t} &= e^{i\mathcal{L}t}\left[\mathcal{P} + (1-\mathcal{P})\right] i\mathcal{L}A_i(t) = i\sum_j \Omega_{ij}A_j(t) \\ &+ e^{i\mathcal{L}t}(1-\mathcal{P})i\mathcal{L}A_i(0)\end{aligned} \tag{1.18}$$

where we have defined a matrix of frequencies Ω that is given by

$$i\Omega_{ij} = \sum_k \left[\langle A(0)|A(0)\rangle^{-1}\right]_{ik} \langle A_k(0)|i\mathcal{L}A_j(0)\rangle \ . \tag{1.19}$$

Using the Laplace transform we can rewrite the last term in (1.18) in the following way

$$e^{i\mathcal{L}t}(1-\mathcal{P})i\mathcal{L}A_i(0) = \int_0^t \mathrm{d}\tau e^{i\mathcal{L}(t-\tau)} i\mathcal{P}\mathcal{L}f_i(\tau) + f_i(t) \tag{1.20}$$

where

$$f_i(t) = e^{i(1-\mathcal{P})\mathcal{L}t} i(1-\mathcal{P})\mathcal{L}A_i(0) \tag{1.21}$$

Using the equation just given and the properties of the projector operator it can be proved that the equation for $A_i(t)$ can be written in this way [84]

$$\frac{\mathrm{d}A_i(t)}{\mathrm{d}t} = \sum_j^N \left[i\Omega_{ij}A_j(t) - \int_0^t \mathrm{d}\tau\, M_{ij}(\tau)A_j(t-\tau)\right] + f_i(t) \tag{1.22}$$

where the memory function is given by [84]

$$M_{ij}(t) = \sum_k \left[\langle A(0)|A(0)\rangle^{-1}\right]_{ik} \langle f(0)|f(t)\rangle \ . \tag{1.23}$$

If we want the two time correlation functions for the quantities A_i we have just to multiply the previous equation for $A_j(0)$ and average over the equilibrium distribution of the initial coordinates of the phase space. Then, due to the fact that $\langle A_i(0)|f_j(t)\rangle = 0$ one obtains

$$\frac{\mathrm{d}C_{ij}(t)}{\mathrm{d}t} = i\sum_k^N \Omega_{ik}C_{kj}(t) - \int_0^t \mathrm{d}\tau \sum_k^N M_{ik}(\tau)C_{kj}(t-\tau) \tag{1.24}$$

where we have introduced the correlation matrix $C_{ij}(t) = \langle A_i(0)|A_j(t)\rangle$. Note that because the function F defined in (1.16) satisfies the Liouville equation it follows that the correlation functions are time translational invariant and they satisfy the

fluctuation-dissipation theorem. Moreover, from these assumptions, it follows that we cannot obtain informations in an out-of-equilibrium regime. What happens at the glass transition is a dynamical arrest. In terms of free energy landscape, the system enters in a phase where the free energy is full of valleys separated by very large barriers so that the equilibration time grows very fast (in the mean field regime it diverges) and the system is stuck in an out-of-equilibrium situation. It follows that the mode-coupling equations are ill defined going beside the mode-coupling temperature altought some attempts to generalize them has been done in this direction [23]. Note that all the topological aspects of the correlation functions, namely their dependence from spatial coordinates, have been suppressed to simplify the notation. However one can consider phase space functions that depend explicitly on the distance between points.

In the case of the theory of glasses the above equation can be rewritten defining the following quantities

$$\rho(\vec{n}q,t)=\sum_{i=1}^{N}e^{i\vec{n}q\cdot\vec{n}r_i(t)} \qquad F(q,t)=\frac{1}{N}\langle\rho(\vec{n}q,t)|\rho(\vec{n}q,0)\rangle \qquad S(q)=F(q,0); \tag{1.25}$$

the first one is the Fourier transform of the density of particles, the second is the dynamical structure factor while the third one is the static structure factor. Define now the quantity $\Phi(q,t)=F(q,t)/S(q)$; the normalization factor is such that $\Phi(q,0)=1$. The mode-coupling equation for the quantity just defined is the following

$$\ddot{\Phi}(q,t)+\Omega^2(q)\Phi(q,t)+\int_0^t \mathrm{d}\tau\tilde{M}(q,t-\tau)\dot{\Phi}(q,t)=0 \tag{1.26}$$

where $\Omega^2(q)=q^2/(\beta m S(q))$ and m is the mass of the particles and β is the inverse of the temperature (the Boltzmann constant is set to one). The memory function can be splitted in two parts:

$$\tilde{M}(q,t-\tau)=M_{reg}(q,t-\tau)+\Omega^2 M(q,t-\tau)\,; \tag{1.27}$$

the first term controls the behavior of Φ in the short timescale and is almost irrelevant to describe the behavior near the glass transition. The second term has the following expression

$$M(q,t)=\frac{1}{2(2\pi)^3}\int \mathrm{d}\vec{n}kV^{(2)}(q,k,|\vec{n}q-\vec{n}k|)\Phi(k,t)\Phi(|\vec{n}q-\vec{n}k|,t) \tag{1.28}$$

where the vertex is given by

$$\begin{aligned}V^{(2)}(q,k,|\vec{n}q-\vec{n}k|)=&\frac{n}{q^2}S(q)S(k)S(|\vec{n}q-\vec{n}k|)\times\\ &\times\left(\frac{\vec{n}q}{q}\cdot[\vec{n}kc(k)+(\vec{n}q-\vec{n}k)c(|\vec{n}q-\vec{n}k|)]\right)^2\end{aligned} \tag{1.29}$$

and $n=V/N$, $c(q)=n(1-1/S(q))$. Note that we have made the assumption of isotropy of space so that the memory kernel and Φ depend only on the magnitude of the momentum q. The form of the equation above is that of a damped harmonic oscillator of frequency Ω. Let us underline also that the form of the vertex here is

obtained under a set of uncontrolled approximations. Here we do not go into the details but the interested reader can be found them in [84].

We want now to underline some peculiar features of these equations:

- it can be shown that there exists a critical temperature T_c at which the normalized correlation function $\Phi(q,t)$ does not decay to zero at large times signaling a transition from an ergodic state to a non ergodic one. This temperature is indipendent from the wave vector q.

- the dynamical behaviour, apart from the irrelevant factor M_{reg}, is completely determined by the static structure factor $S(q)$ which is a global quantity, and by n and m. This implies that MCT predicts the critical slowing down indipendently from the microscopic details of the system.

- it was observed by Bengtzelius and others [11, 113] that when the temperature is lowered the static structure factor becomes more and more picked. Because of the fact that the memory kernel is a cubic function of the static structure factor one can approximate it by replacing $S(q) = \zeta\delta(q - q_0)$ where q_0 is the momentum at which the static structure factor has a maximum. In this case, if we define $\phi(t) = \Phi(q_0, t)$, then the mode-coupling equations become

$$\ddot{\phi}(t) + \Omega^2\phi(t) + \zeta\Omega^2 \int_0^t \mathrm{d}\tau\phi^2(t-\tau)\dot{\phi}(\tau)\,. \tag{1.30}$$

  This equation is known as a schematic version of the mode-coupling equations. It is very similar to the equation that can be derived for a given class of mean field disordered systems [39].

We want to summarize the main predictions that can be done with this framework. First of all the solution of the equation (1.26) and (1.30) develops a plateau when the temperature is approaching the mode-coupling one. This implies that two relevant times scales appears. The first time scale is the characteristic time needed to approach the plateau and is responsible for the β regime; the second time scales is responsible for the departure from the plateau and is the α relaxation time. The last time scale drives the relaxation to equilibrium because once the correlation function has left the plateau it will decay to zero. At the mode-coupling temperature the length of the plateau diverges. The first prediction is about this divergence that can be described by a critical exponent:

$$\tau_\alpha \sim (T - T_c)^{-\gamma} \tag{1.31}$$

where γ can be computed from the mode-coupling theory. Moreover the correlation function $\phi(t)$ can be studied in a region of time around the plateau so that we can define two exponents [84]

$$\begin{aligned} \phi(t) &= \phi_{EA} + At^{-a} \\ \phi(t) &= \phi_{EA} - Bt^{b} \end{aligned} \tag{1.32}$$

where ϕ_{EA} is the plateau value. It can be proved that the exponents that describe the approach to the plateau of $\phi(t)$ (the exponent a) and the departure from it (the

exponent b) are related by

$$\lambda = \frac{\Gamma(1-a)^2}{\Gamma(1-2a)} = \frac{\Gamma(1+b)^2}{\Gamma(1+2b)} \tag{1.33}$$

and moreover the exponent γ is given by

$$\gamma = \frac{1}{2a} + \frac{1}{2b} \tag{1.34}$$

Eq. 1.33 defines the mode-coupling exponent parameter λ that will be the object of interest of the next chapters.

Another remark should be done about the mode-coupling temperature. In fact what happens is that it is usually higher than the the glass transition temperature. This is another strong evidence about the fact that the mode-coupling approach is a mean field one because in general the mean field structure is responsible for a greater increase of free energy barriers when lowering the temperature so that the transition is reached sooner than in non mean field systems. Moreover let us recall that at an experimental level the divergence of the relaxation time is governed by a Fogel-Vulcher law or by an Ahrrenius behavior. Also this discrepancy may be addressed to the mean field character of the mode-coupling approximation and has to be solved by a better understanding of the non mean field corrections that have to be made to the theory especially pointing out a way to take into account activated processes that are stronger in non mean field systems.

The analysis of MCT as a mean field theory for the dynamics in glasses as been pushed forward in [**?**]. In that paper the general structure of MCT theories has been summarized and it has been shown that this kind of theories can be considered as dynamical Landau theories of the glass transition. This means that regardless the correction to the precise form of the MCT equations, there is a set of predictions that are insensible to them. In particular the relation between the exponents a and b and the square root singularity are really universal properties of the Landau approximation while the dynamical temperature or the value of λ are dependent on the details of the MCT kernel and are not universal as can be expected.

1.2.2 Kinetically constrained models

Kinetically Constrained Models (KCM) have been introduced in glass physics with the scope to highlight the purely dynamical aspects of the physics of glass-forming liquids. This models have been introduced by Frerickson and Andersen [77, 78] and have been studied a lot in recent years. The general idea behind this approach is the following. For all this model the Hamiltonian is the simplest as possible, generally it is a sum of independent terms, so that the statics, namely the calculation of the free energy from the Boltzmann distribution, is always trivial while the dynamical rules that are used employ some constraints that frustrate the dynamics itself producing a glassy behavior. In this way the glassiness and the dramatic slowing down are explained by means of dynamic facilitations instead of a very rough free energy landscape. In practice one can look at the dynamics as a rule to explore phase space. If the rule is such that the phase space is separated in regions that can be esplored only by entering in them along some very particular trajectories, it is

clear that the relaxation is automatically suppressed. One of the most interesting features that are displayed by KCMs is that some of them can have a relaxation time that follows the Arrhenius behavior while some others may have a super-Arrhenius behavior [157] so that they can model both strong and fragile glasses. Moreover they give a natural explanation for the emergence of dynamical heterogeneities.

Most of the KCMs are build with elementary degrees of freedom $n_i = 0, 1$. These degrees of freedom can be put on a given lattice (cubic lattice, Bethe lattice) and represents the two possible states of a coarse grained region of a supercooled liquid. We say that $n_i = 0$ if the particles that are around the site i are mobile while $n_i = 1$ if they are immobile. KCMs divide into conservative and non-conservative models: in the former the total number of occupied (or immobile, or high density) sites $\sum_i n_i$ is taken fixed and is a constant of motion while in the latter it can change in time. The dynamical rules that are used to evolve the systems are standard Markov processes that are such that the passage from one configuration to another is permitted only if a dynamical constraint is satisfied.

There are many possible kind of constraints and each constraint defines a particular kinetically constrained model. Here we give a short (not exhaustive) list of KCMs:

- Fredrikson-Andersen facilitated spin models FA-m: these are non-conservative KCMs that are such that a spin flip is allowed only if the number of empty spins (n=0) surrounding the spin under consideration exceeds m.
- East model: according to this model a spin flip is possible only if the spin on the left of the one we want to flip is empty. This is a non conservative model.
- Kob-Andersen model (KA-m): according to this model the dynamical rule is such that a particle can jump to a neighboring spin only if it has at least m empty nearest neighbor spins both in the initial and final states.

Non-conservative models can be divided in two big classes: non-cooperative and cooperative models. In the first case it is possible construct a sequence of allowed transitions starting from whatever configuration that contain a region of empty variable that are such that the final state of the system is totally empty while in the second case such a possibility is not verified. FA-1 is a non cooperative model while FA-m with $m > 2$ and the East model are cooperative. In general non-cooperative models present Arrhenius relaxation while cooperative models show a super-Arrhenius behavior for the relaxation time [158].

The general Hamiltonian that is considered for all these models is the simplest one of the form

$$H = \sum_i n_i \tag{1.35}$$

This means that, as we have said, the statics is always very simple and free of any kind of phase transition because there is no coupling between different degrees of freedom. However the dynamical constraints can force the system to undergo to dynamical phase transitions. Even if the dynamical rules obey the detailed balance condition this does not mean that the Boltzmann measure will be the limiting probability distribution over the configuration space at large times. This means

that it may happen that for some particular initial conditions, the dynamics is not able to converge to the equilibrium distribution. A natural concept here is the one of ergodicity. Let us consider an initial configuration of the system extracted according to the equilibrium distribution. We say that the system is ergodic if the dynamical averages computed starting from this initial configuration are equal to the equilibrium averages [81]. If this requirement is not satisfied we say that the system is not ergodic. One of the main question is if we decrease the concentration $q \in [0,1]$ of empty sites then an ergodicity breaking transition can occur. Of course one can expect that at sufficiently high q the system will be ergodic but the study of the possibility to have an ergodicity breaking transition is not trivial at all. The known results are that the FA-m models and the KA-m models do have such a transition if they are on the Bethe lattice while they do not present the transition if they are on a cubic d-dimensional lattice for whatever value of d and m.

Once the transition point is determined we need to characterize the transition. The first point we need to investigate is how the relaxation time behaves on approaching the transition. For the FA-1 model the fact that its dynamics is nothing but a diffusion of defects leads directly to the fact that the relaxation time follows an Arrhenius law [93]. The same model FA-m with $m \geq 2$ requires the cooperatively for relaxation and this causes a faster increase of the relaxation time that in this case follows a super-Arrhenius behavior. The divergence of the relaxation time can be analyzed in many KCMs. A remarkable fact is that if we look at the FA model on the Bethe lattice so that is has a transition at a finite value of q, then the relaxation time diverges at the critical point with a power law $q \sim (q - q_c)^{-\gamma}$ with $\gamma \simeq 2.9$. This power law behavior is analogous to what happens in MCT and we have seen it in the previous section.

One of the most interesting things about KCMs is that they can be used to investigate the dynamical heterogeneities and the correlation length associated with them. An important result is that they are a mesoscopic phenomenon in the sense that the correlation length associated does not diverge. To study this it is useful to introduce the persistence field $p_i(t)$. We say that $p_i(t) = 0$ if the site i has change its state at least once from time 0 to time t and we say $p_i(t) = 1$ if it has never changed. We can define a global persistence function as $P(t) = \lim_{N\to\infty} \sum_i p_i(t)$. By running a computer simulation it is possible to follow the persistence field in time. If we define $t_{1/2}$ the time such that $P(t_{1/2}) = 1/2$ then we can plot the persistence field for different temperatures. The result is shown in Fig. 1.10. We can clearly see that a correlation length is growing in decreasing the temperature so that the relaxation dynamics is spatially correlated.

In the case of KCMs, one can study the dynamical heterogeneities by looking at the structure factor defined by

$$S_4(\mathbf{k}, t) = \frac{1}{N}\mathcal{N}(t) \sum_{i,j} \Big[p_i(t)p_j(t) - P^2(t) \Big] e^{i\mathbf{k}\cdot(\mathbf{r}_i - \mathbf{r}_j)} \tag{1.36}$$

where $\mathbf{r}_i$ are the vectors that address specific lattice points. The shape of this function is reported in Fig. 1.11 The first thing to note is that the shape of S_4 is the typical one that can be obtained in finite correlated systems. The zero momentum limit gives the susceptibility $\chi_4(t) = \lim_{\mathbf{k}\to 0} S_4(\mathbf{k}, t)$. We see that the susceptibility

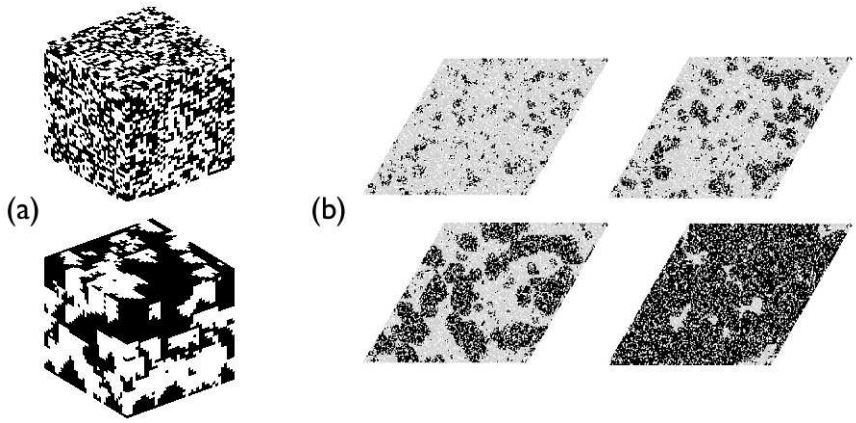

Figure 1.10. a)The persistence field for a three dimensional North-East-Front model (NEF). The figure on the left shows the persistence for $T = 1.0$ while the one on the right shows the same but for $T = 0.15$. Black points are such that $p_i(t) = 0$ while white points are such that $p_i(t) = 1$. These picture are taken from [81]. b) The persistence field for the TGL model for the same density but for different observational times. Taken from [139].

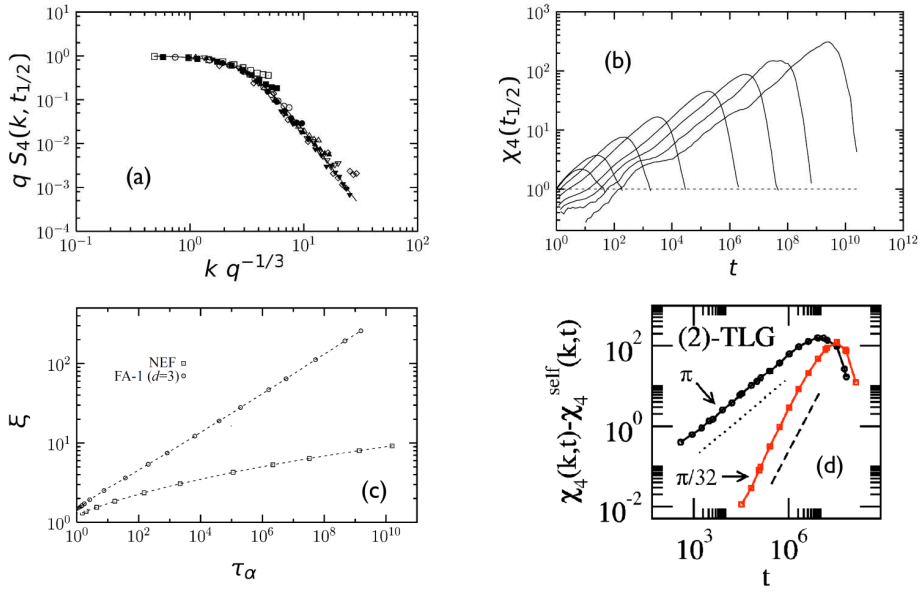

Figure 1.11. a) Four point structure factor for different temperatures in the NEF model b) $\chi_4(t)$ for the NEF model for different temperature as a function of time. As the temperature is decreased the peak of χ_4 grows. c) Scaling of the dynamical correlation length with the relaxation time in the NEF and FA-1 model. d) The behavior of the four point susceptibility for different momenta. The pictures are taken from [81].

is a non monotonic function; moreover because we report its shape for different temperature, one can convince that its peak grows when the temperature is decreased shifting towards larger time. In general it is observed that it appears on times that are of the order of the relaxation time of the persistence function. The peak of χ_4, let us call it χ_4^*, grows as the critical point is approached with a power law $\chi_4^* \sim q^{-\gamma}$ [173] and we expect that $S_4 \simeq \chi_4^* f(k\xi)$ where f is a scaling function being ξ the dynamical correlation length. Moreover one can expect that at $t = t^*$, being t^* the time such that $\chi_4(t^*) = \chi_4^*$, the correlation length behaves like $\xi \sim q^{-\nu}$. Let us conclude that KCMs can be used to see the consequences of the dynamical heterogeneities such as for example the violation of the Stokes-Einstein violation. We will not review this issue here but an almost up-to-date review for this can be found in [81].

1.3 Static Approaches

In the previous sections we have analyzed the problem of the glass transition from a purely dynamical perspective. The mode-coupling theory and the kinetically constrained models, underline that many features of the physics of supercooled liquids may be understood through dynamics without invoking nothing more profound than the concept of dynamical facilitation. Let us also underline that while KCMs are first principles models in the sense that starts from the microscopic details, mode-coupling theory involves a set of some uncontrolled approximation so that it is a more phenomenological theory. Here we want to present two different approaches that are static in nature. They are deeply based on the concept of metastability. The first approach is a mean field one and it is based on a set of mean field spin glass models that display at the dynamical level the same phenomenology of mode-coupling theory. The second approach is a scaling theory based on the mean field results.

1.3.1 Mean field theory

The mean field approach is based on the solution of a set of spin glass models, the p-spin spherical models, that exhibit a dynamical phenomenology similar to what is predicted by the mode-coupling theory and at the static level predict a thermodynamic transition that is in the same spirit of the Kauzmann point in which the excess entropy goes to zero. These models inspired all the mean field treatment of structural glasses and are at the cornerstone of the Random First Order Transition Theory that will be described in the next section. However, before reviewing in detail the p-spin spherical model, we want to underline the principal ideas that are at the basis of the mean field approach that can be successfully applied also for structural glasses in such a way to obtain a mean field theory of structural glasses [125, 128, 129, 130, 142, 131].

Let us consider a system with internal degrees of freedom called σ_i that can be spins or the positions the particles that build the supercooled liquid, and let us consider the hamiltonian of the system $H[\underline{\sigma}]$ where we denote with $\underline{\sigma}$ the whole configuration of the internal degrees of freedom. Then we can consider the free energy of the system as a function of an order parameter $\underline{m}$. For example, in

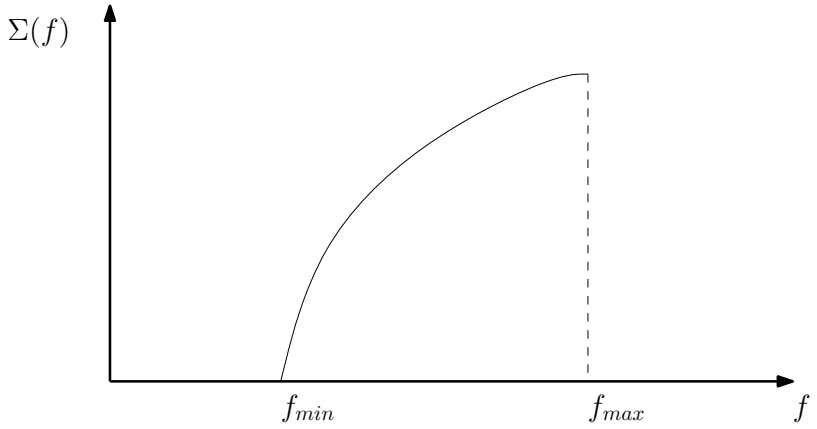

Figure 1.12. The complexity curve in the mean field treatment of structural glasses.

spin system, this could be the configuration of the equilibrium magnetizations on each site and in a system of particles we could be interested in defining the free energy as a functional of the density profile. We assume that at high temperature the free energy as a function of the order parameter is a convex function with a global minimum in the trivial high temperature value of $\underline{m}$ while, on lowering the temperature, at some temperature T_d a set of metastable minima appears in the free energy landscape. These minima are supposed to be in a number that is exponential with the size of the system and can be grouped according to their free energy density f_α. Moreover we assume that the number of minima with free energy density f is given by

$$\mathcal{N}(f,T,N) \sim e^{N\Sigma(f,T)} \tag{1.37}$$

where N is the size of the system. We call $\Sigma(f,T)$ the complexity or configurational entropy of the system. The minima of the free energy are interpreted as possible states of the system and are called TAP states [170]. Another assumption that we make is that below T_d the curve of the complexity is like the one represented in Fig. 1.12.

The total free energy Φ can be computed as follows

$$e^{-\beta N\Phi(T)} = \sum_{\underline{\sigma}} e^{-\beta H[\underline{\sigma}]} \sim \sum_{\alpha} e^{-\beta N f_\alpha} = \int_{f_{min}(T)}^{f_{max(T)}} \mathrm{d}f\, e^{N[\Sigma(f,T)-\beta f]} \tag{1.38}$$

At this point the thermodynamic limit allows us to take the saddle point so that

$$e^{-\beta N\Phi} \simeq e^{N[\Sigma(f^*(T),T)-\beta f^*(T)]} \tag{1.39}$$

where $f^*(T)$ is the solution of the following equation

$$\frac{1}{T} = \left.\frac{\partial\Sigma(f,T)}{\partial f}\right|_{f=f^*(T)} . \tag{1.40}$$

At the dynamical point T_d the solution of this equation is $f^*(T_d) = f_{max}(T_d)$ while when the temperature is lowered the solution is between $f_{min}(T)$ and $f_{max}(T)$. At some point that we call T_K the solution to this equation becomes $f^*(T_K) =$

$f_{min}(T_K)$. This means that the thermodynamics is dominated by the states that have zero configurational entropy that means the states that are in a sub exponential number with respect to the size of the system. This nothing but the Kauzmann point at which the ideal glass transition takes place. For temperature $T < T_K$ the thermodynamics is dominated by the same states that have zero complexity.

At the dynamical level one can expect the following picture. We can do two kinds of dynamical experiments. First of all we can study equilibrium dynamics. This means that we take the system, we let it equilibrate and then we start to look at its dynamics when the starting point is an equilibrium configuration. Because the system has been equilibrated, then it will be in one of the thermodynamically dominant metastable states that are the states with a free energy density that satisfy Eq. 1.40. This implies that the long time properties of the system can be studied in a static way because if we assume true metastability and ergodicity breaking then all the long time properties can be characterized using a statistic measure over the configurations that belong to the equilibrium state in which the system is trapped. The second thing that we can do is to study the off-equilibrium dynamics. In this case the typical experiment is to take the system in its liquid phase and then make a rapid quench to a temperature that is below the dynamical point. Because of the fact that the most numerous states are the threshold ones that have a free energy density equal to $f_{max}(T)$, we can expect that statistically, the initial configuration in which the system starts will be one that belongs to the configurations that are sampled in one of the exponential many threshold states. This means that the dynamical properties of the system, for large times, will be the ones of the threshold states. Let us underline here that at the dynamical point the relaxation time diverges.

From the discussion above it is clear that the most important role here is played by the complexity or configurational entropy. Having a (mean field) way to compute this quantity is crucial for the whole approach. During the years two methods have emerged. The first one is the real replica method introduce by Monasson in [133] while the second one was introduced by Franz and Parisi in [69] and is called the potential method. Here we will describe the real replica method while we leave the discussion of the Franz-Parisi potential to the chapter 3.

The basic idea of the real replica method is that if we consider two copies of the same system and we put a vanishing (*after* the thermodynamic limit) coupling between them then if we are in the liquid phase they are uncorrelated but if we are below the dynamical point they become correlated. We can extend this line of reasoning to more then two copies of the system and consider m copies of it. If we put a small coupling between the m clones and if this small coupling is enough to let all the copies fall down in the same state then we can write the partition function of the cloned system in the following way

$$Z_m = e^{-\beta N \Phi(m,T)} = \sum_{\alpha} e^{-N\beta m f_\alpha} = \int_{f_{min}(T)}^{f_{max}(T)} \mathrm{d}f \, e^{N[\Sigma(f,T) - \beta m f]} \tag{1.41}$$

Taking the thermodynamic limit we can take also the saddle point that gives the equation

$$\frac{m}{T} = \left. \frac{\partial \Sigma(f,T)}{\partial f} \right|_{f^*(m,T)} . \tag{1.42}$$

Moreover we have that

$$\Phi(m,T) = \Sigma(f^*(m,T),T) - \beta m f^*(m,T) \tag{1.43}$$

so that

$$\begin{aligned} f^*(m,T) &= \frac{\partial \Phi(m,T)}{\partial m} \\ \Sigma(m,T) \equiv \Sigma(f^*(m,T),T) &= m^2 \frac{\partial [m^{-1}\beta\Phi(m,T)]}{\partial m} \end{aligned} \tag{1.44}$$

This implies that if we know $\Phi(m,T)$ and we are able to give an analytic continuation of it at non integer value of m then from the parametric plot of $\Sigma(m,T)$ as a function of $f^*(m,T)$ we can reconstruct the shape of $\Sigma(f,T)$. Clearly this is a mean field picture because it assumes the existence of true metastable states while we know that true metastability is not possible in finite dimensions because of nucleation phenomena. This means that the relaxation time can grow very rapidly at the dynamical temperature but cannot diverge remaining finite (even if it can be longer than the typical experimental timescales). The only point where a true divergence can take place is at the Kauzmann transition where the system undergo to an ideal glass transition.

The p-spin spherical model: the statics

Among all the spin glass models that have been studied, the p-spin spherical model is very special. First of all it can be solved in the statics by many methods and moreover also its dynamics can be investigated deeply both in the equilibrium and in the off-equilibrium case. This section follows both the excellent reviews [39, 181] The model is defined by the following disordered Hamiltonian

$$H[\underline{\sigma}] = - \sum_{i_1<i_2<\ldots<i_p} J_{i_1 i_2 \ldots i_p} \sigma_{i_1}\sigma_{i_2}\ldots\sigma_{i_p} \tag{1.45}$$

where the couplings are quenched random variables with zero mean and variance given by

$$\overline{J^2_{i_1 i_2 \ldots i_p}} = \frac{p!}{2N^{p-1}} \tag{1.46}$$

where N is the total number of spins. Moreover we have the spherical constraints

$$1 = \frac{1}{N}\sum_{i=1}^{N} \sigma_i^2 \tag{1.47}$$

We will solve this model using the real replica method even if the standard replica method or the potential method can be employed too. To do this we add $m-1$ copies to the original system. All the copies obey the *same* disorder realization. Moreover we put an infinitesimal coupling between the copies: this will be always hidden in the equations because at the end we will take the limit in which this coupling goes to zero. However it is crucial in order to let all the copies fall down in the same glassy state below the dynamical transition point.

The replicated free energy of the system is given by

$$\Phi(m,T) = \lim_{N\to\infty} \frac{T}{N}\overline{\log Z_m} = \lim_{N\to 0} \frac{T}{N}\overline{\int \mathrm{d}\underline{\sigma}_1 \dots \mathrm{d}\underline{\sigma}_m \, e^{-\beta \sum_a = 1^m H[\underline{\sigma}_a]}} \, . \tag{1.48}$$

Here the replica method is employed to treat the average over the logarithm, as usual

$$\log x = \lim_{n\to 0} \partial_n x^n \tag{1.49}$$

so that the replicated free energy becomes

$$\Phi(m,T) = \lim_{N\to\infty,\ n\to 0} \frac{T}{N}\partial_n \overline{Z_m^n} \tag{1.50}$$

where $\overline{Z_m^n}$ can be computed exactly and it is given by

$$\begin{aligned} \overline{Z_m^n} &= \overline{\int \mathrm{d}\underline{\sigma}_1 \dots \mathrm{d}\underline{\sigma}_{nm} \, e^{-\beta \sum_a = 1^{nm} H[\underline{\sigma}_a]}} \sim \\ &\sim \int \mathrm{d}Q_{ab} e^{NS(Q)} \end{aligned} \tag{1.51}$$

where Q_{ab} is a symmetric $nm \times nm$ matrix whose elements on the diagonal are fixed to be equal to 1 and we have to integrate over the off diagonal elements (provided the symmetric constraint). The action S is given by (we neglect constant terms)

$$S(Q) = \frac{\beta^2}{4} \sum_{ab} Q_{ab}^p + \frac{1}{2} \log\det Q \, . \tag{1.52}$$

The physical meaning of the matrix Q is that its average gives the average of the overlap

$$Q_{ab} = \frac{1}{N} \sum_{i=1}^{N} \sigma_i^{(a)} \sigma_i^{(b)} \tag{1.53}$$

To compute the integral in Eq. 1.51 we can take the saddle point. However it is quite difficult to optimize over all the independent elements of the matrix Q: a possible way out to this is to reduce the space of matrices over which we have to optimize. The simplest ansatz is a 1RSB ansatz that for $n = 2$ and $m = 3$ reads as follows

$$Q = \begin{pmatrix} \begin{pmatrix} 1 & q & q \\ q & 1 & q \\ q & q & 1 \end{pmatrix} & 0 \\ 0 & \begin{pmatrix} 1 & q & q \\ q & 1 & q \\ q & q & 1 \end{pmatrix} \end{pmatrix} \, . \tag{1.54}$$

Note that this ansatz tells us that replicas that belong to different blocks are uncorrelated. This is because the off-block-diagonal matrix elements are set to zero from the beginning. Plugging this ansatz into the form of S we obtain that

$$\begin{aligned} S(Q) &= -\beta n m \phi_{1RSB}(m,q,T) \\ \phi_{1RSB}(m,q,T) &= -\frac{1}{2\beta} \left\{ \frac{\beta^2}{2}[1 + (m-1)q^p] + \frac{m-1}{m} \log(1-q) + \right. \\ &\left. + \frac{1}{m} \log\left[1 + (m-1)q\right] \right\} \, . \end{aligned} \tag{1.55}$$

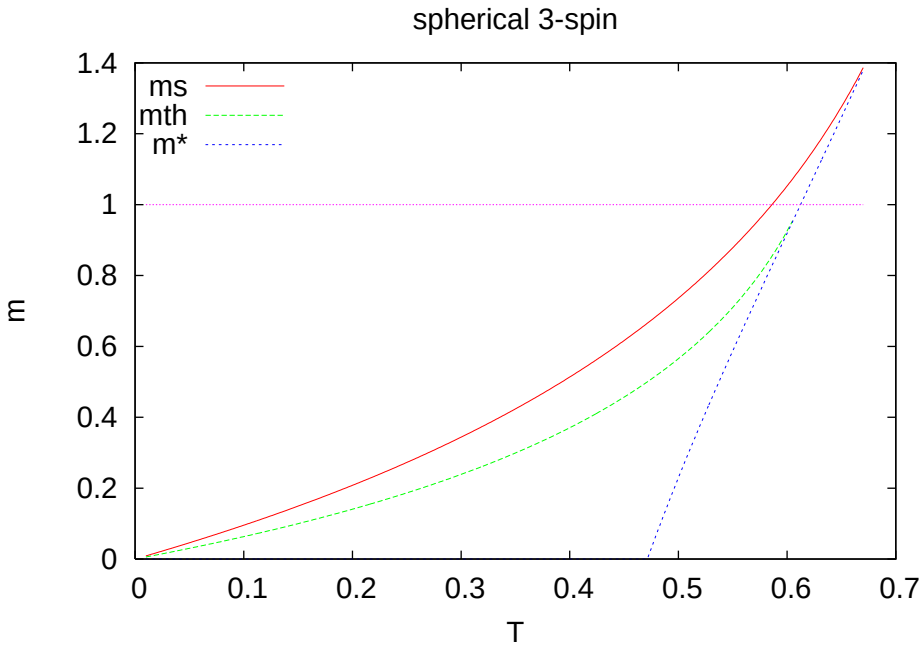

Figure 1.13. The phase diagram of the replicated 3-spin spherical model. Above the dashed blue line there exists a non trivial solution with $q^* > 0$. The plot is taken from [181].

so that the free energy is given by

$$\Phi(m,T) = -\frac{T}{N}\lim_{n\to 0}\partial_n \exp\left[-\beta n m N \phi_{\text{1RSB}}(m,q^*,T)\right] = m\phi_{\text{1RSB}}(m,q^*,T)\ , \quad (1.56)$$

where q^* is the non trivial solution of the saddle point equation. The saddle point equation admits always a trivial high temperature solution that is $q^* = 0$. However we have to remember that we have put a coupling between the replicas. This is why we need to choose the non trivial solution whenever it is available: having a non trivial solution means that replicas can be correlated.

Treating m as a continuous parameter we can first look at where the non trivial solution appears in the (m,T) plane. By solving numerically the saddle point equation we can see a non trivial q^* can be found above the dashed blue line of Fig. 1.13. To compute the configurational entropy we need to compute the quantities in Eq. 1.44. By doing this, we can write the green dashed line on the phase diagram. This line that is denoted with $m_d(T)$ is the line that at fixed temperature corresponds to the value of m in correspondence of which the complexity has its maximum. This line crosses the line $m = 1$ at the dynamical temperature. The line $m = 1$ is the equilibrium one because we need to set $m \to 1$ in order to recover the non-replicated system. The point in which the red line crosses the line $m = 1$ is the Kauzmann point. At that point the states that dominate the Gibbs measure are the one with zero complexity.

An important remark is that between T_K and T_d the free energy of the system that comes from the most relevant metastable states is exactly equal to the one

of the paramagnet even if the paramagnet does not exist below T_d. Below the Kauzmann point the free energy of the system is given by $f_{min}(T)$. In order to compute it we can choose m in such a way that the complexity is zero because we know that those states are the one with $f_{min}(T)$. The red line, that we call $m_s(T)$ is exactly the value of m as a function of the temperature that does this job. This means that the free energy of the glass below the Kauzmann temperature is given by

$$f_{min}(T) = \left.\frac{\Phi(m,T)}{m}\right|_{m=m_s(T)} = \phi_{\text{1RSB}}(m_s(T), q^*(T), T) \ . \tag{1.57}$$

Between the green line and the blue line, the non trivial solution of the saddle point equation $q^* > 0$ is unphysical.

Interestingly enough the green line corresponds to the instability line of the 1RSB ansatz. This means that below it the ansatz (1.54) becomes unstable and the system would break the replica symmetry [132]. This situation is very general and many other models possess this instability line. However, the p-spin spherical model is special because below the green line, no fullRSB solution does exist while in the general case a fullRSB branch is possible [135, 134]. This is what happens for example for hard spheres in high dimensions and will be analyzed in chapter 4. In this case, the branch of the complexity curve that is drawn from the fullRSB part of the phase diagram has a different interpretation. In fact the real replica method at the 1RSB level allows us to compute the complexity that is the logarithm of the number of well defined metastable states in the free energy landscape. If the 1RSB solution is unstable and the solution becomes fullRSB then this means that the bottom of the metastable 1RSB states is not stable and well defined but contains unstable directions. This means that in the fullRSB case the complexity does not count for the number of metastable states, but it counts the number of metabasins inside each of which there is a fullRSB structure of states organized in a hierarchical way as in the Sherrington-Kirkpatrick model [132].

The p-spin spherical model: the dynamics

The Langevin dynamics of this model can be solved exactly too. Consider now the stochastic equation

$$\dot{\phi}_i(t) = -\frac{\partial H_J}{\partial \phi_i} - \mu(t)\phi_i(t) + \xi_i(t) \tag{1.58}$$

where $\xi_i(t)$ are gaussian random variables that play the role of the white noise so that

$$\langle \xi_i(t) \rangle_\xi = 0 \quad \forall t \quad \text{and} \quad i = 1, \dots, N \tag{1.59}$$

$$\langle \xi_i(t)\xi_j(t') \rangle_\xi = 2T\delta_{ij}\delta(t-t') \implies P[\{\xi\}] \propto \exp\left\{ -\frac{1}{4T} \sum_{i=1}^{N} \int \mathrm{d}t\, \xi_i^2(t) \right\} \tag{1.60}$$

being T the temperature of the external thermal bath. Moreover we have to require that the spins live on a sphere of radius N for every time t so that we have to translate the spherical constraint in the dynamical language

$$\frac{1}{N} \sum_{i=1}^{N} \phi_i^2(t) = 1 \quad \forall t \, . \tag{1.61}$$

This constraint can be satisfied by adding a parameter in the Langevin equation. This parameter is $\mu(t)$. The line of reasoning is the following: instead of solving the dynamical equations with the spherical constraint we prefer to solve the parametric version of the dynamical equations (where we have inserted the parameter μ) with no constraint and we can put the parameter μ in a self consistent way, at the end of the calculation, in the form so that the constraint (1.61) is satisfied. Clearly we are interested in the computation of the two time correlation and response functions defined by

$$C(t,t') = \frac{1}{N}\sum_{i=1}^{N}\overline{\langle\phi_i(t)\phi_i(t')\rangle} \qquad R(t,t') = \frac{1}{N}\sum_{i=1}^{N}\overline{\left\langle\frac{\delta\phi_i(t)}{\delta\xi_i(t')}\right\rangle}. \tag{1.62}$$

where the thermal average over the noise ξ is denoted by the brackets while the average over the disorder is indicated with the overline.

We can solve the dynamical problem using the formalism introduced in [123]. De Dominicis and Peliti [55, 58] have noted that in the dynamical approach we have not the necessity to introduce replicas to treat the disorder. In fact the dynamical partition function is equal to one for every realization of the disorder. With functional methods we can write

$$1 = Z = \overline{\left\langle\int\prod_{i=1}^{N}\mathcal{D}\phi_i\,\delta\left(\phi_i(t)-\phi_i^{(\xi)}(t)\right)\right\rangle} \tag{1.63}$$

where $\phi_i^{(\xi)}(t)$ is a particular solution of the Langevin equation. Expressing the functional Dirac delta function in terms of its Fourier transform we obtain[2]

$$\begin{aligned} Z &= \overline{\left\langle\int\prod_{i=1}^{N}\mathcal{D}\phi_i\mathcal{D}\hat{\phi}_i\exp\left\{i\sum_{i=1}^{N}\int\mathrm{d}t\,\hat{\phi}_i(t)\left[\dot{\phi}_i+\frac{\partial H_J}{\partial\phi_i}+\mu(t)\phi_i(t)-\xi_i(t)\right]\right\}\right\rangle} = \\ &= \int\prod_{i=1}^{N}\mathcal{D}\phi_i\mathcal{D}\hat{\phi}_i\exp\left\{i\sum_{i=1}^{N}\int\mathrm{d}t\,\hat{\phi}_i(t)\left[\dot{\phi}_i(t)+\mu(t)\phi_i(t)\right]-T\sum_{i=1}^{N}\int\mathrm{d}t\,\hat{\phi}_i^2(t)\right\}\times \\ &\qquad\times\overline{\exp\left\{i\sum_{i=1}^{N}\int\mathrm{d}t\,\hat{\phi}_i\frac{\partial H_J}{\partial\phi_i}\right\}}. \end{aligned}$$

At this point it is very useful to introduce Grassmann[3] variables [109, 49]. Define the superfield

$$\Phi_i(a) = \phi_i(t) + i\theta\hat{\phi}_i(t) \qquad \theta^2 = 0 \tag{1.64}$$

[2] We have taken into account that the Jacobian that should to be put inside the functional integral is independent from the field variables if you use the Ito discretization rule for the Langevin equation so that it doesn't give any contribution to the calculation.

[3] Here we introduce the supersymmetric formalism in a more compact way. In fact, generally one deals with the superfields only to take into account the determinant that defines the Jacobian produced by the manipulation of the Dirac delta functions. However this Jacobian is a constant. In general, to produce the determinant you need a couple of Grassmann variables. Here we use a coincise notation so that $\theta \to \overline{\theta}\theta$. The full supersymmetric version of this formalism is very powerful because it can be shown that it encodes a supersymmetry that can reproduce the fluctuation-dissipation theorem and whose dynamical breaking can be regarded as a signal of the crossover from the equilibrum to the non-equilibrium situation.

where $a = (t, \theta)$ and the dynamical order parameter as

$$Q(a,b) = \frac{1}{N}\sum_{i=1}^{N}\Phi_i(a)\Phi_i(b)\,; \tag{1.65}$$

we can rewrite the dynamical generating functional as

$$Z = \int\prod_{i=1}^{N}\mathcal{D}\Phi_i\int\mathcal{D}Q\int\mathcal{D}\overline{Q}\exp\left\{-\frac{1}{2}\sum_{i=1}^{N}\int \mathrm{d}a\mathrm{d}b\,\Phi_i(a)\overline{Q}(a,b)\Phi_i(b) + \right. \tag{1.66}$$

$$\left. +\frac{N}{4}\int\mathrm{d}a\int\mathrm{d}b\,Q^p(a,b) + \frac{N}{2}\int\mathrm{d}a\mathrm{d}b\,\left[\delta(a-b)\left(\hat{D}+\mu(t_a)\right)+\overline{Q}(a,b)\right]Q(a,b)\right\} \tag{1.67}$$

where

$$\hat{D} \equiv 2T\frac{\partial}{\partial\theta} + \frac{\partial}{\partial t} - 2\theta\frac{\partial^2}{\partial t\partial\theta}\,. \tag{1.68}$$

If we want to compute the correlation and response functions we have to evaluate the average of the dynamical order parameter which is given by

$$\langle Q(a,b)\rangle = \int\mathcal{D}Q\mathcal{D}\overline{Q}\,Q(a,b)\exp\left\{-\frac{N}{2}\mathrm{Tr}\log\overline{Q} + \frac{N}{4}\int\mathrm{d}a\int\mathrm{d}b\,Q^p(a,b) + \right. \tag{1.69}$$

$$\left. + \frac{N}{2}\int\mathrm{d}a\mathrm{d}b\,\left[\delta(a-b)\left(\hat{D}+\mu(t_a)\right)+\overline{Q}(a,b)\right]Q(a,b)\right\} \tag{1.70}$$

and if we take the large N limit we can take the saddle point approximation so that

$$\langle Q(a,b)\rangle = Q_{SP}(a,b) \tag{1.71}$$

where $Q_{SP}(a,b)$ satisfies the following equation

$$\left(\hat{D}_1+\mu(t_1)\right)Q_{SP}(a_1,a_2) + \delta(a_1-a_2) + \frac{p}{2}\int\mathrm{d}a' Q_{SP}^{p-1}(a_1,a')Q_{SP}(a',a_2) = 0\,. \tag{1.72}$$

The correlation and response function, at the leading order, are embedded in the dynamical order parameter $Q_{SP}(a_1,a_2)$

$$Q_{SP}(a_1,a_2) = C(t_1,t_2) - \theta_1 R(t_2,t_1) - \theta_2 R(t_1,t_2) \tag{1.73}$$

Note that it can be proved that the term $\theta_1\theta_2\left\langle\hat{\phi}_i(t)\hat{\phi}_i(t')\right\rangle$ vanishes.

The dynamical equations for $C(t_1,t_2)$ and $R(t_1,t_2)$ can be recovered from (1.72) by simply equating to zero the coefficient of the Grassmann polynomial. If we suppose that $t_1 > t_2$ then causality implies that $R(t_2,t_1) = 0$ and we obtain[4]

$$\begin{aligned}
\frac{\partial C(t_1,t_2)}{\partial t_1} &= -\mu(t_1)C(t_1,t_2) + \frac{p}{2}\int\mathrm{d}t\,C^{p-1}(t_1,t)R(t_2,t) \\
&\quad + \frac{p(p-1)}{2}\int\mathrm{d}t R(t_1,t)C^{p-2}(t_1,t)C(t,t_2) + 2TR(t_2,t_1) \\
\frac{\partial R(t_1,t_2)}{\partial t_1} &= -\mu(t_1)R(t_1,t_2) \\
&\quad + \delta(t_1-t_2) + \frac{p(p-1)}{2}\int\mathrm{d}t C^{p-2}(t,t_2)R(t,t_2)R(t_1,t)\,.
\end{aligned} \tag{1.74}$$

[4]Note that in the equation below we have left the explicit dependence of the correlation function from $R(t_2,t_1)$ because, although it is zero when $t_2 < t_1$ it is important in the derivation of the equation for the Lagrange mutiplier μ.

Now we have to write down a self consistent equation for the parameter $\mu(t)$ in order to ensure the spherical constraint. This can be done by simply using the fact that

$$C(t,t) = 1 \quad \forall t \tag{1.75}$$

from which follows directly that

$$0 = \frac{\partial C(t_1,t_1)}{\partial t_1} = \lim_{t_2 \to t_1^-} \left[\frac{\partial C(t_1,t_2)}{\partial t_1} + \frac{\partial C(t_1,t_2)}{\partial t_2} \right] . \tag{1.76}$$

Now, using the fact that

$$\lim_{t_2 \to t_1^-} R(t_1,t_2) = 1 \tag{1.77}$$

you can easily see that

$$\mu(t_1) = T + \frac{p^2}{2} \int \mathrm{d}t R(t_1,t) C^{p-1}(t_1,t) \, . \tag{1.78}$$

We are now able to discuss our results.

The equation we have derived can be solved in the equilibrium and off equilibrium regimes. In the equilibrium regime we can use time-translational invariance that tells that the correlation and response functions are actually dependent on the difference between the two times and we can also use the fluctuation-dissipation theorem that relates the response function with the time derivative of the correlation function. The result is a schematic mode-coupling equation that displays a dynamical transition at a temperature T_d that coincides with the temperature that can be obtained from the statics and that has been discussed previously. The correlation displays a two steps relaxation whose dynamical exponents around the plateau follows the relation (1.33). We will study this equation in chapter 3. Also the aging regime can be studied and solved [51].

Here we want to use the theory described here also to study the dynamical fluctuations. By going back to the dynamical action and by optimizing over $\overline{Q}$ we have that the new dynamical generating function can be written in terms of the action

$$S(Q) = \frac{\beta^2}{4} \int \mathrm{d}a\mathrm{d}b Q(a,b)^p + \frac{1}{2} \log\det Q + \frac{1}{2} \int \mathrm{d}a \left[\hat{D} + \mu \right] Q(a,a). \tag{1.79}$$

By developing the action around the saddle point value Q_{SP} we obtain a quadratic term that is a mass term whose inverse gives the four point correlation function of the fields Φ_i. The mass term is given by

$$M[a,b;c,d] = \frac{\beta^2 p(p-1)}{4} Q^{p-2}(a,b)\delta(a,c)\delta(b,d) - \frac{1}{2} Q^{-1}(b,c) Q^{-1}(a,d) \tag{1.80}$$

To invert this operator one can do the following thing. Let us define the following operators

$$\begin{aligned} A[a,b;c,d] &= -\frac{1}{2} Q^{-1}(a,d) Q^{-1}(b,c) \\ B[a,b;c,d] &= \frac{\beta^2 p(p-1)}{4} Q^{p-2}(a,b)\delta(a,c)\delta(b,d) \end{aligned} \tag{1.81}$$

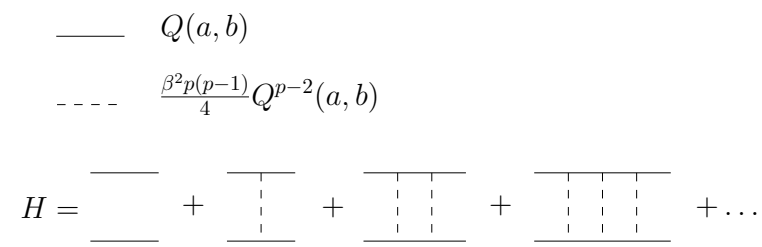

Figure 1.14. The diagrammatic expansion for the four point dynamical correlation function.

Then if we define $H = M^{-1}$ then we can write

$$H = A^{-1} + C \tag{1.82}$$

where the operator C satisfied the following equation

$$C = -\left[A^{-1}BA^{-1} + A^{-1}BC\right] \tag{1.83}$$

that can be solved iteratively. The perturbative series can be represented in an iterative way as shown in Fig. 1.14. This calculation has been done in the more general framework of mode-coupling theory in [18]. However it is difficult to extract the critical properties from this expansion because the resummation of the diagrams is difficult to do. In the next chapter we will follow a different route based on equilibrium thermodynamics that is capable to obtain this correlation function for times that are such that the correlation function $C(t)$ is close to its plateau variable.

1.3.2 Random First Order Transition Theory

The understanding of the fact that the mean field approach may be relevant for the theoretical comprehension of the glass transition problem has come in a series of papers by Kirkpatrick, Thirumalai and Wolynes [102, 103, 97, 98, 99, 101]. They used the insight of mean field models to start a scaling theory of the glass transition. The theory that emerged has been called the Random First Order Transition theory (RFOT) and there are now many reviews that describe it in a deep way. A basic and pedagogical introduction can be found in [40] and a critical review is in [20]. The whole theory can be seen as a revision of the Adam-Gibbs-Di Marzio theory that was introduced in the 60's to explain in a phenomenological (but also very elegant) way the Kauzmann paradox.

The Adam-Gibbs-Di Marzio theory

When the Kauzmann paradox came in, Gibbs was not very satisfied by the resolution that Kauzmann proposed. In particular he noticed that the temperature at which the viscosity diverges is quite close to the one at which the configurational entropy goes to zero as we have underlined in the previous sections. If this is a coincidence or not must be investigated. The pragmatic point is to assume that the two temperatures are related and try to explain this relation.

The key idea of Adam and Gibbs [1] was to connect the slow relaxation in supercooled liquids with the idea that as temperature is decreased the system must rearrange cooperatively larger and larger regions of the system, the so called Cooperative Rearranging Regions (CRR). They are defined as the smallest regions of the systems that can be rearranged independently from the surrounding. This means that in the language of states, each CRR is in a definite glassy state. They assumed that the number of states in which each CRR can be is Ω and it is of order one. Then, because different CRR interacts weakly, the total number of states in which the system can be is

$$\mathcal{N} = \Omega^{N/n} \tag{1.84}$$

where N is the total number of particles while n is the number of particles that belong to a typical CRR. This means that the configurational entropy of the system is given by

$$S_c(T) = \frac{1}{N} \log \mathcal{N}(T) = \frac{1}{n(T)} \log \Omega \tag{1.85}$$

so that

$$n(T) = \frac{\log \Omega}{S_c(T)} \tag{1.86}$$

This means that if there is a configurational entropy vanishing transition, the size of the CRRs diverges. Moreover, if we assume that the free energy barrier that we must cross in order to cooperatively rearrange a CRR is given by the size of the CRR then the relaxation time is given by

$$\tau_R = \tau_0 \exp\left[\frac{B}{T S_c(T)}\right] \tag{1.87}$$

where B contains all constant factors and τ_0 is a timescale. Again, we see that if the configurational entropy vanishes at some temperature, the relaxation time diverges.

In order to see the precise form of this divergence we can estimate the configurational entropy using the entropy of the (supercooled) liquid state and the entropy of the crystal. Then we have

$$\frac{\mathrm{d}S_c}{\mathrm{d}T} = \frac{\mathrm{d}}{\mathrm{d}T}\left(S_{liq} - S_{cr}\right) = c_p^{liq} - c_p^{cr} = \Delta c_p \tag{1.88}$$

where c_p is the specific heat so that

$$S_c(T) - S_c(T_K) = \int_{T_K}^{T} \mathrm{d}t \frac{\Delta c_p(T)}{T} \,. \tag{1.89}$$

If we assume that Δc_p is independent on T we obtain

$$S_c(T) = \Delta c_p \log(T/T_k) \tag{1.90}$$

and around T_K we have

$$S_c(T) \sim \Delta c_p \frac{T - T_K}{T_K} \tag{1.91}$$

so that the the relaxation time become

$$\tau_R = \tau_0 \exp\left[\frac{A}{T - T_k}\right] \tag{1.92}$$

where A is a constant with the dimension of a temperature. We see that the Adam-Gibbs-Di Marzio theory provide a natural explanation of the VFT law for the relaxation time.

The mosaic theory

The theory defined above seems very promising but it relies on some facts that must be settled on more general and solid grounds. One of the main point of the theory is the existence of the CRRs and especially the definition of the states in which they can be. The mean field theory provides an answer to this. In fact one could think that the CRRs can be in one of the TAP states available. However, although in mean field the TAP states are well defined, in finite dimension we know that the free energy must be convex and all the metastable states must be smoothed out due to nucleation. This can be understood in the simplest case of the Ising model.

Suppose to take an Ising model in three dimensions in a positive magnetic field under the critical temperature. Then, at the mean field level the free energy density will have two minima: one in the correspondence of the stable state of positive magnetization and one in correspondence of the metastable state of negative magnetization. At the mean field level, these two minima are separated by a finite barrier. However as soon as finite dimensional effects are taken into account we recognize that the barrier must disappear and a Maxwell construction is needed. This is because if we start from a metastable configuration with negative magnetization, then thermal fluctuation will restore the state with positive magnetization by nucleating it. How this is done can be thought in the following way. Suppose to have a system that is in its metastable negative magnetization state and suppose that at some point a ball of radius R of positive magnetization nucleates in the metastable configuration. The free energy difference between the two configuration is given by

$$\Delta(R) = (f_+ - f_-)\Omega_d R^d + \Gamma S_d R^{d-1} \tag{1.93}$$

where f_+ and f_- are the free energy density of the corresponding stable and metastable states and Ω_d and S_d are the volume and surface of a sphere of radius one. The second therm of Eq. 1.93 is the increase in free energy due to the mismatch of the two configurations on the surface of the ball and its relevance is controlled by the surface tension Γ. The free energy difference $\Delta(R)$ has a maximum in

$$R^* = \frac{\Gamma(d-1)}{f_- - f_+} \tag{1.94}$$

so that if the radius of the ball is $R < R^*$ then the ball will shrink to zero otherwise it will indefinitely expand all over the system nucleating the stable state. The time it takes to nucleate a droplet of size R^* in the metastable system is given by

$$\tau(R^*) \sim \exp\left[\frac{\Delta(R^*)}{T}\right] . \tag{1.95}$$

If we want do the same thing on the glass side we need to consider the metastable TAP states. In [101], Kirkpatrick, Thirumalai and Wolynes considered the free energy of the dominant equilibrium TAP state with respect to the liquid (or paramagnetic) phase. If the free energy given by the equilibrium TAP states between T_K and

T_d is equal to the free energy of the liquid as happens in the p-spin spherical model then we can say that the role played by $f_- - f_+$ is here played by $f^* - f_p = T\Sigma(T)$ where again $\Sigma(T)$ is the complexity of the relevant equilibrium TAP state and f_p is the free energy density of the liquid state. Let us suppose now that the energy mismatch between the glassy state and the liquid state is given by a surface term of the form $\Upsilon_o(T)R^\theta$ where $\theta \leq d-1$. Then we can write the difference in free energy as before

$$\Delta(R) = -T\Sigma(T)\Omega_d R^d + \Upsilon_o(T)R^\theta \tag{1.96}$$

and by finding the maximum value we obtain that for $R \geq l^*$ the liquid will nucleate in the glassy state where

$$l^* = \left(\frac{\theta\Upsilon_0(T)}{T\Sigma(T)\Omega_d d}\right)^{\frac{1}{d-\theta}} . \tag{1.97}$$

One of the main problem of this approach is that in the standard picture, the liquid state is given by a superposition of the thermodynamically relevant TAP states. It is not clear how a superposition like this could be nucleated. A possible way of thinking is the following [24].

Consider a system of particles or spins and suppose that we are able to select a given metastable TAP state, let us call it the state α. Then we take a cavity of radius R inside the system and we freeze all the degrees of freedom outside the cavity. Then we let the interior of the cavity relax. The cavity can be now in one of the exponential many metastable states. However we expect that if the radius of the cavity is small so that the term $\Sigma(T)R^d$ is small then the accessible states are not too many and the cavity will be in the state α because it is favored by the boundary condition. If the radius is increased then all the other states can start to play a role. Let us assume that the surface tension is the same for all couples of different TAP states and is equal to Υ_0. Then the partition function of the cavity can be written as

$$\begin{aligned} Z_\alpha(R,T) &= \exp\left[-\Omega_d R^d \frac{f_\alpha}{T}\right] + \sum_{\gamma\neq\alpha} \exp\left[-\beta\Omega_d R^d f_\gamma + \beta\Upsilon_0 R^\theta\right] = \\ &= \exp\left[-\Omega_d R^d \frac{f_\alpha}{T}\right] + \int_{f_{min}(T)}^{f_{max}(T)} \mathrm{d}f \exp\left[\left(\Sigma(f,T) - \beta f\right)\Omega_d R^d - \beta\Upsilon_0 R^\theta\right] \end{aligned} \tag{1.98}$$

Let us consider the temperature regime in which $T \to T_K$. Then we expect that the relevant R is large so that we can take the saddle point in evaluating the integral. Let us also choose a state α that is an equilibrium state. This means that the boundary of the cavity was properly thermalized and the dynamics inside the cavity is done at the same temperature of the boundary. In this case the partition function of the droplet is given by

$$Z(R,T) \simeq \exp\left[-\Omega_d R^d \beta f^*\right]\left(1 + \exp\left[\Sigma(f^*,T)\Omega_d R^d - \beta\Upsilon_0 R^\theta\right]\right) \tag{1.99}$$

This means that the probability that the droplet is the same state of the boundary is given by

$$p_{in}(R) = \frac{\exp\left[\beta\Upsilon_0 R^\theta\right]}{\exp\left[\beta\Upsilon_0 R^\theta\right] + \exp\left[\Sigma(T)R^d\right]} \tag{1.100}$$

while the probability it is not is

$$p_{out}(R) = \frac{\exp\left[\Sigma(T)R^d\right]}{\exp\left[\beta\Upsilon_0 R^\theta\right] + \exp\left[\Sigma(T)R^d\right]} \tag{1.101}$$

This means that if $R < l^*$, where l^* is the one defined in Eq. 1.97, the surface tension term wins and

$$\begin{aligned} p_{in}(R) &\simeq 1 \\ p_{out}(R) &\simeq 0 \end{aligned} \tag{1.102}$$

while if $R > l^*$ then the configurational entropy drives the nucleation of the supercooled liquid in the metastable state

$$\begin{aligned} p_{in}(R) &\simeq 0 \\ p_{out}(R) &\simeq 1\,. \end{aligned} \tag{1.103}$$

This means that metastable states can be defined only up to a scale $R \leq l^*$.

The result of this discussion is that the CRRs can be identified with regions of the systems that are in a given metastable states and have a size smaller than l^* so that they are stable against nucleation. Moreover we see that if $\Sigma(T)$ vanishes at T_K as predicted by the Adam-Gibbs-Di Marzio theory we immediately see that the typical size of the CRRs grows in decreasing the configurational entropy on approaching T_K so that mean field theory becomes more and more exact on approaching the Kauzmann point. How to detect the growing amorphous order related to the CRR? A possible way to do is to follow exactly the procedure we have introduced before in order to test the stability of a TAP state towards nucleation. We can take a supercooled liquid well thermalized at a given temperature and we can freeze it outside a sphere of a given radius R. Then we can let evolve the interior of the sphere towards its equilibrium configuration and then we can measure the similarity between the final configuration and the initial configuration inside the sphere [21]. This can be done by defining an overlap between different configurations. In Fig. 1.15 we see exactly the plot of the overlap as a function of the radius of the cavity for different temperatures. a high value of the overlap means that the final state is very close to the initial one while a low value of the overlap means that the final state is different from the one present on the boundary of the cavity. An important remark should be done. From the plot we see that the overlap when the radius is small is not close to one. This is because at small radius we expect that the system inside the cavity is in the same state of the one at the boundary so that the initial and final configurations should have an overlap that is the self-overlap of the initial state and that is in general lower than one.

Let us conclude this section by saying that the overlap defined above between the initial and final configuration of the interior of the cavity can be obtained as a sum of a set of *point-to-set* correlation functions. We denote with σ_i the degrees of freedom of the system and with v the set of degrees of freedom that are inside a ball of radius R around a given point in the system. Moreover we denote with $\overline{v}$ the set of degrees of freedom outside the ball v. We can consider a two measures. A standard Bolzmann-Gibbs measure, and a constrained one. The constrained one

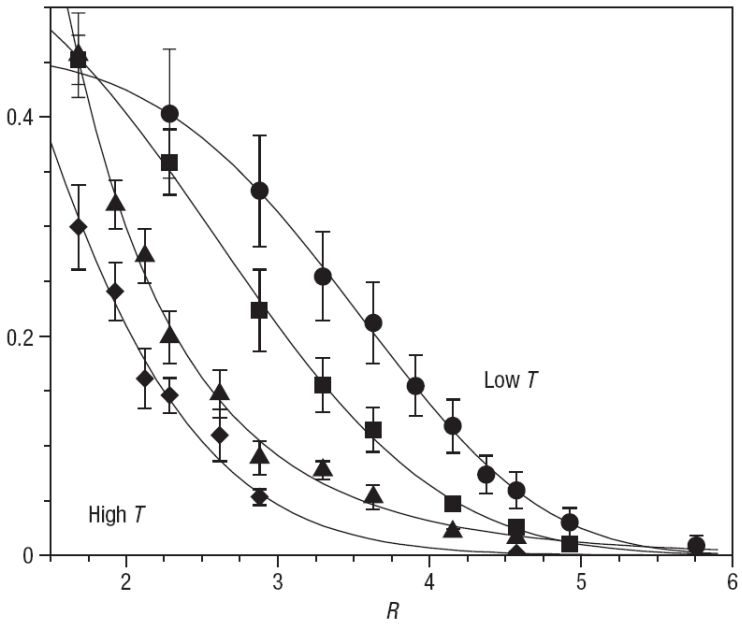

Figure 1.15. The plot show the shape of the overlap between the initial configuration of the cavity with the final state as a function of the radius of the cavity and for different temperatures. The plot is taken from [21].

is such that it is a Boltzmann-Gibbs measure on the degrees of freedom in v having fixed the values of the degrees of freedom $\sigma_{\overline{v}}$. If we indicate with $\langle\cdot\rangle$ the standard Boltzmann-Gibbs measure and with $\langle\cdot\rangle_{\sigma_{\overline{v}}}$ the one constrained with external degrees of freedom $\sigma_{\overline{v}}$ we can define the following correlation function

$$q(R) = \frac{1}{|v|}\sum_{i\in v}\langle\sigma_i\langle\sigma_i\rangle_{\sigma_{\overline{v}}}\rangle = \frac{1}{|v|}\sum_{i\in v} C(i,\overline{v})\,. \tag{1.104}$$

This is a sum of point-to-set correlation function. In fact each $C(i,\overline{v})$ is a correlation function between the degree of freedom i inside v and all the degrees of freedom in $\overline{v}$. This kind of correlation functions is crucial for the whole development of the mosaic theory that, at this stage, is nothing but a scaling theory for the glass transition. How to obtain all the critical properties is not clear up to now even if some work in this direction has been done [35, 34].

Chapter 2

Theory of fluctuations in structural glass models

2.1 Introduction

The study of the fluctuations of the order parameter in statistical physics is crucial to understand the universal properties of phase transitions. In particular, the analysis of the correlation decay with the distance between the degrees of freedom of a system is very important in defining the correlation length that plays a crucial role in standard second order phase transition [141]. In fact by recognizing that that there is a diverging correlation length on approaching the phase transition point, we can build all the machinery of renormalization group calculations that is deeply related to the scale invariance properties of the system near the critical point. For structural glass models all these aspects have emerged only recently. In particular the characterization of the dynamical fluctuations near the dynamical (mean field) transition point is one of the mostly debated topic. In fact in recent years much progress in the understanding in the slow relaxation physics of the glass transition has come from the study of the so called dynamical heterogeneities [12]. As we have seen in the previous chapter, it has been investigated both in simulation and experiments [105] the fact that when the temperature is lowered, the system that is undergoing a glass transition, starts to develop spatial regions with different mobility and of typical size that grows when the transition point is approached possibly diverging at the (mean field) transition point. Interestingly enough, both the approaches to the dynamical glass transition, the mode-coupling theory and replica theory, can describe qualitatively and quantitatively this phenomenon and predict a diverging dynamical correlation function. The main differences of the theory of glasses with respect to standard second order phase transitions are in the definition of the order parameter and on the nature of the correlators that one has to look for in searching of criticality.

This chapter is devoted to the study of this problem in structural glass models. Our perspective will be the one of replica theory. We will start from the theoretical understanding of schematic mean field models that are in the 1RSB universality class [99, 71]. For this models the relation between static and dynamical aspects is very well understood and the relation with schematic mode-coupling theory is

well established. Here we want to apply this theoretical achievements to the structural glass side. The important advantage of replica theory is that it gives a static prescription to compute dynamical properties of the system. In fact solving the dynamics is very complicated also for the simplest structural glass models and one has usually to rely on mode-coupling theory that involves a set of (probably) mean field approximation that are not very well understood. Instead, in replica theory one can give a physical interpretation of what is going on while approaching the dynamical transition and moreover, because the calculations are static, one could try to use standard techniques of phase transition theory.

One of the main result of this chapter is the development of a Landau action for structural glasses [74, 67, 68]. We underline here that this action is valid only to study the dynamical fluctuations in the β regime but we don't know if these results can be extended also in the long time α regime. The theory we will derive will be analyzed at the Gaussian level and we will be able to derive a Ginzburg criterion that states where the Gaussian level gives correct results and where it fails. Moreover in the same framework we will be able to give a general expression for the mode-coupling exponent parameter λ starting from the microscopic descriptions of the system (i.e. starting from the microscopic potential). This is an important point because we have said that if we exclude the case of schematic models, it is not clear the relation between replica theory and mode-coupling theory because in general they address different problems and compute different quantities. Here we will compute a dynamical quantity, namely λ, within replica theory. All the results will be general and can be used in any context. However to extract quantitative results we have to rely in some approximation schemes and here we choose the simplest one that is the replicated Hypernetted Chain approximation of liquid theory. For the sake of clarity, we start the chapter by reviewing some of aspects of the theory of fluctuations in standard phase transition and we will analyze the prototypical Ising model that is in the universality class of the φ^4 theory. We will review all the results that will be extended to the structural glass side.

The content of this chapter is contained in [67, 68].

2.2 The ferromagnetic transition as a paradigm

The first part of this chapter is devoted to recall the building blocks of the standard theory of second order phase transitions in ferromagnetic models. Our goal will be to follow strictly this kind of construction in the structural glass case. In fact we want to build a Landau theory that arises from the microscopic description of the system and deduce from it a set of mean field critical exponents. This is done in two steps. The first one is the study of the mean field theory of a spatial uniform order parameter and then considering small spatial variation of the order parameter to produce a gradient expansion from which we can extract the mean field correlation length and the region of validity of the mean field prediction through a Ginzburg criterion. Of course, in standard second order phase transition this is nothing but a preparatory work for a renormalization calculation of the critical exponents. In the structural or spin glass cases the renormalization group computations are very complicated and a final theoretical non-mean field description is lacking. We will

not go inside any renormalization group calculation so that we will not recall it for the ferromagnetic case. We will derive only the Gaussian predictions that can be extracted from the Landau action we will derive.

2.2.1 Landau theory and the mean field approximation

We want to study a microscopic system that present a ferromagnetic transition on lowering the temperature. The simplest model that has this kind of behavior is the ferromagnetic Ising model in $D > 1$ dimensions. The microscopic Hamiltonian that defines this system is

$$H[\sigma] = -\frac{1}{2D}\sum_{\langle i,j\rangle}\sigma_i\sigma_j \ . \tag{2.1}$$

Note that we have rescaled the coupling constant with the dimension D. The reason is that in the infinite dimensional limit we will have that each spin will act with all the others (the dimension cannot exceed the size of the system) so that we will have $D \sim N$ and we will recover the Curie-Weiss model.

The standard procedure is to start from this microscopic Hamiltonian and to construct the free energy as a function of the order parameter that is the magnetization $\phi_i = \langle\sigma_i\rangle$. To do this we introduce the free energy as a function of an external local magnetic field

$$W[h] = \log Z[h] = \log \sum_{\{\sigma_i=\pm 1\}} e^{-\beta H[\sigma]+\sum_i h_i\sigma_i} \ . \tag{2.2}$$

Here we have ignored some standard constant factors like the temperature in the expression above that are not important for the discussion that will follow. Taking a Legendre transform [141, 183, 47] with respect to the external magnetic field we obtain

$$\Gamma[\phi] = \sum_i h_i^*\phi_i - W[h^*] \ , \tag{2.3}$$

so that

$$e^{-\Gamma[\phi]} = \sum_{\{\sigma_i=\pm 1\}} e^{-\beta H[\sigma]+\sum_i h_i^*(\sigma_i-\phi_i)} \ , \tag{2.4}$$

where h^* is the solution of $\frac{dW[h]}{dh_i} = \phi_i$. The function $\Gamma[\phi]$ is the free energy of the system as a function of the magnetization field.

To see if a phase transition is present, we want to control the small ϕ behavior of $\Gamma[\phi]$. Now we assume that *that* $\Gamma[\phi]$ *is an analytic function of* ϕ *around* $\phi = 0$. We know that this is wrong in finite dimensions and at the critical point or below it but for the moment let us assume that this is true. Suppose that we consider a magnetization profile ϕ that is uniform in space and suppose that we expand $\Gamma[\phi]$ around $\phi = 0$. The symmetries of the Hamiltonian force us to have an expansion of the following form

$$\Gamma[\phi] = V\left\{\frac{1}{2}m_0^2\phi^2 + \frac{g}{4!}\phi^4 + \cdots\right\} \ , \tag{2.5}$$

which is the celebrated Landau free energy (here V is the volume of the system). A systematic way to compute the coefficients m_0^2 and g from the microscopic Hamiltonian is to perform an high temperature expansion [82]. For the D-dimensional

Ising model defined by 2.1 where the coupling constant is $J = 1/(2D)$ it gives at the leading order $m_0^2 = 1 - \beta$. If we consider more terms of the high temperature expansion we obtain and expansion of m_0^2 in powers of β.

Let us note that for the Ising model (2.1), the real expansion parameter is βJ, that is the temperature in units of the coupling constant. Because $J = 1/(2D)$, to obtain a finite limit $D \to \infty$, the expansion parameter must be $\beta/(2D)$ which means that the high temperature expansion is also a large dimension expansion around the $D \to \infty$ limit. To extract the equilibrium value of the magnetization that we denote with $\overline{\phi}$ we have to minimize the free energy $\Gamma[\phi]$. The high temperature expansion shows that m_0^2 vanishes as $m_0^2 \propto T/T_c - 1 = \epsilon$ when the critical temperature T_c is approached. For example, in $D = 3$ an accurate estimate of the critical temperature can be obtained by considering the cubic term in the small β expansion. When m_0^2 is negative, the magnetization is non-zero and it is given by $\overline{\phi} \sim |m_0^2|^{1/2} \sim \epsilon^{1/2}$ which gives the critical exponent β. The other critical exponents can be obtained in a similar way from the expansion 2.5.

2.2.2 Gradient expansion around the mean field solution

In the previous section we have recall the free energy of a ferromagnetic system for a spatial uniform magnetization. The next step is to try to compute a correlation length. This can appear only if we allow spatial fluctuation for the magnetization profile. In particular a uniform magnetization profile can be present only in systems where the space dimension plays no role. Such systems are exactly mean field systems or infinite dimensional systems.

Here we want to include the effect of spatial fluctuation. This is done by considering a gradient expansion around a slowly varying magnetization field. We will continue to assume that the free energy admits a regular expansion around $\phi = 0$. In order to keep the simplest possible set up we will perform a continuum limit of the model and we will denote with $\varphi(x)$ the continuum limit of the spin field σ_i and with $\phi(x) = \langle \varphi(x) \rangle$ the local average magnetization. The Landau free energy at the quadratic order becomes of the following standard form:

$$\Gamma[\phi] = \frac{1}{2} \int \mathrm{d}x \, \phi(x) \left(-\vec{\nabla}^2 + m_0^2 \right) \phi(x) \, . \tag{2.6}$$

The correlation function of the local magnetization profile is given by [183, 141]

$$G(x-y) = \langle \varphi(x) \varphi(y) \rangle = \left[\frac{\partial^2 \Gamma}{\partial \phi(x) \partial \phi(y)} \right]^{-1} \tag{2.7}$$

so that at the quadratic order it is given by

$$G_0(p) = \frac{1}{p^2 + m_0^2} \, , \qquad G_0(x) = \langle \varphi(x) \varphi(0) \rangle \sim_{x \to \infty} x^{\frac{4-D-3}{2}} e^{-m_0 x} \, , \tag{2.8}$$

which is often called the *bare propagator*[1]. This expression shows that the correlation length is $\xi = 1/m_0 \sim \epsilon^{-1/2}$ and the magnetic susceptibility is given by $\chi \propto G_0(p = 0) \sim \epsilon^{-1}$.

[1] The expression in real space can be obtained by noting that $1/(p^2 + m_0^2) = \int_0^\infty dt \, e^{-(p^2 + m_0^2)t}$

2.2.3 From the microscopic details to a coarse grained field theory

As already explained, the discussion we have made is based on the assumption that $\Gamma[\phi]$ can be expanded as an analytic function of ϕ. This assumption is valid at the mean field level (for example for the Curie-Weiss model it is exact because for this model $\Gamma[\phi]$ is also the large deviation function of the magnetization due to a saddle point calculation). However for finite dimensional systems it happens that critical fluctuation induce a singular behavior of $\Gamma[\phi]$ for small ϕ. This means that it is crucial to understand the limits of validity of the Landau expansion by studying the effect of the critical fluctuations on the mean field predictions.

One of the main issue for this program is that the definition of Γ that has been given in Eq. (2.4) is not very practical to make an expansion around the mean field theory. It would be better to have an effective action that is a functional integral over a continuous spin field $\varphi(x)$

$$e^{-\Gamma[\phi]} = \int \mathcal{D}\varphi \, e^{-S[\varphi]+\int \mathrm{d}x h(x)[\varphi(x)-\phi(x)]} \; . \tag{2.10}$$

However we must ensure that

1. the mean field can be obtained by a saddle point calculation of the functional integral so that at the mean field level $\Gamma[\phi] = S[\phi]$. This implies directly that $S[\varphi]$ must have the same form of the Landau action

$$S[\varphi] = \frac{1}{2}\int \mathrm{d}x \, \varphi(x)(-\nabla^2 + m_0^2)\varphi(x) + \frac{g}{4!}\int \mathrm{d}x \varphi^4(x) \; , \tag{2.11}$$

   so that in the mean field approximation we have Eqs. (2.5) and (2.6). Moreover this means that if we want include thermal fluctuations we can treat them by a systematic loop expansion around the mean field solution.

2. The coefficients m_0^2 and g that appear in the definition of $S[\varphi]$ must be *reasonable* approximation of the microscopic coefficients that can be deduced from the microscopic Hamiltonian so that at the mean field level we have a good approximation for the quantities we want compute and we expect that loop correction will improve their estimation when included. By doing this we can guarantee that the criterion of validity of mean field theory has a quantiative meaning for the original microscopic Hamiltonian $H[\sigma]$.

This means that we need to give an appropriate definition of $S[\varphi]$ in terms of a continuum field φ that satisfies the above requirements.

We can use many ways to build such a functional. The best one is given by a non-perturbative renormalization group approach [60]. In this case one can define a functional $\Gamma_\ell[\varphi(x)]$ by integrating the small-scale spin fluctuations on length scales smaller than ℓ, see e.g. [60, Eq. (28)]. Then one can defines a 'coarse-graining"

and changing variable to $y = t/x^2$. Then

$$G_0(x) \propto x^{2-D}\int_0^\infty dy \, e^{-(m_0 x)^2 y - \frac{1}{4y}} y^{-D/2} = x^{2-D} f(m_0 x) \; . \tag{2.9}$$

If $x \gg 1/m_0$, we can take a saddle point so that $f(z) \sim z^{(D-3)/2} e^{-z}$, from which Eq. (2.8) follows.

length ℓ_0 that is bigger than the lattice spacing (in such a way that the average over this size produce a reasonably smooth function) but smaller than the correlation length. In this way $\Gamma_\ell[\varphi(x)]$ is an analytic function of φ at small φ, because the singularity is only developed at the critical point for $\ell \to \infty$ [60]. This implies that Eq. (2.10) is almost exact with S replaced by Γ_{ℓ_0}. In this way we can develop Γ_{ℓ_0} around $\varphi = 0$ and use this as the bare action S in Eq. (2.10) to compute loop corrections. This strategy is very general and can be applied in many contexts. In the liquid case it is quite involved [147, 28] and we need something simpler.

A different and simpler way to obtain a reasonable form of $S[\varphi]$ is to use the high temperature expansion. Let us define Γ_k as the truncation at a finite order β^k of the high temperature expansion of Γ, as given in [82]. By construction we know that $\Gamma_k[\phi]$ is an analytic function of ϕ for any finite k, hence $\Gamma_k[\phi]$ cannot be a good approximation of $\Gamma[\phi]$ at the critical point and below it because in this region we know that $\Gamma[\phi]$ is not analytic. The non analyticity properties of $\Gamma[\phi]$ at the critical point can be detected by seeing that its high temperature expansion is divergent at the critical point. The assumption now is that $\Gamma_k[\varphi]$ *gives a good approximation for* $S[\varphi]$. In fact we see immediately that the two requirements above are satisfied if $S[\varphi] = \Gamma_k[\varphi]$. First of all at the saddle point level we have $\Gamma[\phi] = S[\phi] = \Gamma_k[\phi]$, and we already know that for $k = 1$ this is the correct mean field result, while for $k > 1$ we will obtain an "improved" mean field result. Moreover we have already said that the coefficients of $\Gamma_k[\phi]$ are, for large enough k, good estimates of the microscopic properties of the model (for example the critical temperature). It is important to say also that the high temperature expansion, at whatever order k, is only sensitive to the local physics up to a scale $\ell(k)$ that grows with k. This means that if we cut the high temperature series at a finite order k this should be equivalent to perform an integration over the microscopic degrees of freedom on a scale smaller than $\ell(k)$. This procedure can be applied to our case if we note that the high temperature expansion can be replaced by the low density virial series in the theory of liquids.

Having in mind this, we will use the prescription $S[\varphi] = \Gamma_k[\varphi]$ and then we will expand $S[\varphi]$ in the form of Eq. (2.11), and use it in the functional integral (2.10) to compute $\Gamma[\phi]$ in a loop expansion around mean field. Once the loop expansion is performed we will obtain some non-singular contributions to Γ which were taken in part in the bare action $S[\varphi] = \Gamma_k[\varphi]$. This means that this procedure can produce some "double counting" of non-singular contributions related to the short range physics. In Appendix A we discuss this double counting problem in the case of the ϕ^4 theory. Still, our aim here is to find a Ginzburg criterion that identifies the region where these singular loop corrections are small, and the mean field approximations remains correct: we find that if the Ginzburg criterion is formulated in terms of physical quantities, then double countings are irrelevant. This is shown in next section 2.2.4 and in Appendix A.

2.2.4 The Ginzburg criterion

Once we have a prescription to obtain an action from the microscopic details of the system we can see where the mean field results are valid. This can be done by looking at the first correction to the saddle point approximation that appears performing a loop expansion. We will follow strictly the derivation that is given

in [3, 4].

We start from the bare action

$$S[\varphi] = \frac{1}{2}\int \mathrm{d}x\, \varphi(x)(-\nabla^2 + m_0^2)\varphi(x) + \frac{g}{4!}\int \mathrm{d}x \varphi^4(x) \ . \tag{2.12}$$

We need here to consider explicitly the presence of an ultraviolet cutoff. It is natural, from the discussion we made, to consider the cutoff of the order of $\ell_0(k)$. To do the loop expansion we have to introduce the bare propagator

$$G_0(p) = \frac{1}{p^2 + m_0^2} \ . \tag{2.13}$$

This quantity gives the two point correlation function at the Gaussian level. If we include the one loop correction to it we will have [141]

$$G(p) = G_0(p) - \frac{g}{2}G_0(p)^2 \int^{\Lambda} \frac{\mathrm{d}q}{(2\pi)^D} G_0(q) \ . \tag{2.14}$$

If we consider the inverse of the propagator we have at one loop

$$G^{-1}(p) = G_0(p)^{-1} + \frac{g}{2}\int^{\Lambda} \frac{\mathrm{d}q}{(2\pi)^D} G_0(q) \ , \tag{2.15}$$

that can be seen also as a Dyson resummation of the tadpole diagrams, or as an inversion of the perturbation expansion to obtain directly the second derivative of the Legendre transform of the generating functional. From the physical point of view, $G^{-1}(p=0)$ is the "renormalized mass" or inverse magnetic susceptibility:

$$m_R^2 = G^{-1}(p=0) = m_0^2 + \frac{g}{2}\int^{\Lambda} \frac{\mathrm{d}q}{(2\pi)^D}\frac{1}{q^2+m_0^2} = m_0^2 + \frac{g}{2}\int^{\Lambda} \frac{\mathrm{d}q}{(2\pi)^D}\frac{1}{q^2+m_R^2} \ , \tag{2.16}$$

and we have assumed that the last equality holds at first order in g. As it is mandatory for this kind of calculations, we need to replace m_0 with m_R because the perturbative expansion must be done at a fixed distance from the true critical point [141]. The definition of the critical point is the temperature at which the susceptibility diverges or, in other words where $m_R^2 = 0$

$$m_0^2 = -\frac{g}{2}\int^{\Lambda} \frac{\mathrm{d}q}{(2\pi)^D}\frac{1}{q^2} \ . \tag{2.17}$$

Let us note that from the equation above we see that the shift of the critical temperature is divergent in the ultraviolet (UV divergent) for $D \geq 2$: in fact this is not a universal quantity and it depends on the microscopic details of the system we are studying. Let us define the distance from the critical point as

$$t = m_0^2 + \frac{g}{2}\int^{\Lambda} \frac{\mathrm{d}q}{(2\pi)^D}\frac{1}{q^2} \ , \tag{2.18}$$

then we can rewrite Eq. (2.16) as

$$t = m_R^2\left(1 - \frac{g}{2}\int^{\Lambda} \frac{\mathrm{d}q}{(2\pi)^D}\frac{1}{q^2(q^2+m_R^2)}\right) \ . \tag{2.19}$$

The importance of this relation is that it connects the inverse susceptibility to the distance from the true critical point.

The Ginzburg criterion states where the mean field result is not spoiled by the first loop correction, namely when $t = m_R^2$. We can have two cases

- if the dimension is less than 4, $D < 4$, then the first loop correction is UV convergent and infrared (IR) divergent. This means that we can send the ultraviolet cutoff to infinity so that we obtain

$$\begin{aligned} t =& m_R^2 \left(1 - \frac{g}{2}\int^{\infty} \frac{\mathrm{d}^D q}{(2\pi)^D} \frac{1}{q^2(q^2+m_R^2)}\right) \\ =& m_R^2 - \frac{g}{2}\, m_R^{D-2} \frac{\Omega_D}{(2\pi)^D} \int_0^{\infty} \mathrm{d}x\, x^{D-1} \frac{1}{x^2(x^2+1)} \end{aligned} \tag{2.20}$$

  and it is simple to see that the integral over x is finite. Moreover, because $D < 4$, the second term will be the dominant one if we are close enough to the critical point. The Ginzburg criterion is equivalent to impose that the first term dominates

$$1 \gg g\, m_R^{D-4} C_D = g\xi^{4-D} C_D = \mathrm{Gi}\, \xi^{4-D} \,, \tag{2.21}$$

  and here we used that if this condition is satisfied we are in the mean field region so that the correlation length is $\xi = 1/m_R$. In this way we can define the Ginzburg number $\mathrm{Gi} = gC_D$ that is a universal constant in this case. All this shows that the loop correction always spoil the mean field behavior if we are very close to the critical point and the Ginzburg number tells us at which length scale the fluctuations will be so important to destroy the validity of the mean field approximation $\xi \sim 1/(\mathrm{Gi})^{1/(4-D)}$.

- If $D \geq 4$ we clearly see that the first loop correction is UV divergent and IR convergent. This means that the Ginzburg criterion in this case cannot be universal and depends on the details of the regularization. If we fix the UV cutoff then the integral remains finite at $m_R^2 = 0$ and the mean field behavior is always correct:

$$t = m_R^2 \left(1 - \frac{g}{2}\int^{\Lambda} \frac{\mathrm{d}q}{(2\pi)^D} \frac{1}{q^4}\right) \,. \tag{2.22}$$

  However it is clear that the one loop correction give a strong renormalization on the relation between t and m_R^2. If we impose that this conditions are small we get

$$1 \gg \frac{g}{2}\int^{\Lambda} \frac{\mathrm{d}^D q}{(2\pi)^D} \frac{1}{q^2(q^2+m_R^2)} \tag{2.23}$$

  and this gives a Ginzburg criterion for a given UV cutoff Λ. When this condition is satisfied the mean field calculation is qualitatively and quantitatively correct. Because of the fact that the integral is upper-bounded by its value in $m_R = 0$ then, if $1 \gg gC\Lambda^{D-4}$, the condition above is always satisfied and the one loop contribution is small also at the critical temperature. However if $gC\Lambda^{D-4} \geq 1$ then we obtain that the Ginzburg criterion defines a region around the critical temperature where loop corrections spoil the mean field results.

2.3 Dynamical heterogeneities and replicas

Now we want to repeat what we did for the ferromagnetic case, in the more complicated situation of the glass transition. However there are many obstacles to this program:

1. In the glass transition problem, we need to introduce replicas to define a proper order parameter for the transition;

2. Differently from the ferromagnetic case, the nature of the order parameter is not a real number like the magnetization but it is a function $\widetilde{g}(x-y)$ that describes inter-replicas correlations. This means that if we want to define a scalar order parameter we need a smoothing function $f(x)$ that allows us to introduce $q \sim \int f(x)\widetilde{g}(x)$. We will require later that all the prediction of the theory on universal quantities must be independent on the smoothing function.

3. The nature of the dynamical glass transition is different from the ferromagnetic one because it is discontinuous in the order parameter. In fact at the transition point it jumps from zero to a finite value while in the ferromagnetic case, strictly at the transition point the magnetization is zero and it become continuously non zero when the temperature is decreased. This means that the nature of the transition is not connected to the instability of the high temperature solution but it is more similar to a spinodal point where a new low temperature solution first appears. As a consequence, we need to compute the effective free energy at values of the order parameter that are at a finite distance from its typical high temperature value. This means that if we resum a finite number of the high temperature expansion we cannot have access to the low temperature solution. To have have a good starting point we need in fact to resum an infinite number of terms and from that resummation we will be able to extract the first mean field results.

4. As a consequence of the previous points, we can argue that we will end up with a cubic field theory. However it is well known that due to nucleation, the theory is not really well defined in finite dimensions. This is not a big problem if we are interested in the mean field or one loop calculation but it will become a serious issue if we want to go beyond these results to construct a systematic epsilon expansion. We will not try to discuss this point here but this is of course one of the hot topic that must be studied for the next future [152].

In this section we will start with the first two points of the series above. We will give the basic definitions of dynamical heterogeneities and we will see how the problem of characterizing their behavior at the transition point can be addressed by replicas. However to start the discussion we need to introduce the order parameter of the dynamical glass transition and this will be done in Sec. 2.3.1. Then in Sec. 2.3.3 we will see how replicas provide a precise recipe to compute this order parameter and its correlation functions. Finally, in Sec. 2.3.4 we will define the full replicated theory from which we will start the Landau expansion around the glassy solution.

Because we are in the structural glass case we will always consider in this chapter a system of N particles inside a volume V. The particles interact with a pairwise potential $v(r)$ in a D dimensional space. The density field at point x in space and time t is defined as

$$\hat{\rho}(x,t) = \sum_{i=1}^{N} \delta(x - x_i(t)) \ . \tag{2.24}$$

For what will follow we will consider a generic dynamics that can be Newtonian or stochastic or a Langevin dynamics. In every case we will focus on equilibrium dynamics that means that the we will always start from an equilibrated configuration and we will evolve it according to the dynamical rules. In this way the thermal history of the system will be parametrized by the initial configuration of the particles $\{x_i(0)\}$ and by the dynamical noise. The latter can be given by a set of random initial velocities extracted from the Maxwell distribution if we are doing Newtonian dynamics or it will be the random forces if we are treating stochastic dynamics. In the same spirit of [74] we will separate the dynamical average in two parts. We will denote with $\langle \bullet \rangle$ the average over the dynamical noise at fixed initial condition and with $\mathbf{E}[\bullet]$ the average over the initial condition. This means that if we combine the two averages we will obtain the equilibrium average. For the density we will have

$$\rho = \mathbf{E}[\langle \hat{\rho}(x,t) \rangle] \ . \tag{2.25}$$

2.3.1 The dynamical order parameter: two point functions

As we have seen in the introductory chapter, the dynamical glass transition is marked by an (apparent) divergent relaxation time for the fluctuations of the density field. This fluctuations are said to be frozen in the glass phase. This means that the transition can be studied by looking directly at the correlation functions of the density.

Let us take the density profile at a given space point x but for two different times, let's say time 0 and time $t > 0$. The density profile will be respectively $\rho(x,0)$ and $\rho(x,t)$. Then we can introduce the following quantity

$$\begin{aligned} \hat{C}(r,t) &= \int \mathrm{d}x f(x) \hat{\rho}\left(r + \frac{x}{2}, t\right) \hat{\rho}\left(r - \frac{x}{2}, 0\right) \\ &= \sum_{ij} \delta\left(r - \frac{x_i(t) + x_j(0)}{2}\right) f(x_i(t) - x_j(0)) \ . \end{aligned} \tag{2.26}$$

that tells us how the two configurations at the two different times are similar around the point r. This quantity plays the same role of the overlap in spin glass physics. As we have said before, the function $f(x)$ is nothing but a short ranged smoothing function that is normalized in such a way that $\int \mathrm{d}x f(x) = 1$. For example we can choose $f(x) = \theta(a - |x|)/V_d(a)$, where $V_d(a)$ is the volume of a sphere of radius a. If a is much smaller than the typical inter particle distance and if the time t is not so far from zero, then we can expect that $f(x_i(t) - x_j(0))$ vanishes unless $i = j$. This means that

$$\hat{C}(r,t) \approx \sum_{i} \delta\left(r - \frac{x_i(t) + x_i(0)}{2}\right) f(x_i(t) - x_i(0)) \tag{2.27}$$

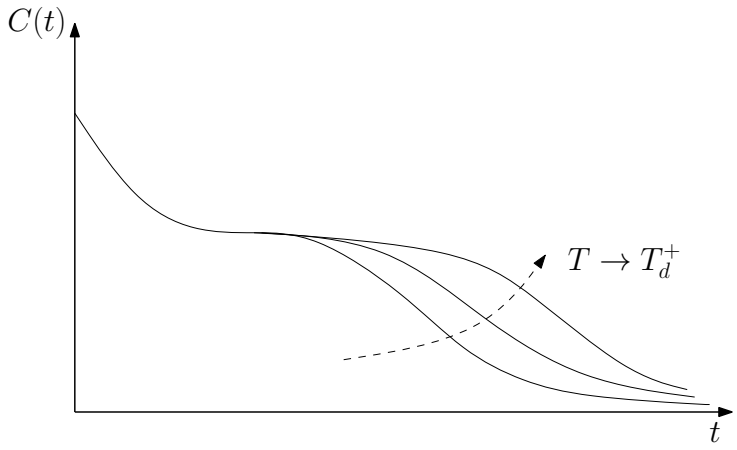

Figure 2.1. The typical shape of $C(t)$ when the dynamical glass transition point is approached. The length of the plateau is diverging as the temperature is lowered towards the dynamical one.

and therefore we have the physical interpretation of $C(r,t)$ as a "mobility" field because it counts how many particles that are around r have moved less then a in time t. More simply we can take Eq. (2.27) as the definition of a *self* two point correlation function. Let us note that the definition of $C(r,t)$ is dependent on the smoothing function we have chosen. However in what will follow, we will show that as far as critical properties are concerned, the particular form of f will be irrelevant.

Let us now introduce

$$C(t) = V^{-1} \int \mathrm{d}r \mathbf{E}[\langle \hat{C}(r,t) \rangle] - \rho^2 \tag{2.28}$$

that is the spatial and thermal average of the connected correlation function of the density. What happens in general is that when the dynamical transition point T_d is approached, the typical picture of $C(t)$ is the one represented in Fig. 2.1 so that it will display the standard two steps relaxation. This kind of behavior is described by a first fast "β-relaxation" occurring on short timescales up to the plateau and by a much slower "α-relaxation" that range from the plateau to zero [84].

As we have said in the introductory chapter if we are in a region of times such that $C(t)$ is close to its plateau value we can fit the shape of the correlation function with two power laws

$$\begin{aligned} C(t) &\sim C_\mathrm{d} + \mathcal{A}\, t^{-a} \qquad \text{last part of the } \beta\text{-relaxation} \\ C(t) &\sim C_\mathrm{d} - \mathcal{B}\, t^{b} \qquad \text{beginning of the } \alpha\text{-relaxation} \end{aligned} \tag{2.29}$$

Moreove if we define the α-relaxation time by $C(\tau_\alpha) = C(0)/e$ than we will see an apparent divergence

$$\tau_\alpha \sim |T - T_\mathrm{d}|^{-\gamma} \tag{2.30}$$

As we have seen in the introduction, this kind of behavior is well predicted by the mode-coupling theory [84]. At this level, all the exponents are related to the

exponent parameter

$$\lambda = \frac{\Gamma(1-a)^2}{\Gamma(1-2a)} = \frac{\Gamma(1+b)^2}{\Gamma(1+2b)} \ , \qquad \gamma = \frac{1}{2a} + \frac{1}{2b} \ , \tag{2.31}$$

In low dimensions, a rapid crossover to a different regime dominated by activation is observed and the divergence at T_d is avoided; however, the power-law regime is the more robust the higher the dimension [44, 43] or the longer the range of the interaction [92].

2.3.2 Fluctuations of the order parameter and four point functions

As in the ferromagnetic case, we expect that on approaching the dynamical glass transition point, the fluctuations of the order parameter will increase. In recent times, it has been seen both in numerical simulation and at the experimental and theoretical level [71, 61, 13, 12] that the dynamical slowing down, on approaching $T_{\rm d}$ is accompanied by a growing heterogeneity of the local relaxation. This means that the correlations $\hat{C}(r,t)$ will have stronger and stronger fluctuations when the dynamical temperature is approached.

The entity of such fluctuations can be quantified through the introduction of an appropriate correlation function

$$G_4(r,t) = \mathbf{E}[\langle \hat{C}(r,t)\hat{C}(0,t)\rangle] - \mathbf{E}[\langle \hat{C}(r,t)\rangle]\mathbf{E}[\langle \hat{C}(0,t)\rangle] \ . \tag{2.32}$$

Note that this is a four point correlation function with respect to the density field (in the standard ferromagnetic case the role played by G_4 is given by the correlation function of the local magnetization which is a two point correlation function). We expect that this function will decay as $G_4(r,t) \sim \exp(-r/\xi(t))$ where we call $\xi(t)$ the dynamical correlation length. The shape of $\xi(t)$ will be the following: it will grow at the end of the β-regime and it will have a maximum $\xi = \xi(t \sim \tau_\alpha)$ whose height will diverge (apparently) with a power law when the temperature approaches the dynamical point. Both in standard MCT [84] and in its extensions [22, 19, 14, 15, 162, 163] we can study this kind of behavior to extract quantitative predictions on the critical exponents .

If we play a little bit with the two different averages, the one over the initial condition of the dynamics, and the other over the thermal history, we are able to define also the following four point correlation function [74]

$$G_{th}(r,t) = \mathbf{E}\left[\langle \hat{C}(r,t)\hat{C}(0,t)\rangle - \langle \hat{C}(r,t)\rangle\langle \hat{C}(0,t)\rangle\right] \ . \tag{2.33}$$

We say that this function describes the *isoconfigurational* fluctuations of the two point correlations, i.e. the fluctuations due to the noise of the dynamical process at fixed initial condition. Moreover to enhance the effect of the initial conditions we could define the following correlation function

$$G_{het}(r,t) = \mathbf{E}\left[\langle \hat{C}(r,t)\rangle\langle \hat{C}(0,t)\rangle\right] - \mathbf{E}\left[\langle \hat{C}(r,t)\rangle\right]\mathbf{E}\left[\langle \hat{C}(0,t)\rangle\right] \ . \tag{2.34}$$

For each of these correlations, we can define the corresponding susceptibility

$$\begin{aligned}
\chi_4(t) &= \int \mathrm{d}r G_4(r,t) = \mathbf{E}\left[\left\langle\left(\frac{1}{V}\int \mathrm{d}r\hat{C}(r,t)\right)^2\right\rangle\right] - \mathbf{E}\left[\left\langle\frac{1}{V}\int \mathrm{d}r\hat{C}(r,t)\right\rangle\right]^2 , \\
\chi_{th}(t) &= \int \mathrm{d}r G_{th}(r,t) = \mathbf{E}\left[\left\langle\left(\frac{1}{V}\int \mathrm{d}r\hat{C}(r,t)\right)^2\right\rangle - \left\langle\frac{1}{V}\int \mathrm{d}r\hat{C}(r,t)\right\rangle^2\right] \\
\chi_{het}(t) &= \int \mathrm{d}r\, G_{het}(r,t) = \mathbf{E}\left[\left\langle\frac{1}{V}\int \mathrm{d}r\hat{C}(r,t)\right\rangle^2\right] - \mathbf{E}\left[\left\langle\frac{1}{V}\int \mathrm{d}r\hat{C}(r,t)\right\rangle\right]^2 .
\end{aligned} \tag{2.35}$$

so that

$$\chi_4(t) = \chi_{het}(t) + \chi_{th}(t) . \tag{2.36}$$

2.3.3 The key connection between replicas and dynamics

As we have seen in the introductory chapter, we know that replicas can be employed to describe the dynamical glass transition. In fact according to the mean field picture the dynamical transition is nothing but the signature of the appearance of an exponential number of metastable states. In this way the β regime is identified with the dynamics "inside a metastable state", while the α regime is identified with "transitions between different states". This picture will be also clarified in the next chapter. In what follows we will give the replica prescription to compute the dynamical averages.

Let us start from the following two quantities

$$\begin{aligned}
\langle\hat{C}(r,t\to\infty)\rangle &= \int \mathrm{d}x f(x)\left\langle\hat{\rho}\left(r+\frac{x}{2}\right)\right\rangle_{\mathrm{m}}\left\langle\hat{\rho}\left(r-\frac{x}{2}\right)\right\rangle_{\mathrm{m}} , \\
\mathbf{E}[\langle\hat{C}(r,t\to\infty)\rangle] &= \int \mathrm{d}x f(x)\overline{\left\langle\hat{\rho}\left(r+\frac{x}{2}\right)\right\rangle_{\mathrm{m}}\left\langle\hat{\rho}\left(r-\frac{x}{2}\right)\right\rangle_{\mathrm{m}}} .
\end{aligned} \tag{2.37}$$

The physical meanings of the two averages that we have introduced on the right here are the following. If we fix the initial condition, then the infinite time limit of the equilibrium dynamics (if the initial condition is a typical equilibrium condition) is given by the average over a replicated measure that provides the statistical typical aspects of the metastable states in which the dynamics is trapped. This average is denoted with $\langle\bullet\rangle_{\mathrm{m}}$. The average over the initial condition can be performed in a second time and we denote it with an overline. Note that here the initial condition plays the role of a quenched disorder. The meaning of the average over the initial condition is that in this way we are averaging over the possible metastable states in which the dynamics can remain trapped in.

If we apply this line of reasoning to the four point function that we have intro-

duced in the last section we obtain

$$\begin{aligned} G_4(r,t\to\infty) &= \int \mathrm{d}x\mathrm{d}y\, f(x)f(y)\,[\overline{\langle\hat\rho(r-x/2)\hat\rho(-y/2)\rangle_{\mathrm{m}}\langle\hat\rho(r+x/2)\hat\rho(y/2)\rangle_{\mathrm{m}}}] \\ &\quad - \mathbf{E}[\langle\hat C(r,t\to\infty)\rangle]\mathbf{E}[\langle\hat C(0,t\to\infty)\rangle]\ , \\ G_{th}(r,t\to\infty) &= \int \mathrm{d}x\mathrm{d}y\, f(x)f(y)\,[\overline{\langle\hat\rho(r-x/2)\hat\rho(-y/2)\rangle_{\mathrm{m}}\langle\hat\rho(r+x/2)\hat\rho(y/2)\rangle_{\mathrm{m}}}] \\ &\quad - \int \mathrm{d}x\mathrm{d}y\, f(x)f(y)\,[\overline{\langle\hat\rho(r-x/2)\rangle_{\mathrm{m}}\langle\hat\rho(-y/2)\rangle_{\mathrm{m}}\langle\hat\rho(r+x/2)\hat\rho(y/2)\rangle_{\mathrm{m}}}]\ . \end{aligned} \tag{2.38}$$

We will not discuss G_{het} because in the following we will not be interested in it even if the formalism can be easily extended to compute also this quantity. The form of the second term in the expression for $G_{th}(r,t\to\infty)$ is due to the fact that the densities at time zero come from the same initial equilibrium condition so that they are correlated but then they evolve independenty so that the densities at time $t\to\infty$ become uncorrelated. This means that we can study the infinite time limit of equilibrium dynamics by means of a static replica prescription [100, 133, 127]. The great advantage of the replica method is that we can compute such averages without solving the dynamics. Let us see how.

The method we will describe here is a development of the potential method [69] that will be deeply studied in the next chapter, with the real replica method [133]. We introduce for every particle in the system, $m-1$ additional particles identical to the first ones in such a way that we have m replicas for any given particle. This means that now we have a replicated system and we address each replica by a label $a=1,\dots,m$. We will allow different replicas to interact with a potential $v_{ab}(r)$. If the two replicas are the same $a=b$ then $v_{aa}(r)=v(r)$ so that particles in the same replica interact through the microscopic interaction potential. If the particles belong to different replicas $a\neq b$ then the potential $v_{ab}(r)$ will be an infinitesimal attractive potential. The role of this attractive potential is the one of a symmetry breaking field. We expect that if we are at the dynamical point or below it this infinitesimal coupling is enough to let all the replicas fall in the same metastable state. However the crucial observation is that all the replicas in the same state will be uncorrelated when $v_{a\neq b}\to 0$. Because we have different replicas, it is mandatory to introduce also a replicated version of the density field so that we can define

$$\begin{aligned} \hat\rho_a(x) &= \sum_{i=1}^{N}\delta(x-x_i^a)\ , \\ \hat\rho^{(2)}_{ab}(x,y) &= \hat\rho_a(x)\hat\rho_b(y)-\hat\rho_a(x)\delta_{ab}\delta(x-y)\ . \end{aligned} \tag{2.39}$$

where x_i^a is intended to be the position of the particle i of the replica a. As it happens in schematic models we can detect the dynamical transition by looking at the two point correlation functions when the inter-replica potential goes to zero and in the limit $m\to 1$ so that the original model is reproduced [133, 127]. We denote by $\langle\bullet\rangle_{\mathrm{r}}$ the equilibrium average for the replicated system under the conditions stated above.

All these considerations lead to the following dictionary

- replace $\langle \bullet \rangle_{\rm r} = \overline{\langle \bullet \rangle_{\rm m}}$,
- factorize the averages $\langle \bullet \rangle_{\rm m}$ when they involve different replicas, and
- remove the replica indexes.

Let us consider the density field for any spatial argument and for $a \neq b$; for example we have

$$\langle \hat{\rho}_a \hat{\rho}_b \rangle_{\rm r} = \overline{\langle \hat{\rho}_a \hat{\rho}_b \rangle_{\rm m}} = \overline{\langle \hat{\rho}_a \rangle_{\rm m} \langle \hat{\rho}_b \rangle_{\rm m}} = \overline{\langle \hat{\rho} \rangle_{\rm m} \langle \hat{\rho} \rangle_{\rm m}} \tag{2.40}$$

that is one of the averages that we want to compute. Another slightly more complex example is the following. Assuming that different letters mean different values of the replica indices we have:

$$\begin{aligned} \langle \hat{\rho}_a \hat{\rho}_a \hat{\rho}_b \rangle_{\rm r} &= \overline{\langle \hat{\rho}_a \hat{\rho}_a \hat{\rho}_b \rangle_{\rm m}} = \overline{\langle \hat{\rho}_a \hat{\rho}_a \rangle_{\rm m} \langle \hat{\rho}_b \rangle_{\rm m}} = \overline{\langle \hat{\rho} \hat{\rho} \rangle_{\rm m} \langle \hat{\rho} \rangle_{\rm m}} \ , \\ \langle \hat{\rho}_a \hat{\rho}_b \hat{\rho}_c \rangle_{\rm r} &= \overline{\langle \hat{\rho}_a \hat{\rho}_b \hat{\rho}_c \rangle_{\rm m}} = \overline{\langle \hat{\rho}_a \rangle_{\rm m} \langle \hat{\rho}_b \rangle_{\rm m} \langle \hat{\rho}_c \rangle_{\rm m}} = \overline{\langle \hat{\rho} \rangle_{\rm m} \langle \hat{\rho} \rangle_{\rm m} \langle \hat{\rho} \rangle_{\rm m}} \end{aligned} \tag{2.41}$$

At this point we can introduce a space dependent order parameter

$$\hat{q}_{ab}(r) = \int {\rm d}x \, f(x) \, \hat{\rho}^{(2)}_{ab}(r - x/2, r + x/2) \ , \tag{2.42}$$

and the two-replica correlation function

$$\begin{aligned} C_{ab}(r) &= \langle \hat{q}_{ab}(r) \rangle_{\rm r} - \rho^2 \\ &= \int {\rm d}x \ f(x) [\langle \hat{\rho}^{(2)}_{ab}(r - x/2, r + x/2) \rangle_{\rm r} - \langle \hat{\rho}_a(r - x/2) \rangle_{\rm r} \langle \hat{\rho}_b(r + x/2) \rangle_{\rm r}] \ , \end{aligned} \tag{2.43}$$

where $f(x)$ is once again an arbitrary short ranged function and the results that we will obtain about the critical properties will be independent on its specific form. To detect the dynamical transition, we are interested in the functions just defined for $a \neq b$. Using the dictionary between averages we obtain

$$C_{ab}(r) = \int {\rm d}x \, f(x) \, [\overline{\langle \hat{\rho}_a(r - x/2) \rangle_{\rm m} \langle \hat{\rho}_b(r + x/2) \rangle_{\rm m}}] - \rho^2 \ . \tag{2.44}$$

Because of replica equivalence inside a metastable state, we can drop out the replica indices so that we get

$$C_{ab}(r) = \int {\rm d}x \, f(x) \, [\overline{\langle \hat{\rho}(r - x/2) \rangle_{\rm m} \langle \hat{\rho}(r + x/2) \rangle_{\rm m}} - \rho^2 = \mathbf{E}[\langle \hat{C}(r, t \to \infty) \rangle] - \rho^2 \ . \tag{2.45}$$

The above equation is crucial because it gives the replica prescription to compute the long time limit of the dynamics inside a metastable state.

Using the same strategy we can give the replica prescription to compute the long time limit of the four point correlation functions. Let us define the correlation matrix of the order parameter (for $a \neq b$ and $c \neq d$):

$$G^{(f)}_{ab;cd}(r) = \langle \hat{q}_{ab}(r) \hat{q}_{cd}(0) \rangle_{\rm r} - \langle \hat{q}_{ab}(r) \rangle_{\rm r} \langle \hat{q}_{cd}(0) \rangle_{\rm r} \ ; \tag{2.46}$$

The superscript f only reminds us about the dependence of this matrix on the smoothing function that we used to define the matrix $\hat{q}$. By doing the same steps that we did for the two point functions we have

$$\begin{aligned} G^{(f)}_{ab;cd}(r) = \int \mathrm{d}x\mathrm{d}y\, f(x)f(y)\, [\overline{\langle \hat{\rho}_a(r-x/2)\hat{\rho}_b(r+x/2)\hat{\rho}_c(-y/2)\hat{\rho}_d(y/2)\rangle_{\mathrm{m}}}] \\ - \mathbf{E}[\langle \hat{C}(r, t\to\infty)\rangle]\mathbf{E}[\langle \hat{C}(0, t\to\infty)\rangle] \ ; \end{aligned} \tag{2.47}$$

we see that the first term in the average in the r.h.s. can be factorized over different replica indices. In this way we obtain the final replica prescription for the four point correlation function in the long time limit

$$\begin{aligned} G_4(r, t\to\infty) &= G^{(f)}_{ab;ab}(r) \ , \\ G_{th}(r, t\to\infty) &= G^{(f)}_{ab;ab}(r) - G^{(f)}_{ab;ac}(r) \ . \end{aligned} \tag{2.48}$$

2.3.4 The replicated free energy for structural glasses

Here we introduce the replicated free energy that will play the major role in the following. We use the standard notation of liquid theory as in [89] and we adapt it to a replicated system. Let us take the grand canonical partition function of a system of particles in D-dimensions that interact with a pairwise potential v. The chemical potential is denoted by μ and we introduce also an external field Ψ that is useful to obtain correlation functions by derivatives. The logarithm of the partition function is given by

$$\begin{aligned} &W[\nu, w] = \ln Z[\nu, w] \\ &= \ln \sum_{N=0}^{\infty} \frac{1}{N!} \int \left[\prod_{i=1}^{N} \mathrm{d}x_i\right] \exp\left(\frac{1}{2}\int \mathrm{d}x\mathrm{d}y\ \hat{\rho}^{(2)}(x,y)w(x,y) + \int \mathrm{d}x\ \nu(x)\hat{\rho}(x)\right) \end{aligned} \tag{2.49}$$

where the fields that appear in the above expression are defined by

$$\begin{aligned} \hat{\rho}(x) &= \sum_{i=1}^{N} \delta(x - x_i) \ , \\ \hat{\rho}^{(2)}(x,y) &= \sum_{i=1}^{N}\sum_{j\neq i} \delta(x-x_i)\delta(y-x_j) = \hat{\rho}(x)\hat{\rho}(y) - \hat{\rho}(x)\delta(x-y) \ . \end{aligned} \tag{2.50}$$

The expressions above are completely general. The microscopic characteristics of the system are encrypted in

$$\begin{aligned} \nu(x) &= \beta\mu - \beta\Psi(x) \ , \\ w(x,y) &= -\beta v(x,y) \ . \end{aligned} \tag{2.51}$$

By following the discussion above, we will introduce a replicated version of the system [133, 127]. The interaction between different replicas will be $w_{ab} = -\beta v_{ab}$

so that the logarithm of the replicated gran canonical partition function will be

$$W[\{\nu_a\},\{w_{ab}\}] = \ln Z[\{\nu_a\},\{w_{ab}\}] = \ln \sum_{N=0}^{\infty} \frac{1}{(N!)^m} \int \left(\prod_{a=1}^{m} \prod_{i=1}^{N} \mathrm{d}x_i^{(a)} \right) \times \exp\left(\frac{1}{2} \sum_{a,b}^{1,m} \int \mathrm{d}x\mathrm{d}y \; \hat{\rho}_{ab}^{(2)}(x,y) w_{ab}(x,y) + \sum_{a=1}^{m} \int \mathrm{d}x \; \nu_a(x) \hat{\rho}_a(x) \right) . \tag{2.52}$$

The replicated one and two point density fields are defined as in 2.39. For simplicity, in the following we will use the shorthand notations (when there is no ambiguity):

1. for spatial positions we will often write $f(1) \to f(x_1)$, $f(1,2) \to f(x_1,x_2)$;
2. in a similar way we will use $\int \mathrm{d}x_1 \to \int_1$;
3. ignore the space and replica indices to denote $\hat{\rho} \to \{\hat{\rho}_a(1)\}$, $\hat{\rho}^{(2)} \to \{\hat{\rho}_{ab}^{(2)}(1,2)\}$;

and similarly for all the complex quantities that can be written in the same way.

The dynamical glass transition can be studied by looking at the behavior of $\hat{\rho}$ and $\hat{\rho}^{(2)}$ when the control parameter (the temperature or the average density) is changed. To stress this, as in standard phase transition, it is very convenient to produce the Legendre transform with respect to these fields [137, 57, 47]. If we denote with ρ and $\rho^{(2)}$ the averages of $\hat{\rho}$ and $\hat{\rho}^{(2)}$ then we obtain [127]

$$\Gamma[\rho,\rho^{(2)}] = \sum_a \int \rho_a(1)\nu_a^*(1) + \frac{1}{2} \sum_{a,b} \int_{1,2} \rho_{ab}^{(2)}(1,2) w_{ab}^*(1,2) - W[\nu^*,w^*] \; , \tag{2.53}$$

where ν^* and w^* are the solution of the two equations

$$\left.\frac{\delta W[\nu,w]}{\delta \nu_a(1)}\right|_{\nu^*,w^*} = \rho_a(1) \quad \text{and} \quad \left.\frac{\delta W[\nu,w]}{\delta w_{ab}(1,2)}\right|_{\nu^*,w^*} = \frac{1}{2}\rho_{ab}^{(2)}(1,2). \tag{2.54}$$

The advantage in producing the Legendre transform is that we can safely take the limit in which the interaction between different replicas goes to zero and we can then search for a non trivial glassy solution in replica space. In [137], Morita and Hiroike showed that the Legendre transform can be written in the following way

$$\Gamma[\rho,\rho^{(2)}] = \Gamma_{\mathrm{id}}[\rho,\rho^{(2)}] + \Gamma_{\mathrm{ring}}[\rho,\rho^{(2)}] + \Gamma_{\mathrm{2PI}}[\rho,\rho^{(2)}] \; , \tag{2.55}$$

where

$$\begin{aligned} \Gamma_{\mathrm{id}}[\rho,\rho^{(2)}] &= \sum_a \int_1 \rho_a(1) \left[\ln \rho_a(1) - 1\right] \\ &\quad + \frac{1}{2} \sum_{a,b} \int_{1,2} \left[\rho_{a,b}^{(2)}(1,2) \ln\left(\frac{\rho_{a,b}^{(2)}(1,2)}{\rho_a(1)\rho_b(2)} \right) - \rho_{a,b}^{(2)}(1,2) + \rho_a(1)\rho_b(2) \right] \; , \\ \Gamma_{\mathrm{ring}}[\rho,\rho^{(2)}] &= \frac{1}{2} \sum_{n\geq 3} \frac{(-1)^n}{n} \sum_{a_1,\ldots,a_n} \int_{1,\ldots,n} \rho_{a_1}(1) h_{a_1 a_2}(1,2) \cdots \rho_{a_n}(n) h_{a_n a_1}(n,1) \end{aligned} \tag{2.56}$$

and we have introduced

$$h_{ab}(1,2) = \frac{\rho^{(2)}_{a,b}(1,2)}{\rho_a(1)\rho_b(2)} - 1 \ . \tag{2.57}$$

The term $\Gamma_{2\mathrm{PI}}$ denotes the sum of all the two-particle irreducible diagrams whose precise definition is given in [137, 57, 47]. We will not enter in the precise study of this term because for the following discussion its particular form will not be relevant. In particular when we will do practical calculations we will always neglect it. However it must be taken under consideration for future works in the case in which we want to improve over the approximation we will use.

As it is usual in standard liquid theory, we introduce the direct correlation function in order to simplify our equations. However here we have the necessity of a replicated direct correlation function $c_{ab}(1,2)$ defined through a replicated version of the Ornstein-Zernike (OZ) equations

$$h_{ab}(1,2) = c_{ab}(1,2) + \sum_c \int_3 h_{ac}(1,3)\rho_c(3)c_{cb}(3,2) \ . \tag{2.58}$$

Of course, the solution of $c_{ab}(1,2)$ in terms of $h_{ab}(1,2)$ can always be obtained in terms of a series expansion

$$c_{ab}(1,2) = \sum_{n\neq 1}(-1)^n \sum_{a_2,\ldots,a_{n-1}} \int_{3,\ldots,n-1} h_{aa_1}(1,3)\rho_{a_1}(3)h_{a_1a_2}(3,4)\cdots \tag{2.59}$$

$$\cdots \rho_{a_{n-1}}(n-1)h_{a_{n-1}b}(n-1,2). \tag{2.60}$$

Finally, the free energy is given by computing Γ on the solutions of the saddle point equation [137, 57, 47]

$$\left.\frac{\delta\Gamma[\rho,\rho^{(2)}]}{\delta\rho^{(2)}_{ab}(1,2)}\right|_{\overline{\rho}_{ab}} = \frac{1}{2}w_{ab}(1,2). \tag{2.61}$$

An analogous equation can be written for the saddle point value of $\rho_a(1)$ in terms of the chemical potential. However here we are interested in a situation in which $\rho_a(1) = \rho$ so that we will not consider this equation and we will directly put the one point density function to a constant value. Actually, the value of the density will play the role of the control parameter for athermal systems like hard spheres. Moreover we look for a solution for the two point density correlator that has a 1RSB structure that in this real replicas calculation is equivalent to require that it is of the form

$$\overline{\rho^{(2)}}_{ab}(1,2) = \delta_{ab}\rho^2 g(1,2) + (1-\delta_{ab})\rho^2\tilde{g}(1,2) \tag{2.62}$$

The dynamical transition is signaled by the following fact. In the high temperature (or low density) phase, the saddle point value for $\tilde{g}$ is trivially one. However once we cross the dynamical point a non trivial solution for $\tilde{g}$ appears. Moreover we want to underline that the 1RSB structure is expected to be valid only in a first approximation. We know that it gives the exact result only for few schematic models (the p-spin spherical model) but for the general case we have to expect that at some poin fullRSB effects may become important. This is shown for example in

chapter 4 where we will see that a Gardner transition can be present in the low temperature (high density) region. However, in general, what happens is that fullRSB effects may be relevant for the equilibrium low temperature phase well below T_d and for the off equilibrium dynamics but as we look to the physics around T_d and equilibrium dynamics, fullRSB effects should not appear.

2.4 Landau expansion of the free energy around the glassy solution

As explained in the previous sections, we want to produce a Landau expansion for the free energy in such a way that we are able not only to obtain the mean field results, but also to see where they are valid. The first important difference with respect to the case of the ferromagnetic model is in the fact that here the order parameter is not a number (the magnetization) but it is a non trivial function $\widetilde{g}(x_1 - x_2)$. The second crucial difference is that the transition is of the *random first order* type, namely it is a second order phase transition from the thermodynamic point of view but the order parameter jumps discontinuously at the dynamical point. The main consequence is that we cannot approach the transition from the high temperature (low density) region but we must be in the low temperature phase to produce an expansion of the free energy around the non trivial glassy solution. In what will follow we will always assume that we are slightly in the glass phase so that $T < T_d$ (or $\rho > \rho_d$) where $\widetilde{g}$ is non-trivial. Then we will study the limit in which $\epsilon = T_d - T \to 0^+$.

In Sec. 2.4.1 we introduce an appropriate scalar order parameter and perform a Landau expansion of the free energy for small deviations of the order parameter around the critical point. In Sec. 2.4.2 we show how this expansion can be used to compute the MCT exponents, in particular the exponent parameter λ, following [29]. In Sec. 2.4.3 we perform a more detailed study of the mass matrix, i.e. the quadratic term of the expansion. In Sec. 2.4.4 we use this to show that the value of the MCT critical exponents do not depend on the details of the definition of the scalar order parameter; as a side product we obtain a much simpler expression for these exponents. Interestingly enough we will see in the next chapter the expression for the exponent parameter in the Hypernetted Chain approximation can be obtained also following a different strategy.

2.4.1 Free energy for a uniform field

Let us consider again the order parameter $C_{ab}(r)$, defined in Eq. (2.43). We want to produce the free energy as a function of this order parameter when we restrict to the case in which it is a constant over space. We can do this by just maximizing the free energy with respect to $\rho^{(2)}$ provided that C_{ab} is given by (2.43). We can enforce this through a Lagrange multiplier ε_{ab}:

$$\Gamma[C_{ab}] = \max_{\rho^{(2)}, \varepsilon_{ab}} \left[\Gamma[\rho, \rho^{(2)}] - \sum_{a \neq b} \varepsilon_{ab} \left(V C_{ab} - \int_{1,2} f(1,2)[\rho^{(2)}_{ab}(1,2) - \rho_a(1)\rho_b(2)] \right) \right] . \tag{2.63}$$

If $\varepsilon_{ab} = 0$, because we are in the glass phase, the free energy will be maximized by $\rho^{(2)} = \overline{\rho^{(2)}}$, Eq. (2.62), that will correspond to some value of $\overline{C}_{ab}$. We now want to make an expansion around this reference value. Let us define $\Delta\rho^{(2)} = \rho^{(2)} - \overline{\rho^{(2)}}$ and $\Delta C_{ab} = C_{ab} - \overline{C}_{ab}$ the displacements from this reference value. Moreover let us use a global index to address both replica and space indices $A = \{a, b, 1, 2\}$, $B = \{c, d, 3, 4\}$. We also use Einstein's convention in which repeated indices are summed.

Let us expand $\Gamma[\rho, \rho^{(2)}]$ around the reference solution: we get

$$\begin{aligned}\Delta\Gamma[\Delta C_{ab}] = \max_{\Delta\rho^{(2)},\ \varepsilon_{ab}} \Bigg\{ & \frac{1}{2}\frac{\delta^2\Gamma[\rho, \overline{\rho^{(2)}}]}{\delta\rho^{(2)}_A \delta\rho^{(2)}_B}\Delta\rho^{(2)}_A \Delta\rho^{(2)}_B \\ & + \frac{1}{6}\frac{\delta^3\Gamma[\rho, \overline{\rho^{(2)}}]}{\delta\rho^{(2)}_A \delta\rho^{(2)}_B \delta\rho^{(2)}_C}\Delta\rho^{(2)}_A \Delta\rho^{(2)}_B \Delta\rho^{(2)}_C \\ & - \sum_{a\neq b}\varepsilon_{ab}\left(V\Delta C_{ab} - \int_{1,2} f(1,2)\Delta\rho^{(2)}_{ab}(1,2)\right)\Bigg\} ,\end{aligned} \tag{2.64}$$

and it must be assumed that all the derivatives are computed on the reference solution. We introduce now the mass matrix and the cubic interaction term

$$\begin{aligned} M_{AB} &= \frac{\delta^2\Gamma[\rho, \overline{\rho^{(2)}}]}{\delta\rho^{(2)}_A \delta\rho^{(2)}_B} , \\ L_{ABC} &= \frac{\delta^3\Gamma[\rho, \overline{\rho^{(2)}}]}{\delta\rho^{(2)}_A \delta\rho^{(2)}_B \delta\rho^{(2)}_C} , \end{aligned} \tag{2.65}$$

Moreover we denote $\varepsilon_A = \varepsilon_{ab} f(1,2)$ and we assume $\varepsilon_{aa} = 0$. The saddle point equation becomes

$$0 = M_{AB}\Delta\rho^{(2)}_B + \frac{1}{2}L_{ABC}\Delta\rho^{(2)}_B\Delta\rho^{(2)}_C + \varepsilon_A , \tag{2.66}$$

and we can solve it in perturbation theory

$$\Delta\rho^{(2)}_A = -M^{-1}_{AB}\varepsilon_B - \frac{1}{2}M^{-1}_{AB}L_{BCD}M^{-1}_{CC'}\varepsilon_{C'}M^{-1}_{DD'}\varepsilon_{D'} + O(e^3) . \tag{2.67}$$

By inserting the above expression inside the free energy we get

$$\begin{aligned}\Delta\Gamma[\Delta C_{ab}] = \max_{\varepsilon_{ab}} \Bigg[& -\frac{1}{2}\varepsilon_A M^{-1}_{AB}\varepsilon_B - \frac{1}{6}L_{ABC}M^{-1}_{AA'}M^{-1}_{BB'}M^{-1}_{CC'}\varepsilon_{A'}\varepsilon_{B'}\varepsilon_{C'} \\ & - V\sum_{a\neq b}\varepsilon_{ab}\Delta C_{ab}\Bigg] .\end{aligned} \tag{2.68}$$

We introduce the notation $(M^{-1}M^{-1}M^{-1}L)_{ABC} = M^{-1}_{AA'}M^{-1}_{BB'}M^{-1}_{CC'}L_{A'B'C'}$ and

$$\begin{aligned} V\mathcal{M}^{-1}_{ab,cd} &= \int_{1,2,3,4} f(1,2)M^{-1}_{ab,cd}(1,2,3,4)f(3,4) , \\ V\mathcal{L}_{ab,cd,ef} &= \int_{1,\cdots,6} f(1,2)f(3,4)f(5,6)(M^{-1}M^{-1}M^{-1}L)_{ab,cd,ef}(1,2;3,4;5,6) . \end{aligned} \tag{2.69}$$

In this way Eq. (2.68) becomes

$$\Delta\Gamma[\Delta C_{ab}] = V \max_{\varepsilon_{ab}} \left[-\frac{1}{2}\varepsilon_{ab}\mathcal{M}^{-1}_{ab,cd}\varepsilon_{cd} - \frac{1}{6}\mathcal{L}_{ab,cd,ef}\varepsilon_{ab}\varepsilon_{cd}\varepsilon_{ef} - \sum_{a\neq b}\varepsilon_{ab}\Delta C_{ab} \right] . \tag{2.70}$$

If we derive with respect to ε_{ab} we get

$$\Delta C_{ab} = -\mathcal{M}^{-1}_{ab,cd}\varepsilon_{cd} - \frac{1}{2}\mathcal{L}_{ab,cd,ef}\varepsilon_{cd}\varepsilon_{ef} , \tag{2.71}$$

that can be inverted to obtain

$$\varepsilon_{ab} = -\mathcal{M}_{ab,cd}\Delta C_{cd} - \frac{1}{2}\mathcal{M}_{ab,cd}\mathcal{L}_{cd,ef,gh}\mathcal{M}_{ef,e'f'}\Delta C_{e'f'}\mathcal{M}_{gh,g'h'}\Delta C_{g'h'} . \tag{2.72}$$

At this point we can insert this in Eq. (2.70). The result is

$$\begin{aligned} \Delta\Gamma[\Delta C_{ab}] &= V\left\{\frac{1}{2}\Delta C_{ab}\mathcal{M}_{ab,cd}\Delta C_{cd} + \frac{1}{6}\mathcal{W}_{ab,cd,ef}\Delta C_{ab}\Delta C_{cd}\Delta C_{ef} + \cdots\right\} , \\ \mathcal{W}_{ab,cd,ef} &= \mathcal{M}_{ab,a'b'}\mathcal{M}_{cd,c'd'}\mathcal{M}_{ef,e'f'}\mathcal{L}_{a'b',c'd',e'f'} . \end{aligned} \tag{2.73}$$

that is the Landau expansion of the free energy at the third order around the non trivial glassy solution.

2.4.2 Computation of λ

In this section we will give the precise expression for the replica prescription to compute the mode-coupling exponent parameter λ. The replica recipe for this quantity has been first introduced for schematic models where it can be seen that it gives the correct results [29, 32, 31, 66, 143]. This result is quite important for the following reason. In general, the replica method and mode-coupling theory treat different aspects of the dynamical glass transition problem. In fact the first one focuses on the static aspects, namely the characterization of the metastable states that appear at the transition point, while the latter studies mainly the dynamical aspects. This means that often the two methods address different problems and are complementary. In this way it is not very simple to relate them. This result allows a comparison between the two methods because with the replica method we have access to a completely dynamical quantity. It has been obtained with the following line of reasoning.

Suppose to study the Langevin dynamics using the Martin-Siggia-Rose formalism [123]. It is well known that this technique can be improved by going to a supersymmetric action [109, 183]. In this formalism one obtains a dynamical free energy that has exactly the same functional form of the static free energy (apart from a kinetic term that controls the short time dynamics and that is irrelevant in the long time limit). It is instructive to see this in the case of the p-spin spherical model by comparing Eq. 1.79 with Eq. 1.52. In particular the mapping from the dynamical free energy and its static counterpart can be made if we replace super-times with replica indices and integrals over time and Grassman variables with sums over the replica indices. By looking at the dynamical action it is simple to see that

the exponent parameter is given by the ratio between two of the coefficients that define the cubic terms in the expansion of the dynamical free energy around the saddle point solution. Actually these two coefficients can be related to six points dynamical correlation function whose long time limit can be computed using the replica recipe given in the previous section. This means that if we are in a region of time such that the correlation function is close to its plateau value that is the region of times relevant to compute λ the two coefficients are exactly given by the corresponding cubic coefficients in the static replicated free energy. This concludes the strategy.

In the structural glass case we cannot prove that the replica prescription gives the correct results because we cannot solve the dynamics. However we can see if it agrees with the experiments and numerical simulations. Let us now go deeply in the details of the calculation. The cubic terms of the expansion of the replicated free energy around the glassy solution that are relevant to obtain the exponent parameter are

$$-\frac{w_1}{6}\mathrm{Tr}(\Delta C)^3 - \frac{w_2}{6}\sum_{a\neq b}\Delta C_{ab}^3 \,. \tag{2.74}$$

and the replica prescription for the exponent parameter is given by

$$\lambda = \frac{w_2}{w_1} \,. \tag{2.75}$$

The cubic terms are obtained analyzing the derivatives in (2.65). We have said that these must be computed on the glassy solution that here has a 1RSB structure and in replica space is replica symmetric. In [169], Temesvari, De Dominicis and Pimentel have shown that for a replica symmetric saddle point the two coefficients w_1 and w_2 can be written as

$$\begin{aligned} w_1 &= \mathcal{W}_1 - 3\mathcal{W}_5 + 3\mathcal{W}_7 - \mathcal{W}_8 \,, \\ w_2 &= \frac{1}{2}\mathcal{W}_2 - 3\mathcal{W}_3 + \frac{3}{2}\mathcal{W}_4 + 3\mathcal{W}_5 + 2\mathcal{W}_6 - 6\mathcal{W}_7 + 2\mathcal{W}_8 \,, \end{aligned} \tag{2.76}$$

where

$$\begin{aligned} \mathcal{W}_1 &= \mathcal{W}_{ab,bc,ca} \,, \\ \mathcal{W}_2 &= \mathcal{W}_{ab,ab,ab} \,, \\ \mathcal{W}_3 &= \mathcal{W}_{ab,ab,ac} \,, \\ \mathcal{W}_4 &= \mathcal{W}_{ab,ab,cd} \,, \\ \mathcal{W}_5 &= \mathcal{W}_{ab,ac,bd} \,, \\ \mathcal{W}_6 &= \mathcal{W}_{ab,ac,ad} \,, \\ \mathcal{W}_7 &= \mathcal{W}_{ac,bc,de} \,, \\ \mathcal{W}_8 &= \mathcal{W}_{ab,cd,ef} \,. \end{aligned} \tag{2.77}$$

This means that the final expression for λ is given by

$$\lambda = \frac{w_2}{w_1} = \frac{\frac{1}{2}\mathcal{W}_2 - 3\mathcal{W}_3 + \frac{3}{2}\mathcal{W}_4 + 3\mathcal{W}_5 + 2\mathcal{W}_6 - 6\mathcal{W}_7 + 2\mathcal{W}_8}{\mathcal{W}_1 - 3\mathcal{W}_5 + 3\mathcal{W}_7 - \mathcal{W}_8} \,. \tag{2.78}$$

An important thing that we have to say now is that the expression above depends implicitly by the specific form of the smoothing function $f(x)$ that we have chosen to define the order parameter. We will see in what follows that actually, in the end, the dependance on f disappears. Moreover let us note that the above expression is very complicated because to obtain the cubic coefficients $\mathcal{W}$ we need to obtain $\mathcal{M}$ that is a complex operation (see Eq. (2.69),) and then we need to do a convolution with $\mathcal{L}$ as it is written in Eq. (2.73). This sequence of operations is in general very hard to do. However we recall here that we need to compute everything at the critical point. The crucial observation is that at the dynamical transition the mass matrix defined in (2.65) develops a zero mode. This will simplify enormously the calculation.

2.4.3 The mass matrix and the zero mode

Let us recall that we are studying the case in which the system is homogeneous that means that in Eq. (2.62) we have $\tilde{g}(x_1, x_2) = \tilde{g}(x_1 - x_2)$. This implies that $\tilde{g}$ is a function of just one variable. The solution of the saddle point in the high temperature (low density) phase gives $\tilde{g}(x) = 1$ and this is the trivial solution. When the dynamical point is crossed, we will have a non trivial solution for $\tilde{g}(x)$. The appearance of this new solution is discontinuous and can be regarded, as in first order transitions, like a bifurcation phenomenon. This means that it can be detected only by coming from the glass phase and otherwise, if we come from the liquid phase, nothing special will happen. We call $\epsilon = T_d - T$ the distance from the critical point (if the control parameter is the density then $\epsilon = \rho - \rho_d$). We will always refer to the temperature as the control parameter but everything can be rewritten easily in terms of the density. We will be always in the region where ϵ is small and positive. For $\epsilon \to 0^+$ we have

$$\widetilde{g}(1,2;\epsilon) = \widetilde{g}(1,2;0) + 2\sqrt{\epsilon}\,\kappa\, k_0(1,2) + O(\epsilon)\ . \tag{2.79}$$

Here, the function k_0 is normalized by $V^{-1}\int_{1,2} k_0(1,2)^2 = \int \mathrm{d}x k_0(x)^2 = 1$, which defines implicitly the constant κ. Deriving this relation with respect to the control parameter we get

$$\frac{d\overline{\rho}_{ab}(1,2)}{d\epsilon} = \frac{\rho^2}{\sqrt{\epsilon}}(1-\delta_{ab})\,\kappa\, k_0(1,2) + O(1)\ . \tag{2.80}$$

Now we consider again the saddle point equation (2.61). We look to the case in which $a \neq b$ so that $w_{a\neq b} = 0$. If we take the derivative with respect to the control parameter we obtain

$$\begin{aligned} 0 = \frac{d}{d\epsilon}\left.\frac{\delta\Gamma[\rho,\rho^{(2)}]}{\delta\rho^{(2)}_{ab}(1,2)}\right|_{\widetilde{\rho}_{ab}} &= \sum_{c\neq d}\int_{3,4}\left.\frac{\delta^2\Gamma[\rho,\rho^{(2)}]}{\delta\rho^{(2)}_{ab}(1,2)\delta\rho^{(2)}_{cd}(3,4)}\right|_{\overline{\rho}_{ab}}\frac{d\overline{\rho}_{cd}(3,4)}{d\epsilon} \\ &+ \sum_{c}\int_{3,4}\left.\frac{\delta^2\Gamma[\rho,\rho^{(2)}]}{\delta\rho^{(2)}_{ab}(1,2)\delta\rho^{(2)}_{cc}(3,4)}\right|_{\overline{\rho}_{ab}}\frac{d\overline{\rho}_{cc}(3,4)}{d\epsilon} + \left.\frac{\delta^2\Gamma[\rho,\rho^{(2)}]}{\delta\rho^{(2)}_{ab}(1,2)\delta\epsilon}\right|_{\overline{\rho}_{ab}} \end{aligned} \tag{2.81}$$

If we recall that the definition of the "mass operator" in Eq. (2.65) is

$$M_{ab;cd}(1,2;3,4) = \left.\frac{\delta^2\Gamma[\rho,\rho^{(2)}]}{\delta\rho^{(2)}_{ab}(1,2)\delta\rho^{(2)}_{cd}(3,4)}\right|_{\overline{\rho}_{ab}} \tag{2.82}$$

for $a \neq b$ and $c \neq d$ then Eq. (2.81) can be rewritten as

$$0 = \sum_{c \neq d} \int_{3,4} M_{ab;cd}(1,2;3,4) \frac{d\overline{\rho}_{cd}(3,4)}{d\epsilon} + \mathcal{K}(1,2) \tag{2.83}$$

where $\mathcal{K}(1,2)$ is a finite contribution at the critical point and does not depend on $a \neq b$ because of the symmetry of the saddle point.

From Eq. (2.80) we see that the derivative $d\overline{\rho}_{cd}(3,4)/d\epsilon$ is divergent as $\epsilon^{-1/2}$ when the transition point is approached. In this way we conclude that the mass operator must develop a zero mode in order to cancel the divergence coming from the the derivative of the saddle point solution. This means that

$$\sum_{c \neq d} \int_{3,4} M_{ab;cd}(1,2;3,4) k_0(3,4) = \mu \sqrt{\epsilon} k_0(1,2) \ . \tag{2.84}$$

By exploiting the replica symmetry of the saddle point solution it can be proved that the mass matrix has the following replica structure [169]

$$\begin{aligned} M_{ab;cd}(1,2;3,4) =& M_1(1,2;3,4) \left(\frac{\delta_{ac}\delta_{bd} + \delta_{ad}\delta_{bc}}{2} \right) \\ &+ M_2(1,2;3,4) \left(\frac{\delta_{ac} + \delta_{ad} + \delta_{bc} + \delta_{bd}}{4} \right) + M_3(1,2;3,4) \end{aligned} \tag{2.85}$$

Moreover the matrices of the form (2.85) form a closed algebra and we can search for the inverse of the mass matrix as a matrix that has the same replica structure

$$\begin{aligned} G_{ab;cd}(1,2;3,4) =& G_1(1,2;3,4) \left(\frac{\delta_{ac}\delta_{bd} + \delta_{ad}\delta_{bc}}{2} \right) \\ &+ G_2(1,2;3,4) \left(\frac{\delta_{ac} + \delta_{ad} + \delta_{bc} + \delta_{bd}}{4} \right) + G_3(1,2;3,4) \ . \end{aligned} \tag{2.86}$$

The equation for G is

$$\begin{aligned} &\sum_{c \neq d} \int_{3,4} M_{ab;cd}(1,2;3,4) G_{cd;ef}(3,4;5,6) = \\ &= \frac{\delta_{ae}\delta_{bf} + \delta_{af}\delta_{be}}{2} \frac{\delta(1,5)\delta(2,6) + \delta(1,6)\delta(2,5)}{2} \end{aligned} \tag{2.87}$$

so that if we consider the equilibrium replica limit $m \to 1$ we obtain

$$\begin{aligned} G_1 &= M_1^{-1} \\ G_2 &= -2[2M_1 - M_2]^{-1} \otimes M_2 \otimes M_1^{-1} \\ G_3 &= M_1^{-1} \otimes \left\{ M_2 \otimes [2M_1 - M_2]^{-1} \otimes M_2 - M_3 \right\} \otimes M_1^{-1} \ . \end{aligned} \tag{2.88}$$

where we have denoted with $\otimes$ the convolution in the space variables ($a \otimes b = \int_{3,4} a(1,2,;3,4) b(3,4;5,6)$).

From Eq. (2.80) it follows that the zero mode does not have any replica structure. This implies that

$$\begin{aligned}
&\lim_{m\to 1}\sum_{c\neq d}\int_{3,4} M_{ab;cd}(1,2;3,4)k_0(3,4) = \\
&= \lim_{m\to 1}\int_{3,4}\left[m(m-1)M_3(1,2;3,4) + M_1(1,2;3,4) + (m-1)M_2(1,2;3,4)\right]k_0(3,4) \\
&= \int_{3,4} M_1(1,2;3,4)k_0(3,4)
\end{aligned} \tag{2.89}$$

from which it follows that k_0 is a zero mode (with eigenvalue proportional to $\sqrt{\epsilon}$) only for the term of the mass operator defined by the kernel $M_1(1,2;3,4)$. Moreover M_2 and M_3 are regular at the transition and do not present any zero mode. In this way we have

$$\int_{3,4} M_1(1,2;3,4)k_0(3,4) = \mu\sqrt{\epsilon}k_0(1,2)\ , \tag{2.90}$$

or equivalently (recall that $\int_{1,2} k_0(1,2)^2 = V$):

$$M_1^{-1}(1,2;3,4) = \frac{1}{V\,\mu\sqrt{\epsilon}}k_0(1,2)k_0(3,4) + O(1)\ . \tag{2.91}$$

From this it follows that if we look at (2.88) we recognize that the operator G_1 and G_2 have a single pole (a divergent eigenvalue) while the operator G_3 has a double pole at the dynamical transition point.

This is a generalization of the results obtained in [74] to the physical situation in which we need to take into account the spatial structure of the quantities involved in the definition of the free energy. We can rewrite (2.88) in the following way

$$\begin{array}{llll}
G_2 = O_2 \otimes M_1^{-1} & \text{with} & O_2 = -2[2M_1 - M_2]^{-1}\otimes M_2 \\
G_3 = M_1^{-1}\otimes O_3 \otimes M_1^{-1} & \text{with} & O_3 = \left[M_2\otimes[2M_1 - M_2]^{-1}\otimes M_2 - M_3\right]
\end{array} \tag{2.92}$$

so that by knowing the behavior of the smallest eigenvalue for M_1 we can infer the divergent behavior of such kernel operators

$$\begin{array}{l}
G_1(1,2;3,4) \simeq \frac{1}{V\,\mu\sqrt{\epsilon}}k_0(1,2)k_0(3,4) + O(1) \\
G_2(1,2;3,4) \simeq \frac{1}{V\,\mu\sqrt{\epsilon}}k_2(1,2)k_0(3,4) + O(1) \\
G_3(1,2;3,4) \simeq \frac{\kappa_3}{V\,\mu^2\epsilon}k_0(1,2)k_0(3,4) + O\Big(\frac{1}{\sqrt{\epsilon}}\Big)
\end{array} \tag{2.93}$$

where

$$\begin{aligned}
k_2(1,2) &= \int_{3,4} O_2(1,2;3,4)k_0(3,4) \\
\kappa_3 &= \frac{1}{V}\int_{1,2,3,4} k_0(1,2)O_3(1,2;3,4)k_0(3,4)
\end{aligned} \tag{2.94}$$

Form the expressions above we clearly see the double pole structure of G_3. However in G_3 a single pole divergence is also present and it depends on the excited states of the kernel operator M_1. We will see later that this will not play any role in the calculation of λ.

2.4.4 Analysis of the cubic terms and computation of λ

From the analysis of the critical behavior of the mass matrix we have all the ingredients to compute a simple and universal expression for λ. Because of the fact that λ is given by the ratio of cubic coefficients we start from their generic expression given in (2.73). If we use Eq. (2.69) we obtain

$$\begin{aligned}\mathcal{W}_{ab,cd,ef} &= \mathcal{M}_{ab;a'b'}\mathcal{M}_{cd;c'd'}\mathcal{M}_{ef;e'f'}\frac{1}{V}\int_{1,\dots,6;1',\dots,6'} f(1,2)M^{-1}_{a'b';a''b''}(1,2;1',2')\times \\ &\times f(3,4)M^{-1}_{c'd';c''d''}(3,4;3',4')f(5,6)M^{-1}_{e'f';e''f''}(5,6;5',6') \\ &\times L_{a''b'';c''d'';e''f''}(1',2';3',4';5',6') \\ &= \frac{1}{V}\int_{1',\dots,6'}\Delta_{ab;a''b''}(1',2')\Delta_{cd;c''d''}(3',4')\Delta_{ef;e'',f''}(5',6') \\ &\times L_{a''b'';c''d'';e''f''}(1',2';3',4';5',6')\ ,\end{aligned} \tag{2.95}$$

where we have defined

$$\begin{aligned}\Delta_{ab;a''b''}(1',2') &= \mathcal{M}_{ab;a'b'}\int_{1,2} f(1,2)M^{-1}_{a'b';a''b''}(1,2;1',2') \\ &= \Delta_1(1',2')\frac{\delta_{a,a''}\delta_{b,b''}+\delta_{a,b''}\delta_{b,a''}}{2} \\ &+ \Delta_2(1',2')\frac{\delta_{a,a''}+\delta_{b,a''}+\delta_{a,b''}+\delta_{b,b''}}{4}+\Delta_3(1',2')\ .\end{aligned} \tag{2.96}$$

The constant (that means that it does not depend on space variables) matrix $\mathcal{M}_{ab;cd}$ inherits the replica structure from the mass matrix $M_{ab;cd}(1,2;3,4)$. From Eq. (2.69) we obtain

$$\begin{aligned}\mathcal{M}^{-1}_{ab,cd} &= \mathcal{G}_1\left(\frac{\delta_{ac}\delta_{bd}+\delta_{ad}\delta_{bc}}{2}\right)+\mathcal{G}_2\left(\frac{\delta_{ac}+\delta_{ad}+\delta_{bc}+\delta_{bd}}{4}\right)+\mathcal{G}_3\ , \\ \mathcal{M}_{ab,cd} &= \mathcal{M}_1\left(\frac{\delta_{ac}\delta_{bd}+\delta_{ad}\delta_{bc}}{2}\right)+\mathcal{M}_2\left(\frac{\delta_{ac}+\delta_{ad}+\delta_{bc}+\delta_{bd}}{4}\right)+\mathcal{M}_3\ ,\end{aligned} \tag{2.97}$$

The quantities $\mathcal{G}_i$ are f-dependent and are defined in the following way

$$\mathcal{G}_i = \frac{1}{V}\int_{1,2,3,4} f(1,2)G_i(1,2;3,4)f(3,4)\ , \tag{2.98}$$

The expression of $\mathcal{M}_i$ in terms of the $\mathcal{G}_i$ is simply obtained and it is given by

$$\begin{aligned}\mathcal{M}_1 &= \frac{1}{\mathcal{G}_1}\ , \\ \mathcal{M}_2 &= -\frac{2\mathcal{G}_2}{\mathcal{G}_1(2\mathcal{G}_1-\mathcal{G}_2)}\ , \\ \mathcal{M}_3 &= \frac{\mathcal{G}_2^2}{\mathcal{G}_1^2(2\mathcal{G}_1-\mathcal{G}_2)}-\frac{\mathcal{G}_3}{\mathcal{G}_1^2}\ .\end{aligned} \tag{2.99}$$

The next step is to study the matrix Δ in Eq. (2.95). Using the explicit expressions for $\mathcal{M}_i$ we obtain

$$\begin{aligned}
\Delta_1(1',2') &= f \star \frac{1}{\mathcal{G}_1} G_1 \ , \\
\Delta_2(1',2') &= f \star \frac{2(\mathcal{G}_1 G_2 - G_1 \mathcal{G}_2)}{\mathcal{G}_1(2\mathcal{G}_1 - \mathcal{G}_2)} \ , \\
\Delta_3(1',2') &= f \star \frac{\mathcal{G}_2^2 G_1 + 2\mathcal{G}_1(\mathcal{G}_1 G_3 - \mathcal{G}_3 G_1) + \mathcal{G}_2(\mathcal{G}_3 G_1 - \mathcal{G}_1(G_2 + G_3))}{\mathcal{G}_1^2(2\mathcal{G}_1 - \mathcal{G}_2)} \ ,
\end{aligned} \tag{2.100}$$

and we have introduced the notation

$$(f \star G_i)(1',2') = \int_{1,2} f(1,2) G_i(1,2;1',2') \tag{2.101}$$

At this point by inserting the critical behavior of the G_i given in Eq. (2.93) into the above expressions for Δ we see that the divergent parts appear both at the numerator and denominator of that expressions so that we can extract the finite contributions in the limit $\epsilon \to 0^+$ by only looking at them. By doing explicitly the calculations we see that some non-trivial cancellations happen and we get

$$\begin{aligned}
\Delta_1(1,2) &= \frac{k_0(1,2)}{f \star k_0} \ , \\
\Delta_2(1,2) &= 0 \ , \\
\Delta_3(1,2) &= 0 \ ,
\end{aligned} \tag{2.102}$$

where we have defined

$$f \star k_0 = V^{-1} \int_{1,2} f(1,2) k_0(1,2) = \int \mathrm{d}x f(x) k_0(x) \ . \tag{2.103}$$

Using this result into Eq. (2.95) we obtain the final expression for the cubic terms of the Landau expansion of the free energy

$$\mathcal{W}_{ab;cd;ef} = \frac{1}{(f \star k_0)^3} \frac{1}{V} \int_{1,2;3,4;5,6} k_0(1,2) k_0(3,4) k_0(5,6) L_{ab;cd;ef}(1,2;3,4;5,6) \ . \tag{2.104}$$

Finally, using Eq. (4.79), the two cubic coefficients relevant for the computation of λ are given by

$$\begin{aligned}
w_2 = {} & \frac{1}{(f \star k_0)^3} \frac{1}{V} \int_{1,2;3,4;5,6} k_0(1,2) k_0(3,4) k_0(5,6) \Big(\frac{1}{2} L_{ab,ab,ab} - 3 L_{ab,ab,ac} \\
& + \frac{3}{2} L_{ab,ab,cd} + 3 L_{ab,ac,bd} + 2 L_{ab,ac,ad} - 6 L_{ac,bc,de} + 2 L_{ab,cd,ef} \Big)(1,2;3,4;5,6) \\
w_1 = {} & \frac{1}{(f \star k_0)^3} \frac{1}{V} \int_{1,2;3,4;5,6} k_0(1,2) k_0(3,4) k_0(5,6) (L_{ab,bc,ca} - 3 L_{ab,ac,bd} \\
& + 3 L_{ac,bc,de} - L_{ab,cd,ef})(1,2;3,4;5,6) \ .
\end{aligned} \tag{2.105}$$

Because of the fact that λ is given by the ratio of the two coefficients above it is straightforward to see that it will not depend on the smoothing function f as it was said before. Moreover we see that the expressions above are very simple once we have the zero mode k_0 because we do not need to do any operator inversion.

2.5 Gradient expansion around the mean field uniform solution

The scope of this section is to investigate the critical behavior of the four point correlation functions $G_{th}(r)$ and $G_4(r)$. To do this, we pointed out in the case of the ferromagnetic model, that we need to allow a slight dependance of the order parameter on the spatial structure and then we need to perform a gradient expansion again around the saddle point solution. Here we will do this in the structural glass case. The two four point correlation functions $G_{th}(r)$ and $G_4(r)$ can be related to the inverse of the mass operator $G_{ab;cd}(1,2;3,4)$, Eqs. (2.85) and (2.86). In fact we should invert the mass operator $M_{ab;cd}(1,2;3,4)$ and perform the convolution with the smoothing function $f(x)$ to obtain the replica correlation $G^{(f)}_{ab;cd}(r)$ that enters in Eq. (2.48). This procedure is very hard to do in practical calculation. However we should be able to take advantage from the fact that we are interested in the long distance behavior of the four point correlation functions. This will be reflected in the fact that we can focus only on the critical properties of the mass matrix. To show this we make a gradient expansion in which we consider a field $\Delta\rho^{(2)}_{ab}(1,2)$ which is almost uniform. Recall that in the uniform case $\Delta\rho^{(2)}_{ab}(x_1,x_2) = \Delta\rho^{(2)}_{ab}(x_1 - x_2)$ so that here we add a dependance on the variable $(x_1+x_2)/2$ and we consider the case in which this dependance is weak.

2.5.1 Fourier transform

Let us consider the Fourier transform of $\Delta\rho^{(2)}_{ab}(1,2)$ with respect to the translational invariant variable $x_1 - x_2$ and the center of mass variable $(x_1+x_2)/2$

$$\begin{aligned}\Delta\rho^{(2)}_{ab}(p,q) &= \int \mathrm{d}x_1\mathrm{d}x_2\, e^{ip\left(\frac{x_1+x_2}{2}\right)+iq(x_1-x_2)}\Delta\rho^{(2)}_{ab}(x_1,x_2)\ ,\\ \Delta\rho^{(2)}_{ab}(x_1,x_2) &= \int \frac{\mathrm{d}p\,\mathrm{d}q}{(2\pi)^{2D}}\, e^{-ip\left(\frac{x_1+x_2}{2}\right)-iq(x_1-x_2)}\Delta\rho^{(2)}_{ab}(p,q)\ .\end{aligned} \tag{2.106}$$

We see that p is the momentum associated to the spatial variation of $\Delta\rho^{(2)}$ that is assumed to be weak and q is the momentum that is coupled to the local displacement. If we are interested in the long distance behavior we have to look at the small p limit.

Consider now the quadratic part of the expansion of the free energy around the glassy solution. We can insert this Fourier representation inside this term to obtain

$$\begin{aligned}\Delta_2\Gamma &= \frac{1}{2}\sum_{a\neq b}\sum_{c\neq d}\int_{1,2,3,4}\Delta\rho^{(2)}_{ab}(1,2)M_{ab;cd}(1,2,3,4)\Delta\rho^{(2)}_{cd}(3,4)\\ &= \frac{1}{2}\sum_{a\neq b}\sum_{c\neq d}\int\frac{\mathrm{d}p\,\mathrm{d}\hat{p}\,\mathrm{d}q\,\mathrm{d}k}{(2\pi)^{4D}}\Delta\rho^{(2)}_{ab}(p,q)M_{ab;cd}(-p,-\hat{p};-q,-k)\Delta\rho^{(2)}_{cd}(\hat{p},k)\end{aligned} \tag{2.107}$$

where

$$M_{ab;cd}(p,\hat{p};q,k) = \int_{1,2,3,4} e^{ip\left(\frac{x_1+x_2}{2}\right)+iq(x_1-x_2)+i\hat{p}\left(\frac{x_3+x_4}{2}\right)+ik(x_3-x_4)}M_{ab;cd}(1,2;3,4) \tag{2.108}$$

The saddle point glassy solution is translational invariant. Because the mass matrix is given by the second derivative of the free energy computed on the glassy solution we obtain that it is translationally invariant too. This means that we can perform a change of variable $X = (x_1 + x_2 + x_3 + x_4)/4$ and $u_i = x_i - X$, with $\sum_{i=1}^4 u_i = 0$ so that $M(1,2;3,4)$ will not depend on X. Calling $\mathcal{D}u = \mathrm{d}u_1\mathrm{d}u_2\mathrm{d}u_3\mathrm{d}u_4\delta\left(\frac{1}{4}\sum_{i=1}^4 u_i\right)$ we obtain

$$\begin{aligned} M_{ab;cd}(p,\hat{p};q,k) = \int \mathrm{d}X\mathcal{D}u\, e^{i(p+\hat{p})X + ip\left(\frac{u_1+u_2}{2}\right) + iq(u_1-u_2) + i\hat{p}\left(\frac{u_3+u_4}{2}\right) + ik(u_3-u_4)} \\ \times M_{ab;cd}(u_1,u_2;u_3,u_4) = (2\pi)^D\delta(p+\hat{p})M^{(p)}_{ab;cd}(q,k)\ , \end{aligned} \tag{2.109}$$

$$M^{(p)}_{ab;cd}(q,k) = \int \mathcal{D}u\, e^{ip\left(\frac{u_1+u_2}{2} - \frac{u_3+u_4}{2}\right) + iq(u_1-u_2) + ik(u_3-u_4)} M_{ab;cd}(u_1,u_2;u_3,u_4)\ . \tag{2.110}$$

The four point correlation function that we want to study is given by

$$\begin{aligned} G^{(p)}_{ab;cd}(q,k) &= \int \mathcal{D}u\, e^{ip\left(\frac{u_1+u_2}{2} - \frac{u_3+u_4}{2}\right) + iq(u_1-u_2) + ik(u_3-u_4)} \\ &\times \langle \Delta\hat{\rho}^{(2)}_{ab}(u_1,u_2)\Delta\hat{\rho}^{(2)}_{cd}(u_3,u_4)\rangle_{\mathrm{r}} = \\ &= \int \mathcal{D}u\, e^{ip\left(\frac{u_1+u_2}{2} - \frac{u_3+u_4}{2}\right) + iq(u_1-u_2) + ik(u_3-u_4)} G_{ab;cd}(u_1,u_2;u_3,u_4)\ , \end{aligned} \tag{2.111}$$

and we are looking at the situation in which the couple of points $u_1,\ u_2$ is far away from the couple $u_3,\ u_4$. This is equivalent to look at the small p limit and we need to develop the mass matrix around this limit. The correlation function that appears in the expression above is given by the inverse of the mass matrix. If we transform Eq. (2.87) in Fourier space we obtain

$$\begin{aligned} \sum_{c\neq d}\int \frac{\mathrm{d}k}{(2\pi)^D} M^{(p)}_{ab;cd}(q,k)G^{p}_{cd;ef}(-k,q') = \\ = \frac{\delta_{ae}\delta_{bf} + \delta_{af}\delta_{be}}{2}(2\pi)^D\frac{\delta(q-q') + \delta(q+q')}{2}\ . \end{aligned} \tag{2.112}$$

Moreover, going back to Eq. (2.88) we have

$$\begin{aligned} G^{(p)}_{ab;cd}(q,k) &= \left(\frac{\delta_{ac}\delta_{bd} + \delta_{ad}\delta_{bc}}{2}\right) G^{(p)}_1(q,k) \\ &+ \left(\frac{\delta_{ac} + \delta_{ad} + \delta_{bc} + \delta_{bd}}{4}\right) G^{(p)}_2(q,k) + G^{(p)}_3(q,k)\ , \\ G^{(p)}_1 &= \left[M^{(p)}_1\right]^{-1}\ , \\ G^{(p)}_2 &= -2\left[2M^{(p)}_1 - M^{(p)}_2\right]^{-1} \otimes M^{(p)}_2 \otimes \left[M^{(p)}_1\right]^{-1}\ , \\ G^{(p)}_3 &= \left[M^{(p)}_1\right]^{-1} \otimes \left\{M^{(p)}_2 \otimes \left[2M^{(p)}_1 - M^{(p)}_2\right]^{-1} \otimes M^{(p)}_2 - M^{(p)}_3\right\} \otimes \left[M^{(p)}_1\right]^{-1}. \end{aligned} \tag{2.113}$$

The convolution and inversion operations appearing in Eq. (2.113) are given by

$$\begin{aligned}[A\otimes B](q,q') &= \int \frac{\mathrm{d}k}{(2\pi)^D} A^{(p)}(q,k)B^{(p)}(-k,q') \ , \\ [A\otimes A^{-1}](q,q') &= (2\pi)^D \frac{\delta(q-q')+\delta(q+q')}{2} \ .\end{aligned} \tag{2.114}$$

The four point function $G^{(f)}_{ab;cd}(r-r')$ defined in Eq. (2.46) can be rewritten as

$$G^{(f)}_{ab;cd}(r-r') = \int \mathrm{d}x\mathrm{d}y\, f(x)f(y)\, G_{ab;cd}\left(r+\frac{x}{2}, r-\frac{x}{2}; r'+\frac{y}{2}, r'-\frac{y}{2}\right) \ . \tag{2.115}$$

By going to Fourier space we obtain

$$\begin{aligned}&(2\pi)^D\delta(p+\hat{p})G^{(f)}_{ab;cd}(p) = \int \mathrm{d}r\mathrm{d}r' e^{ipr+i\hat{p}r'} \\ &\times \int \mathrm{d}x\mathrm{d}y\, f(x)f(y)\, G_{ab;cd}\left(r+\frac{x}{2}, r-\frac{x}{2}; r'+\frac{y}{2}, r'-\frac{y}{2}\right) \\ &= \int \frac{\mathrm{d}q\,\mathrm{d}k}{(2\pi)^{2D}} f(-q)f(-k) \int \mathrm{d}r\mathrm{d}r'\mathrm{d}x\mathrm{d}y\, e^{ipr+i\hat{p}r'+iqx+iky} \\ &\times G_{ab;cd}\left(r+\frac{x}{2}, r-\frac{x}{2}; r'+\frac{y}{2}, r'-\frac{y}{2}\right) \\ &= \int \frac{\mathrm{d}q\,\mathrm{d}k}{(2\pi)^{2D}} f(-q)f(-k) \int_{1,2,3,4} e^{ip\left(\frac{x_1+x_2}{2}\right)+\hat{p}\left(\frac{x_3+x_4}{2}\right)+iq(x_1-x_2)+ik(x_3-x_4)} \\ &\times G_{ab;cd}(1,2;3,4) = (2\pi)^D\delta(p+\hat{p}) \int \frac{\mathrm{d}q\,\mathrm{d}k}{(2\pi)^{2D}} f(-q)f(-k)G^{(p)}_{ab;cd}(q,k) \ .\end{aligned} \tag{2.116}$$

so that

$$G^{(f)}_{ab;cd}(p) = \int \frac{\mathrm{d}q\,\mathrm{d}k}{(2\pi)^{2D}} f(-q)f(-k)G^{(p)}_{ab;cd}(q,k) \ . \tag{2.117}$$

If we use this in Eq. (2.48) we arrive at

$$\begin{aligned}G_{th}(p) &= \int \frac{\mathrm{d}q\,\mathrm{d}k}{(2\pi)^{2D}} f(-q)f(-k)\left[G^{(p)}_{ab;ab}(q,k) - G^{(p)}_{ab;ac}(q,k)\right] \\ &= \int \frac{\mathrm{d}q\,\mathrm{d}k}{(2\pi)^{2D}} f(-q)f(-k)\left[\frac{1}{2}G^{(p)}_1(q,k) + \frac{1}{4}G^{(p)}_2(q,k)\right] \ .\end{aligned} \tag{2.118}$$

Moreover using Eq. (2.113) we have

$$\begin{aligned}\frac{G_1}{2}+\frac{G_2}{4} &= \frac{1}{M_1} + \left[\frac{1}{M_2-2M_1}M_2 - 1\right]\frac{1}{2M_1} \\ &= \frac{1}{M_1} + \left[\frac{1}{M_2-2M_1}M_2 - \frac{1}{M_2-2M_1}(M_2-2M_1)\right]\frac{1}{2M_1} \\ &= \frac{1}{M_1} + \left[\frac{1}{M_2-2M_1}2M_1\right]\frac{1}{2M_1} \\ &= \frac{1}{M_1} + \frac{1}{M_2-2M_1}\end{aligned} \tag{2.119}$$

from which we see that the critical behavior is driven by the zero mode sector of the kernel operator M_1

$$G^{sing}_{th}(p) = \int \frac{\mathrm{d}q\,\mathrm{d}k}{(2\pi)^{2D}} f(-q)f(-k)\left[M^{(p)}_1\right]^{-1}(q,k) \ . \tag{2.120}$$

2.5.2 Analysis of the spectrum of the mass matrix

From the sections above we have seen that the long range behavior of the four point correlation functions we are interested in, is dominated by the zero mode sector of the kernel operator M_1. We now want to study in more details the spectral properties of this operator and to relate them to the correlations we are looking at.

We have seen that M_1 develops a zero eigenvalue at the dynamical transition point. Moreover we know that the eigenvector associated to this eigenvalue is translationally invariant. Because of the fact that the whole mass matrix is translationally invariant, we have that M_1 is proportional to $\delta(p+\hat{p})$ in Fourier space which means that we can diagonalize $M_1^{(p)}(q,k)$ at fixed external momentum p. In this way we can write the following spectral decomposition

$$M_1^{(p)}(q,k) = \lambda_0(p^2)\psi_0^{(p)}(q)\psi_0^{(p)}(k) + \sum_{\alpha\geq 1}\lambda_\alpha(p^2)\psi_\alpha^{(p)}(q)\psi_\alpha^{(p)}(k) \tag{2.121}$$

where the term associated to the lowest eigenvalue has been put in evidence for future convenience and where

$$\begin{aligned} &\int \frac{\mathrm{d}k}{(2\pi)^D}\, M_1^{(p)}(q,k)\psi_\alpha^{(p)}(-k) = \lambda_\alpha(p^2)\psi_\alpha^{(p)}(q)\ , \\ &\int \frac{\mathrm{d}k}{(2\pi)^D}\, \psi_\alpha^{(p)}(k)\psi_{\alpha'}^{(p)}(-k) = \delta_{\alpha,\alpha'}\ . \end{aligned} \tag{2.122}$$

The crucial assumption that we will do in the following is that there is a persistent mass gap between the zeroth order eigenvalue and the first excited state when the dynamical glass transition point is approached. In particular we know that the zeroth order eigenvalue is collapsing to zero at the dynamical point and we suppose that all the excited states will have finite positive eigenvalues. Let us come back to Eq. (2.90) that defines the zero mode

$$\int_{3,4} M_1(x_1,x_2,x_3,x_4)k_0(x_3-x_4) = (\mu\sqrt{\epsilon}+O(\epsilon))k_0(x_1-x_2)\ ; \tag{2.123}$$

if we go in Fourier space we get

$$\int \frac{\mathrm{d}k}{(2\pi)^D} M_1^{(p=0)}(q,-k)k_0(k) = (\mu\sqrt{\epsilon}+O(\epsilon))k_0(q)\ . \tag{2.124}$$

This means that

$$\psi_0^{(p=0)}(q) = k_0(q)\ , \qquad \lambda_0(p=0) = \mu\sqrt{\epsilon}+O(\epsilon)\ . \tag{2.125}$$

We define for $i=1,2,3$ the following constants

$$m_i = \int \frac{\mathrm{d}q\,\mathrm{d}k}{(2\pi)^{2D}} k_0(-q)M_i^{(p=0)}(q,k)k_0(-k)\ , \tag{2.126}$$

so that

$$\lambda_0(p^2) = m_1 + \sigma p^2 + O(p^4) = \mu\sqrt{\epsilon} + \sigma p^2 + O(\epsilon, p^4)\ . \tag{2.127}$$

This means that if we are close to the transition point $\lambda_0(p^2)$ is small for small external momentum p. This implies that the leading term in the spectral decomposition of M_1^{-1} is given by the zero mode:

$$\begin{aligned}\left[M_1^{(p)}\right]^{-1}(q,k) &= \frac{1}{\lambda_0(p^2)}\psi_0^{(p)}(q)\psi_0^{(p)}(k) + \sum_{\alpha\geq 1}\frac{1}{\lambda_\alpha(p^2)}\psi_\alpha^{(p)}(q)\psi_\alpha^{?}(k) \\ &\simeq \frac{1}{\lambda_0(p^2)}\psi_0^{(p)}(q)\psi_0^{(p)}(k)\end{aligned} \tag{2.128}$$

From the discussion above we see that

$$\mu = \lim_{\epsilon\to 0}\frac{\mathrm{d}m_1}{\mathrm{d}\sqrt{\epsilon}} = \lim_{\epsilon\to 0}\frac{\mathrm{d}}{\mathrm{d}\sqrt{\epsilon}}\int\frac{\mathrm{d}^D q\,\mathrm{d}^D k}{(2\pi)^{2D}}k_0(-q)M_1^{(p=0)}(q,k)k_0(-k)\ . \tag{2.129}$$

The coefficient σ can be obtained using perturbation theory because if we develop the operator M_1 around $p=0$ we get

$$M_1^{(p)}(q,k) = M_1^{(p=0)}(q,k) + p^2\left.\frac{\partial}{\partial p^2}M_1^{(p)}(q,k)\right|_{p=0} + O(p^4)\ . \tag{2.130}$$

We know that k_0 is the fundamental state of the unperturbed operator $M_1^{(p=0)}(q,k)$ so that we can treat the second term of the expansion above like a perturbation that is small by construction because we are at $p\simeq 0$. This means that the shift in the ground state eigenvalue is given by

$$\lambda_0(p^2) - m_1 = p^2\lim_{\epsilon\to 0}\int\frac{\mathrm{d}q\,\mathrm{d}k}{(2\pi)^{2D}}k_0(-q)\left.\frac{\partial}{\partial p^2}M_1^{(p)}(q,k)\right|_{p=0}k_0(-k)\ , \tag{2.131}$$

so that

$$\sigma = \lim_{\epsilon\to 0}\int\frac{\mathrm{d}q\,\mathrm{d}k}{(2\pi)^{2D}}k_0(-q)\left.\frac{\partial}{\partial p^2}M_1^{(p)}(q,k)\right|_{p=0}k_0(-k)\ . \tag{2.132}$$

From Eq. (2.127) and (2.128) we finally obtain that close to the transition point we have for small external momentum p

$$\left[M_1^{(p)}\right]^{-1}(q,k) \simeq \frac{1}{\mu\sqrt{\epsilon}+\sigma p^2}k_0(q)k_0(k) \tag{2.133}$$

Inserting this in Eq. (2.120) we get, with the same definition of the $\star$ product as before:

$$G_{th}^{sing}(p) = \frac{(f\star k_0)^2}{\mu\sqrt{\epsilon}+\sigma p^2} = \frac{G_0\epsilon^{-1/2}}{1+\xi^2p^2}\ , \qquad f\star k_0 = \int\frac{\mathrm{d}q}{(2\pi)^D}f(-q)k_0(q)\ . \tag{2.134}$$

From this result we see that the correlation length is

$$\xi = \sqrt{\frac{\sigma}{\mu}}\epsilon^{-1/4} \tag{2.135}$$

and

$$G_0 = \frac{(f\star k_0)^2}{\mu}\ . \tag{2.136}$$

In this way we have completely analyzed the Gaussian part of the gradient expansion of the free energy around the glassy solution and we have extracted the first mean field predictions. Now we need to see where these results are valid.

2.6 Ginzburg criterion

The purpose of this section is to discuss systematically where the Gaussian results that we have derived above give accurate estimates of the four point correlation functions and where they fails. To do this we assume that the free energy Γ comes from the truncation of a high temperature expansion (this point will be considered again in Sec. 2.7) and we use this mean field free energy as a bare action to perform a loop calculation in order to obtain a Ginzburg criterion for the dynamical glass transition. The general expectation is that the Gaussian predictions are valid everywhere in the temperature-density plane if we are above the upper critical dimension. However if we are below it these prediction are valid up to a certain distance from the critical point where the fluctuations destroy the mean field behavior. How to precisely define the order of magnitude of this distance can be done by looking at which point the first correction to the Gaussian prediction for the correlation functions becomes of the same order of the leading term. The Gaussian bare propagator is $G^{(p)}_{ab;cd}(q,k)$ given in Eq. (2.113). To compute the loop correction we should compute all the diagrammatics that comes from the cubic vertices. This is a very complicated calculations. However a wonderful result allows us to simplify enormously this task.

2.6.1 Projection on the critical mode

First of all a great simplification arise if we focus on the long distance behavior so that we look at the critical part of the correlation functions. In particular we have shown that the major role in this is played by the zero mode of the kernel operator M_1. For example, if we consider Eqs. (2.120) we have that because of (2.133), the thermal four point correlation function will be dominated by the zero mode of M_1. However let us specify that the full behavior of G_{th} depends also on the excited states of M_1 but they do not give the dominant contribution at long distance so that we neglect them.

To simplify drastically the things, a simple way to neglect all the excited states is to set their eigenvalues to infinity so that we do not allow thermal fluctuations along these excited states and the theory becomes defined only for a field that is parallel to the zero mode, being the orthogonal fluctuations frozen. This means that we can consider an effective low-energy theory where only the fluctuations along the zero mode are allowed so that we choose

$$\Delta\rho^{(2)}_{ab}(p,q) = \phi_{ab}(p)k_0(q) \ . \tag{2.137}$$

In this way the bare action simplify drastically because it does not include all the fluctuations orthogonal to the zero mode. The quadratic part of the action is obtained by inserting Eq. (2.137) in Eq. (2.107). The relevant cubic terms according to [169, 74] can be obtained by inserting Eq. (2.137) in the cubic part of

the expansion and using similar considerations as in Sec. 2.4.2. The result is

$$\begin{aligned}\Gamma[\phi_{ab}] = \frac{1}{2}\int \frac{\mathrm{d}p}{(2\pi)^D} \Bigg(& \sum_{a\neq b}(\mu\sqrt{\epsilon}+\sigma p^2)|\phi_{ab}(p)|^2 \\ & + m_2 \sum_a \left|\sum_b \phi_{ab}(p)\right|^2 + m_3 \left|\sum_{a\neq b}\phi_{ab}(p)\right|^2 \Bigg) \\ & + \frac{w_1}{6}\sum_{a\neq b\neq c\neq a}\int \frac{\mathrm{d}p\mathrm{d}p'}{(2\pi)^{2D}}\phi_{ab}(p)\phi_{bc}(p')\phi_{ca}(-p-p') \\ & + \frac{w_2}{6}\sum_{a\neq b}\int \frac{\mathrm{d}p\mathrm{d}p'}{(2\pi)^{2D}}\phi_{ab}(p)\phi_{ab}(p')\phi_{ab}(-p-p') \ ,\end{aligned} \tag{2.138}$$

and all the coefficients that appear here are the ones computed in the previous sections. Let us stress that by focusing on the fluctuations along the zero mode, all the momentum structure of the theory has been greatly simplified.

2.6.2 The mapping on the φ^3 theory in random field

Having the action we have written above, we should now start the one loop computation of the first correction to the Gaussian contribution to the correlation function. This calculation is extremely complex due to the replica structure of the vertices involved. Moreover let us remember that at the end of the computation we should take the limit $m \to 1$. A *crucial* result of [74] is that the perturbative expansion of a replica field theory of the form (2.138) can be mapped to the study of a scalar field theory that satisfies a particular cubic stochastic field equation. To obtain this result it has been introduced a particular transformation of the replicated fields that is reminiscent of the Cardy's treatment of the random field Ising model [37, 38]. Using the techniques developed by Parisi and Sourlas in [146, 144], it can be shown that the solution of this stochastic equation describes also the leading critical behavior of a cubic field theory in a random field.

The action of this *spinodal* field theory is

$$\begin{aligned}S(\varphi) = & \frac{1}{2}\int \mathrm{d}x\, \varphi(x)(-\nabla^2 + m_0^2)\varphi(x) + \frac{g}{6}\int \mathrm{d}x\varphi^3(x) \\ & + \int \mathrm{d}x(h_0(x) + \delta h(g,\Delta))\varphi(x)\end{aligned} \tag{2.139}$$

where $h_0(x)$ is a Gaussian random field with zero mean and variance given by

$$\overline{h_0(x)h_0(y)} = \Delta\delta(x-y) \ , \tag{2.140}$$

The mapping between the coefficients of the replica field theory and the random field theory is the following

$$\begin{aligned} m_0^2 &= \mu\sqrt{\epsilon}/\sigma \ , \\ g &= (w_1 - w_2)/\sigma^{3/2} \ , \\ \Delta &= -(m_2+m_3)/\sigma \ . \end{aligned} \tag{2.141}$$

In the action (2.139) we added a counterterm δh, that will be used to avoid that one loop corrections shift the position of the critical point. The counterterm δh can be seen also as a redefinition of the mean value for the random field h_0. The bare propagator of the theory is, as usual, given by $G_0(p) = (p^2 + m_0^2)^{-1}$.

Let us now write the generating functional of the connected diagrams

$$W[J] = \ln Z[J] \ , \tag{2.142}$$

where $J(x)$ is given by

$$J(x) = h_0(x) + \delta h(g, \Delta) \ . \tag{2.143}$$

We introduce the following diagrammatic notation that will be used soon

(2.144)

so that

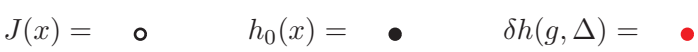

(2.145)

Let us give the diagrammatic expansion for $W[J]$ up to second order in g

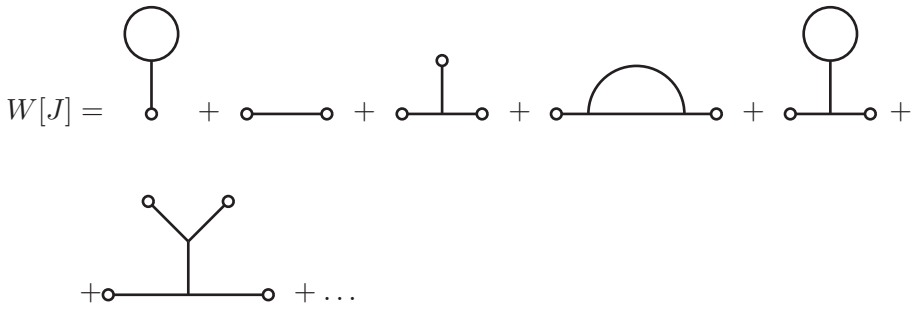

(2.146)

Let us now compute $\langle \varphi(x) \rangle$ up to first order in perturbation theory. If we average over the random field we will have, as usual in these cases, single and doubled propagator [144]. We denote the doubled propagator with a blue dot so that the expansion of $\langle \varphi(x) \rangle$ is given by

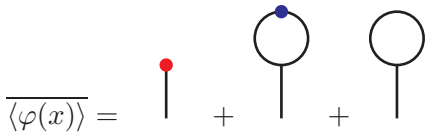

(2.147)

In the previous equation we have assumed that the counterterm δh is proportional to g so that we have retained only the diagrams up to second order in g. This hypothesis must be checked *a posteriori*.

As we have seen in the ferromagnetic case the important point is that we want to make a perturbative expansion in terms of the distance from the true critical

point. We must ensure in this way that it is not shifted so we require $\overline{\langle\varphi(x)\rangle} = 0$. This means that in perturbation theory we have

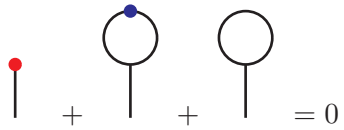

(2.148)

so that we have that $\delta h \propto g$. Now let us focus on the main quantity we want to compute: the two point correlation function. The perturbative expansion gives

$\overline{\langle\varphi(x)\varphi(y)\rangle} = G_0(x-y) +$

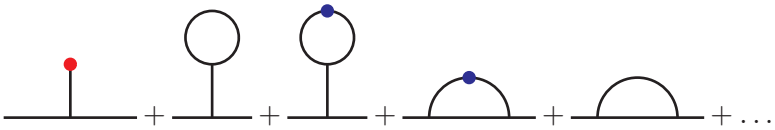

$= G_0(x-y) +$

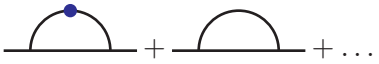

and we have used the result (2.148). Because of the fact that we are interested in the most infrared divergent diagrams we can neglect the second term that is subdominant. However let us note that this diagram is divergent in the ultraviolet regime as soon as $D > 4$. At zero external momentum we have

$$G(p=0) = G_0(p=0) + G_0(p=0)^2 \frac{\Delta g^2}{2} \int^{\Lambda} \frac{\mathrm{d}q}{(2\pi)^D} G_0(q)^3 \ . \tag{2.149}$$

Now we will follow closely the line of reasoning of Sec. 2.2.4. By inverting the relation above we get

$$\begin{aligned} m_R^2 = G^{-1}(p=0) &= m_0^2 - \frac{\Delta g^2}{2} \int^{\Lambda} \frac{\mathrm{d}q}{(2\pi)^D} \frac{1}{(q^2+m_0^2)^3} \\ &= m_0^2 - \frac{\Delta g^2}{2} \int^{\Lambda} \frac{\mathrm{d}q}{(2\pi)^D} \frac{1}{(q^2+m_R^2)^3} \ . \end{aligned} \tag{2.150}$$

The correction to the mass is UV divergent for $D \geq 6$ and leads to a non-universal shift of the critical point that corresponds to

$$m_0^2 = \frac{\Delta g^2}{2} \int^{\Lambda} \frac{\mathrm{d}q}{(2\pi)^D} \frac{1}{q^6} \ . \tag{2.151}$$

We define the distance from the critical point with

$$t = m_0^2 - \frac{\Delta g^2}{2} \int^{\Lambda} \frac{\mathrm{d}q}{(2\pi)^D} \frac{1}{q^6} \ , \tag{2.152}$$

so that Eq. (2.150) becomes

$$m_R^2 = t - \frac{\Delta g^2}{2} \int^{\Lambda} \frac{\mathrm{d}q}{(2\pi)^D} \left(\frac{1}{(q^2+m_R^2)^3} - \frac{1}{q^6} \right) \ . \tag{2.153}$$

The Ginzburg criterion amounts to say the the correction is small so that the mean field result $m_R^2 = t$ is valid. A simpler and completely equivalent (apart from a pre factor) condition can be obtained if we consider the derivative of t with respect to m_R^2 that gives

$$\frac{dt}{dm_R^2} = 1 - 3\frac{\Delta g^2}{2}\int^{\Lambda} \frac{\mathrm{d}q}{(2\pi)^D}\frac{1}{(q^2+m_R^2)^4} \ , \tag{2.154}$$

so that the mean field results will be correct if the second term is smaller than one. This term is convergent in the ultraviolet and divergent in the infrared regime in $D < 8$. In this case a renormalized theory exist and it leads to a universal form of the Ginzburg criterion. Moreover we clearly see that the upper critical dimension is 8 If we send the ultraviolet cutoff to ∞ and we consider the Schwinger representation for the propagator [141]

$$\frac{1}{p^2+m^2} = \int_0^{\infty} \mathrm{d}\alpha\, e^{-\alpha(p^2+m^2)} \ ,$$

by taking the derivative with respect to m_R^2 we obtain

$$\frac{dt}{dm_R^2} = 1 - \frac{\Delta g^2}{4(4\pi)^{D/2}}\Gamma\left(4-\frac{D}{2}\right) m_R^{D-8} \tag{2.155}$$

and finally the Ginzburg criterion

$$1 \gg \frac{g^2\Delta}{4(4\pi)^{D/2}}\Gamma\left(4-\frac{D}{2}\right) m_R^{D-8} \ . \tag{2.156}$$

For $D > 8$ the Ginzburg criterion is not universal because it is strictly dependent on the ultraviolet cutoff. Coming from the mean field region where $\xi = 1/m_R$ we can write

$$1 \gg \mathrm{Gi}\,\xi^{8-D} \ , \qquad \mathrm{Gi} = \frac{g^2\Delta}{4(4\pi)^{D/2}}\Gamma\left(4-\frac{D}{2}\right) \ . \tag{2.157}$$

2.7 Explicit calculations in the Hypernetted Chain approximation (HNC)

All the theory developed up to here is completely general and can be applied in any desired context. However for the practical use it relies on the knowledge of the expression of the the free energy Γ that in general is unknown or not exactly computable. Instead, the general situation is the one in which one has an approximation for Γ. Actually this is good for our purpose because we know that below the transition , up to the transition point, the free energy is not analytic while we want to have an analytic function that can be expanded to obtain a Landau action. However let us remember that the glass transition is discontinuous so that it cannot be obtained in perturbation theory from the liquid state. This means that it is reasonable that if we obtain Γ from a high temperature expansion we need to perform a resumation of an infinite class of diagrams in order to obtain a free energy that admits a non perturbative solution different from the one of the liquid

state. Once a given resummation with non-trivial glassy behavior has been chosen, we will choose it as the mean field approximation of Γ and then we will perform the Landau expansion around the non trivial saddle point solution. At that point we will perform a one loop calculation to see where this approximation is valid and where it fails.

Coming from liquid theory there are many possible schemes that give partial resummation of the diagrammatic expansion for Γ [89]. We will choose the simplest one that is the hypernetted chain approximation (HNC) which amounts to neglect completely the 2PI diagrams that contribute to Γ as it is written in Eq. 2.55. In order to be clear we review here the results of the previous sections in order to apply them to the HNC case

- once the analytic approximation for Γ has been chosen, we need to identify a critical dynamical temperature T_d (or a dynamical density ρ_d) where the off diagonal part $\widetilde{g}$ of the physical correlation defined in Eq. (2.62) jumps from the trivial value $\widetilde{g} = 1$ to a non-trivial function.

- then we need to obtain the zero mode k_0 of the mass operator that we know is developing at the transition point. The zero mode can be extracted from the direct diagonalization of the mass operator defined in Eqs. (2.82) and (2.85). However we have seen that it is actually the lowest eigenvalue of the kernel operator M_1 so that we need to study only this term.

  All this kind of operations are quite involved and a simpler route to extract k_0 exist. In fact once we have the behavior of $\widetilde{g}$ close to the transition point, we can extract the zero mode from Eq. (2.79).

- Once we have the zero mode and the order parameter computed at the transition point, we can easily expand the mean field approximation to Γ. Then we can start to compute all the mean field observables we are interested in. The first one is the exponent parameter λ. Remember that in doing all the calculation we need to introduce a smoothing function f but we have seen that its precise form is irrelevant for this calculation.

- The next step is to look at the gradient expansion for the fluctuations along the zero mode. We will give the expression the masses m_2 and m_3 from Eq. (2.126). The critical part is once again related to the zero mode of M_1, as expressed in Eqs. (2.127) and (2.128). Moreover the other two coefficients μ and σ are given respectively by Eqs. (2.129) and (2.132). From these we have the singular part of the four point correlations, Eq. (2.134), with the dynamical correlation length given in Eq. (2.135) and the f-dependent prefactor given in Eq. (2.136).

- Finally, using the gradient expansion we can perform a one-loop calculation to obtain the Ginzburg number.

Let us underline here that the hypernetted chain approximation is not the better one that we can choose because we know that it gives only qualitatively good results around the dynamical transition point [127, 36, 145]. In fact the quantitative agreement with numerical and experimental data is not good: a classical example

is the prediction of the non-ergodicity factor that turns out to be in disagreement with experiments and numerical simulations. The fact that this approximation is not so good will be confirmed by the prediction of the exponent parameter that is not in agreement with the usual values that can be found in experiments. However we will see in chapter 4 that better approximation schemes give better quantitative results for λ. Moreover we hope that at least the order of magnitude of the Ginzburg number is not affected by the poor quality of the hypernetted chain approximation.

2.7.1 The saddle point equations in HNC

The first thing to do is to identify a dynamical transition point in the HNC approximation. This can be done by looking at the HNC expression of the free energy, taking the first derivative and imposing the saddle point equations. The HNC expression of the free energy is given by

$$\begin{aligned}\Gamma[\rho,\rho^{(2)}] &= \sum_a \int_1 \rho_a(1)\left[\ln\rho_a(1)-1\right] \\ &+ \frac{1}{2}\sum_{a,b}\int_{1,2}\left[\rho^{(2)}_{a,b}(1,2)\ln\left(\frac{\rho^{(2)}_{a,b}(1,2)}{\rho_a(1)\rho_b(2)}\right)-\rho^{(2)}_{a,b}(1,2)+\rho_a(1)\rho_b(2)\right] \\ &+ \frac{1}{2}\sum_{n\geq 3}\frac{(-1)^n}{n}\sum_{a_1,\dots,a_n}\int_{1,\dots,n}\rho_{a_1}(1)h_{a_1a_2}(1,2)\cdots\rho_{a_n}(n)h_{a_na_1}(n,1)\end{aligned} \tag{2.158}$$

and by extremizing we obtain the following equations

$$\ln[h_{ab}(x,y)+1]+\beta\phi_{ab}(x,y) = h_{ab}(x,y)-c_{ab}(x,y) \tag{2.159}$$

$$c_{ab}(x,y) = h_{ab}(x,y) - \sum_{c=1}^{n}\int \mathrm{d}z h_{ac}(x,z)\rho_c c_{cb}(z,y) \tag{2.160}$$

where $\phi_{ab}(x,y)$ is the interparticle potential. The direct correlation function is defined by the replicated Ornstein-Zernike equation that we write here for convenience.

If we look for a translational invariant solution and we search for a replica symmetric solution, we can call $h(x)=h_{a=b}(x)$ and $\tilde{h}(x)=h_{a\neq b}(x)$. The equations above give

$$\ln[h(x)+1]+\beta\phi(x) = h(x)-c(x) \tag{2.161}$$

$$\ln[\tilde{h}(x)+1] = \tilde{h}(x)-\tilde{c}(x) \tag{2.162}$$

$$h(q) = c(q)+\rho\left[h(q)c(q)+(m-1)\tilde{h}(q)\tilde{c}(q)\right] \tag{2.163}$$

$$\tilde{h}(q) = \tilde{c}(q)+\rho\left[h(q)\tilde{c}(q)+c(q)\tilde{h}(q)+(m-2)\tilde{h}(q)\tilde{c}(q)\right] \tag{2.164}$$

and the Ornstein-Zernike equation has been rewritten in Fourier space. The dynamical point is controlled by the limit $m\to 1$ in which the equations become

$$\ln[h(x)+1]+\beta\phi(x) = h(x)-c(x) \tag{2.165}$$

$$\ln[\tilde{h}(x)+1] = \tilde{h}(x)+\tilde{c}(x) \tag{2.166}$$

$$h(q) = c(q)+\rho\left[h(q)c(q)+\tilde{h}(q)\tilde{c}(q)\right] \tag{2.167}$$

$$\tilde{h}(q) = \tilde{c}(q)+\rho\left[h(q)\tilde{c}(q)+c(q)\tilde{h}(q)-\tilde{h}(q)\tilde{c}(q)\right]\ . \tag{2.168}$$

These equations have the desired behavior because they admit the trivial solution $\tilde{h} = 0$ in the high temperature-low density phase and a glassy solution in the low temperature-high density regime. We will now suppose that we know the non-trivial solution to these equations (that can be solved numerically for a given potential) and we will compute the expression of the derivative of the HNC free energy that, it will be assumed, will be computed on that solution.

2.7.2 Derivatives of the free energy

The expansion of the HNC free energy is built upon the derivative of the free energy computed on the glassy solution. Here we will compute the derivative that we need in order to compute the mass term and the cubic interactions of the Landau expansion. In order to be as simple as possible we will first perform the calculation without taking into account the symmetries on the replica and spatial indices, and then, at the end, we will symmetrize our results. We can use the notation $\delta_{ab}(1,2) = \delta_{ab}\delta(x_1 - x_2)$. Let us take the first derivative of the HNC free energy

$$\frac{\delta\Gamma[\rho,\rho^{(2)}]}{\delta\rho^{(2)}_{ab}(1,2)} = \frac{1}{2}\log\left[\frac{\rho^{(2)}_{ab}(1,2)}{\rho_a(1)\rho_b(2)}\right] + \frac{1}{2}\left[c_{ba}(2,1) - h_{ba}(2,1)\right] \ , \tag{2.169}$$

that can be proved using the diagrammatic expansion for the term Γ_{ring} that appears in (2.56). Moreover we have

$$\begin{aligned}\frac{\delta c_{ab}(1,2)}{\delta h_{cd}(3,4)} &= \left[\delta_{ac}(1,3) - \rho_c(3)c_{ac}(1,3)\right]\left[\delta_{db}(4,2) - \rho_d(4)c_{db}(4,2)\right] \\ &= \rho_c(3)\rho_d(4)\Gamma^{(2)}_{ac}(1,3)\Gamma^{(2)}_{db}(4,2)\end{aligned} \tag{2.170}$$

where we have introduced

$$\Gamma^{(2)}_{ab}(1,2) = \frac{1}{\rho_a(1)}\delta_{ab}(1,2) - c_{ab}(1,2) \ . \tag{2.171}$$

It follows that the second derivative of the free energy that gives the mass term is given by

$$\begin{aligned}&\frac{\delta^2\Gamma[\rho,\rho^{(2)}]}{\delta\rho^{(2)}_{ab}(1,2)\delta\rho^{(2)}_{cd}(3,4)} = \frac{1}{2}\left[\frac{\delta_{ac}(1,3)\delta_{db}(4,2)}{\rho^{(2)}_{ab}(1,2)} - \frac{\delta_{ad}(1,4)\delta_{bc}(2,3)}{\rho_a(1)\rho_b(2)}\right] \\ &+ \frac{1}{2}\frac{1}{\rho_c(3)\rho_d(4)}\left[\delta_{bc}(2,3) - \rho_c(3)c_{bc}(2,3)\right]\left[\delta_{da}(4,1) - \rho_d(4)c_{da}(4,1)\right] \\ =&\frac{1}{2}\left[\frac{\delta_{ac}(1,3)\delta_{db}(4,2)}{\rho^{(2)}_{ab}(1,2)} - \frac{\delta_{ad}(1,4)\delta_{bc}(2,3)}{\rho_a(1)\rho_b(2)}\right] + \frac{1}{2}\Gamma^{(2)}_{bc}(2,3)\Gamma^{(2)}_{da}(4,1) \ .\end{aligned} \tag{2.172}$$

The third derivative is computed in the same way and it gives the cubic coeffi-

cients

$$\begin{aligned}
&\frac{\delta^3\Gamma[\rho,\rho^{(2)}]}{\delta\rho^{(2)}_{ab}(1,2)\delta\rho^{(2)}_{cd}(3,4)\delta\rho^{(2)}_{ef}(5,6)} = -\frac{1}{2}\delta_{ac}(1,3)\delta_{db}(4,2)\delta_{ae}(1,5)\delta_{fb}(6,2)\frac{1}{[\rho^{(2)}_{ab}(1,2)]^2}\\
&-\frac{1}{2}\frac{1}{\rho_c(3)\rho_e(5)\rho_f(6)}\left[\delta_{bc}(2,3)-\rho_c(3)c_{bc}(2,3)\right]\frac{\delta c_{da}(4,1)}{\delta h_{ef}(5,6)}\\
&-\frac{1}{2}\frac{1}{\rho_d(4)\rho_e(5)\rho_f(6)}\frac{\delta c_{bc}(2,3)}{\delta h_{ef}(5,6)}\left[\delta_{da}(4,1)-\rho_d(4)c_{da}(4,1)\right]\\
&=-\frac{1}{2}\delta_{ac}(1,3)\delta_{db}(4,2)\delta_{ae}(1,5)\delta_{fb}(6,2)\frac{1}{[\rho^{(2)}_{ab}(1,2)]^2}\\
&-\frac{1}{2}\left[\Gamma^{(2)}_{bc}(2,3)\Gamma^{(2)}_{de}(4,5)\Gamma^{(2)}_{fa}(6,1)+\Gamma^{(2)}_{be}(2,5)\Gamma^{(2)}_{cf}(3,6)\Gamma^{(2)}_{da}(4,1)\right]
\end{aligned} \tag{2.173}$$

The explicit expansion of the free energy around the glassy solution is then $\Delta\Gamma = \Gamma[\rho,\rho^{(2)}] - \Gamma[\rho,\overline{\rho^{(2)}}]$ and inserting the replica symmetric parametrization of this solution we obtain

$$\begin{aligned}
\Delta^2\Gamma &= \frac{1}{4\rho^2}\sum_{a\neq b}\int_{1,2}\left[\frac{1}{\widetilde{g}(1,2)}-1\right][\Delta\rho_{ab}(1,2)]^2\\
&\quad+\frac{1}{4}\sum_{a\neq b,c\neq d}\int_{1,2,3,4}\Delta\rho_{ab}(1,2)\Gamma^{(2)}_{bc}(2,3)\Delta\rho_{cd}(3,4)\Gamma^{(2)}_{da}(4,1)\ ,\\
\Delta^3\Gamma &= -\frac{1}{12\rho^4}\sum_{a\neq b}\int_{1,2}\frac{1}{[\widetilde{g}(1,2)]^2}[\Delta\rho_{ab}(1,2)]^3\\
&\quad-\frac{1}{6}\sum_{a\neq b,c\neq d,e\neq f}\int_{1,2,3,4,5,6}\Delta\rho_{ab}(1,2)\Gamma^{(2)}_{bc}(2,3)\Delta\rho_{cd}(3,4)\\
&\quad\times\Gamma^{(2)}_{de}(4,5)\Delta\rho_{ef}(5,6)\Gamma^{(2)}_{fa}(6,1)\ .
\end{aligned} \tag{2.174}$$

Let us note that Eq. (2.172) and (2.173) are not symetrized, but obviously when they are inserted in the free energy to compute $\Delta^2\Gamma$ and $\Delta^3\Gamma$ they are contracted with symmetric functions so the result is correct. However, in the following section we will have to symmetrize them explicitly in order to insert them in the expressions for the coefficients of the action, where the symmetry properties have been used explicitly.

2.7.3 The mass matrix

Due to the symmetry properties of the saddle point solution in replica space, we have that the mass matrix can be put in the form (2.85) by a proper symmetrization of the indices in Eq. (2.172). The expression of the three kernels that define the

mass term are given by

$$\begin{aligned} M_1(1,2;3,4) &= \frac{1}{2\rho^2}\frac{\delta(1,3)\delta(2,4)}{\tilde{g}(1,2)} - \frac{1}{2\rho}\left[\delta(1,4)\Delta c(2,3) + \delta(2,3)\Delta c(1,4)\right] \\ &\quad + \frac{1}{2}\Delta c(1,4)\Delta c(2,3) \\ M_2(1,2;3,4) &= -\frac{1}{2}\tilde{c}(1,4)\left(\frac{1}{\rho}\delta(2,3) - \Delta c(2,3)\right) - \frac{1}{2}\tilde{c}(2,3)\left(\frac{1}{\rho}\delta(1,4) - \Delta c(1,4)\right) \\ M_3(1,2;3,4) &= \frac{1}{2}\tilde{c}(1,4)\tilde{c}(2,3) \end{aligned} \tag{2.175}$$

where we have defined

$$\Delta c(1,2) = c(1,2) - \tilde{c}(1,2)\ . \tag{2.176}$$

It is important to note that Eq. (2.172) has not been symetrized over spatial indices in such a way that it is invariant under the exchange $1 \leftrightarrow 2$ and $3 \leftrightarrow 4$. In fact this is not required because we will apply this operator only to symmetric functions.

2.7.4 Expression of λ

Let us now consider the cubic terms from which we can obtain the expression for the exponent parameter λ. We need to put Eq. (2.173) into Eqs. (2.105) to obtain w_1 and w_2. However firstly we have to symmetrize Eq. (2.173) with respect to $a \leftrightarrow b$, $c \leftrightarrow d$, $e \leftrightarrow f$, $ab \leftrightarrow cd$, $ab \leftrightarrow ef$, $cd \leftrightarrow ef$ because these properties have been explicitly used to obtain Eqs. 2.105. If fact they are crucial in Eqs. (4.79) and (2.77) As we did for the mass matrix analysis, it is very important to symmetrize over the replica indices while the spatial variables can also not to be symetrized because we will integrate them combined with symmetric functions. Let us write the two terms in Eq. (2.173) underlining the replica structure

$$\begin{aligned} L^{(1)}_{ace,bdf}(1,2;3,4;5,6) &= \delta_{ac}(1,3)\delta_{db}(4,2)\delta_{ae}(1,5)\delta_{fb}(6,2)\frac{1}{[\rho^{(2)}_{ab}(1,2)]^2}\ , \\ L^{(2)}_{bc,de,fa}(1,2;3,4;5,6) &= \Gamma^{(2)}_{bc}(2,3)\Gamma^{(2)}_{de}(4,5)\Gamma^{(2)}_{fa}(6,1)\ . \end{aligned} \tag{2.177}$$

It follows that the once we symmetrized over the replica indices we obtain

$$\begin{aligned} L_{ab,cd,ef} = &-\frac{1}{8}\left(L^{(1)}_{ace,bdf} + L^{(1)}_{acf,bde} + L^{(1)}_{adf,bce} + L^{(1)}_{ade,bcf}\right) \\ &-\frac{1}{8}\left(L^{(2)}_{ac,bf,de} + L^{(2)}_{ac,be,df} + L^{(2)}_{ad,be,cf} + L^{(2)}_{ad,bf,ce}\right. \\ &\left.+L^{(2)}_{ae,bc,df} + L^{(2)}_{ae,bd,cf} + L^{(2)}_{af,bc,de} + L^{(2)}_{af,bd,ce}\right) \end{aligned} \tag{2.178}$$

Now we can use this expression to obtain the two cubic terms that are needed

to compute the exponent parameter

$$
\begin{aligned}
w_2 &= -\frac{1}{16}\frac{1}{(f\star k_0)^3\,V}\int_{1,2;3,4;5,6} k_0(1,2)k_0(3,4)k_0(5,6) \\
&\quad\times \delta(1,3)\delta(2,4)\delta(1,5)\delta(2,6)\left(\frac{1}{\rho^4\tilde{g}^2(1,2)}\right)\,, \\
w_1 &= -\frac{1}{8}\frac{1}{(f\star k_0)^3\,V}\int_{1,2,3,4,5,6} k_0(1,2)k_0(3,4)k_0(5,6) \\
&\quad\times \left[\Gamma(2,3)\Gamma(4,5)(\Gamma(6,1)-3\tilde{\Gamma}(6,1))+(3\Gamma(2,3)-\tilde{\Gamma}(2,3))\tilde{\Gamma}(4,5)\tilde{\Gamma}(6,1)\right]\,,
\end{aligned}
\tag{2.179}
$$

The final expression for the exponent parameter is given by

$$
\lambda = \frac{1}{2}\frac{\int \mathrm{d}r \frac{k_0(r)^3}{\rho^4\tilde{g}(r)^2}}{\int \frac{\mathrm{d}q}{(2\pi)^D}k_0(q)^3\left[\Gamma(q)-\tilde{\Gamma}(q)\right]^3} = \frac{1}{2}\frac{\frac{1}{\rho^4}\int \mathrm{d}r \frac{k_0^3(r)}{\tilde{g}^2(r)}}{\frac{1}{\rho^3}\int \frac{\mathrm{d}q}{(2\pi)^D}k_0^3(q)\left[1-\rho\Delta c(q)\right]^3}\,. \tag{2.180}
$$

2.7.5 Computation of μ and σ

The last part of the theoretical work, before entering in the numerical solution of the HNC equations, is the calculation of the coefficients that appear in the mass matrix in the gradient expansion μ, σ, m_2, m_3. We have that

$$
\begin{aligned}
m_1(p) &= \int \frac{\mathrm{d}q\mathrm{d}k}{(2\pi)^{2D}}k_0(q)M_1^{(p)}(q,k)k_0(k) \\
&= \frac{1}{2\rho^2}\int \mathrm{d}r\frac{k_0^2(r)}{\tilde{g}(r)} - \frac{1}{2\rho}\int \frac{\mathrm{d}q}{(2\pi)^D}k_0^2(q)\left[\Delta c\left(\frac{p}{2}+q\right)+\Delta c\left(\frac{p}{2}-q\right)\right] \\
&+ \frac{1}{2}\int \frac{\mathrm{d}q}{(2\pi)^D}k_0^2(q)\Delta c\left(\frac{p}{2}+q\right)\Delta c\left(\frac{p}{2}-q\right)\,,
\end{aligned}
\tag{2.181}
$$

so that we obtain simply

$$
\mu = \lim_{\epsilon\to 0}\frac{\mathrm{d}m_1(p=0)}{\mathrm{d}\sqrt{\epsilon}}\,. \tag{2.182}
$$

From Eq. (2.79) we see that

$$
\kappa k_0(r) = \lim_{\epsilon\to 0}\sqrt{\epsilon}\frac{\mathrm{d}\tilde{g}(r)}{\mathrm{d}\epsilon} \implies \tilde{g}(r,\epsilon) = \tilde{g}(r,0) + 2\sqrt{\epsilon}\kappa k_0(r) + O(\epsilon)\,. \tag{2.183}
$$

so that, by using the Ornstein-Zernike equation we get

$$
g(q) - \tilde{g}(q) = \frac{\Delta c(q)}{1-\rho\Delta c(q)}\,, \tag{2.184}
$$

from which

$$
\begin{aligned}
\tilde{c}(q,\epsilon) &= \tilde{c}(q,0) + \sqrt{\epsilon}c_0(q) + O(\epsilon) \\
c_0(q) &= \lim_{\epsilon\to 0}\frac{\mathrm{d}\tilde{c}(q)}{\mathrm{d}\sqrt{\epsilon}} = 2\kappa k_0(q)\left[1-\rho\Delta c(q)\right]^2\,.
\end{aligned}
\tag{2.185}
$$

It follows that the expression for the coefficient μ is given by

$$\mu = -\frac{\kappa}{\rho^2}\int \mathrm{d}r \frac{k_0^3(r)}{\tilde{g}^2(r)} + \frac{2\kappa}{\rho}\int \frac{\mathrm{d}q}{(2\pi)^D} k_0^3(q)\left[1-\rho\Delta c(q)\right]^3 \tag{2.186}$$

and σ is given by

$$\sigma = \lim_{\epsilon\to 0} \left.\frac{\mathrm{d}m_1(p)}{\mathrm{d}p^2}\right|_{p=0} . \tag{2.187}$$

The last expression can be computed using

$$\begin{aligned} f\left(\left|\frac{p}{2}+q\right|\right) \simeq f(q) + \frac{1}{2}\frac{f'(q)}{q}(q\cdot p) \\ + \frac{1}{2}\left[\frac{1}{4}\frac{f''(q)}{q^2}(q\cdot p)^2 + \frac{1}{4}\frac{f'(q)}{q}p^2 - \frac{1}{4}\frac{f'(q)}{q^3}(q\cdot p)^2\right] \end{aligned} \tag{2.188}$$

so that σ becomes finally

$$\sigma = \frac{1}{8\rho}\int \frac{\mathrm{d}q}{(2\pi)^D} k_0^2(q)\left[\rho\Delta c(q)-1\right]\left[\left(\Delta c''(q) - \frac{\Delta c'(q)}{q}\right)\cos^2\theta + \frac{\Delta c'(q)}{q}\right] \tag{2.189}$$

$$-\frac{1}{8}\int \frac{\mathrm{d}q}{(2\pi)^D} k_0^2(q)\left(\Delta c'(q)\right)^2\cos^2\theta \tag{2.190}$$

where we have introduced the angle θ between the D-dimensional vector q and one of the axis of the D-dimensional hyperplane. In three dimensions we obtain

$$\sigma = \frac{1}{48\pi^2}\int_0^\infty \mathrm{d}q\, k_0^2(q)\left\{\frac{1}{\rho}\left[\rho\Delta c(q)-1\right]\left[q^2\Delta c''(q) + 2q\Delta c'(q)\right] - q^2\left(\Delta c'(q)\right)^2\right\} . \tag{2.191}$$

Finally the parameters m_2 and m_3 are given by

$$\begin{aligned} m_2 &= -\int \frac{\mathrm{d}q}{(2\pi)^D} k_0^2(q)\tilde{c}(q)\left[\frac{1}{\rho} - \Delta c(q)\right] \\ m_3 &= \frac{1}{2}\int \frac{\mathrm{d}q}{(2\pi)^D} k_0^2(q)\tilde{c}^2(q) . \end{aligned} \tag{2.192}$$

2.7.6 Numerical results

We will now describe how we have obtained the numerical results for the quantities we are going to list in Tab. 2.1, 2.2.

We focused on the three dimensional case. In this case the HNC saddle point equations can be solved using a standard iteration scheme so that the solution of the equations is seen as a fixed point of the iteration. At high temperature/low density only the trivial non-glassy solution appears while when we lower the temperature or increase the density and we start from a suitable initial guess for the off diagonal element $\widetilde{g}$ of the parametrization of the two point correlation matrix, then a non-trivial glassy solution appears. Because we have seen that the quantities we want to compute depend critically on the zero mode, and because we have seen that the latter can be computed from the behavior of $\widetilde{g}$ nearby the critical point, once we have determined the position of the critical point we have analyzed the behavior of $\widetilde{g}$

System	T	ρ_d	$-w_1$	$-w_2$	m_2	m_3	σ	μ	λ	ξ_0	G_0	Gi
SS-6	1	6.691	$3.88{\cdot}10^{-6}$	$1.35{\cdot}10^{-6}$	-0.000925	0.000110	0.000195	0.000525	0.348	0.601	224	0.0267
SS-9	1	2.912	0.0000772	0.0000272	-0.00539	0.000633	0.00163	0.00543	0.353	0.548	34.3	0.0125
SS-12	1	2.057	0.000275	0.0000973	-0.0116	0.00132	0.00378	0.0152	0.354	0.498	14.2	0.0118
LJ	0.7	1.407	0.00106	0.000376	-0.0258	0.00290	0.00989	0.0414	0.355	0.489	6.00	0.00833
HarmS	10^{-3}	1.336	0.00129	0.000465	-0.0336	0.00343	0.00772	0.0779	0.359	0.315	2.82	0.0434
HarmS	10^{-4}	1.196	0.00165	0.000622	-0.0403	0.00386	0.00819	0.109	0.378	0.274	1.69	0.0632
HarmS	10^{-5}	1.170	0.00174	0.000663	-0.0416	0.00395	0.00845	0.109	0.382	0.278	1.66	0.0635
HS	0	1.169	0.00174	0.000664	-0.0418	0.00397	0.00847	0.108	0.381	0.280	1.67	0.0639

Table 2.1. Numerical values of the coefficients of the effective action and the physical quantities from the HNC approximation. For each potential, lengths are given in units of r_0 and energies in units of ε, with $k_B = 1$. Data at fixed temperature, using density as a control parameter with $\epsilon = \rho_d - \rho$. The data are taken from [68].

System	ρ	T_d	$-w_1$	$-w_2$	m_2	m_3	σ	μ	λ	ξ_0	G_0	Gi
LJ	1.2	0.336	0.00186	0.000663	-0.0361	0.00403	0.0147	0.0572	0.356	0.507	4.56	0.00730
LJ	1.27	0.438	0.00153	0.000541	-0.0321	0.00370	0.0128	0.0447	0.353	0.536	5.74	0.00771
LJ	1.4	0.684	0.00108	0.000383	-0.0260	0.00293	0.0100	0.0292	0.355	0.586	8.52	0.00825
WCA	1.2	0.325	0.00195	0.000686	-0.0389	0.00426	0.0133	0.0607	0.351	0.467	4.37	0.0134
WCA	1.4	0.692	0.00111	0.000388	-0.0270	0.00301	0.00966	0.0291	0.350	0.576	8.67	0.0106

Table 2.2. Numerical values of the coefficients of the effective action and the physical quantities from the HNC approximation. For each potential, lengths are given in units of r_0 and energies in units of ε, with $k_B = 1$. Data at fixed density, using temperature as a control parameter with $\epsilon = T_d - T$. The data are taken from [68].

when approaching the dynamical transition from the glass phase. In particular the zero mode is obtained from a numerical derivative of $\widetilde{g}$ with respect to the control parameter (namely the temperature or the density). By using directly Eq. 2.79. We check the the calculation of the zero mode is consistent by computing it for two slightly different densities or temperatures very close to the dynamical point in order to see that it does not depend on the density if we are sufficiently close to the transition. Moreover the dynamical point is obtained by fitting the derivative of $\widetilde{g}$ with the square root behavior.

In Fig. 2.2 we show the typical shape for the zero mode and $\widetilde{g}$. Both quantities are given in real and Fourier space.

We considered different microscopic pairwise potential of monodisperse systems. The models we used are

- Hard spheres (HS):

$$v(r) = \begin{cases} \infty & \text{if } r < r_0 \\ 0 & \text{if } r > r_0 \end{cases} , \tag{2.193}$$

- Harmonic spheres (HarmS):

$$v(r) = \begin{cases} \varepsilon(1 - r/r_0)^2 & \text{if } r < r_0 \\ 0 & \text{if } r > r_0 \end{cases} , \tag{2.194}$$

  for various temperatures (note that for $\beta \to \infty$ this potential reduces to the hard-spheres potential),

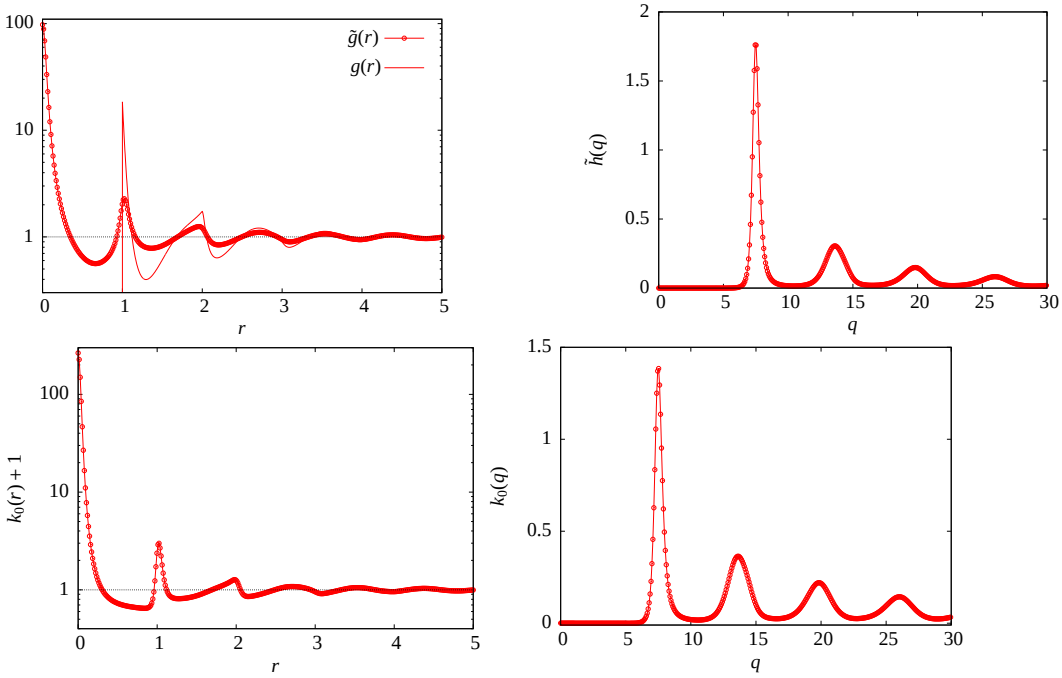

Figure 2.2. Off-diagonal correlations and the zero mode, all computed at ρ_d for hard spheres in $D = 3$. The data are taken from [68].

- Lennard-Jones (LJ):

$$v(r) = 4\varepsilon \left[\left(\frac{r_0}{r} \right)^{12} - \left(\frac{r_0}{r} \right)^{6} \right], \tag{2.195}$$

- Weeks-Chandler-Andersen (WCA):

$$v(r) = 4\varepsilon \left[\left(\frac{r_0}{r} \right)^{12} - \left(\frac{r_0}{r} \right)^{6} + \frac{1}{4} \right] \theta(r_0 2^{1/6} - r), \tag{2.196}$$

- Soft-spheres (SS):

$$v(r) = \varepsilon \left(\frac{r_0}{r} \right)^{n} \tag{2.197}$$

  for $n = 6, 9, 12$.

for these models the length are measured in terms of the particle diameter that is r_0 while and the temperatures in unit of the energy scale of the potential ε. Note that for Hard-Spheres temperature is irrelevant and for soft spheres temperature and density are not independent so that we use the density as the control parameter that drives the transition.

By computing all the quantities very closely to the dynamical point, we can obtain

- The value of λ given by Eq. (2.180).

- The prefactor $\xi_0 = \sqrt{\sigma/\mu}$ of the correlation function $\xi = \xi_0 \epsilon^{-1/4}$, see Eq. (2.135).
- The prefactor of the divergent part of the four point correlation function G_{th} as given in Eq. (2.136).
- The prefactor of the Ginzburg criterion given by Eqs. (2.157) and (2.141).

Moreover let us note that the prefactor of the divergent part of the thermal four point correlation function depends on the smoothing function f. Here we have chosen a box function

$$f(x) = (2A)^{-D} \prod_{i=1}^{D} \theta(A^2 - x_i^2) \ , \tag{2.198}$$

where $\theta(x)$ is the Heaviside step function. We choose $A = 0.1 r_0$. The results are collected in the Tab.s 2.1, 2.2 We underline that the zero mode computed numerically includes the prefactor κ. However all the physical quantities λ, ξ_0, G_0, Gi, are independent of this normalization as of f. All the other quantities are multiplied by a factor κ-dependent. The numerical calculations depend on the cutoffs, ultraviolet and infrared, that are needed to discretize the functions that appear in the HNC equations. We note that they are significant altering the results on our predictions within 10^{-3}.

We have not done a systematic analysis of the cutoff dependance because the numerical precision we have is enough to compare our results with the experiments where the exact value of the quantities studied is affected by the difficulty of accessing the critical region close to the glass transition. We remark that our numerical result for $\lambda \approx 0.35$ is quite bad if compared with the common value $\lambda \approx 0.7$ that is obtained in experiments and well reproduced by mode-coupling theory [10, 9, 84]. However we have underlined before that it is well known that the HNC approximation is not a very good approximation to produce accurate quantitative results [145]. Finally in order to compare our results for the other quantities we computed we note that not many experimental data are available in the first β regime and it would be very welcome if these prediction could be compared by some experiments. The only simulation data we found are reported in [161] and we checked that our results are roughly consistent with them.

2.8 Conclusions and perspectives

In this chapter we have studied the replica approach to the critical dynamical correlations in the β regime for structural glass models. The difference with respect to mean field schematic models is that the spatial structure complicates all the analysis. We have been able to produce a Landau free energy that has been used to obtain the critical part of the four point correlation functions. Moreover we have used this action as the starting point to make a one loop calculation that is able to predict the regions of validity of the Gaussian approximation. All the theory is based on the presence of a zero mode in the spectrum of the kernel operator that defines the Gaussian part of the Landau free energy. This eigenvector is the one

responsible for the dynamical criticality of the correlations we computed. In replica language it is the structural glass counterpart of the replicon eigenmode of the Hessian matrix in replica space for schematic models. Moreover, based on some results obtained for schematic models, we were able to compute the general expression for the mode-coupling exponent parameter from replica theory.

All the theory developed is very general. To produce quantitative results we analyzed a particular simple mean field approximation for the free energy which is the Hypernetted Chain approximation where we were able to find the expressions for all the critical quantities we are interested in.

Let us underline here that the theory above is valid only in the β regime. This means that it gives predictions only for the fluctuations of the dynamical correlation function for times such that this correlator is close to its plateau value. . We do not know if these results can be extended to the α regime where the dynamical correlation decays from the plateau. The main problem in addressing the dynamical fluctuations in the α regime is that we do not have a replica prescription to compute the quantities we are interested in. However, recently, a very nice work has been done in this direction [72]. Starting from the assumption that the dynamics in the α regime is a quasi equilibrium exploration process of metastable states, we are now able to give a replica prescription to study the α regime. This will be discussed in the next chapter. Another point to discuss is how to go beyond mean field results. First of all it is not clear if the results on the RFIM recently obtained in [167, 168, 171, 172] apply to the structural glass case at the dynamical transition. Moreover we should take into account activated processes. Instantons will probably the key tool to extend the approach to the finite dimensional case. This is left for future work.

Chapter 3

The Boltzmann Pseudodynamic approach to long time dynamics

In this chapter we will start by reviewing the potential method that was introduced by Franz and Parisi in [69]. The potential method is a powerful tool in glass physics and it relies on the key idea that for these systems the relevant order parameter is the overlap between configurations. The potential is nothing but the large deviation function for the overlap. However originally it has been introduced to look at equilibrium physics of glasses. In this chapter, after reviewing the original construction, we will introduce a first generalization that is able to use this construction also to study off-equilibrium and aging situations and we will see how we can obtain informations on the aging dynamics from this generalized construction.

We will then introduce the main subject of this chapter that is a further generalization of the potential method that is called the Boltzmann Pseudodynamics [72]. This new construction is capable to obtain the dynamical equations of a glassy system in the long time α regime. We will prove firstly that it gives the correct results for the p-spin spherical model with $p > 2$; then we will consider the structural glass case and we will focus on the simplest setting that is the replicated liquid theory. We will derive a dynamical version of the Ornstein-Zernike equations and we will use the Hypernetted Chain approximation in order to close them self consistently. The result will be a set of mode-coupling equations that will be solved both in the equilibrium and the aging regime. We will compute the associated mode-coupling exponent parameter λ and the fluctuation-dissipation ratio. A first draft of this work is in [76].

3.1 The Potential Method

The potential method has been introduced firstly by Franz and Parisi in a series of work [69, 70]. In this approach one is interested in the study of the free energy of a system that is constrained to be at a fixed overlap with a reference one whose configurations are extracted according to the Bolzmann-Gibbs measure. In other words, this potential is nothing but the large deviation function for the overlap that here plays the central role of the order parameter. This potential is a key tool both in spin-glass models and in structural glasses. The importance relies in the fact

that while the replica method is clearly applicable in spin glass systems where the overlap as an order parameter emerges quite naturally, in structural glass models it is not clear how the overlap emerges in the static treatment. The potential method approach is pragmatic. The basic assumption is that if the relevant order parameter is the overlap then we must be able to construct a large deviation function for it.

In order to define an overlap we need two configurations and a natural way to define the potential is then

$$V(q) = \lim_{N\to\infty} -\frac{1}{\beta N} \sum_{\underline{\tau}} \frac{e^{-\beta H[\underline{\tau}]}}{Z(\beta)} \ln \sum_{\underline{\sigma}} e^{-\beta H[\underline{\sigma}]} \delta\left(q - Q(\underline{\sigma}, \underline{\tau})\right) \tag{3.1}$$

$$Z(\beta) = \sum_{\underline{\tau}} e^{-\beta H[\underline{\tau}]} \tag{3.2}$$

where $H[\underline{\tau}]$ is the Hamiltonian of the system and $Q(\underline{\sigma}, \underline{\tau})$ is a proper definition of the overlap. Note that here the notation is quite general in the sense that $\underline{\sigma}$ can be both a spin configurations in the case we are treating spin glasses and a set of positions for the particles if we are playing with structural glass systems. Even the definition of the overlap function is left free in order to be adapted both to the spin glass and the structural glass case. By looking directly at the expression of the potential we immediately see that even if the model is without quenched disorder in the Hamiltonian, a natural quenched disorder is clearly introduced. In fact the first system, the one whose configurations are indicated with $\underline{\tau}$, acts as a quenched disorder for the system $\underline{\sigma}$.

Here we will give a qualitative description of how the shape of the potential is. We will leave the explicit computation of the potential for the next section where its off-equilibrium generalization will be given and computed. The shape of the potential can be understood on the following ground. At high temperature the system is in its paramagnetic phase and the reference configuration and the constrained one will be extracted from the global paramagnetic minimum of the free energy landscape. Two configurations that belong to this minimum are uncorrelated and the overlap between the two will be zero. This implies that the shape of the potential will be a convex function with a global minimum in $q = 0$. When we lower the temperature, at some point, the dynamical point T_d, the system starts to develop metastable glassy states. These states are represented by local minima in the free energy landscape. This implies that the reference system below the dynamical temperature, will be in one of the many (exponential) metastable states. The constrained configuration will be able to be in the same metastable state of the reference configuration or in a different one. In the first case the overlap between two typical configurations will be different from zero while in the second case it will be zero. This implies that at the dynamical point a local minimum at $q > 0$ in the shape of the potential will appear.

However if the temperature is greater then the Kauzmann point T_K, the local minimum at $q > 0$ is metastable while at the Kauzmann point it will become the global one. The interpretation of this fact goes as follows. The key point is that we have said that in a glassy system there is an exponential (in the size of the system and at the mean field level) number of metastable states. This implies that the system at equilibrium will select a metastable state not only according to its free

energy but also according on how much this metastable state will be typical among all the other states. In other words, the number of metastable states will play a role; let us see how.

The shape of the potential for different temperature is reported in fig. 3.1 In the

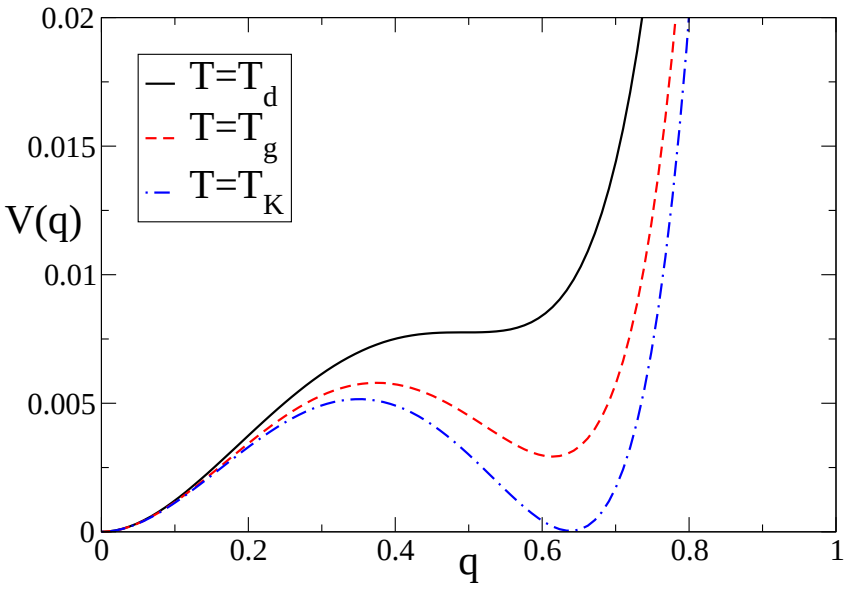

Figure 3.1. The potential as a function of the overlap for different temperatures.

figure we have not plotted exactly the potential but we have plotted $V(q,T) - F(T)$ where $F(T)$ is the free energy density of a system that is unconstrained (or in other words $F(T) = \int \mathrm{d}q V(q,T)$. Let us analyze what happens at the local minimum for $T \in [T_K, T_d]$. In this regime, the potential is nothing but the free energy of the equilibrium TAP metastable states that dominate the measure. We indicate this free energy with $f^*(T)$. Then, because of the fact that

$$F(T) = f^*(T) - T\Sigma(f^*(T)) \tag{3.3}$$

where $\Sigma(f^*(T))$ is the complexity of the states that dominate the measure, we have that the height of the local minimum of the potential is

$$V(q_{min}(T), T) - F(T) = T\Sigma(f^*(T)) \tag{3.4}$$

so that from the shape of the potential we can compute the complexity of the equilibrium metastable states. In this way it is clear why the Kauzmann point is identified with the temperature at which the height of the local minimum is equal to the height in the minimum at $q = 0$. In fact in this case the complexity of the equilibrium states becomes exactly zero and the ideal glass transition is reached.

However here we make an important remark. Suppose that we have a model that is described exactly by the picture we have shown up to now. Moreover suppose

that we can solve separately the dynamics and the potential method. It will turn out that at the dynamical point, the dynamical correlation function will develop a plateau and the potential will develop a saddle. However the value of q at which the saddle is developed is exactly equal to the height of the dynamical correlation function at the plateau. If we think that when we are asymptotically close to the dynamical point, the plateau value of the correlation function is the first point of the long time relaxation, we can think that the potential gives us the first point of the long time relaxation of the dynamical correlation function. This observation goes in the direction that with the potential method we can understand how the dynamics samples phase space in the long time regime and actually it is one of the observations that are at the basis of the Boltzmann Pseudodynamics construction that will be introduced quite soon in this chapter.

Let us conclude this section by underlining that the statements above are valid at the mean field level. What happens in the non mean field region is different. In particular, what is expected is that in finite dimensional systems the potential should be convex. In fact true metastability can exist only in infinite dimensional models while in finite dimensions, nucleation should destroy the pure dynamical transition leaving only a phenomenological dynamical crossover. In this way one expects as in standard first order phase transitions that a Maxwell construction should be found. However, even if the dynamical transition is destroyed by nucleations the situation is more controversial at the Kauzmann point where a true thermodynamic transition could be present.

3.2 The potential method for non equilibrium states

In this section we will introduce a generalization of the potential method to study non equilibrium TAP states. This generalization is a hybrid combination of the Monasson real replicas method with the standard potential that has been introduced in the previous section. In fact we can use the real replica method to select the TAP states that dominate the reference measure and then let the slave system to fall into them. To do this let us introduce the following potential

$$\begin{aligned} V(\tilde{p},\beta,m) = -\lim_{N\to\infty}\frac{1}{\beta N}\mathbf{E}_J\frac{1}{Z_m}\sum_{\underline{\sigma}^{(1)}}\dots\sum_{\underline{\sigma}^{(m)}} e^{-\beta\sum_{a=1}^{m}H[\underline{\sigma}^{(a)}]}\times \\ \times\ln\left[\sum_{\underline{\tau}} e^{-\beta H[\underline{\tau}]}\delta\left(\tilde{p}-q(\sigma^{(1)},\tau)\right)\right] \end{aligned} \tag{3.5}$$

where $\mathbf{E}_J$ is the average over the quenched disorder (if it is present) and

$$Z_m = \sum_{\underline{\sigma}^{(1)}}\dots\sum_{\underline{\sigma}^{(m)}} e^{-\beta\sum_{a=1}^{m}H[\underline{\sigma}^{(a)}]+\epsilon\sum_{a<b}q(\underline{\sigma}^{(a)},\underline{\sigma}^{(b)})} \tag{3.6}$$

and the m replicas σ are virtually coupled with an infinitesimal coupling ϵ (that will be hidden from now on) that will play the role of the replica symmetry breaking field. We see that the standard potential is just the special case $m = 1$. Here we want to use the freedom to choose m in such a way that the measure of the reference replicas will peaked on the TAP states that we want to study.

Suppose now that we choose $T \in [T_K, T_d]$. Then we know that the standard potential will have a local stable minimum at an overlap greater then zero. This minimum will correspond to the equilibrium TAP states that dominate the measure of the reference configuration. We know that at fixed temperature we have a set of metastable TAP states that differ according to their complexity. We want to prove that if we decrease m, we will change the shape the potential in such a way that when we reach the threshold states at that temperature, the generalized potential will have saddle instead of a minimum. Let us be more precise. Let us introduce the effective temperature $T' = T/m$. Then we want to show that if we lower the value of m at some value $m_{th}(T)$ the local minimum will become a saddle as depicted in fig. 3.2. The statement here is that the value of m_{th} coincides with the fluctuation-

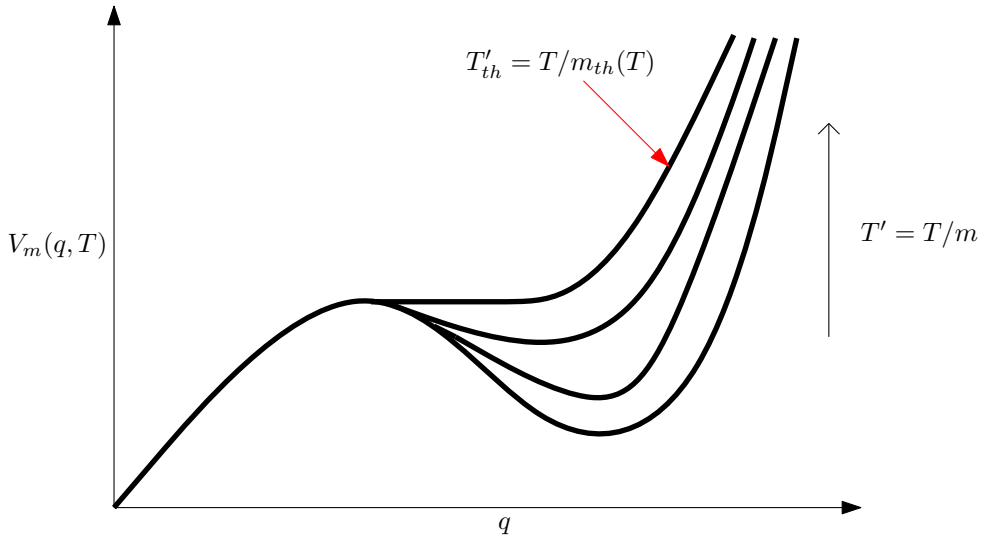

Figure 3.2. The off equilibrium potential as a function of the overlap at a fixed temperature $T \in [T_k, T_d[$ for different values of the Parisi breaking point m .

dissipation ratio that can be computed by solving the aging dynamics of the model. Here we will prove this statement in the framework of the p-spin spherical model. However let us point out a remarkable fact. This statement is valid whenever the 1RSB picture is exact or whenever we are dealing with a 1RSB approximation. If the system undergoes a Gardner transition the situation will change and up to now a lot of work is in progress in order to extend this kind of phenomenology within a fullRSB approach. We will see what happens at the static level in chapter 4 where exactly this problem will appear.

Let us start the computation of this off-equilibrium potential by using the replica method. We have

$$V(\tilde{p},\beta,m) = -\lim_{N\to\infty}\lim_{n\to 0}\lim_{s\to m}\frac{1}{\beta N n}\times$$
$$\times\frac{\partial}{\partial s}\mathbf{E}_J\left\{\left[\sum_{\underline{\sigma}^{(1)}}\cdots\sum_{\underline{\sigma}^{(m)}} e^{-\beta\sum_{a=1}^{m}H[\underline{\sigma}^{(a)}]}Z[\tilde{p},\beta,\underline{\sigma}^{(1)}]^{s-m}\right]^n\right\} \tag{3.7}$$

where

$$Z[\tilde{p},\beta,\underline{\sigma}^{(1)}] = \sum_{\underline{\tau}} e^{-\beta H[\underline{\tau}]}\delta\left(\tilde{p} - q(\underline{\sigma}^{(1)},\underline{\tau})\right) . \tag{3.8}$$

By introducing replicas and averaging over the couplings we obtain that

$$V = -\lim_{N\to\infty}\lim_{n\to 0}\lim_{s\to m}\frac{1}{\beta N n}\frac{\partial}{\partial s}\int\left\{\mathrm{d}\hat{Q}\right\}e^{Nf(\hat{Q})} \tag{3.9}$$

and

$$f(\hat{Q}) = \frac{\beta^2}{4}\sum_{a,b=1}^{s}\sum_{\alpha,\beta=1}^{n}\hat{Q}^p_{\alpha a,\beta b} + \frac{1}{2}\mathrm{Tr}\ln\hat{Q} . \tag{3.10}$$

At this point we make the following ansatz

$$\hat{Q}_{\alpha a,\beta b} = \delta_{\alpha\beta}Q_{ab} \tag{3.11}$$

and this implies

$$V = -\frac{1}{\beta}\lim_{s\to m}\frac{\partial}{\partial s}f(Q^*) \tag{3.12}$$

where Q^* is the particular value of Q that satisfies the saddle point condition. The ansatz simply tells that replicas belonging to different blocks are uncorrelated and only the groups of s replicas are correlated. Moreover we use a replica-symmetric ansatz that tells that the matrix Q can be decomposed in the following way

$$Q = \begin{pmatrix} A & B \\ B^T & D \end{pmatrix} \tag{3.13}$$

where A is an $m\times m$ matrix that is given by

$$A_{ab} = \delta_{ab} + (1-\delta_{ab})q \tag{3.14}$$

and D is a $(s-m)\times(s-m)$ matrix

$$D_{ab} = \delta_{ab} + (1-\delta_{ab})r . \tag{3.15}$$

The off-diagonal blocks are given by

$$B_{ab} = \tilde{p}\delta_{a1} + (1-\delta_{a1})p \tag{3.16}$$

where B is a $m\times(s-m)$ matrix (m being the number of rows).

Now we have to put the parametrization (3.13) into the expression for f and then compute the saddle point equations in order to obtain Q^*. By looking directly at the expression of the function f we realize that the only problematic term is the computation of the trace-log term, namely the computation of the determinant of the overlap matrix Q. The determinant of Q can be computed according the following formula

$$\det Q = (\det A)\det\left(D - (B^T)A^{-1}B\right) . \tag{3.17}$$

The inverse of the matrix A is given by

$$A^{-1} = x\delta_{ab} + (1-\delta_{ab})y \tag{3.18}$$

where

$$\begin{aligned} x &= \frac{1-2q+mq}{(1-q)(1+(m-1)q)} \\ y &= \frac{q}{(q-1)(1+(m-1)q)} \,. \end{aligned} \tag{3.19}$$

At this point it is easy to compute

$$\left(A^{-1}B\right)_{ab} = \hat{\alpha}\delta_{a1} + (1-\delta_{a1})\hat{\beta} \tag{3.20}$$

where

$$\begin{aligned} \hat{\alpha} &= \tilde{p}x + (m-1)py \\ \hat{\beta} &= xp + \tilde{p}y + (m-2)py \end{aligned} \tag{3.21}$$

and finally

$$\left((B^T)A^{-1}B\right)_{ab} = \hat{\gamma} \tag{3.22}$$

where

$$\hat{\gamma} = \tilde{p}\hat{\alpha} + (m-1)p\hat{\beta} \,. \tag{3.23}$$

In the end we have to evaluate the determinant of the matrix A that is given by [48, 181]

$$\det A = (1-q)^{m-1}\,(1+(m-1)q) \tag{3.24}$$

and the determinant of the matrix

$$\left[D - B^T A^{-1} B\right]_{ab} = \hat{x}\delta_{ab} + \hat{y}(1-\delta_{ab}) \qquad \hat{x} = 1-\hat{\gamma} \quad \hat{y} = r-\hat{\gamma} \tag{3.25}$$

that is given by

$$\det\left[D - B^T A^{-1} B\right] = \hat{x}^{s-m}\left(1-\frac{\hat{y}}{\hat{x}}\right)^{s-m-1}\left[1+(s-m-1)\frac{\hat{y}}{\hat{x}}\right] \tag{3.26}$$

so that we get

$$\begin{aligned} \det Q = (1-q)^{m-1}\,(1+(m-1)q)\,\hat{x}^{s-m}\left(1-\frac{\hat{y}}{\hat{x}}\right)^{s-m-1} \times \\ \times\left[1+(s-m-1)\frac{\hat{y}}{\hat{x}}\right] \,. \end{aligned} \tag{3.27}$$

The final expression for $f(Q)$ is given by

$$\begin{aligned} f(Q) = \frac{\beta^2}{4}\,(s + m(m-1)q^u + 2\tilde{p}^u(s-m) + 2p^u(s-m)(m-1) + \\ +(s-m)(s-m-1)r^u) + \frac{1}{2}\ln\det Q \,. \end{aligned} \tag{3.28}$$

At this point we want to search for a stationary point solution for the potential. We want to solve the following equation

$$0 = \frac{\mathrm{d}V[\tilde{p},m,\beta]}{\mathrm{d}\tilde{p}} = -\frac{\mathrm{d}}{\mathrm{d}\tilde{p}}\lim_{s\to m}\frac{\partial}{\partial s}f[\tilde{p},\{q_i(\tilde{p},m,s)\},m,s,\beta] \tag{3.29}$$

where $q_1 = q$, $q_2 = p$ and $q_3 = r$ and they are just a relabeling of the variables. One has to observe that the subsystem composed by the first m replicas is independent from all the other replicas while the other replicas clearly depend on the first m replicas. In order to show this point let us introduce the variable $t = s - m$. The potential can be rewritten as

$$0 = V[\tilde{p}, m, \beta] = -\lim_{t\to 0} \frac{\partial}{\partial t} f[\tilde{p}, \{q_i(\tilde{p}, m, t)\}, m, t, \beta] \tag{3.30}$$

where in principle we should write $f[\tilde{p}, \{q_i(\tilde{p}, m, t+m)\}, m, t+m, \beta]$ in order to be coherent with the previous notation but we have used a simplified notation. Because we are looking at the limit $t \to 0$ we can expand the function f at the first order in t at fixed parameter $\{q_i\}$ and $\tilde{p}$. We have

$$f[Q] = f_0[q_1, m, \beta] + t f_1[\tilde{p}, \{q_i\}, m, \beta] \tag{3.31}$$

where we used the fact that by construction f_0 cannot depend on all the parameters except from q_1 and m (and actually is the replicated free energy in 1RSB ansatz of the Monasson method). The two functions above are defined by

$$\begin{aligned} f_0[q_1, m, \beta] &= f[Q]|_{t=0} \\ f_1[\tilde{p}, \{q_i\}, m, \beta] &= \left.\frac{\partial f[Q]}{\partial t}\right|_{t=0} . \end{aligned} \tag{3.32}$$

At the lowest order in t the saddle point equations for the parameter q_i are given by

$$0 = \frac{\partial [f_0 + t f_1]}{\partial q_i} . \tag{3.33}$$

The solution can be written as

$$q_i(\tilde{p}, m, t, \beta) = q_i^*(\tilde{p}, m, \beta) + \mathcal{O}(t) . \tag{3.34}$$

From the saddle point we see that q_1^* satisfies the equation

$$0 = \frac{\partial f_0}{\partial q_1} \implies \frac{q_1}{(q_1 - 1)(1 + (m-1)q_1)} + \frac{\beta^2 u}{2} q_1^{u-1} = 0 \tag{3.35}$$

and its solution is *independent* on $\tilde{p}$. The parameters q_2^* and q_3^* satisfy the equations

$$0 = \left.\frac{\partial f_1}{\partial q_{2,3}}\right|_{q_1 = q_1^*(m)} . \tag{3.36}$$

At this point we want to put the solutions (3.34) inside the expression of $f[Q]$. We see that the terms proportional to t for the solution of the saddle point equations give rise to terms of order t^2 in the expansion for $f(Q)$. This is quite simple to see for the parameters $q_{2,3}$ but it is less intuitive for q_1. However it can be easily see that because of the equation (3.35) we have that the correction for the f_0 term is of order t^2 too. This is actually a very general feature. If a saddle point equation is

corrected by a small part of order ϵ than the functional from where it comes from is corrected at the order ϵ^2 [1].

Now we want to select the stationary points of V that are also saddles. First of all let us discuss the stationarity equation.

$$0 = \frac{\mathrm{d}V[\tilde{p}, m, \beta]}{\mathrm{d}\tilde{p}} = -\frac{\mathrm{d}f_1[\tilde{p}, q_1^*(m), q_{2,3}^*(\tilde{p}, m), m, \beta]}{\mathrm{d}\tilde{p}} \,. \tag{3.37}$$

Because of the fact that $q_{2,3}^*$ are solutions of the saddle point equations (3.36) this equation is equivalent to the requirement that the gradient vector of f_1 computed at $q_1^*(m)$ vanishes

$$\nabla f_1[\tilde{p}, q_1^*(m), q_{2,3}, m, \beta] = \left(\frac{\partial f_1}{\partial \tilde{p}}, \frac{\partial f_1}{\partial q_2}, \frac{\partial f_1}{\partial q_3}\right) = 0 \,. \tag{3.38}$$

It can be seen by inspection that a replica symmetric solution for these equation exist and it is

$$q_{2,3}^* = \tilde{p} = q_1^*(m) \tag{3.39}$$

In an analogous way, the equation for the requirement that the stationary point is a saddle can be written as

$$0 = \frac{\mathrm{d}^2 V}{\mathrm{d}\tilde{p}^2} = $$
$$= \det \begin{pmatrix} \frac{\partial^2 f_1[\tilde{p},q_1^*(m),q_{2,3},m,\beta]}{\partial \tilde{p}^2} & \frac{\partial^2 f_1[\tilde{p},q_1^*(m),q_{2,3},m,\beta]}{\partial \tilde{p}\partial q_2} & \frac{\partial^2 f_1[\tilde{p},q_1^*(m),q_{2,3},m,\beta]}{\partial \tilde{p}\partial q_3} \\ \frac{\partial^2 f_1[\tilde{p},q_1^*(m),q_{2,3},m,\beta]}{\partial \tilde{p}\partial q_2} & \frac{\partial^2 f_1[\tilde{p},q_1^*(m),q_{2,3},m,\beta]}{\partial q_2^2} & \frac{\partial^2 f_1[\tilde{p},q_1^*(m),q_{2,3},m,\beta]}{\partial \tilde{q}_3\partial q_2} \\ \frac{\partial^2 f_1[\tilde{p},q_1^*(m),q_{2,3},m,\beta]}{\partial \tilde{p}\partial q_3} & \frac{\partial^2 f_1[\tilde{p},q_1^*(m),q_{2,3},m,\beta]}{\partial \tilde{q}_3\partial q_2} & \frac{\partial^2 f_1[\tilde{p},q_1^*(m),q_{2,3},m,\beta]}{\partial q_3^2} \end{pmatrix} \Bigg|_{q_{2,3}^*=\tilde{p}=q_1^*(m)} \tag{3.40}$$

It turns out that the above equation can be reduced to

$$-\frac{1}{(1-q_1^*(m))^2} + \frac{\beta^2 u(u-1)}{2} q_1^*(m)^{u-2} = 0 \,. \tag{3.41}$$

This is nothing but the marginal stability condition of aging dynamics that fixes the value of the fluctuation dissipation ratio X to be equal to m_{th}. In other words, equation (3.35) and equation (3.41) fix the overlap of the threshold states at the temperature T and the value of the Parisi breaking point m that selects the threshold states. The value of m_{th} is exactly the value of the fluctuation dissipation ratio computed in [51].

3.3 The Boltzmann Pseudodynamics construction

The Boltzmann Pseudodynamics construction is a method introduced in [72] that is capable to obtain the dynamical equations for a glassy system in the α-regime. It is based on the following intuitive idea.

[1] See for example Giorgio Parisi, *Statistical Field Theory*.

The mean field glassy dynamics at the mode-coupling transition point can be thought in the following way. At high temperature the dynamical correlator decays rapidly to zero while when the temperature is lowered, on approaching the dynamical point, an exponential number of metastable states start to appear so that it develops a plateau whose length diverges at the dynamical point. The standard interpretation of the two steps relaxation of the dynamical correlation function goes as follows. The first relaxation, up to the plateau, describes how the system relaxes in the first metastable state available to the dynamics. Moreover, the long time relaxation, the one that starts from the plateau value, describes the relaxation from a metastable state to another in a free energy landscape that is very rugged. However one can conjecture that the exploration of each metastable state can be done in a quasi-ergodic way before escaping from it. It is natural that in this way some equilibrium construction should be doable for the whole long time dynamics.

The simplest way to obtain this quasi equilibrium construction is to generalize the Franz-Parisi potential. The reason is that we have seen that at the dynamical point the potential develops a saddle and the point at which the saddle is developed, is exactly the plateau value of the dynamical correlation function that can be thought as the first point of the correlator in the α regime. Moreover, by looking at how the potential is constructed, we can see that it incorporates the idea that it is related to a restricted measure over the metastable states. Starting from all these ideas we can think about a generalization of the potential method that should be capable to describe in a quasi equilibrium way how the phase space is explored in the long time regime of the dynamics. Moreover let us point out that in the α-regime the shape of the dynamical correlator should be almost independent on the details of the dynamics [88]. In particular we can imagine that if we use a local dynamics, the details through which it is defined should become less and less important in the long time regime where the quasi equilibrium behavior is satisfied. In practice we can expect that if we have an exponential number of metastable states and if the true dynamics is such that it does not facilitate the cooperative rearrangement of extensive part of the system, then this construction will give the correct dynamical equations. This statement is far from being rigorously proved and a major effort in this direction should be made in order to give to this new equilibrium construction an universal value.

In the following subsection we will review the Boltzmann Pseudodynamics construction recently introduced in [72] and we will show some generalities about correlation and response function that can be computed using this formalism.

3.3.1 The general definition

Suppose that we have a system described by a set of internal degrees of freedom that we call S_i (our notation is very close to the one encountered in spin systems but can also be used to treat particles in a liquid where the internal degrees of freedom are the position of the particles). In the following we will define a dynamical rule to evolve such system so that we will indicate with $S_i(t)$ the configuration of the system at time t.

The Boltzmann Pseudodynamics is a discrete time dynamics defined from the following dynamical rule: given the configuration of the spins (we will call the spins

the internal degrees of freedom even if it is simple to adapt our jargon to other kind of systems) at time t, the configuration at time $t+1$ occur with a probability that is given by

$$\begin{aligned} M(\underline{S}(t+1)|\underline{S}(t)) &= \frac{1}{Z[\beta_{t+1};\underline{S}(t)]}\mathrm{e}^{-\beta_{t+1}H[\underline{S}(t+1)]}\delta\left(\tilde{C}(t,t+1)-q\left(\underline{S}(t),\underline{S}(t+1)\right)\right) \\ Z[\beta_{t+1};\underline{S}(t)] &= \sum_{\underline{S}(t+1)}\mathrm{e}^{-\beta_{t+1}H[\underline{S}(t+1)]}\delta\left(\tilde{C}(t,t+1)-q\left(\underline{S}(t),\underline{S}(t+1)\right)\right) \end{aligned} \tag{3.42}$$

The function $q(\sigma,\tau)$ is a properly defined overlap used to measure the similarity between the configurations σ and τ and for spin system can be defined simply by $q(\sigma,\tau)=\sum_i \sigma_i\tau_i/N$ while for particle system it can be defined in a similar way as it has been done in the previous chapter. The probability of a trajectory given an initial configuration at time $t=0$ is given by

$$P[\underline{S}(t),\underline{S}(t-1),\ldots,\underline{S}(1)|\underline{S}(0)] = \hat{P}[\underline{S}(0)]\prod_{k=1}^{t-1}M(\underline{S}(t+1)|\underline{S}(t)) \tag{3.43}$$

where $\hat{P}$ is a given initial probability measure over the space of configurations of the system. Note that the above dynamics is defined using a set of variables $\{\tilde{C}(t+1,t)\}$ and by a set of "temperatures" $\{\beta_t\}$ that can be fixed from the outside. Given this construction we can study the standard time dependent correlation and response functions.

3.3.2 Response functions

The analysis of linear response functions provides a fundamental characterization of the dynamics just introduced. Consider the dynamics (3.42) in a time dependent field h_t coupled with an observable $m(\underline{S}(t))$, function of the system configuration $\underline{S}(t)$. The Hamiltonian in presence of the field is

$$H_h(\underline{S}(t)) = H(\underline{S}(t)) - h(t)m(\underline{S}(t)). \tag{3.44}$$

The response function is defined as usual

$$R(t,s) = \frac{\partial\langle m(\underline{S}(t))\rangle}{\partial h(s)} \tag{3.45}$$

where the average is done over the multiple realizations of the trajectories of the system. Moreover, because of the causal structure of the Markov Chain (3.42), the response function is non zero only if $t>s$. To compute this quantity we start from

$$\begin{aligned} &\frac{\partial}{\partial h(s)}P\left(\underline{S}(t),\underline{S}(t-1),\ldots,\underline{S}(1)|\underline{S}(0)\right) = \\ &\beta_s\left[m(\underline{S}(s)) - \mathcal{E}\left[m|\underline{S}(s-1)\right]\right]P\left(\underline{S}(t),\underline{S}(t-1),\ldots,\underline{S}(1)|\underline{S}(0)\right) \end{aligned} \tag{3.46}$$

where

$$\mathcal{E}\left[m|\underline{S}(s-1)\right] = \frac{1}{Z[\beta_s;\underline{S}(s-1)]}\sum_S e^{-\beta_s H(\underline{S})}m(\underline{S})\delta\left(q(\underline{S},\underline{S}(s-1)) - \tilde{C}(s,s-1)\right). \tag{3.47}$$

This leads to

$$\begin{aligned} R(t,s) &= \beta_s[\langle m(\underline{S}(t))m(\underline{S}(s))\rangle - \langle m(t)\mathcal{E}(m|\underline{S}(\sigma-1))\rangle] = \\ &= \beta_s[C(t,s) - \langle m(t)\mathcal{E}(m|\underline{S}(s-1))\rangle] \end{aligned} \tag{3.48}$$

where

$$\langle A(\underline{S}(s))\rangle = \sum_{\underline{S}(t)} \dots \sum_{\underline{S}(0)} A(\underline{S}(s)) P\left(\underline{S}(t), \underline{S}(t-1), \dots, \underline{S}(1)|\underline{S}(0)\right) \hat{P}(\underline{S}(0)) \,. \tag{3.49}$$

Note that if $s = 0$ than the last term factorizes (if there is no disorder over which we have to take the average)

$$\langle m(t)E(m|S_{\sigma-1})\rangle = \langle m(t)\rangle m_0 \tag{3.50}$$

where

$$m_0 = \sum_{\underline{S}} m(\underline{S})\hat{P}(\underline{S}) \,. \tag{3.51}$$

is the average value of the observable m when computed using the initial probability distribution that is unconstrained from the others.

3.3.3 Equilibrium measure

In general, for time independent temperature $\beta_\sigma = \beta$ and correlation $C(\sigma+1,\sigma) = C$, the Markov chain (3.42) is ergodic. However, the ordinary Boltzmann distribution is not the stationary measure. In fact we can notice that the detailed balance is verified with respect to the modified distribution

$$\mu(S) = \frac{1}{Z_2} e^{-\beta H(\underline{S})} Z(\beta, \underline{S}) \tag{3.52}$$

where

$$Z_2 = \sum_{\underline{S},\underline{S}'} e^{-\beta[H(\underline{S})+H(\underline{S}')]} \delta\left(q(\underline{S},\underline{S}') - C\right) \tag{3.53}$$

This is therefore the equilibrium distribution of the chain.

3.4 The p-spin spherical model

In this section we will discuss in detail the Boltzmann Pseudodynamics construction for the disordered p-spin spherical model. To do this let us recall its Hamiltonian

$$H_J[\underline{\sigma}; h] = -\sum_{i_1<\dots<i_p} J_{i_1,\dots,i_p}\sigma_{i_1}\dots\sigma_{i_p} - \sum_{i=1}^{N} h_i\sigma_i \qquad \sum_{i=1}^{N}\sigma_i^2 = N \tag{3.54}$$

$$P[J_{i_1\dots i_p}] \propto \exp\left[-\frac{N^{p-1}}{p!}J^2_{i_1\dots i_p}\right] \tag{3.55}$$

where we have put a magnetic field that is site dependent so that we will use it in order to define and compute the correlation and response functions.

Let us also introduce the generalized Franz-Parisi potential [69] that is defined as follows:

$$V\left[\{\beta_k\};\{\tilde{C}(k-1,k)\}\right] = \frac{1}{N}\mathbf{E}_J \sum_{\underline{\sigma}_1} \cdots \sum_{\underline{\sigma}_{L-1}} \frac{1}{Z} \mathrm{e}^{-\beta_1 H_J[\underline{\sigma}_1]} \times$$
$$\times \prod_{k=1}^{L-2} M(\underline{\sigma}_{k+1}|\underline{\sigma}_k) \ln \sum_{\underline{\sigma}_L} \mathrm{e}^{-\beta_L H_J[\underline{\sigma}_L]} \delta\left(\tilde{C}(L-1,L) - q(\underline{\sigma}_{L-1},\underline{\sigma}_L)\right) \tag{3.56}$$

where $\mathbf{E}_J$ indicates the average over the quenched disorder and where we have defined the transfer matrix of the Boltzmann Pseudodynamics as

$$M(\underline{\sigma}_k|\underline{\sigma}_{k-1}) = \frac{1}{Z(\underline{\sigma}_{k-1})} \mathrm{e}^{-\beta_k H_J[\underline{\sigma}_k]} \delta\left(\tilde{C}(k-1,k) - q(\underline{\sigma}_{k-1},\underline{\sigma}_k)\right) . \tag{3.57}$$

The overlap and the normalization factors are defined as follows

$$q(\underline{\sigma}_{k-1},\underline{\sigma}_k) = \frac{1}{N}\sum_{i=1}^{N} \sigma_i(k-1)\sigma_i(k) \tag{3.58}$$

$$Z(\underline{\sigma}_{k-1}) = \sum_{\underline{\sigma}_k} \mathrm{e}^{-\beta_k H_J[\underline{\sigma}_k]} \delta\left(\tilde{C}(k-1,k) - q(\underline{\sigma}_{k-1},\underline{\sigma}_k)\right) . \tag{3.59}$$

The notation has to be intended in the following way: with $\underline{\sigma}_k$ we denote the whole spin configuration of the system at the position k along the chain. Moreover with $\sigma_i(k)$ we denote the spin i of the k-system. The parameters $\{\tilde{C}(k,k+1)\}$ are fixed from the outside. Moreover we have left the freedom to choose different temperatures for different positions along the Markov Chain. This can be used in principle to use the Boltzmann Pseudodynamics to treat the problem of how to follow Gibbs states in temperature.

The physical interpretation of the generalized Franz-Parisi potential is that it gives the free energy of the last system in the Markov Chain. The main claim of this section is that if we want to minimize this potential with respect to the parameters $\{\tilde{C}(k,k+1)\}$ we will end up with the dynamical equations for this model in the long time limit. Note that if we restrict to the case in which the chain contains only two systems we recover the standard Franz-Parisi potential. In order to study this potential let us first of all introduce a further generalization of it. We can assume that the first system, the free one, will be replicated n_1 times and we can put a vanishing coupling between these n_1 real replicas. This produce a hybrid version of the generalization of the potential method with the real replica method developed in [133] and analogous to the off-equilibrium potential method introduced in the previous section. If we want to recover the equilibrium we can send at the end $n_1 \to 1$ but if we want to study off-equilibrium this generalization is very useful both from the practical and the theoretical point of view.

This generalized potential can be written in the following way

$$V\left[\{\beta_k\};\{\tilde{C}(k-1,k)\}\right]=\frac{1}{N}\mathbf{E}_J\sum_{\underline{\sigma}_1}\cdots\sum_{\underline{\sigma}_{L-1}}\frac{1}{Z_{n_1}}\mathrm{e}^{-\beta_1\sum_{a=1}^{n_1}H_J[\underline{\sigma}_1^{(a)}]}\times$$
$$\times\prod_{k=1}^{L-2}M(\underline{\sigma}_{k+1}|\underline{\sigma}_k)\ln\sum_{\underline{\sigma}_L}\mathrm{e}^{-\beta_L H_J[\underline{\sigma}_L]}\delta\left(\tilde{C}(L-1,L)-q(\underline{\sigma}_{L-1},\underline{\sigma}_L)\right)\cdot \tag{3.60}$$
$$Z_{n_1}=\sum_{\underline{\sigma}_1^{(1)}}\cdots\sum_{\underline{\sigma}_1^{(n_1)}}\exp\left[-\beta_1\sum_{a=1}^{n_1}H[\underline{\sigma}_1^{(a)}]\right]$$

Let us now start the computation of this expression. It is easy to realize that some technical difficulties arise because of the last logarithm function and of the normalization factors of the restricted Bolzmann measures that define the Markov chain for the pseudodynamic process. However these problems can be overcome by introducing replicas. In fact we have that

$$\ln\sum_{\underline{\sigma}_L}e^{-\beta_L H_J[\underline{\sigma}_L]}\delta\left[\tilde{C}(L-1,L)-q(\underline{\sigma}_{L-1},\underline{\sigma}_L)\right]=$$
$$\lim_{n_L\to0}\frac{\mathrm{d}}{\mathrm{d}n_L}\left(\sum_{\underline{\sigma}_L}e^{-\beta_L H_J[\underline{\sigma}_L]}\delta\left[\tilde{C}(L-1,L)-q(\underline{\sigma}_{L-1},\underline{\sigma}_L)\right]\right)^{n_L}=$$
$$=\lim_{n_L\to0}\frac{\mathrm{d}}{\mathrm{d}n_L}\sum_{\underline{\sigma}_L^{(1)}}\cdots\sum_{\underline{\sigma}_L^{(n_1)}}e^{-\beta_L\sum_{a=1}^{n_L}H_J[\underline{\sigma}_L^{(a)}]}\prod_{a=1}^{n_L}\delta\left[\tilde{C}(L-1,L)-q(\underline{\sigma}_{L-1},\underline{\sigma}_L^{(a)})\right] \tag{3.61}$$

where to get from the first line to second one we have assumed that the number of replicas is an integer and the replica prescription makes sense only if we manage to compute the replicated potential as a function of n_L so that in the end we can produce an analytic continuation through we can take safely the limit $n_L\to0$. In an analogous way, the normalization factors read

$$\frac{1}{Z[\underline{\sigma}_{t-1}]}=\lim_{n_t\to0}\left(\sum_{\underline{\sigma}_t}e^{-\beta_t H_J[\underline{\sigma}_t]}\delta\left[\tilde{C}(t-1,t)-q(\underline{\sigma}_{t-1},\underline{\sigma}_t)\right]\right)^{n_t-1}=$$
$$=\lim_{n_t\to0}\sum_{\underline{\sigma}_t^{(2)}}\cdots\sum_{\underline{\sigma}_t^{(n_t)}}e^{-\beta_t\sum_{a=2}^{n_t}H_J[\underline{\sigma}_t^{(a)}]}\prod_{a=2}^{n_t}\delta\left[\tilde{C}(t-1,t)-q(\underline{\sigma}_{t-1},\underline{\sigma}_t^{(a)})\right] \tag{3.62}$$

where we have introduced the notation according to which the spin i in the k-position along the chain belonging to the replica a is denoted with $\sigma_i^{(a)}(k)$. With these tools we can compute the generalized potential in the thermodynamic limit. Let us see how.

By replicating every normalization factor and the final logarithm we get

$$
\begin{aligned}
V = & \frac{1}{N} \lim_{r_1 \to 0} \lim_{\{n_k \to 0\}_{k=2,\dots,L}} \frac{1}{r_1} \frac{\mathrm{d}}{\mathrm{d}n_L} \mathbf{E}_J \left\{ \int \left(\prod_{k=1}^{L} \prod_{a=1}^{n_k} \prod_{i=1}^{N} \mathrm{d}\sigma_i^{(a)}(k) \right) \times \right. \\
& \times \left[\prod_{k=1}^{L} \prod_{a=1}^{n_k} \delta(1 - q(\underline{\sigma}_k^{(a)}, \underline{\sigma}_k^{(a)})) \right] \exp \left[- \sum_{k=1}^{L} \beta_k \sum_{a=1}^{n_k} H_J[\underline{\sigma}_k^{(a)}] \right] \\
& \left. \prod_{k=1}^{L-1} \prod_{a=1}^{n_k} \delta \left[\tilde{C}(k, k+1) - q(\underline{\sigma}_k^{(1)}, \underline{\sigma}_{k+1}^{(a)}) \right] \right\}^{r_1} = \\
= & \lim_{r_1 \to 0} \lim_{\{n_k \to 0\}_{k=2,\dots,L}} \frac{1}{r_1} \frac{\mathrm{d}}{\mathrm{d}n_L} \int \left(\prod_{s=1}^{r_1} \prod_{k=1}^{L} \prod_{a=1}^{n_k} \prod_{i=1}^{N} \mathrm{d}\sigma_i^{(a)}(k, s) \right) \times \\
& \times \left[\prod_{s=1}^{r_1} \prod_{k=1}^{L} \prod_{a=1}^{n_k} \delta(1 - q(\underline{\sigma}^{(a)}(k, s), \underline{\sigma}^{(a)}(k, s))) \right] \times \\
& \times \left[\mathbf{E}_J \exp \left[- \sum_{s=1}^{r_1} \sum_{k=1}^{L} \beta_k \sum_{a=1}^{n_k} H_J[\underline{\sigma}^{(a)}(k, s)] \right] \right] \times \\
& \times \prod_{s=1}^{r_1} \prod_{k=1}^{L-1} \prod_{a=1}^{n_k} \delta \left[\tilde{C}(k, k+1) - q(\underline{\sigma}^{(1)(k,s)}, \underline{\sigma}_{k+1}^{(a)}(k+1, s)) \right]
\end{aligned}
\tag{3.63}
$$

Because of the fact that the quenched disorder is Gaussian, we can take the average over it. The relevant term for this operation is the following

$$
\begin{aligned}
& \mathbf{E}_J \exp \left[- \sum_{s=1}^{r_1} \sum_{k=1}^{L} \beta_k \sum_{a=1}^{n_k} H_J[\underline{\sigma}^{(a)}(k, s)] \right] = \\
& = \exp \left[\frac{N}{4} \sum_{s,s'=1}^{r_1} \sum_{k,j=1}^{L} \beta_k \beta_j \sum_{a=1}^{n_k} \sum_{b=1}^{n_j} \left(\frac{1}{N} \sum_{i=1}^{N} \sigma_i^{(a)}(k, s) \sigma_i^{(b)}(j, s') \right)^p \right]
\end{aligned}
\tag{3.64}
$$

where in the final result we have neglected at the exponent subdominant terms that will vanish in the thermodynamic limit.

Now we can introduce the overlap matrix as follows

$$
Q_{ab}^{(s,s')}(k; j) = \frac{1}{N} \sum_{i=1}^{N} \sigma_i^{(a)}(k, s) \sigma_i^{(b)}(j, s') \tag{3.65}
$$

The generalized potential can be written as a function of the overlap. This can be done by using a set of Dirac delta functions to enforce (3.65)

$$
\prod_{\langle (k,s,a);(j,s',b) \rangle} \delta \left[N Q_{ab}^{(s,s')}(k; j) - \sum_{i=1}^{N} \sigma_i^{(a)}(k, s) \sigma_i^{(b)}(j, s') \right] \tag{3.66}
$$

where the notation $\langle (k, s, a); (j, s', b) \rangle$ means that if we organize the variables $Q_{ab}^{(s,s')}(k; j)$ in a symmetric matrix, than the product runs only on the upper triangular part of that matrix (diagonal included). In this way the expression for the generalized

potential becomes

$$
\begin{aligned}
V = & \frac{1}{N} \lim_{r_1 \to 0} \lim_{\{n_k \to 0\}_{k=2,\dots,L}} \frac{1}{r_1} \frac{\mathrm{d}}{\mathrm{d}n_L} \int \left(\prod_{s=1}^{r_1} \prod_{k=1}^{L} \prod_{a=1}^{n_k} \prod_{i=1}^{N} \mathrm{d}\sigma_i^{(a)}(k,s) \right) \times \\
& \times \left[\prod_{s=1}^{r_1} \prod_{k=1}^{L} \prod_{a=1}^{n_k} \delta(1 - q(\underline{\sigma}^{(a)}(k,s), \underline{\sigma}^{(a)}(k,s))) \right] N^{\gamma} \times \\
& \times \int \left(\prod_{\langle (k,s,a);(j,s',b) \rangle} \mathrm{d}Q_{ab}^{(s,s')}(k;j)\, \delta \left[N Q_{ab}^{(s,s')}(k;j) - \sum_{i=1}^{N} \sigma_i^{(a)}(k,s) \sigma_i^{(b)}(j,s') \right] \right) \cdot \\
& \times \left[\prod_{s=1}^{r_1} \prod_{k=1}^{L} \prod_{a=1}^{n_k} \delta \left(\tilde{C}(k,k+1) - Q_{1a}^{(s,s)}(k;k+1) \right) \right] \cdot \\
& \times \exp \left[\frac{N}{4} \sum_{s,s'=1}^{r_1} \sum_{k,j=1}^{L} \beta_k \beta_j \sum_{a=1}^{n_k} \sum_{b=1}^{n_j} \left[Q_{ab}^{(s,s')}(k;j) \right]^p + \sum_{s=1}^{r_1} \sum_{k=1}^{L} \beta_k \sum_{i=1}^{N} h_i(k) \sum_{a=1}^{n_k} \sigma_i^{(a)}(k,s) \right]
\end{aligned}
\tag{3.67}
$$

where γ is a constant (dependent on N) that will not play any role in the following.

By expanding the Dirac deltas with their Fourier representation we get

$$
\begin{aligned}
V = & \lim_{r_1 \to 0} \lim_{\{n_k \to 0\}_{k=2,\dots,L}} \frac{1}{r_1} \frac{\mathrm{d}}{\mathrm{d}n_L} \int \left(\prod_{[\langle (k,s,a);(j,s',b) \rangle]} \mathrm{d}Q_{ab}^{(s,s')}(k;j) \right) \\
& \int \left(\prod_{\langle (k,s,a);(j,s',b) \rangle} \mathrm{d}\tilde{Q}_{ab}^{(s,s')}(k;j) \right) \exp \left[\frac{N}{4} \sum_{s,s'=1}^{r_1} \sum_{k,j=1}^{L} \beta_k \beta_j \sum_{a=1}^{n_k} \sum_{b=1}^{n_j} \left[Q_{ab}^{(s,s')}(k;j) \right]^p \right] \\
& \int \left(\prod_{s=1}^{r_1} \prod_{k=1}^{L} \prod_{a=1}^{n_k} \prod_{i=1}^{N} \mathrm{d}\sigma_i^{(a)}(k,s) \right) \exp \left[N \sum_{\langle (k,s,a);(j,s',b) \rangle} Q_{ab}^{(s,s')}(k;j) \tilde{Q}_{ab}^{(s,s')}(k;j) \right. \\
& \left. - \sum_{i=1}^{N} \sum_{\langle (k,s,a);(j,s',b) \rangle} \tilde{Q}_{ab}^{(s,s')}(k;j) \sigma_i^{(a)}(k,s) \sigma_i^{(b)}(j,s') + \sum_{s=1}^{r_1} \sum_{k=1}^{L} \beta_k \sum_{i=1}^{N} h_i(k) \sum_{a=1}^{n_k} \sigma_i^{(a)}(k,s) \right]
\end{aligned}
\tag{3.68}
$$

where we have used some Dirac deltas to fix the value of some elements of the overlap matrix Q. In fact the integration denoted with $[\langle (k,s,a);(j,s',b) \rangle]$ is done over the same variables than before except the variables $Q_{aa}^{(s,s)}(k;k)$ that are fixed to 1 and for $Q_{1a}^{(s,s)}(k;k+1)$ that must be equal to $\tilde{C}(k,k+1)$. In order to simplify the computation we introduce the symmetric matrix

$$
\underline{Q}_{ab}^{(s,s')}(k;j) = \frac{1}{2} \tilde{Q}_{ab}^{(s,s')}(k;j) + \frac{1}{2} \delta_{ab} \delta_{kj} \delta_{ss'} \tilde{Q}_{ab}^{(s,s')}(k;j) \tag{3.69}
$$

that allow us to perform the Gaussian integral over the spin variables

$$\int \left(\prod_{s=1}^{r_1} \prod_{k=1}^{L} \prod_{a=1}^{n_k} \prod_{i=1}^{N} \mathrm{d}\sigma_i^{(a)}(k,s) \right) \exp \left[\sum_{s=1}^{r_1} \sum_{k=1}^{L} \beta_k \sum_{i=1}^{N} h_i(k) \sum_{a=1}^{n_k} \sigma_i^{(a)}(k,s) - \right.$$
$$- \sum_{i=1}^{N} \sum_{\langle (k,s,a);(j,s',b) \rangle} \tilde{Q}_{ab}^{(s,s')}(k;j) \sigma_i^{(a)}(k,s) \sigma_i^{(b)}(j,s') \Bigg] = \mathcal{K} \exp \left[-\frac{N}{2} \mathrm{Tr} \ln \underline{Q} \right. \tag{3.70}$$
$$\left. + \frac{1}{4} \sum_{s,s'}^{r_1} \sum_{i=1}^{N} \sum_{k,j=1}^{L} \beta_k \beta_j \sum_{a=1}^{n_k} \sum_{b=1}^{n_j} h_i(k) \left[\underline{Q}^{-1} \right]_{ab}^{(s,s')} (k;j) h_i(j) \right]$$

where the constant $\mathcal{K}$ will play no role in what follows because it is independent on Q and $\tilde{Q}$. At this point we need to set the external fields to zero in order to take the saddle point in the integral. However we included these fields in our computation because they are useful to compute the pseudodynamic response function that gives an interpretation of the ansatz given in [72] for the parametrization of the overlap matrix.

Suppose that we want to compute the change of the average value of the magnetization at time s due to a change of the external field at time t where $1 < t < s$. From how the Markov Chain is constructed we see that the Markov property guarantees us that the systems that are along the chain beyond the s-system can be integrated out. This is nothing but the causality structure induced by the chain. In this way, without loosing generality we can consider $s = L$. The response function is given by

$$R(L,t) = \frac{1}{N} \sum_{i=1}^{N} \frac{\mathrm{d}}{\mathrm{d}h_i(t)} \mathbf{E}_J \left\langle \sigma_i^{(L)} \right\rangle_{\text{chain}} \Bigg|_{\{h_i(k)=0\}_{k=1\dots L}} =$$
$$= \frac{1}{N\beta_L} \sum_{i=1}^{N} \frac{\mathrm{d}^2}{\mathrm{d}h_i(t)\mathrm{d}h_i(L)} \mathbf{E}_J \sum_{\underline{\sigma}_1} \cdots \sum_{\underline{\sigma}_{L-1}} \frac{1}{Z} \mathrm{e}^{-\beta_1 H_J[\underline{\sigma}_1]} \left[\prod_{k=1}^{L-1} M(\underline{\sigma}_{k+1} | \underline{\sigma}_k) \right] \cdot$$
$$\cdot \ln \sum_{\underline{\sigma}_1} \mathrm{e}^{-\beta_L H_J[\underline{\sigma}_L]} \delta \left(\tilde{C}(L-1,L) - q(\underline{\sigma}_{L-1}, \underline{\sigma}_L) \right) \Bigg|_{\{h_i(k)=0\}_{k=1\dots L}} = \tag{3.71}$$
$$= \lim_{n_1 \to 1} \frac{1}{\beta_L} \sum_{i=1}^{N} \frac{\mathrm{d}}{\mathrm{d}h_i(t)} \frac{\mathrm{d}}{\mathrm{d}h_i(L)} V \left[\{\beta_k\}; \left\{ \tilde{C}(t+1,t) \right\}, \{h_i(t)\} \right] \Bigg|_{\{h_i(k)=0\}_{k=1\dots L}}$$

Now we can use the expression we have derived for the generalized potential to

obtain the response function. Let us take first the saddle point over $\tilde{Q}$

$$
\begin{aligned}
R(L,t) = \beta_s \lim_{n_1\to 1} \lim_{\{r_1,n_k\to 0\}_{k=2,\ldots,L}} \frac{1}{r_1}\frac{\mathrm{d}}{\mathrm{d}n_L} \int \left(\prod_{[\langle (k,s,a);(j,s',b)\rangle]} \mathrm{d}Q_{ab}^{(s,s')}(k;j) \right) \\
\int \left(\prod_{\langle (k,s,a);(j,s',b)\rangle} \mathrm{d}\tilde{Q}_{ab}^{(s,s')}(k;j) \right) \left[\frac{1}{2} \sum_{s,s'=1}^{r_1} \sum_{a=1}^{n_t} \sum_{b=1}^{n_L} \left[\underline{Q}^{-1}\right]_{ab}^{(s,s')}(t;L) \right] \\
\exp\left[\mathbf{K} + \frac{N}{4} \sum_{s,s'=1}^{r_1} \sum_{k,j=1}^{L} \beta_k\beta_j \sum_{a=1}^{n_k}\sum_{b=1}^{n_j} \left[Q_{ab}^{(s,s')}(k;j)\right]^p + \right. \\
\left. + \frac{1}{4} \sum_{s,s'}^{r_1} \sum_{i=1}^{N} \sum_{k,j=1}^{L} \beta_k\beta_j \sum_{a=1}^{n_k}\sum_{b=1}^{n_j} h_i(k) \left[\underline{Q}^{-1}\right]_{ab}^{(s,s')}(k;j) h_i(j) - \frac{N}{2}\mathrm{Tr}\ln \underline{Q} \right]
\end{aligned}
\tag{3.72}
$$

where $\mathbf{K}$ is a constant that can be also proportional to N but which doesn't enter in the rest of the calculation because it is independent on Q. By taking firstly the saddle point over $\tilde{Q}$ and then the saddle point over Q, and by assuming the final replica symmetric ansatz that says

$$
Q^{*}{}_{ab}^{(s,s')}(k;j) = \delta_{s,s'} Q_{ab}^{SP}(k,j) \tag{3.73}
$$

one easily sees that the response function is given by

$$
R(L,s) = \beta_s \lim_{n_1\to 1} \lim_{\{n_k\to 0\}_{k=2,\ldots,L}} \frac{\mathrm{d}}{\mathrm{d}n_L} \left(\sum_{a=1}^{n_t}\sum_{b=1}^{n_L} Q_{ab}^{SP}(t,L) \right) \tag{3.74}
$$

where $Q_{ab}^{SP}(s,L)$ is the saddle point solution that satisfies the equation

$$
\frac{\beta_t\beta_s p}{2} \left[Q_{ab}(t,s)\right]^{p-1} + \left[Q^{-1}\right]_{ab}(t,s) = 0 \tag{3.75}
$$

In order to solve these equations we must choose an ansatz for the overlap matrix so that we can reduce the degrees of freedom of the system and simplify the calculation. The simplest ansatz is a replica symmetric one where here replica symmetric means an ansatz with the lowest number of degrees of freedom and compatible with the constraint of the matrix. This ansatz is the one given in [72] and it is

$$
\begin{aligned}
Q_{ab}(t,s) &= C(t,s) + \delta_{ab}\delta_{su}\Delta C(s,s) + \Theta_{>}(s-t)\delta_{a1}\Delta C(t,s) + \\
&\quad + \Theta_{>}(t-s)\delta_{b1}\Delta C(s,t) \\
\Delta C(t,s) &= \tilde{C}(t,s) - C(t,s)
\end{aligned}
\tag{3.76}
$$

where $C(t,s)$ are parameters over which we want to optimize and where the function $\Theta_{>}(x)$ is equal to one only if $x > 0$. By doing this, it is simple to see that

$$
R(L,t) = \beta_s \left(\tilde{C}(t,L) - C(t,L) \right) \tag{3.77}
$$

that clearly justify the assumption done in [72]. However let us note that if $t = 1$, because of the fact that the number of replicas of the first system goes to one

we obtain that $R(L,1) = \tilde{C}(L,1)$. This difference can be seen by looking at the correlation function representation for the response function.

Let us compute the response function again directly

$$
\begin{aligned}
R(L,s) &= \frac{1}{N}\sum_{i=1}^{N}\frac{\mathrm{d}}{\mathrm{d}h_i(s)}\,\mathbf{E}_J[\langle\sigma_i(L)\rangle] = \\
&= \beta_s \mathbf{E}_J \sum_{\underline{\sigma}_1}\frac{\mathrm{e}^{-\beta_1 H_J[\underline{\sigma}_1;\underline{h}_1]}}{Z[\underline{h}_1]}\sum_{\underline{\sigma}_2}\frac{\mathrm{e}^{-\beta_2 H_J[\underline{\sigma}_2;\underline{h}_2]}}{Z[\underline{\sigma}_1;\underline{h}_2]}\delta\left[\tilde{C}(1,2)-q(\underline{\sigma}_1,\underline{\sigma}_2)\right]\times \\
&\ldots\times\sum_{\underline{\sigma}_s}\frac{\mathrm{e}^{-\beta_s H_J[\underline{\sigma}_s;\underline{h}_s]}}{Z[\underline{\sigma}_{s-1};\underline{h}_s]}\sigma_i(s)\delta\left[\tilde{C}(s-1,s)-q(\underline{\sigma}_{s-1},\underline{\sigma}_s)\right]\times\ldots \\
&\ldots\times\sum_{\underline{\sigma}_L}\frac{\mathrm{e}^{-\beta_L H_J[\underline{\sigma}_L;\underline{h}_L]}}{Z[\underline{\sigma}_{L-1};\underline{h}_L]}\sigma_i(L)\delta\left[\tilde{C}(L-1,L)-q(\underline{\sigma}_{L-1},\underline{\sigma}_L)\right]- \\
&-\beta_s \mathbf{E}_J \sum_{\underline{\sigma}_1}\frac{\mathrm{e}^{-\beta_1 H_J[\underline{\sigma}_1;\underline{h}_1]}}{Z[\underline{h}_1]}\sum_{\underline{\sigma}_2}\frac{\mathrm{e}^{-\beta_2 H_J[\underline{\sigma}_2;\underline{h}_2]}}{Z[\underline{\sigma}_L;\underline{h}_2]}\delta\left[\tilde{C}(1,2)-q(\underline{\sigma}_1,\underline{\sigma}_2)\right]\times\ldots \\
&\ldots\times\sum_{\underline{\sigma}_s}\frac{\mathrm{e}^{-\beta_s H_J[\underline{\sigma}_s;\underline{h}_s]}}{Z[\underline{\sigma}_{s-1};\underline{h}_s]}\delta\left[\tilde{C}(s-1,s)-q(\underline{\sigma}_{s-1},\underline{\sigma}_s)\right]\times \\
&\times\sum_{\underline{\sigma}_s}\frac{\mathrm{e}^{-\beta_s H_h[\underline{\sigma}_s;\underline{h}_s]}}{Z[\underline{\sigma}_{s-1};\underline{h}_s]}\sigma_i(s)\delta\left[\tilde{C}(s-1,s)-q(\underline{\sigma}_{s-1},\underline{\sigma}_s)\right]\times \\
&\ldots\times\sum_{\underline{\sigma}_L}\frac{\mathrm{e}^{-\beta_L H_J[\underline{\sigma}_L;\underline{h}_L]}}{Z[\underline{\sigma}_{L-1};\underline{h}_L]}\sigma_i(L)\delta\left[\tilde{C}(L-1,L)-q(\underline{\sigma}_{L-1},\underline{\sigma}_L)\right]= \\
&= \frac{\beta_s}{N}\sum_{i=1}^{N}\mathbf{E}_J\left[\langle\sigma_i(s)\sigma_i(L)\rangle-\langle\sigma_i(L)\,\langle\sigma_i(s)|t<s\rangle\rangle\right]
\end{aligned}
\tag{3.78}
$$

where in the last term we have indicated the correlation between the spin $\sigma_i(L)$ and the mean value of the spin $\sigma_i(s)$ that is conditioned to have the same history of the spin $\sigma_i(L)$. It is clear that if we take $s = 1$ the two spins in the last term are coupled only because of the disorder while if $s > 1$ there is coupling also coming from the history.

At this point we want to analyze the saddle point equation (3.75). An important remark should be done. Where do the indices in that equation run? In general the procedure should be the following. One first optimize the potential over the overlap matrix elements that are not constrained by the constraints of the pseudodynamics. Then, the solution of the saddle point equations are functions of the constraints and one should optimize over the constraints. Moreover the indices do not run on the diagonal part of the overlap matrix. There is also the tricky point that the inversion of the overlap matrix is very complicated also in the simplest replica symmetric ansatz. How to solve all these problems? The first problem can be solved quite simply. In fact one can optimize from the beginning with both the free matrix elements and the constrained ones. This implies that in the equation above, the indices can run also to the values of the constraints. However we have the problem that the indices cannot be such that we are taking diagonal elements. This problem can be solved by simply introducing a Lagrange multiplier and letting the matrix

elements on the diagonal to be free. The new form of the generalized Franz-Parisi potential is given by

$$\begin{aligned} &V(\{\beta_s\},\{\tilde{C}(s,s+1)\}) = \\ &\lim_{r_1\to 0}\lim_{\{n_k\to 0\}_{k=2,\dots,L}} \frac{1}{r_1}\frac{\mathrm{d}}{\mathrm{d}n_L}\int\left[\prod_{\langle\langle(k,s,a);(j,s',b)\rangle\rangle}\mathrm{d}Q_{ab}(k,s;j,s')\right]\cdot \\ &\cdot\exp\left[\mathbf{K}+\frac{N}{4}\sum_{s,s'=1}^{r_1}\sum_{k,j=1}^{L}\beta_k\beta_j\sum_{a=1}^{n_k}\sum_{b=1}^{n_j}\left[Q_{ab}(k,s;j,s')\right]^p+\right. \\ &\left.+\frac{N}{2}\mathrm{Tr}\ln Q-\frac{N}{2}\sum_{s=1}^{r_1}\sum_{k=1}^{L}\nu_k(s)\sum_{a=1}^{n_k}\left(Q_{aa}(k,s;k,s)-1\right)\right] \end{aligned} \tag{3.79}$$

where the notation $\langle\langle(k,a);(j,b)\rangle\rangle$ indicates that the integral is over all the matrix elements in the upper triangular part of the overlap matrix including the diagonal and excluding the constraints elements (but however we can take the derivative also with respect to them because we want to optimize). By taking the large N limit, we can write down the saddle point equations. With the ansatz (3.73), the saddle point equations are given by

$$\frac{\beta_k\beta_j p}{2}\left[Q_{ab}(k,j)\right]^{p-1}+\left[Q^{-1}\right]_{ab}(k,j)-\nu_k\delta_{kj}\delta_{ab}=0 \tag{3.80}$$

By taking all the temperatures equal to β and multiplying the equation above for Q and summing over the indices we obtain

$$\frac{\beta^2 p}{2}\sum_{z=1}^{L}\sum_{c=1}^{n_z}\left[Q_{ac}(k,z)\right]^{p-1}Q_{cb}(z,j)+\delta_{kj}\delta_{ac}-\nu_k Q_{ab}(k,j)=0 \tag{3.81}$$

Note that the equations above are the standard saddle point equations for the overlap matrix of the p-spin spherical model but with an ansatz that is more structured than the standard one. The structure of the replica matrix is naturally induced by the Markov Chain construction. This is a key observation because it tells that given a model, whatever it will be, if its solution can be computed using the replica method through a set of closed equations for the overlap matrix, than the pseudodynamic construction can be implemented by taking the same equations and then by putting in the equations the structure for the overlap matrix that we have just discussed.

At this point, we insert the replica symmetric ansatz in the saddle point equations just derived. At the first order in $\tilde{C}-C$ one has

$$\begin{aligned} \left[Q_{ab}(k,j)\right]^{p-1} = {} & C^{p-1}(k,j)+\delta_{ab}\delta_{kj}\Delta C_{p-1}(k,k)+\delta_{a1}\Theta_{>}(p-1)C^{p-2}(k,j)\Delta C(k,j)+ \\ & +\delta_{b1}\Theta_{>}(k-j)(p-1)C^{p-2}(k,j)\Delta C(k,j) \end{aligned} \tag{3.82}$$

where

$$\Delta C_{p-1}(\alpha,\alpha)=1-C^{p-1}(\alpha,\alpha) \tag{3.83}$$

At this point we can compute the matrix product in the first term of the saddle point equation (3.81). This can be done in the following way

$$
\begin{aligned}
&\sum_{z=1}^{L}\sum_{c=1}^{n(z)}\left[Q_{ac}(s,z)\right]^{p-1}Q_{cb}(z,u) = \sum_{z=1}^{L}\sum_{c=1}^{n(z)}\Big[C^{p-1}(s,z)+\delta_{ac}\delta_{sz}\Delta C_{p-1}(s,s)+\\
&+\Theta_{>}(z-s)\delta_{a1}(p-1)C^{p-2}(s,z)\Delta C(s,z)+\Theta_{>}(s-z)\delta_{c1}(p-1)C^{p-1}(s,z)\Delta C(s,z)\Big]\cdot\\
&\cdot\left[C(z,u)+\delta_{cb}\delta_{zu}\Delta C(u,u)+\Theta_{>}(u-z)\delta_{c1}\Delta C(z,u)+\Theta_{>}(z-u)\delta_{b1}\Delta C(z,u)\right] =\\
&=\sum_{z=1}^{L}n(z)C^{p-1}(s,z)C(z,u)+C^{p-1}(s,u)\Delta C(u,u)+\sum_{z=1}^{u-1}C^{p-1}(s,z)\Delta C(z,u)+\\
&+\sum_{z=u+1}^{L}n(z)\delta_{b1}C^{p-1}(s,z)\Delta C(z,u)+\Delta C_{p-1}(s,s)C(s,u)+\\
&+\Theta_{>}(u-s)\delta_{a1}\Delta C_{p-1}(s,s)\Delta C(s,u)+\Theta_{>}(s-u)\delta_{b1}\Delta C_{p-1}(s,s)\Delta C(s,u)+\\
&+\sum_{z=s+1}^{L}n(z)\delta_{a1}(p-1)C^{p-2}(s,z)\Delta C(s,z)C(z,u)+\\
&+\Theta_{>}(s-u)\delta_{a1}(p-1)C^{p-2}(s,s)\Delta C(s,s)\Delta C(u,u)+\\
&+\Theta_{>}(u-s)\sum_{z=s+1}^{u-1}\delta_{a1}(p-1)C^{p-2}(s,z)\Delta C(s,z)\Delta C(z,u)+\\
&+\sum_{z=\max(s,u)+1}^{L}n(z)\delta_{a1}\delta_{b1}(p-1)C^{p-2}(s,z)\Delta C(s,z)\Delta C(z,u)+\\
&+\sum_{z=1}^{s-1}(p-1)C^{p-2}(s,z)\Delta C(s,z)C(z,u)+\delta_{ab}\delta_{su}\Delta C_{p-1}(s,s)\Delta C(s,s)+\\
&\Theta_{>}(s-u)\delta_{b1}(p-1)C^{p-2}(s,u)\Delta C(s,u)\Delta C(u,u)+\\
&+\sum_{z=1}^{\min(s,u)-1}(p-1)C^{p-2}(s,z)\Delta C(s,z)\Delta C(z,u)+\\
&+\Theta_{>}(s-u)\sum_{z=u+1}^{s-1}\delta_{b1}(p-1)C^{p-2}(s,z)\Delta h(s,z)\Delta C(z,u)\,.
\end{aligned}
\tag{3.84}
$$

The next step is to consider the infinite chain limit. To do this we use the result about the response function and we put the reasonable ansatz [72]

$$
\frac{1}{\beta}R(u,s)\mathrm{d}s = \Theta_{>}(u-s)\Delta C(s,u) \tag{3.85}
$$

Using this, the product of the two matrices becomes

$$\sum_{z=1}^{L}\sum_{c=1}^{n(z)}[Q_{ac}(s,z)]^{p-1}Q_{cb}(z,u) \to C^{p-1}(s,u)\Delta C(u,u) + \Delta C_{p-1}(s,s)C(s,u) + \\ + \frac{1}{\beta}\int_0^u \mathrm{d}z C^{p-1}(s,z)R(u,z) + \frac{1}{\beta}\int_0^s \mathrm{d}z(p-1)C^{p-2}(s,z)R(s,z)C(z,u) + \\ + C^{p-1}(s,0)C(0,u) + \delta_{ab}\delta_{su}\left[\Delta C_{p-1}(s,s)\Delta C(s,s)\right] + \\ + \Theta_{>}(u-s)\delta_{a1}\left[\frac{1}{\beta}\Delta C_{p-1}(s,s)R(u,s) + \frac{1}{\beta}(p-1)C^{p-2}(u,s)R(u,s)\Delta C(u,u) + \right. \\ \left. + \frac{1}{\beta^2}\int_s^u \mathrm{d}z(p-1)C^{p-2}(s,z)R(z,s)R_c(u,z)\right] + \\ + \Theta_{>}(s-u)\delta_{b1}\left[\frac{1}{\beta}\Delta C_{p-1}(s,s)R(s,u) + \frac{1}{\beta}(p-1)C^{p-2}(s,u)R(s,u)\Delta C(u,u)\right. \\ \left. + \frac{1}{\beta^2}\int_u^s \mathrm{d}z(p-1)C^{p-2}(s,z)R(s,z)R(z,u)\right] \tag{3.86}$$

Note that to obtain the above result we have taken the replica limit $n_1 \to 1$ that tells that we are looking at the equilibrium TAP states. In the end one obtains the following equation for the "scalar" part

$$\nu(t)C(t,u) = \frac{\beta^2 p}{2}\left[C^{p-1}(t,u)\Delta C(u,u) + \Delta C_{p-1}(t,t)C(t,u) + C^{p-1}(t,0)C(u,0) + \right. \\ \left. + \frac{1}{\beta}\int_0^u \mathrm{d}z\, C^{p-1}(t,z)R(u,z) + \frac{p-1}{\beta}\int_0^t \mathrm{d}z\, C^{p-2}(t,z)R(t,z)C(z,u)\right] \tag{3.87}$$

From the "response" part of the equation one gets

$$\frac{1}{\beta}\nu(t)R(t,u) = \frac{\beta^2 p}{2}\left[\frac{1}{\beta}\Delta C_{p-1}(t,t)R(t,u) + \frac{p-1}{\beta}C^{p-2}(t,u)R(t,u)\Delta C(u,u) + \right. \\ \left. \frac{p-1}{\beta^2}\int_u^t \mathrm{d}z\, C^{p-2}(t,z)R(t,z)R(z,u)\right] \tag{3.88}$$

Moreover from the diagonal part we can obtain the equation for the Lagrange multiplier that were needed to fix the spherical constraints

$$\nu(t)\Delta C(t,t) = \frac{\beta^2 p}{2}\Delta C_{p-1}(t,t)\Delta C(u,u) + 1\,. \tag{3.89}$$

Note that because of the fact that we have taken the infinite chain limit and the continuum ansatz for the correlation and response functions we have substituted (k,j) with (t,u) in order to make the notation clearer. The Lagrange multiplier is fixed by the fact that we want a solution where $\tilde{C}(t,t) = 1 \quad \forall t$ (and this has been used in (3.83)).

At this point we search for a solution where

$$\Delta C(t,t) = 1 - q_d \qquad \forall t \tag{3.90}$$

It follows that the Lagrange multiplier is given by

$$\nu(t) = \frac{\beta^2 p}{2}\left(1 - q_d^{p-1}\right) + \frac{1}{1-q_d} \tag{3.91}$$

We are now equipped to study both the equilibrium and the off-equilibrium dynamics.

3.4.1 Equilibrium dynamics

We will search for a solution of the equations (3.87) and (3.88) that is time translational invariant (TTI) and that satisfies the fluctuation-dissipation theorem (FDT). Under this assumption we obtain that the equations can be rewritten in the following way

$$\begin{aligned} 0 = &-\frac{C(t)}{1-q_d} + \frac{\beta^2 p}{2}\left[C^{p-1}(t) - C^p(t) - q_d^{p-1}C(t)\right] - \\ &- \frac{\beta^2 p}{2}\int_0^t \mathrm{d}z \dot{C}(z)\left[C^{p-1}(t-z) - C^{p-1}(t)\right] \end{aligned} \tag{3.92}$$

that is the dynamical equation for the correlation function asymptotically close to the dynamical point. It is quite easy to show that by evaluating the equation in $t = 0$ and by imposing that $C(0) = q_d$ we obtain the equation for both the critical temperature and the plateau value q_d.

Computation of λ

Having the equation in the equilibrium regime we want to compute the exponent parameter λ in the p-spin spherical model. The calculation of this parameter has been done several times and is a standard quantity that can be computed within any mode-coupling like equation. However we prefer to recall it here because it will be a good guideline when we will discuss the application of Boltzmann Pseudodynamics to the structural glass case. The known result is that $\lambda = 1/2$ for every p and we want to derive again this by using the equation of the Boltzmann Pseudodynamics.

Because of the fact that λ is the exponent parameter that controls how the correlation function behaves when it is around the plateau, we will try to stay at times such that asymptotically we are near the plateau. This means that we develop

$$C(t) = q_d + At^b \tag{3.93}$$

where A is a constant that cannot be determined (even if we know that it should be negative). The ansatz above is valid only near the plateau. At this point we want to develop the equation (3.92) in powers of t^b. We note that the first non trivial term is proportional to t^{2b} because the zeroth order and the first one vanish due to the fact that q_d is a double root of the same equation evaluated in $t = 0$. This means that we have to take the second variation of the above equation. In this way, expanding the equation at the second order, it becomes

$$\begin{aligned} 0 = t^{2b}A^2 \Bigg\{ &\frac{(p-1)(p-2)}{2} q_d^{p-3} - \frac{p(p-1)}{2} q_d^{p-2} - \\ &- (p-1) q_d^{p-2} \int_0^t \mathrm{d}z\, b z^{b-1}\left((t-z)^b - t^b\right)\Bigg\} \end{aligned} \tag{3.94}$$

The last term can be evaluated as follows

$$\begin{aligned}\int_0^t \mathrm{d}z\, bz^{b-1}\left((t-z)^b - t^b\right) &= t^{2b}\int_0^t \frac{\mathrm{d}z}{z}\, b\left(\frac{z}{t}\right)^{b-1}\left[\left(\frac{t}{z}-1\right)^b - \left(\frac{t}{z}\right)^b\right] = \\ &= t^{2b}\int_1^\infty \mathrm{d}y\, by^{-2b-1}\left[(y-1)^b - y^b\right] = \\ &= t^{2b}\left[-1 + \int_1^\infty \mathrm{d}y\, by^{-2b-1}(y-1)^b\right].\end{aligned} \tag{3.95}$$

The integral in the last line is given by

$$\begin{aligned}&\int_1^\infty \mathrm{d}y\, by^{-2b-1}(y-1)^b = \int_1^\infty \mathrm{d}y\, \frac{b}{\Gamma(1+2b)}\int_0^\infty \mathrm{d}s\, e^{-sy}s^{2b}(y-1)^b = \\ &= \frac{b}{\Gamma(1+2b)}\int_0^\infty \mathrm{d}s s^{b-1}e^{-s}\int_0^\infty \mathrm{d}z\, e^{-z}z^b = \frac{\Gamma^2(1+b)}{\Gamma(1+2b)}\end{aligned} \tag{3.96}$$

where in the last equalities we have used the standard relation

$$\frac{1}{x^n} = \frac{1}{\Gamma(n)}\int_0^\infty \mathrm{d}t t^{n-1}e^{-xt}\,. \tag{3.97}$$

It follows that

$$\int_0^t \mathrm{d}z\, bz^{b-1}\left((t-z)^b - t^b\right) = t^{2b}\left[-1 + \frac{\Gamma^2(1+b)}{\Gamma(1+2b)}\right] \tag{3.98}$$

Putting everything into the dynamical equation for the correlation function we obtain

$$0 = \frac{p-2}{2q_d} - \frac{p}{2} - \left(-1 + \frac{\Gamma^2(1+b)}{\Gamma(1+2b)}\right) \tag{3.99}$$

and by using that

$$q_d = \frac{p-2}{p-1} \tag{3.100}$$

we obtain

$$\lambda = \frac{\Gamma^2(1+b)}{\Gamma(1+2b)} = \frac{1}{2} \tag{3.101}$$

that is the known result.

3.4.2 Off-equilibrium dynamics

The aging dynamics can be obtained by noting that the term proportional to $C^{p-1}(t,0)C(u,0)$ is zero in the asymptotic aging time window. The new equations of motion are

$$\begin{aligned}0 &= C(t,u)\left[-\frac{1}{1-q_d} + \frac{\beta^2 p}{2}(1-q_d)C^{p-2}(t,u)\right] + \\ &+ \frac{\beta p}{2}\int_0^u \mathrm{d}z\, C^{p-1}(t,z)R(u,z) + \frac{\beta p(p-1)}{2}\int_0^t \mathrm{d}z\, C^{p-2}(t,z)R(t,z)C(u,z)\end{aligned} \tag{3.102}$$

$$
\begin{aligned}
0 = R(t,u)\left[-\frac{1}{1-q_d} + \frac{\beta^2 p(p-1)}{2}(1-q_d)C^{p-2}(t,u)\right] + \\
+ \frac{\beta p(p-1)}{2}\int_u^t \mathrm{d}z\, C^{p-2}(t,z)R(t,z)R(z,u)
\end{aligned}
\tag{3.103}
$$

At this point we make the following ansatz. For $t > u$ we assume

$$
\begin{aligned}
C(t,u) &= \mathcal{C}\left(\frac{u}{t}\right) \\
R(t,u) &= \frac{1}{t}\mathcal{R}\left(\frac{u}{t}\right)
\end{aligned}
\tag{3.104}
$$

and denoting $\lambda = u/t$ we obtain that the dynamical equations become

$$
\begin{aligned}
0 = \mathcal{C}(\lambda)\left[-\frac{1}{1-q_d} + \frac{\beta^2 p}{2}(1-q_d)\mathcal{C}^{p-2}(\lambda)\right] + \frac{\beta p}{2}\int_0^\lambda \frac{\mathrm{d}\lambda'}{\lambda}\,\mathcal{C}^{p-1}(\lambda')\mathcal{R}\left(\frac{\lambda'}{\lambda}\right) + \\
+ \frac{\beta p(p-1)}{2}\int_0^1 \mathrm{d}\lambda'\,\mathcal{C}^{p-2}(\lambda')\mathcal{R}(\lambda')\mathcal{C}\left[\left(\frac{\lambda}{\lambda'}\right)^{\mathrm{sgn}(\lambda'-\lambda)}\right]
\end{aligned}
\tag{3.105}
$$

$$
\begin{aligned}
0 = \mathcal{R}(\lambda)\left[-\frac{1}{1-q_d} + \frac{\beta^2 p(p-1)}{2}(1-q_d)\mathcal{C}^{p-2}(t,u)\right] + \\
+ \frac{\beta p(p-1)}{2}\int_\lambda^1 \frac{\mathrm{d}\lambda'}{\lambda'}\,\mathcal{C}^{p-2}(\lambda')\mathcal{R}(\lambda')\mathcal{R}\left(\frac{\lambda}{\lambda'}\right)
\end{aligned}
\tag{3.106}
$$

that are exactly the equations for the aging part of the correlation and response functions in the aging regime. It follows that the FDT-ration x is exactly the one found by Cugliandolo and Kurchan [51]. Moreover let us underline a basic fact that will be useful in the structural glass computation. In order to have a non-vanishing response function in the low temperature phase, the quantity inside the square brackets in the second equation should vanish. This gives an equation for q_d in the low temperature phase and this equation is what is known as the marginal stability condition.

3.5 Boltzmann Pseudodynamics for HNC liquids

In order to extend the Boltzmann Pseudodynamics in the structural glass case we will start from the Ornstein-Zernike equations and we will close them with the Hypernetted Chain approximation. Let us write them again

$$
\ln[h_{ab}(x,y)+1] + \beta\phi_{ab}(x,y) = h_{ab}(x,y) - c_{ab}(x,y) \tag{3.107}
$$

$$
c_{ab}(x,y) = h_{ab}(x,y) - \sum_{c=1}^{n}\int \mathrm{d}z h_{ac}(x,z)\rho_c c_{cb}(z,y) \tag{3.108}
$$

We will suppose that there is space translational invariance which ensure that all the two point quantities are actually functions only of the distance between the points. Here we choose to change notation to be closer to the one of [72]. Calling $\tilde{h}(x) = h_{a=b}(x)$ and $h(x) = h_{a\neq b}(x)$ and using the analogous notation for the direct

correlation function we have that at the dynamical point the following equations holds

$$\ln[\tilde{h}(x)+1]+\beta\phi(x)=\tilde{h}(x)-\tilde{c}(x) \tag{3.109}$$
$$\ln[h(x)+1]=h(x)-c(x) \tag{3.110}$$
$$\tilde{h}(q)=\tilde{c}(q)+\rho\left[\tilde{h}(q)\tilde{c}(q)+(m-1)h(q)c(q)\right] \tag{3.111}$$
$$h(q)=c(q)+\rho\left[\tilde{h}(q)c(q)+\tilde{c}(q)h(q)+(m-2)h(q)c(q)\right] \tag{3.112}$$

where in (3.108) we have rewritten the convolution as a product in Fourier space. In the limit $m\to 1$ we obtain the HNC equation for the dynamical transition point

$$\ln[\tilde{h}(x)+1]+\beta\phi(x)=\tilde{h}(x)-\tilde{c}(x) \tag{3.113}$$
$$\ln[h(x)+1]=h(x)+c(x) \tag{3.114}$$
$$\tilde{h}(q)=\tilde{c}(q)+\rho\left[\tilde{h}(q)\tilde{c}(q)+h(q)c(q)\right] \tag{3.115}$$
$$h(q)=c(q)+\rho\left[\tilde{h}(q)c(q)+\tilde{c}(q)h(q)-h(q)c(q)\right] \tag{3.116}$$

If one focuses on the differences between diagonal and off diagonal elements like $\Delta h(q)=\tilde{h}(q)-h(q)$ and $\Delta c(q)=\tilde{c}(q)-c(q)$ one sees immediately that

$$\Delta h(q)=\Delta c(q)+\rho\Delta h(q)\Delta c(q)\,. \tag{3.117}$$

The dynamical point appears when $h(x)\neq 0$ and $m=1$.

We will now derive the dynamical equations in the Boltzmann Pseudodynamics directly starting from these equations. To do this, we assume that there is a chain of replicas and for every point z in the chain there are $n(z)$ replicas. In this way, the most natural ansatz for the two matrices is the Franz-Parisi replica symmetric one:

$$\begin{aligned}h_{ab}(x)=&h(s,u;x)+\delta_{ab}\delta_{su}\Delta h(s,s;x)+\Theta_{>}(u-s)\delta_{a1}\Delta h(s,u;x)+\\&+\Theta_{>}(s-u)\delta_{b1}\Delta h(s,u;x)\end{aligned} \tag{3.118}$$

$$\begin{aligned}c_{ab}(x)=&c(s,u;x)+\delta_{ab}\delta_{su}\Delta c(s,s;x)+\Theta_{>}(u-s)\delta_{a1}\Delta c(s,u;x)+\\&+\Theta_{>}(s-u)\delta_{b1}\Delta c(s,u;x)\end{aligned} \tag{3.119}$$

where $\Delta h(q;s,u)=\tilde{h}(q;s,u)-h(q;s,u)$ and an analogous notation holds for $\Delta c(q;s,u)$. Here, again, s and u are the positions of the two groups of replicas inside the chain and in the continuum limit of infinite chain they will become two pseudo-time coordinates. The indices a and b identify two replicas inside the two groups selected by the pseudo-time indices. We will analyze a situation where ρ is a constant.

Now we can see how the replica ansatz above can be put inside the equations. Let us start from the OZ equation in Fourier space

$$h_{ab}(q)=c_{ab}(q)+\rho\sum_{c=1}^{n}h_{ac}(q)c_{cb}(q)\,; \tag{3.120}$$

we note that the last term is the product of two replica matrices and we know how to treat it within the Pseudodynamics parametrization for the replica matrices. In fact, by using the representation (3.118) and (3.119) we get

$$\begin{aligned}
&\sum_{c=1}^{n} h_{ac}(q)c_{cb}(q) = \sum_{z=1}^{L}\sum_{c=1}^{n(z)} h_{ac}(q;s,z)c_{cb}(q;z,u) = \sum_{z=1}^{L}\sum_{c=1}^{n(z)} [h(s,z;q)+ \\
&+\delta_{ac}\delta_{sz}\Delta h(s,s;q) + \Theta_{>}(z-s)\delta_{a1}\Delta h(s,z;q) + \Theta_{>}(s-z)\delta_{c1}\Delta h(s,z;q)] \times \\
&\times [c(z,u;q) + \delta_{cb}\delta_{zu}\Delta c(u,u;q) + \Theta_{>}(u-z)\delta_{c1}\Delta c(z,u;q)+ \\
&+\Theta_{>}(z-u)\delta_{b1}\Delta c(z,u;q)] = \\
&= \sum_{z=1}^{L} n(z)h(q;s,z)c(q;z,u) + h(q;s,u)\Delta c(q;u,u) + \sum_{z=1}^{u-1} h(q;s,z)\Delta c(q;z,u)+ \\
&+ \sum_{z=u+1}^{L} n(z)\delta_{b1}h(q;s,z)\Delta c(q;z,u) + \Delta h(q,s,s)c(q;s,u)+ \\
&+ \delta_{ab}\delta_{su}\Delta h(q;s,s)\Delta c(q;s,s) + \Theta_{>}(u-s)\delta_{a1}\Delta h(q;s,s)\Delta c(q;s,u)+ \\
&+ \Theta_{>}(s-u)\delta_{b1}\Delta h(q;s,s)\Delta c(q;s,u) + \sum_{z=s+1}^{L} n(z)\delta_{a1}\Delta h(q;s,z)c(q;z,u)+ \\
&\Theta_{>}(s-u)\delta_{a1}\Delta h(q;s,s)\Delta c(q;u,u) + \Theta_{>}(u-s)\sum_{z=s+1}^{u-1}\delta_{a1}\Delta h(q;s,z)\Delta c(q;z,u)+ \\
&+ \sum_{z=\max(s,u)+1}^{L} n(z)\delta_{a1}\delta_{b1}\Delta h(q;s,z)\Delta c(q;z,u) + \sum_{z=1}^{s-1}\Delta h(q;s,z)c(q;z,u)+ \\
&+ \Theta_{>}(s-u)\delta_{b1}\Delta h(q;s,u)\Delta c(q;u,u) + \sum_{z=1}^{\min(s,u)-1}\Delta h(q;s,z)\Delta c(q;z,u)+ \\
&+ \Theta_{>}(s-u)\sum_{z=u+1}^{s-1}\delta_{b1}\Delta h(q;s,z)\Delta c(q;z,u)\ .
\end{aligned} \tag{3.121}$$

At this point we have to take the limit of an infinite chain of replicas together with the replica limit. To do this we point out the following things: first of all we have to take the limit in which all the $n(z)$ numbers of replicas go to zero except for the first one $n(1)$ which goes to one. This is because, as discussed for the p-spin case, the idea is that the first replica is unconstrained. Here, because there is no quenched disorder, to pick the Boltzmann measure on the metastable states we can use the Monasson method and replicate the system m times and then let the number of replicas go to one. Moreover the functions $h(q;s,u)$ and $c(q;s,u)$ become continuous functions of the variables $s,\ u$. In this way we put

$$\frac{1}{\beta}R_h(q;u;s)\mathrm{d}s = \Theta_{>}(u-s)\Delta h(q;s,u) \tag{3.122}$$

$$\frac{1}{\beta}R_c(q;u,s)\mathrm{d}s = \Theta_{>}(u-s)\Delta c(q;s,u) \tag{3.123}$$

that is the generalization of the result for the response function that we have found in the previous sections. Using this, the product of the two matrices becomes

$$\begin{aligned}
&\sum_{c=1}^{n} h_{ac}(q)c_{cb}(q) \to \Delta h(q;s,s)c(q;s,u) + \frac{1}{\beta}\int_0^u \mathrm{d}z h(q;s,z)R_c(q;u,z) + \\
&h(q;s,u)\Delta c(q;u,u) + \frac{1}{\beta}\int_0^s \mathrm{d}z R_h(q;s,z)c(q;z,u) + h(q;s,0)c(q;0,u) + \\
&+ \delta_{ab}\delta_{su}\left[\Delta h(q;s,s)\Delta c(q;s,s)\right] + \Theta_>(u-s)\delta_{a1}\left[\frac{1}{\beta}\Delta h(q;s,s)R_c(q;u,s) + \right. \\
&\left. + \frac{1}{\beta}R_h(q;u,s)\Delta c(q;u,u) + \frac{1}{\beta^2}\int_s^u \mathrm{d}z R_h(q;z,s)R_c(q;u,z)\right] + \\
&+ \Theta_>(s-u)\delta_{b1}\left[\frac{1}{\beta}\Delta h(q;s,s)R_c(q;s,u) + \frac{1}{\beta}R_h(q;s,u)\Delta c(q;u,u) + \right. \\
&\left. \frac{1}{\beta^2}\int_u^s \mathrm{d}z R_h(q;s,z)R_c(q;z,u)\right]
\end{aligned} \tag{3.124}$$

This means that the OZ equation generates the following dynamical equations

$$\begin{aligned}
h(q;s,u) = c(q;s,u) + \rho\,&[h(q;s,0)c(q;0,u) + h(q;s,u)\Delta c(q;u,u) + \\
&+\Delta h(q;s,s)c(q;s,u) + \frac{1}{\beta}\int_0^u \mathrm{d}z h(q;s,z)R_c(q;u,z) + \\
&\left.\frac{1}{\beta}\int_0^s \mathrm{d}z R_h(q;s,z)c(q;z,u)\right]
\end{aligned} \tag{3.125}$$

$$\Delta h(q;s,s) = \Delta c(q;s,s) + \rho\Delta h(q;s,s)\Delta c(q;s,s) \tag{3.126}$$

$$\begin{aligned}
R_h(q;u,s) = R_c(q;u,s) + \rho\,&[R_h(q;u,s)\Delta c(q;u,u) + \Delta h(q;s,s)R_c(q;u,s) + \\
&\left.+\frac{1}{\beta}\int_s^u \mathrm{d}z R_h(q;z,s)R_c(q;u,z)\right]
\end{aligned} \tag{3.127}$$

Now let us consider the first constitutive equation (3.107). The idea is to develop the logarithm with a power series and than to look at what happens when we consider an infinite long chain. To do this let us look at the building block of the series

$$\begin{aligned}
h^l_{ab}(x;s,u) = h^l(x;s,u) + \delta_{ab}\delta_{su}\Delta h_l(x;s,u) + \frac{1}{\beta}\delta_{a1}lh^{l-1}(x;s,u)R_h(x;u,s)\mathrm{d}s + \\
+\frac{1}{\beta}\delta_{b1}lh^{l-1}(x;s,u)R_h(x;s,u)
\end{aligned} \tag{3.128}$$

where we have taken into account just the zeroth and first order in $\mathrm{d}s$. Equation (3.107) can be rewritten in the following way

$$\sum_{l=1}^{\infty}\frac{(-1)^l}{l}h^l_{ab}(x) + \beta\phi_{ab}(x) = h_{ab}(x) - c_{ab}(x) \tag{3.129}$$

Using (3.128), the above equation generates the following relations

$$\sum_{l=1}^{\infty} \frac{(-1)^{l+1}}{l} h^l(x;s,u) = h(x;s,u) - c(x;s,u) \tag{3.130}$$

$$\sum_{l=1}^{\infty} \frac{(-1)^{l+1}}{l} \Delta h_l(x;s,s) + \beta\phi(x) = \Delta h(x;s,s) - \Delta c(x;s,s) \tag{3.131}$$

$$\sum_{l=1}^{\infty} (-1)^{l+1} h^{l-1}(x;s,u) R_h(x;s,u) = R_h(x;s,u) - R_c(x;s,u) \tag{3.132}$$

The first equation can be rewritten in the following way

$$\ln[h(x;s,u)+1] = h(x;,s,u) - c(x;s,u) \tag{3.133}$$

while the third one becomes

$$R_c(x;s,u) = R_h(x;s,u) \frac{h(x;s,u)}{1+h(x;s,u)} \,. \tag{3.134}$$

Moreover it is easy to see that eq. (3.131) is nothing but the difference between (3.113) and (3.114). This means that the two quantities $\Delta c(,1,2;s,s)$ and $\Delta h(1,2;s,s)$ are actually independent on s and are exactly the quantities that can be computed by solving the equations (3.113)-(3.116). The fact that these two quantities do not depend on s is because in the equation (3.107) we have not coupling between replicas at different times. In the end we get the following equation

$$\begin{aligned} h(q;s,u) = c(q;s,u) + \rho \Big[& h(q;s,u)\Delta c(q;u,u) + \Delta h(q;s,s) c(q;s,u) + \\ & + h(q;s,0) c(q;0,u) + \frac{1}{\beta} \int_0^u \mathrm{d}z R_c(q;u,z) h(q;s,z) + \\ & + \frac{1}{\beta} \int_0^s \mathrm{d}z R_h(q;s,z) c(q;z,u) \Big] \end{aligned} \tag{3.135}$$

Let us note that actually this is an equation in h and R_h because c and R_c can be computed using the previous equations. The equation for R_h is given by

$$\begin{aligned} R_h(q;u,s) = R_c(q;u,s) + \rho \Big[& R_h(q;u,s)\Delta c(q;u,u) + \Delta h(q;s,s) R_c(q;u,s) + \\ & + \frac{1}{\beta} \int_s^u \mathrm{d}z R_h(q;z,s) R_c(q;u,z) \Big] \,. \end{aligned} \tag{3.136}$$

By construction it is evident that the above equations are covariant under time reparametrization which means that if we have a solution for them, $h(q;s,u)$, $c(q;s,u)$, $R_h(q;s,u)$ and $R_c(q;s,u)$, we can obtain another solution by choosing a monotone increasing function $f(t)$ and writing the new solution in the following way

$$h'(q;s,u) = h(q;f(s),f(u)) \quad c'(q;s,u) = c(q;f(s),f(u)) \tag{3.137}$$

$$R'_h(q;s,u) = \frac{\mathrm{d}f(u)}{\mathrm{d}u} R_h(q;f(s),f(u)) \quad R'_c(q;s,u) = \frac{\mathrm{d}f(u)}{\mathrm{d}u} R_c(q;f(s),f(u)) \tag{3.138}$$

Because of the reparametrization invariance of the equations, we see that the time here is just an arbitrary parameter. To fix it to the physical time we have to "fix the gauge" by choosing a parametrization. In this way we can reduce the degrees of freedom of the above equations. In particular we can choose to fix the gauge in such a way that time translational invariance (TTI) and fluctuation-dissipation relation (FDT) are satisfied.

Although it is evident that a TTI solution is compatible with the equations, it is not evident a priori that also a FDT solution is possible. We will now verify that this is the case as can be argued on the basis of the algebraic properties of the Franz-Parisi matrices that are equivalent to the supersymmetric (*i.e.* FDT) ones of the dynamics [72]. Consider the following FDT ansatz

$$-\beta\frac{\mathrm{d}h(x;s-u)}{\mathrm{d}s}=R_h(x;s-u) \tag{3.139}$$

and consider the derivative with respect to s of the equation (3.133) in its TTI version. It gives

$$-\beta\frac{\mathrm{d}c(z;s-u)}{\mathrm{d}s}=R_h(x;s-u)+\frac{R_h(x;s-u)}{1+h(x;s-u)} \tag{3.140}$$

that is consistent with equation (3.134) if we put

$$-\beta\frac{\mathrm{d}c(z;s-u)}{\mathrm{d}s}=R_c(x;s-u) \tag{3.141}$$

At this point let us consider the equation for $h(q;s,u)$ in its TTI version (we can set $u=0$ due to TTI)

$$\begin{aligned}h(q;s)=c(q;s)+\rho\,[&h(q;s)\Delta c_0(q)+\Delta h_0(q)c(q;s)+\\&+\frac{1}{\beta}\int_0^s\mathrm{d}zR_h(q;s-z)c(q;z)+h(q;s)c(q;0)\Big]\end{aligned} \tag{3.142}$$

where we have introduced the following notation

$$\Delta h(q;s,s)=\Delta h_0(q)=\tilde{h}(q;0)-h(q;0) \tag{3.143}$$

$$\Delta c(q;s,s)=\Delta c_0(q)=\tilde{c}(q;0)-c(q;0) \tag{3.144}$$

Let us apply the operator $-\beta\mathrm{d}/\mathrm{d}s$ to the equation (3.142). Using (3.139) and (3.141) we obtain

$$\begin{aligned}&R_h(q;s)=R_c(q;s)+\rho\,[R_h(q;s)\Delta c_0(q)+\Delta h_0(q)R_c(q;s)+\\&+R_h(q;s)c(q;0)+\int_0^s\mathrm{d}z\frac{\mathrm{d}R_h(q;s-z)}{\mathrm{d}z}c(q;z)-R_h(q;0)c(q;s)\Big]=\\&=R_c(q;s)+\rho\,[R_h(q;s)\Delta c_0(q)+\Delta h_0(q)R_c(q;s)+\\&\frac{1}{\beta}\int_0^s\mathrm{d}zR_h(q;s-z)R_c(q;z)\Big]\end{aligned} \tag{3.145}$$

that is the equation for the response function in the TTI regime. This means that the above equations admit a FDT solution.

Let us now consider the equation for $h(q;s)$. Using TTI and FDT we obtain

$$\begin{aligned} 0 &= c(q,s) - h(q,s) + \rho \Big[h(q;s)\Delta c_0(q) + \Delta h_0(q) c(q;s) - \int_0^s \mathrm{d}z \dot{h}(q;s-z) c(q,z) + \\ &+ h(q;s)c(q;0)] = \\ &= W_q[h] - \rho \int_0^s \dot{h}(q,z)[c(q,s-z) - c(q;s)] \end{aligned} \tag{3.146}$$

where

$$\begin{aligned} W_q[h] = c(q;s) - h(q;s) + \rho \, [h(q;s)\Delta c_0(q) + c(q;s)\Delta h_0(q) + \\ + c(q;0)h(q;s) - (h(q,s) - h(q,0))c(q,s)] \ . \end{aligned} \tag{3.147}$$

This equation is the dynamical equation in the α regime at the dynamical point. Let us note that it is a mode-coupling equation but here the kernel is formally simple because it is given by the direct correlation function. Moreover we want to underline that the coupling between different modes comes from the fact that the relation between the direct correlation function and the function $h(q;t)$ is not diagonal in Fourier space in the sense that $c(q;t)$ depends in a complicated way from $h(k;t)$ as it can be seen by writing the equation (3.133) in Fourier space

$$\begin{aligned} c(q;t) = h(q;t) - \sum_{n=1}^{\infty} \frac{(-1)^{n+1}}{n} \int \frac{\mathrm{d}^D k_1}{(2\pi)^D} \cdots \\ \cdots \int \frac{\mathrm{d}^D k_{n-1}}{(2\pi)^D} h(k_1;t) \ldots h(k_{n-1},t) h(q - k_1 - \ldots - k_{n-1};t) \ . \end{aligned} \tag{3.148}$$

In general, in mode-coupling theory one has a kernel which is a finite polynomial in the dynamical variables (namely the normalized dynamical structure factor) but here we have a kernel which is an infinite series of the dynamical variables.

We will show now how to obtain the exponent parameter λ from this equation. First of all let us prove that the "plateau" solution is determined by putting W_q equal to zero. In fact let us compute

$$\begin{aligned} W_q[h]|_{h(\cdot;0)} &= c(q;0) - h(q;0) + \rho[h(q;0)(\tilde{c}(q;0) - c(q;0)) + \\ &+ c(q;0)(\tilde{h}(q;0) - h(q;0)) + c(q;0)h(q;0)] = \\ &= c(q,0) - h(q;0) + \rho[h(q,0)\tilde{c}(q;0) + c(q:0)\tilde{h}(q;0) - c(q;0)h(q;0)] = 0 \end{aligned} \tag{3.149}$$

where the last equality follows because of equation (3.116). Now let us compute the first derivative of W_q at the dynamical point and at zero time. To do this we need the following basic quantity

$$\frac{\delta c(q;t)}{\delta h(k;t)} = (2\pi)^D \delta(q-k) - \text{T.F.} \left(\frac{1}{\tilde{g}(x)} \right) (q-k) \tag{3.150}$$

where $\tilde{g}(x) = 1 + h(x)$ is the off-diagonal two point density correlation function and T.F.$(\cdot)$ denotes the Fourier transform. From this relation it follows that

$$\begin{aligned} \frac{\delta W_q[h]}{\delta h(k,s)}\Big|_{h(\cdot;0)} = \frac{1}{1-\rho\Delta c(q)} \Big[(2\pi)^D \delta(q-k)(2\rho\Delta c(q) - \rho^2 \Delta c^2(q)) - \\ - \text{T.F.} \left(\frac{1}{\tilde{g}(x)} \right) (q-k) \Big] = -\frac{2\rho^2}{1-\rho\Delta c(q)} M_1^{(p=0)}(q,k) \end{aligned} \tag{3.151}$$

where $M_1^{(p=0)}(q,k)$ is exactly the kernel operator discussed in the previous chapter that has a zero eigenvector at the dynamical transition that we denote with $k_0(k)$. Moreover remember that M_1 is asymmetric so that the kernel operator $\frac{\delta W_q[h]}{\delta h(k,s)}\Big|_{h(\cdot;0)}$ has $k_0(k)$ as right eigenvector and $(1-\rho\Delta c(q))k_0(q)$ as left eigenvector. Now let us put

$$h(q;t) = h(q;0) + G_q(t) \qquad G_q(t) = Ak_0(q)t^b + \delta G_q(t) \tag{3.152}$$

where

$$\int \frac{\mathrm{d}^D q}{(2\pi)^D} k_0(q)\delta G_q(t) = 0 \quad \forall t > 0 \tag{3.153}$$

At this point we should develop the dynamical equation in powers of $G_q(t)$. The zero order is trivially zero because $h(q;0)$ is a solution for the plateau. Moreover the first order is given by the Jacobian matrix (3.151) multiplied by the zero mode which is equal to zero. It follows that the equation reduces to the second variation equal to zero. Moreover the equality remains valid if we multiply all the equation by the left eigenvector of the Jacobian matrix. It follows that we need to compute all the second order variation terms of the dynamical equation. The first term is given by

$$\begin{aligned}
&\frac{\delta^2 W_q[h]}{\delta h(k;s)\delta h(p;s)}\bigg|_{h(\cdot;0)} = -\rho(2\pi)^D\delta(q-p)\left[(2\pi)^D\delta(q-k) - \text{T.F.}\left(\frac{1}{\tilde{g}}\right)(q-k)\right] - \\
&- \rho(2\pi)^D\delta(q-k)\left[(2\pi)^D\delta(q-p) - \text{T.F.}\left(\frac{1}{\tilde{g}}\right)(q-p)\right] + \\
&+ \frac{1}{1-\rho\Delta c(q)}\text{T.F.}\left(\frac{1}{\tilde{g}^2}\right)(q-p-k)
\end{aligned} \tag{3.154}$$

The second term to be computed is the variation of the integral which is given by

$$\begin{aligned}
&\delta^2\int_0^t \mathrm{d}s\dot{h}(q;s)[c(q;t-s) - c(q;t)] = \\
&= k_0(q)\left[k_0(q) - \int\frac{\mathrm{d}^D k}{(2\pi)^D}\text{T.F.}\left(\frac{1}{\tilde{g}}\right)(q-k)k_0(k)\right]t^{2b}\left[-1 + \frac{\Gamma^2(1+b)}{\Gamma(1+2b)}\right]
\end{aligned} \tag{3.155}$$

From all this it follows that the dynamical equation at the second order multiplied on the left by the left eigenvector of the Jacobian matrix is given by

$$\begin{aligned}
0 = &\int_q k_0(q)(1-\rho\Delta c(q))\left[-2\rho k_0^2(q) + 2\rho\int_k k_0(q)\text{T.F.}\left(\frac{1}{\tilde{g}}\right)(q-k)k_0(k) + \right. \\
&\left.\frac{1}{1-\rho\Delta c(q)}\int_{k,p}\text{T.F.}\left(\frac{1}{\tilde{g}^2}\right)(q-k-p)k_0(k)k_0(p)\right]t^{2b} + \\
&- 2\rho\int_q k_0^2(q)(1-\rho\Delta c(q))\left[k_0(q) - \int_k \text{T.F.}\left(\frac{1}{\tilde{g}}\right)(q-k)k_0(k)\right]\times \\
&\times t^{2b}\left[-1 + \frac{\Gamma^2(1+b)}{\Gamma(1+2b)}\right]
\end{aligned} \tag{3.156}$$

from which it follows

$$\lambda = \frac{\Gamma^2(1+b)}{\Gamma(1+2b)} = \\ = \frac{\int_{q,k,p} \text{T.F.}\left(\frac{1}{\tilde{g}^2}\right)(q-k-p)k_0(k)k_0(p)k_0(q)}{2\rho\int_q k_0^2(q)(1-\rho\Delta c(q))\int_k \left[(2\pi)^D\delta(q-k) - \text{T.F.}\left(\frac{1}{\tilde{g}}\right)(q-k)\right]k_0(k)} \tag{3.157}$$

Let us have a look to the denominator that can be rewritten using the fact that

$$\int_k \left.\frac{\delta W_q[h]}{\delta[h(k,s)]}\right|_{h(\cdot;0)} k_0(k) = 0 \tag{3.158}$$

from which it follows that

$$\int_q k_0^2(q)(1-\rho\Delta c(q))\int_k \left[(2\pi)^D\delta(q-k) - \text{T.F.}\left(\frac{1}{\tilde{g}}\right)(q-k)\right]k_0(k) = \int_q k_0^3(q)(1-\rho\Delta c(q))^3. \tag{3.159}$$

The final expression for λ is given by

$$\lambda = \frac{\int \mathrm{d}^D x \frac{k_0^3(x)}{\tilde{g}^2(x)}}{2\rho\int_q k_0^3(q)(1-\rho\Delta c(q))^3} \tag{3.160}$$

that is exactly the one computed in the previous chapter.

3.5.1 The aging regime

At this point we want to study the aging regime of the dynamical equations we have derived before. Because we are in the aging time window, we can set to zero the term $h(q;s,0)c(q;u,0)$ and the dynamical equations become

$$h(q;s,u) = c(q;s,u) + \rho\left[\Delta h(q)c(q;s,u) + \frac{1}{\beta}\int_0^u \mathrm{d}z R_c(q;u,z)h(q;s,z) + \right. \\ \left. + h(q;s,u)\Delta c(q) + \frac{1}{\beta}\int_0^s \mathrm{d}z R_h(q;s,z)c(q;z,u)\right] \tag{3.161}$$

$$R_h(q,s,u) = R_c(q;s,u) + \rho\left[R_h(q;s,u)\Delta c(q) + \right. \\ \left. + \Delta h(q)R_c(q;s,u) + \frac{1}{\beta}\int_u^s \mathrm{d}z R_h(q;z,u)R_c(q;s,z)\right]. \tag{3.162}$$

Now we make the usual aging ansatz so that for $s > u$ we have

$$\begin{aligned} h(q;s,u) &= \underline{h}\left(q;\frac{u}{s}\right) \\ R_h(q;s,u) &= \frac{1}{s}\mathcal{R}_h\left(q;\frac{u}{s}\right) \\ c(q;s,u) &= \underline{c}\left(q;\frac{u}{s}\right) \\ R_c(q;s,u) &= \frac{1}{s}\mathcal{R}_c\left(q;\frac{u}{s}\right) \end{aligned} \tag{3.163}$$

Using these new variables and setting $\lambda = u/s$, the equations become

$$\begin{aligned}\underline{h}(q;\lambda) = \underline{c}(q;\lambda) + \rho\Bigg[\Delta h(q)\underline{c}(q;\lambda) + \frac{1}{\beta}\int_0^\lambda \frac{\mathrm{d}\lambda'}{\lambda}\mathcal{R}_c\left(q;\frac{\lambda'}{\lambda}\right)\underline{h}(q;\lambda') + \\ + \underline{h}(q;\lambda)\Delta c(q) + \frac{1}{\beta}\int_0^1 \mathrm{d}\lambda'\mathcal{R}_h(q;\lambda')\underline{c}\left[q;\left(\frac{\lambda'}{\lambda}\right)^{\mathrm{sgn}(\lambda-\lambda')}\right]\Bigg]\end{aligned} \tag{3.164}$$

$$\begin{aligned}&\mathcal{R}_h(q,\lambda) = \mathcal{R}_c(q;\lambda) + \\ &+\rho\left[\mathcal{R}_h(q;\lambda)\Delta c(q) + \Delta h(q)\mathcal{R}_c(q;\lambda) + \frac{1}{\beta}\int_\lambda^1 \frac{\mathrm{d}\lambda'}{\lambda'}\mathcal{R}_h\left(q;\frac{\lambda}{\lambda'}\right)\mathcal{R}_c(q;\lambda')\right].\end{aligned} \tag{3.165}$$

At this point it is easy to show that these equations are consistent with a quasi-FDT ansatz for the response functions

$$\begin{aligned}\mathcal{R}_h(q;\lambda) &= \beta x\frac{\mathrm{d}}{\mathrm{d}\lambda}\underline{h}(q;\lambda) \\ \mathcal{R}_c(q;\lambda) &= \beta x\frac{\mathrm{d}}{\mathrm{d}\lambda}\underline{c}(q;\lambda)\,.\end{aligned} \tag{3.166}$$

By applying the operator $\beta x\mathrm{d}/\mathrm{d}\lambda$ to the equation (3.164) and by using the following identities

$$\frac{\mathrm{d}}{\mathrm{d}\lambda}f\left(\frac{\lambda'}{\lambda}\right) = -\frac{\lambda'}{\lambda}\frac{\mathrm{d}}{\mathrm{d}\lambda'}\left(\frac{\lambda'}{\lambda}\right) \tag{3.167}$$

$$\beta x\frac{\mathrm{d}}{\mathrm{d}\lambda}\int_0^\lambda \frac{\mathrm{d}\lambda'}{\lambda}\mathcal{R}_c\left(q;\frac{\lambda'}{\lambda}\right)\underline{h}(q;\lambda') = \int_0^\lambda \frac{\mathrm{d}\lambda'}{\lambda^2}\lambda'\mathcal{R}_h(q;\lambda')\mathcal{R}_c\left(q;\frac{\lambda'}{\lambda}\right) \tag{3.168}$$

$$\begin{aligned}\beta x\frac{\mathrm{d}}{\mathrm{d}\lambda}\int_0^1 \mathrm{d}\lambda'\mathcal{R}_h(q;\lambda')\underline{c}\left[q;\left(\frac{\lambda'}{\lambda}\right)^{\mathrm{sgn}(\lambda-\lambda')}\right] = \int_0^\lambda \mathrm{d}\lambda'\mathcal{R}_h(q;\lambda')\mathcal{R}_c\left(q;\frac{\lambda'}{\lambda}\right)\left(-\frac{\lambda'}{\lambda^2}\right) + \\ + \int_\lambda^1 \mathrm{d}\lambda'\mathcal{R}_h(q;\lambda')\mathcal{R}_c\left(q;\frac{\lambda}{\lambda'}\right)\left(\frac{1}{\lambda'}\right)\end{aligned} \tag{3.169}$$

it is possible to show that equation (3.164) becomes (3.165).

We note now that the equations (3.164) and (3.165) derive only from the Ornstein-Zernike equations and are quite general. However we need here the HNC closure that allows us to give a complete set of equations that can be solved. The equations that come from the HNC closure are the following

$$\ln[\underline{h}(x;\lambda)+1] = \underline{h}(x;\lambda) - \underline{c}(x;\lambda) \tag{3.170}$$

$$\sum_{l=1}^{\infty}\frac{(-1)^{l+1}}{l}\Delta\underline{h}_l(x,1) + \beta\phi(x) = \Delta\underline{h}(x;1) - \Delta\underline{c}(x;1) \tag{3.171}$$

$$\mathcal{R}_c(x;\lambda) = \mathcal{R}_h(x;\lambda)\frac{\underline{h}(x;\lambda)}{1+\underline{h}(x;\lambda)}\,. \tag{3.172}$$

At this point let us see what are the equation for the "plateau" functions, namely all the above quantities computed at $\lambda = 1$. By considering the equation (3.164)

computed in $\lambda = 1$ where the ansatz (3.166) can be used, and by using the above equations, we get the following set of equations

$$\begin{aligned} h(q) &= c(q) + \rho\left[h(q)\Delta c(q) + \Delta h(q)c(q) + xc(q)h(q)\right] \\ \ln\left[h(x)+1\right] &= h(x) - c(x) \\ \Delta h(q) &= \delta c(q) + \rho\Delta h(q)\Delta c(q) \\ \Delta h(x) - \Delta c(x) &= \sum_{l=1}^{\infty} \frac{(-1)^{l+1}}{l}\Delta h_l(x) + \beta\phi(x) \end{aligned} \tag{3.173}$$

where we have used the notation $\underline{h}(q;1) = h(q)$ and an analogous for the other functions. It is quite easy to show that the above equations are the same as (3.109)-(3.112) where $x = m$. However up to now, there is no condition that fixes the value of x. In fact its value can be determined by looking at the equation (3.165) in the limit $\lambda = 1$. By denoting $\mathcal{R}_{c,h}(q;1) = R_{c,h}(q)$, this equation can be rewritten in the following way

$$0 = R_c(q)\left(1 + \rho\Delta h(q)\right) - R_h(q)\left(1 - \rho\Delta c(q)\right) \tag{3.174}$$

By using the equation (3.172) we obtain

$$\begin{aligned} 0 = \left(1+\rho\Delta h(q)\right)\int \frac{\mathrm{d}^D k}{(2\pi)^D}\Bigg[&\text{T.F.}\left(\frac{h}{1+h}\right)(q-k)R_h(k) - \\ &-(2\pi)^D\frac{1-\rho\Delta c(q)}{1+\rho\Delta h(q)}\delta(q-k)R_h(k)\Bigg] \end{aligned} \tag{3.175}$$

From this equation we obtain

$$\begin{aligned} 0 = \int \frac{\mathrm{d}^D k}{(2\pi)^D}\Big[&\left(2\rho\Delta c(q) - \rho^2\Delta c^2(q)\right)(2\pi)^D\delta(q-k) - \\ &-\text{T.F.}\left(\frac{1}{\tilde{g}}\right)(q-k)\Big]R_h(k) \end{aligned} \tag{3.176}$$

This equation has a trivial high-temperature solution that is $R_h(q) = 0$. However, as we go beyond the dynamical point, a non trivial solution appears provided that

$$0 = \det\left[\left(2\rho\Delta c(q) - \rho^2\Delta c^2(q)\right)(2\pi)^D\delta(q-k) - \text{T.F.}\left(\frac{1}{\tilde{g}}\right)(q-k)\right] \tag{3.177}$$

that is nothing but the marginal stability condition.

In the end the aging dynamics follows very closely the one that can be learnt from the p-spin model. The fluctuation-dissipation ratio can be computed analytically by solving the replicated Ornstein-Zernike equations (3.109)-(3.112) and by fixing the parameter m in such a way that the condition (3.177) is satisfied. Note that the analogy with the p-spin model is striking in the sense that not only the fluctuation dissipation ratio is determined by the marginal stability condition, but moreover, this condition is fixed by an equation that does not depend on x explicitly.

3.6 Perspectives

In this chapter we have seen how the Boltzmann Pseudodynamics construction can be used to obtain the dynamical equations in the α regime. This result is important

for many reasons. First of all it gives a quantitative understanding of how the dynamics samples the phase space in the long time regime. Moreover this idea of quasi equilibrium sampling of phase space can be made rigorous by studying a generalized version of the Franz-Parisi potential. We have seen that this approach reproduces correctly the dynamical equations for the long time dynamics in the exactly solvable p-spin spherical model and we have applied it also in the structural glass case. This has been possible because the construction is static in nature so that approximation schemes and methods that are well known in the statics can be applied straightforwardly. However there are many important point to be discussed.

First of all it is not clear to what extent these results are valid. In other words, one could ask if this construction is valid for every kind of systems and dynamics. Even if a complete answer to this question is not known now, we can give some general arguments in order to understand for which systems the pseudodynamics gives the correct results. Firstly we have to note is that this approach is not correct for the $p = 2$ spherical model. The reason is the following. Let us consider the Langevin dynamics for this model. We can obtain a set of dynamical equations for the correlation and response functions. Let us have a look at what happens in the long time regime. The key point is that in the standard dynamical equations with $p > 2$ one can prove that the derivative term $\mathrm{d}C(t)/\mathrm{d}t$ that appears in the equation can be neglected because it is subdominant with respect to the others. However for the $p = 2$ case this is not true and the dynamical equation in the long time limit contains such term and of course it cannot be obtained by the pseudodynamics ansatz by construction. However let us note that the $p = 2$ model is pathological in the sense that it is not glassy. If one looks at the statics, one can see that it is a disguised ferromagnet [50, 56] so that there is no complexity and the free energy landscape is simpler than the models with $p > 2$. For these reasons we tend to think that the pseudodynamics approach gives the correct results when the dynamics is dominated by the relaxation in a huge number (exponential) of metastable states while it does not give the correct results whenever the free energy landscape is simple.

Another thing that has not been investigated here is the stability of the pseudodynamics solution. In fact we have computed the generalized Franz-Parisi potential within a replica-symmetric pseudodynamic ansatz. However it could be the case that fullRSB effects appear and the replica-symmetric solution is unstable. This observation is important also because we have seen that the fluctuation dissipation ratio in the aging regime is computed with the marginal stability condition that is the condition that in replica space corresponds to tell where the system becomes unstable towards further replica symmetry breaking solutions. We will see in the next chapter that this is not the general case and that what happens in general is that the vanishing of the 1RSB replicon (the replicon eigenvalue that corresponds to the stability analysis of the 1RSB solution) is not always the condition that is needed to compute the fluctuation dissipation ratio. In fact the general idea is that the aging dynamics is dominated by threshold states. In the spherical p-spin model the effective temperature that corresponds to such states is the same that can be read by imposing the marginal stability condition. However this is a peculiar property of this model while in the general situation this is not the case. It is mandatory to understand how to produce a pseudodynamic RSB ansatz in order to include this

more general phenomenology. This is of course doable but from the technical point of view it is full of difficulties because the RSB ansatz involve many parameters over which we need to take the saddle point. In particular, we know that whenever we have fullRSB effect we have a continuum set of effective temperatures and the FDT-ratio changes as long as we change the time window. The analysis of the aging dynamics in the Sherrington-Kirkpatrick model has been done in [53, 52] and from this analysis it is clear that the extra parameters that should be put in the RSB ansatz are directly correlated to the infinitely many time windows in which the aging dynamics is decomposed.

The things we have just discussed are important in order to make the full approach consistent. However, once this has been done, we could try to use this construction to attack problems that have not been solved yet. One of these is the study of the dynamical fluctuations in the long time α regime. We have seen in the second chapter that in the short time β regime, the theory of the fluctuations is very peculiar in the sense that, by using replicas, it can be shown that it is equivalent to the study of a cubic field theory in a random field. To show this one can look at the Gaussian fluctuations around the saddle point solution for the Franz-Parisi potential. What happens is that at the dynamical point the degeneracy of the longitudinal and replicon eigenvalue is responsible for the appearance of a propagator with a double pole. This kind of behavior with propagators with double poles is typical in random field models and starting from this observation it is possible to show that the dynamical glass transition and the RFIM are connected.

It is not clear if all this can be generalized in the long time regime. To see if this is the case, one should look at the Gaussian fluctuations in replica space around the replica symmetric pseudodynamics saddle point. It is possible that some peculiar behavior could happen. Even if this kind of approach seems very promising, there are many technical difficulties that are related to the study of the replica structure of the stability matrix and we leave this for future work.

Moreover let us underline again that our results are mean field in nature and the extension to the finite dimensional case is rather problematic. In fact we expect that in finite dimensions also the Franz-Parisi potential will change drastically because nucleation will enforce the convexity in its shape deleting the true metastability. How to generalize this to the pseudynamics case is problematic and is not very clear and we hope to be able to study the problem in the next future.

Chapter 4

Theory of dense amorphous hard spheres in high dimensions

In this chapter we examine the glass and jamming transition of hard spheres in the limit of infinite dimensions. We will take the random first order theory perspective and in particular we will show that the 1RSB phase diagram, that was known up to now, is only partially correct and a Gardner transition is present. This implies that fullRSB effects are important especially in the jamming part of the phase diagram. This is a work in progress and despite a very huge amount of theoretical efforts, we are not able yet to extract all the consequences of the fullRSB physics. However we hope that when the fullRSB equations will be solved the new description of the jamming physics will be more accurate. The problem is very interesting and in this thesis our scope is to improve the replica approach to it. The complete characterization of the jamming and glass physics of hard spheres is far from being reached but we hope that our results can be a good mean field starting point that can shed some light on the problem.

Here we present the state of the art and the motivations for this study. At the basis of the idea that fullRSB effects may play some role in the jamming physics there is the fact that in general fullRSB solutions are always marginally stable. While in the 1RSB physics the amorphous jammed states are the bottom of well defined minima of the free energy landscape, in the fullRSB picture, at the bottom of each metastable 1RSB state there is an infinite hierarchy of glassy states separated by flat directions. This idea of marginal stability of jammed packings seems very well established at the phenomenological level and it is mandatory for the replica approach (the one that we adopt here) to reconcile this with the experiments. Moreover it was known that the 1RSB solution suffered of some inconsistencies so that we hope that the fullRSB solution will be able to cure them. This chapter is organized as follows: first of all we introduce the problem of the glass and jamming transition of hard spheres. We will not be able to cover all the aspects of this field but many reviews and monographies are avavilable now so that we will make often reference to them [115, 2, 8, 46, 108, 174, 145].

We will be mainly concerned on the replica approach so that the main reference for this part of the work will be [145] and below we will give many results that will not be proved here but that can be found in this reference. After this we will set

up the problem and we will give some motivations for this study. Then we will go deeply in the hard part of the computations and we will first show that the 1RSB solution suffers of an instability that is responsible for a Gardner transition to a fullRSB phase. In the meanwhile we will be able to compute the mode-coupling exponent parameter λ and we will find a better agreement with experiments. For this part of the chapter we will strictly follow the reference [110].

Once we have recognized that the 1RSB diagram is unstable, we will try to write down the 2RSB solution. We will show that the 2RSB solution can be present only in a certain region of the unstable part of the 1RSB phase diagram and we will compute the 2RSB jamming part of the phase diagram. Then we will derive the fullRSB equations. We will obtain the Parisi equation for the hard-spheres case and we will write down the variational equations for the fullRSB solution. Then we will solve numerically these equations and we will show the numerical evidence that the fullRSB calculation correctly describe the scaling of the infinite time limit of the mean square displacement with the pressure. We will conclude with some interesting perspective about the work done and still to be done.

The original content of this chapter is reported in two papers. The first one [110] is on the Gardner transition and on the calculation of the exponent parameter while the second one [45] is on the 2RSB and fullRSB solution.

4.1 The glass and jamming transition of hard spheres

It has been shown that the study of amorphous hard spheres packings is important for a large class of physical systems and applications that range from liquids, glasses and granular matter to computer science problems like signal digitalization and error correcting codes and it has been investigated widely also by the information theory community [46, 153]. However, up to now, a satisfactory theoretical comprehension of the amorphous packings of identical hard spheres is lacking even if in recent years a large amount of numerical and experimental data has been collected.

Amorphous packings are usually produced according to a given dynamical protocol that has some randomness built in the algorithm. Let us here analyze one of the most common protocol to produce such amorphous packings introduced by Lubachevsky and Stillinger [117]. The idea is to increase the size of the spheres during a molecular dynamics simulation up to the jamming point. Here the relevant parameter is the rate γ at which the diameter is increased. It is believed that in the thermodynamic limit, if we are able to avoid the crystallization transition, the packing fraction (the fraction of the volume covered by the spheres) of the final amorphous state is independent on the randomness built in the algorithm and in three dimension is very close to 0.64 that has been called J-point. Moreover it has been observed that different algorithms have practically the same J-point (even if the real value of this packing fraction is slightly dependent on the details of the dynamics). For this reason it has been proposed to call the $\varphi = 0.64$ point, the random close packing point (RCP). The general phase diagram is reported in Fig. 4.1.

In general the study of such amorphous packings should be done by solving this complicated non equilibrium dynamics. To overcome this difficulty a more

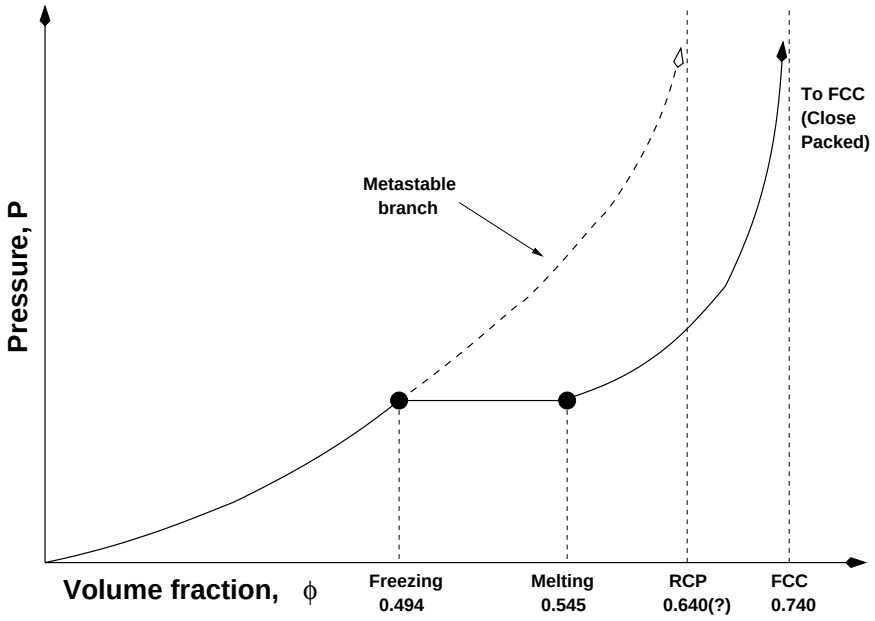

Figure 4.1. The phase diagram of three dimensional hard spheres that emerges in many dynamical protocol used to obtain the amorphous packings. Plot taken from [145]. The full line is the equilibrium line that shows a freezing transition at which the system becomes a crystalline solid. The crystalline structure is arranged around a FCC lattice that represents the lattice around which particles vibrate. At infinite pressure, the vibration is suppressed and we obtain that the equilibrium crystalline packing is a FCC one. If we are able to avoid the freezing transition the liquid enters in a metastable phase. If we compress the hard sphere liquid we obtain an infinite pressure amorphous packing at a packing fraction $\varphi = 0.64$ that is called random close packing point. The value of this packing fraction seems to depend slightly on the compression protocols and on the initial conditions.

pragmatic approach could be used and one could try to identify a class of amorphous packings that could be described by using equilibrium statistical mechanics tools. These packings can be actually defined as infinite pressure limit of glassy states of hard spheres. This idea is very appealing for many reasons. First of all we can use equilibrium techniques instead of solving the dynamics. Secondly, we can study under the same framework the glass and jamming transition problems. This approach is nothing but the application of the RFOT to the case of hard spheres. However we will see that the p-spin spherical model universality class is not sufficient for the jamming side of the phase diagram while it is enough for a large part of the glass phase diagram. Let us underline now that the theory that we will describe below is for frictionless hard spheres of the same size. In experiments friction plays a very important role and in numerical simulations polydispersity is always employed to overcome the crystallization. Here we will neglect completely these aspects to be in the simplest possible framework.

A standard thing that can be done in order to study the metastable branch after the freezing packing fraction φ_f is to assume that the equation of state of the liquid can be continued in this region. However it has been seen that all the possible analytic continuations of the liquid state give an unphysical value for the packing fraction at which the pressure diverges. Moreover there are many inconsistencies of these approaches as for example the fact that the two point density correlation function computed using an analytic continuation of the liquid phase is not observed in amorphous jammed packings where its shape is completely different [145]. A possible way out to this is to assume that a thermodynamic glass transition occurs in the metastable branch of the phase diagram. There are many reasons to think in this way. First of all this kind of phenomenon is predicted in many mean field models; moreover a dynamical phase transition is predicted by many mean field dynamical theories above all which there is mode-coupling theory. The existence of such thermodynamic transition in finite dimension is a highly debated topic and the perspective that will be considered here is pragmatic: we assume that the phase transition occurs and we investigate its consequences. The resulting phase diagram is the one represented in Fig. 4.2.

The signature of the thermodynamic glass transition is a jump in the compressibility of the system. In fact in the dense liquid phase the particles move on two time scales: the fast time scale of the vibrations around metastable equilibrium positions centered in the cages made by the other particles and the slow time scale of the cooperative rearrangments of the particles. Suppose that we change the density by $\Delta\varphi$; then the pressure will suddenly increase by ΔP_0. Then the size of the cages will be reduced and the pressure will relax to $\Delta P_f < \Delta P_0$. Then, on the structural relaxation time scale, a cooperative rearrangment of the particles will take place and the pressure will relax to its asymptotic value $\Delta P_\infty < \Delta P_f$. At the thermodynamic glass transition we expect that the structural relaxation will take place on an infinite time scale so that it is frozen. In this way the increase in pressure due to an increase in density will be larger in the glass phase than in the metastable liquid phase leading to a smaller compressibility $K = \varphi^{-1}\Delta\varphi/\Delta P$.

This picture that is conjectured to be the relevant one in finite dimension, can be complicated in the mean field limit or in infinite dimensions as it happens in the standard RFOT scheme. In fact in general we can expect that before the thermo-

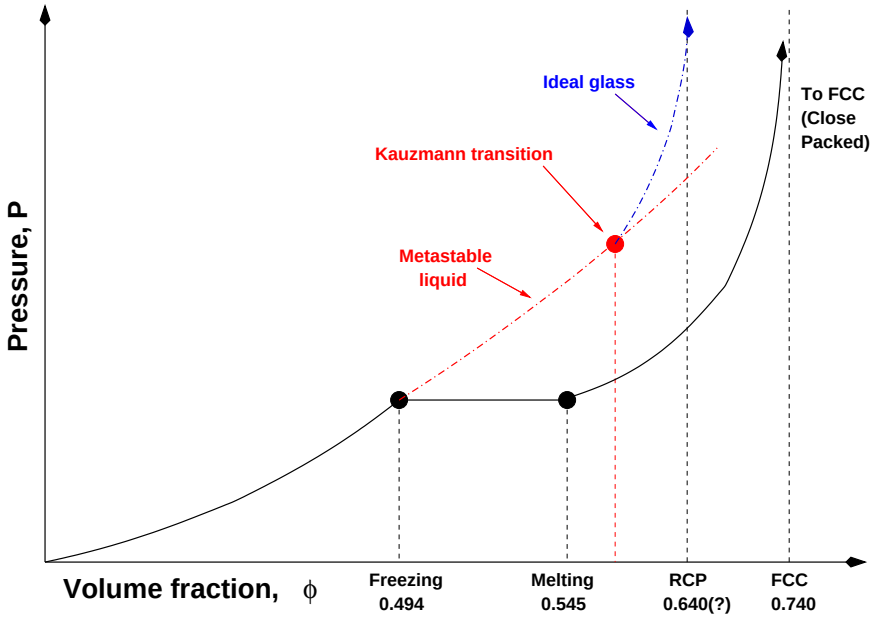

Figure 4.2. The phase diagram of hard spheres with the assumption of a thermodynamic glass transition in the metastable branch. Plot taken from [145].

dynamic glass transition there is a clustering transition that signals the appearance of an exponential number of metastable states and the actual thermodynamic transition is the point in which the configurational entropy of the relevant equilibrium states goes to zero. The final mean field phase diagram in three dimensions is the one reported in Fig. 4.3. Let us review it:

- Coming from the low packing fraction region, at equilibrium, the system is in the liquid phase. If we follow the equilibrium branch than a first order phase transition occur with freezing density φ_f and melting density φ_m. In the high density region the system is in a crystalline phase whose infinite pressure limit is a FCC lattice.

- if we are able to avoid the first order phase transition we enter in a metastable liquid phase.

- At φ_d the first metastable glassy states appear and a clustering transition occurs.

- At φ_K a thermodynamic glass transition occurs. The complexity of the relevant metastable states goes to zero and the compressibility jumps. The equilibrium relaxation time diverges and structural relaxation is frozen.

- For $\varphi \in [\varphi_d, \varphi_K]$ a different group of metastable glassy states dominates the partition function. Each of these states can be followed by compressing the system very fast (faster than the relaxation time) and each state will be characterized by its final jamming density. The states that dominate at φ_d will produced jammed states at φ_{th} and the states that dominate at φ_K will pro-

duce jammed states at φ_{GCP}. The meaning of φ_{GCP} is that it is the density corresponding to the densest amorphous packings (glass close packing).

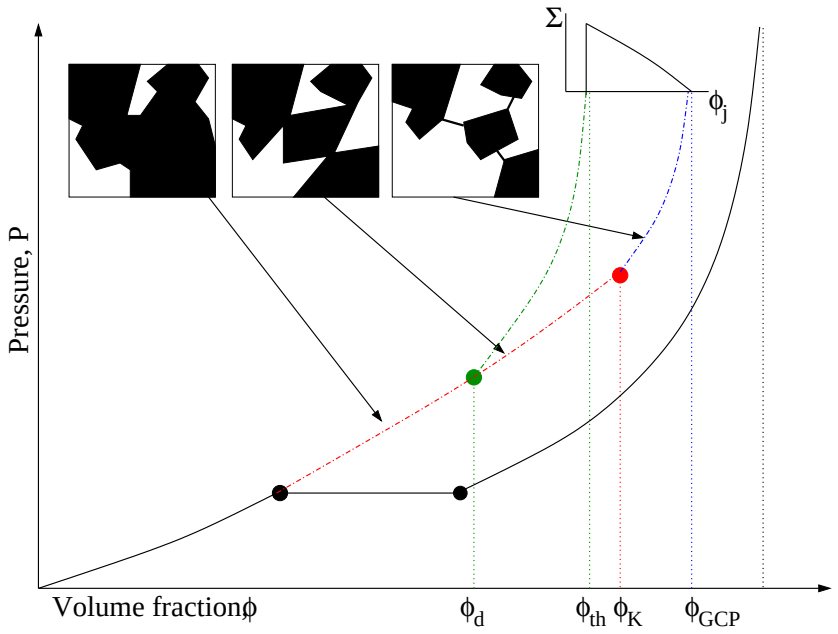

Figure 4.3. The mean field phase diagram of hard spheres. Plot taken form [145]. On the ϕ axis there are all the relevant densities for the metastable branch. After the freezing density, the liquid enters into the metastable phase and at the dynamical transition ϕ_d the ergodicity is broken and there is the appearance of an exponential number of metastable states. If we are in each state we can compress the system to produce amorphous jammed packings. The packings with the lowest packing fraction are produced compressing threshold states and we find them at ϕ_{th}. The packings with highest packing fraction are at ϕ_{GCP}. ϕ_K is the Kauzmann packing fraction that corresponds to the point where the thermodynamics is dominated by the states with higher internal entropy. In the inset on the right there is the plot of the configurational entropy of metastable states as a function of the internal entropy of the states.

The mean field phase diagram is expected to be the correct one in the large space dimension limit. In the following section we will set up the framework in which all the details of this phase diagram can be derived. Note that this phase diagram is 1RSB in nature in the sense that it is expected that the states with packing fraction between the dynamical one and the Kauzmann point are well defined 1RSB states. In the following, we will show that if we compress rapidly these states, at some point during the compression, these states will become unstable towards further RSB states and we expect that they will undergo to a Gardner transition. The Gardner transition has been discovered firstly in mean field spin glass models [**?**]. Strictly speaking this transition happens when the equilibrium metastable states undergo to a fullRSB transition. At equilibrium it can be detected by looking at the divergence of the spin glass susceptibility [132]. However let us underline that we expect that all the metastable states undergo to this transition so that the effect of the fullRSB physics must be detected also in the off-equilibrium dynamics. The effect of this kind of transition on the whole RFOT picture is now under debate.

4.2 Hard Spheres in high dimensions. The replica approach

In this section we will review the real replica method for hard spheres [145]. We will mainly follow the ideas of section 1.3.1 but here we will repeat the line of reasoning for clarity. The basic idea is that here the Parisi parameter m will be conjugated to the internal entropy of the states. As in the previous sections we will treat m as a control parameter that will be used to select a given group of metastable states. In this way we introduce m real copies of our native system of hard spheres and we put a small attractive coupling between these systems in such a way that they tend to be in the same configuration. The partition function of the replicated system will be given by

$$\begin{aligned} Z_m(\varphi) = e^{N\mathcal{S}(m,\varphi)} \sim \sum_\alpha e^{Nms_\alpha} = \int_{s_{min}(\varphi)}^{s_{max}(\varphi)} \mathrm{d}s\, e^{N[\Sigma(s,\varphi)+ms]} \\ \sim e^{N[\Sigma(s^*,\varphi)+ms^*]} \end{aligned} \tag{4.1}$$

where the sum is over all the metastable states that have internal entropy between $s_{min}(\varphi)$ and $s_{max}(\varphi)$ and $\Sigma(s,\varphi)$ is the configurational entropy of the states that have internal entropy s. The value $s^*(m,\varphi)$ is the saddle point value for the integral and tells which states are the relevant ones at the packing fraction φ. From these relations it follows that

$$s^*(m,\varphi) = \frac{\partial \mathcal{S}(m,\varphi)}{\partial m} \tag{4.2}$$

$$\Sigma(m,\varphi) = \Sigma(s^*(m,\varphi),\varphi) = -m^2 \frac{\partial}{\partial m}\left[\frac{1}{m}\mathcal{S}(m,\varphi)\right] \tag{4.3}$$

From the parametric plot of $\Sigma(m,\varphi)$ and $s^*(m,\varphi)$ we can reconstruct $\Sigma(m,\varphi)$.

Let us consider a system of N hard d-dimensional spheres with unit diameter enclosed in a volume V, hence at density $\rho = N/V$. The packing fraction is $\varphi = 2^{-d}\rho V_d$ where $V_d = \pi^{d/2}/\Gamma(1+d/2)$ is the volume of a sphere of radius one. Let us introduce the grand canonical partition function of m coupled systems of hard spheres. Each particle of each system belongs to a molecule of m atoms of coordinate $\overline{x} = (x_1, \ldots, x_m)$. The molecules are in a volume V and we put a harmonic potential between the atoms in each molecule and a hard sphere potential between atoms that belong to the same replica. The replicated partition function is given by

$$\begin{aligned} Z_m(\varepsilon) = \sum_{N=0}^{\infty} z^N \int_V \frac{\mathrm{d}^N x_1 \ldots \mathrm{d}^N x_m}{N!} \left(\prod_{i<j}\prod_{a=1}^{m} \chi(x_{ai}-x_{aj})\right) \times \\ \times \prod_{i=1}^{N} \exp\left[-\frac{\varepsilon}{m}\sum_{a<b}(x_{ai}-x_{bi})^2\right] = \\ = \sum_{N=0}^{\infty} \int_V \frac{\mathrm{d}^N \overline{x}}{N!} \prod_{i=1}^{N} z(\overline{x}_i) \prod_{i<j} \overline{\chi}(\overline{x}_i - \overline{x}_j) \end{aligned} \tag{4.4}$$

where $\chi(x-y) = \theta(|x-y|-1)$, $\overline{\chi}(\overline{x}-\overline{y}) = \prod_{a=1}^{m}\chi(z_a - y_a)$ and

$$z(\overline{x}) = z \exp\left[-\frac{\varepsilon}{m}\sum_{a<b}(x_{ai}-x_{bi})^2\right] \tag{4.5}$$

In the formula above it is implicitly assumed that each component of the N-dimensional vector x_i is a d-dimensional vector.

By using standard liquid theory techniques [137, 57, 90] we can produce the Legendre trasform of the free entropy with respect to $z(\overline{x})$. In this way we produce the entropy as a function of the single molecule density

$$\rho(\overline{x}) = \langle \sum_{i=1}^{N} \delta(\overline{x} - \overline{x}_i) \rangle \qquad \delta(\overline{x} - \overline{x}_i) = \prod_{a=1}^{N} \delta(x_a - x_{ai}). \tag{4.6}$$

The expression of the entropy is given in terms of an infinite sum of diagrams

$$\mathcal{S}[\rho(\overline{x})] = \int \mathrm{d}\overline{x} \rho(\overline{x})[1 - \ln \rho(\overline{x})] + \frac{1}{2} \int \mathrm{d}\overline{x}\mathrm{d}\overline{y} \rho(\overline{x})\rho(\overline{y}) f(\overline{x} - \overline{y}) + [\text{other terms}] \tag{4.7}$$

where $f(\overline{x} - \overline{y}) = -1 + \prod_{a=1}^{m} \theta(|x_a - y_a| - 1)$ is the Mayer function of the replicated system [89]. To compute the thermodynamics of this system one should in principle solve the saddle point equations $\delta\mathcal{S}/\delta\rho(\overline{x}) = 0$ and then take the analytic continuation of the solution as a function of m in order to reconstruct the curve of the configurational entropy. However this is an extremely difficult task to do and some approximation scheme should be used. A first approximation could be to parametrize the density function $\rho(\overline{x})$ by a small number of parameters. In partiular one could look for a Gaussian approximation and then optimize the entropy over the variance [145].

However we can use a different approach if we are in the high dimensional limit. In fact it has been shown in [79] that the "other terms" that appear in (4.7) are exponentially small in the limit of infinite dimensions. The precise statement of this is that each term in the sum is exponentially small but it does not prevent the sum of all these terms to be of order one. Here we will assume that this is not the case and we will neglect these terms. Interestingly enough there exist a hard sphere model where these terms do not appear [122, 121]. In this way the entropy functional will be the sum of the ideal gas term plus the first virial correction. Moreover we restrict the space of solution of the saddle point equation to density fields that are translationally and rotationally invariant. If we put $x_a = X + u_a$ where X is the centre of mass of the molecule, we have that translational invariance demands that the single molecule density does not depend on X. Rotational invariance force ρ to be dependent only on the scalar products $q_{ab} = u_a \cdot u_b$. Moreover, because $\sum_{a=1}^{m} u_a = 0$ we get that the matrix $\hat{q}$ is Laplacian that means that $\sum_a q_{ab} = \sum_b q_{ab} = 0$. A *crucial* result of [111] is that a Gaussian ansatz for the single molecule density gives the correct result for the thermodynamic quantities. In this way we can study the problem by introducing a proper Gaussian approximation for $\rho(\overline{x})$: we can consider the following parametrization

$$\rho(\overline{u}) = \frac{\rho m^{-d}}{(2\pi)^{(m-1)d/2} \det(\hat{A}^{m,m})^{d/2}} e^{-1/2 \sum_{a,b=1}^{m-1} (\hat{A}^{m,m})^{-1} u_a \cdot u_b} \tag{4.8}$$

where $\hat{A}$ is a symmetric $m \times m$ matrix such that $\sum_{a=1}^{m} A_{ab} = \sum_{b=1}^{m} A_{ab} = 0$. Moreover we have indicated with $\hat{A}^{m,m}$ the matrix that can be obtained from the matrix $\hat{A}$ by removing the last row and the last column. The normalization factor in front of the exponential function is such that $\int \mathcal{D}\overline{u} \rho(\overline{u}) = \rho$ and

$\mathcal{D}\overline{u} = m^d \delta\left(\sum_a u_a\right) \mathrm{d}u_1 \ldots \mathrm{d}u_m$. The parameters A_{ab} give the average of the scalar products of the displacements

$$\langle u_a \cdot u_b \rangle = \frac{1}{\rho} \int \mathcal{D}\overline{u} \rho(\overline{u}) u_a \cdot u_b = dA_{ab} \tag{4.9}$$

for $a,\ b \in [1, m-1]$, while $\langle u_a \cdot u_m \rangle = -\sum_{b=1}^{m-1} \langle u_a \cdot u_b \rangle = A_{am}$ and $\langle u_m \cdot u_m \rangle = \sum_{a,\ b=1}^{m-1} \langle u_a \cdot u_b \rangle = A_{mm}$. In the limit of large space dimensions, we can change the variables of integration from $\overline{u}$ to $\hat{q}$. By taking the limit $d \to \infty$ all the integrals can be evaluated by saddle point. In fact the integral that give the normalization of the density will be [111]

$$\begin{aligned} \rho &= \int \mathcal{D}\overline{u} \rho(\overline{u}) = \int \mathrm{d}\hat{q} J(\hat{q}) \rho(\hat{q}) \propto \\ &\propto \int \mathrm{d}\hat{q} \prod_{a=1}^{m} \delta\left(\sum_{b=1}^{m} q_{ab}\right) \exp\left[\frac{1}{2}(d-m) \log\det \hat{q}^{m,m} - \frac{1}{2} \sum_{a,b}^{m} (\hat{A}^{m,m})^{-1}_{ab} q_{ab}\right] \end{aligned} \tag{4.10}$$

where here $J(\hat{q})$ is the Jacobian of the change of integration variables whose expression is derived in the appendix. The saddle point value of $\hat{q}$ is given by

$$q^{sp}_{ab} = dA_{ab}\ . \tag{4.11}$$

At this point we can use a result that is given in [111] that states that in the infinite dimension limit

$$\mathcal{S}[\rho(\overline{u})]/N = 1 - \log \rho(\hat{q}^{sp}) - 2^{d-1} \varphi \mathcal{F}\left(\frac{d}{D^2} 2\hat{q}^{sp}\right) \tag{4.12}$$

where D is the diameter of the spheres (in our case we choose $D = 1$) and the function $\mathcal{F}$ is given by

$$\mathcal{F}(\overline{u}) = \int \frac{\mathrm{d}^m \epsilon}{\sqrt{2\pi}^m} \exp\left[-\frac{1}{2} \min_a |\epsilon + u_a|^2\right] \tag{4.13}$$

Note that here the expression above actually depends on the scalar products $u_a \cdot u_b = q_{ab}$.

By inserting the parametrization for the molecule density inside the expression (4.12), the ideal gas term can be written as

$$\begin{aligned} 1 - \log(\hat{q}^{sp}) =& 1 - \log \rho + d \log m + \frac{(m-1)d}{2} + \frac{(m-1)d}{2} \log(2\pi) \\ &+ \frac{d}{2} \log\det \hat{A}^{m,m} \end{aligned} \tag{4.14}$$

and the interaction term is given by

$$2^{d-1} \varphi \mathcal{F}\left(\frac{d}{D^2} 2\hat{q}^{sp}\right) = 2^{d-1} \varphi \mathcal{F}\left(\frac{d^2}{D^2} 2\hat{A}\right)\ . \tag{4.15}$$

so that the final expression of the entropy density is given by

$$\begin{aligned} \frac{\mathcal{S}[\hat{A}]}{N} &= 1 - \log \rho + d \log m + \frac{(m-1)d}{2} \log(2\pi e) + \frac{d}{2} \log\det(\hat{A}^{m,m}) \\ &\quad - 2^{d-1} \varphi\, \mathcal{F}\left(\frac{d^2}{D^2} 2\hat{A}\right)\ . \end{aligned} \tag{4.16}$$

In order to obtain a simple limit $d \to \infty$, we can define a matrix $\hat{\alpha} = \frac{d^2}{D^2}\hat{A}$ and a reduced packing fraction $\widehat{\varphi} = 2^d\varphi/d$ so that the entropy density will become

$$\begin{aligned} s[\hat{\alpha}] = \frac{\mathcal{S}[\hat{\alpha}]}{N} &= 1 - \log\rho + d\log m + \frac{(m-1)d}{2}\log(2\pi e D^2/d^2) \\ &+ \frac{d}{2}\log\det(\hat{\alpha}^{m,m}) - \frac{d}{2}\widehat{\varphi}\,\mathcal{F}\left(2\hat{\alpha}\right) \ . \end{aligned} \tag{4.17}$$

The matrix $\hat{\alpha}$ is a variational parameter and is therefore determined by the optimization of the entropy. Let us call $\hat{\alpha}^*$ and m^* the saddle point value of $\hat{\alpha}$ and m for the entropy density. Then the reduced pressure $p = \beta P/\rho$ of the equilibrium glass is given by

$$p_{glass}(\varphi) = -\frac{\varphi}{m^*}\frac{\partial s[\hat{\alpha}^*]}{\partial\varphi} = \frac{1}{m^*}\left[1 + \frac{d}{2}\widehat{\varphi}\,\mathcal{F}\left(2\hat{\alpha}^*\right)\right] \ . \tag{4.18}$$

This result shows that the pressure diverges whenever $m^* \to 0$ as $p \sim 1/m^*$. Hence, the density at which $m^* \to 0$ defines the jamming point [145].

4.3 The 1RSB phase diagram

The 1RSB calculation consists in computing the entropy density under a 1RSB ansatz for the single molecule density profile. In particular the 1RSB ansatz is provided by a specific parametrization of the matrix $\hat{\alpha}$ that defines the single molecule density. As in the standard real replicas calculations, the 1RSB calculation corresponds to take a replica symmetric parametrization compatible with the constraints of the problem so that we choose

$$\alpha_{ab}^{\mathrm{1RSB}} = \widehat{A}\left(\delta_{ab} - \frac{1}{m}\right) \ , \tag{4.19}$$

and the form of the matrix is such that the sum of the elements in each row or column is zero so that translational invariance is preserved. By inserting this parametrization inside the expression of the entropy density and by using the fact that

$$\log\det\left(\left[\widehat{A}(\delta_{ab} - \frac{1}{m})\right]^{m,m}\right) = (m-1)\log\widehat{A} - \log m \tag{4.20}$$

we obtain

$$\begin{aligned} s[\hat{\alpha}^{\mathrm{1RSB}}] &= 1 - \log\rho + \frac{d}{2}\log m + \frac{(m-1)d}{2} \\ &+ \frac{(m-1)d}{2}\log\left(\frac{2\pi D^2\widehat{A}}{d^2}\right) - \frac{d}{2}\widehat{\varphi}\mathcal{F}[\hat{\alpha}^{1RSB}] \end{aligned} \tag{4.21}$$

Let us compute the interaction term. Here we will introduce a replica trick that is the key ingredient for all the calculations that will appear in the following. We

need to compute the following quantity

$$\begin{aligned}\mathcal{F}[\hat{v}] &= \int \frac{\mathrm{d}^m\epsilon}{(\sqrt{2\pi})^m}\exp\left[-\frac{1}{2}\min_a|\epsilon+x_a|^2\right] = \\ &= \lim_{n\to 0}\sum_{n_1,\ldots,n_m;\sum_a^m n_a=n}\frac{n!}{n_1!\ldots n_m!}\exp\left[-\frac{1}{2}\sum_{a=1}^m\frac{n_a}{n}|x_a|^2+\frac{1}{2}\sum_{a,b}^{1,m}\frac{n_an_b}{n^2}x_a\cdot x_b\right] \\ &= \lim_{n\to 0}\sum_{n_1,\ldots,n_m;\sum_a^m n_a=n}\frac{n!}{n_1!\ldots n_m!}\exp\left[-\frac{1}{2}\sum_{a=1}^m\frac{n_a}{n}\upsilon_{aa}+\frac{1}{2}\sum_{a,b}^{1,m}\frac{n_an_b}{n^2}\upsilon_{ab}\right]\end{aligned} \tag{4.22}$$

where here $\hat{v}=\hat{v}^{1RSB}=2\hat{\alpha}^{1RSB}$. By inserting the parametrization of the 1RSB matrix we have

$$\begin{aligned}\mathcal{F}[\hat{v}^{\mathrm{1RSB}}] &= \lim_{n\to 0}\sum_{n_1,\ldots,n_m;\sum_a^m n_a=n}\frac{n!}{n_1!\ldots n_m!}\exp\left[-\frac{1}{2}\sum_{a=1}^m\frac{n_a}{n}\upsilon_{aa}^{\mathrm{1RSB}}+\frac{1}{2}\sum_{a,b}^{1,m}\frac{n_an_b}{n^2}\upsilon_{ab}^{\mathrm{1RSB}}\right] \\ &= \lim_{n\to 0}e^{-\widehat{A}}\sum_{n_1,\ldots,n_m;\sum_a^m n_a=n}\frac{n!}{n_1!\ldots n_m!}\exp\left[\widehat{A}\sum_{a=1}^m\frac{n_a^2}{n^2}\right] \\ &= \lim_{n\to 0}e^{-\widehat{A}}\sum_{n_1,\ldots,n_m;\sum_a^m n_a=n}\frac{n!}{n_1!\ldots n_m!} \\ &\times\int\left(\prod_{a=1}^m\frac{\mathrm{d}\lambda_a}{\sqrt{2\pi}}\right)\exp\left[-\sum_{a=1}^m\frac{\lambda_a^2}{2}-\sqrt{2\widehat{A}}\sum_{a=1}^m\frac{n_a\lambda_a}{n}\right] \\ &= \int\left(\prod_{a=1}^m\frac{\mathrm{d}\lambda_a}{\sqrt{2\pi}}\right)\exp\left[-\sum_{a=1}^m\frac{\lambda_a^2}{2}-\sqrt{2\widehat{A}}\min_a\lambda_a-\widehat{A}\right] \\ &= \int\left(\prod_{a=1}^m\frac{\mathrm{d}\lambda_a}{\sqrt{2\pi}}\right)\exp\left[-\frac{1}{2}\sum_{a=1}^m\left(\lambda_a+\sqrt{2\widehat{A}}\,\delta_{a,\min}\right)^2\right] \\ &= m\int_{-\infty}^{\infty}\frac{\mathrm{d}\lambda_1}{\sqrt{2\pi}}e^{-\frac{1}{2}\left(\lambda_1+\sqrt{2\widehat{A}}\right)^2}\left[\int_{\lambda_1}^{\infty}\frac{\mathrm{d}\lambda}{\sqrt{2\pi}}e^{-\frac{1}{2}\lambda^2}\right]^{m-1} \\ &= m\int_{-\infty}^{\infty}\frac{\mathrm{d}\lambda_1}{\sqrt{2\pi}}e^{-\frac{1}{2}\left(\lambda_1+\sqrt{2\widehat{A}}\right)^2}\left[\Theta\left(-\frac{\lambda_1}{\sqrt{2}}\right)\right]^{m-1}\end{aligned} \tag{4.23}$$

where we have defined

$$\mathrm{erf}(x)=\frac{2}{\sqrt{\pi}}\int_0^x\mathrm{d}y\,e^{-y^2}\qquad\qquad\Theta(x)=\frac{1}{2}+\frac{1}{2}\mathrm{erf}(x)=\frac{1}{\sqrt{\pi}}\int_{-x}^{\infty}\mathrm{d}y\,e^{-y^2} \tag{4.24}$$

We also define for later convenience

$$\Theta_k(x)=\frac{1}{\sqrt{2\pi}}\int_x^{\infty}\mathrm{d}y\,y^k\,e^{-\frac{1}{2}y^2}\,. \tag{4.25}$$

Note that

$$\begin{aligned}
\Theta_0(x) &= \Theta(-x/\sqrt{2}) \\
\Theta_1(x) &= e^{-\frac{1}{2}x^2}/\sqrt{2\pi} \\
\Theta_2(x) &= x\Theta_1(x) + \Theta(-x/\sqrt{2}) \\
\Theta_3(x) &= \Theta_1(x)(2+x^2) \\
\Theta_4(x) &= x(3+x^2)\Theta_1(x) + 3\Theta_0(x)
\end{aligned} \tag{4.26}$$

and so on.

By inserting the result for the interaction term inside the expression for the entropy density we obtain [145]

$$\begin{aligned}
s[\hat{\alpha}^{\mathrm{1RSB}}] &= 1 - \log\rho + \frac{d}{2}\log m + \frac{(m-1)d}{2} \\
&\quad + \frac{(m-1)d}{2}\log\left(\frac{2\pi D^2 \widehat{A}}{d^2}\right) - \frac{d}{2}\widehat{\varphi}[1 - \mathcal{G}_m(\widehat{A})] \,, \\
\mathcal{G}_m(\widehat{A}) &= 1 - m\int_{-\infty}^{\infty}\frac{d\lambda}{\sqrt{2\pi}}e^{-\frac{1}{2}\lambda^2}\left[\frac{1}{2}\left(1 + \mathrm{erf}\left(\frac{\sqrt{2\widehat{A}} - \lambda}{\sqrt{2}}\right)\right)\right]^{m-1} .
\end{aligned} \tag{4.27}$$

At this point we have to take the saddle point over $\widehat{A}$. The saddle point equation is

$$\frac{1}{\widehat{\varphi}} = \frac{\widehat{A}}{1-m}\frac{\partial \mathcal{G}_m(\widehat{A})}{\partial \widehat{A}} \equiv \mathcal{F}_m(\widehat{A}) \tag{4.28}$$

The shape of the function $\mathcal{F}_m(\widehat{A})$ is reported in fig. (4.4). From this, it follows that a solution of the saddle point equation exists only for reduced packing fraction that are such that

$$\widehat{\varphi} \geq \frac{1}{\max_{\widehat{A}}\mathcal{F}_m(\widehat{A})} = \widehat{\varphi}_d(m) \tag{4.29}$$

For $m = 1$ we obtain the clustering or dynamical phase transition point

$$\widehat{\varphi}_d = \widehat{\varphi}_d(1) = 4.8 \,. \tag{4.30}$$

If we want to look for the J-point, namely the lowest density at which the pressure is infinite we need to set $m \to 0$. However in this limit the cage radius $\widehat{A}$ goes to zero as well so that to perform the calculation we must scale $\widehat{A} = m\hat{\alpha}$. In this way, the saddle point equation becomes

$$\frac{1}{\widehat{\varphi}} = \mathcal{F}_0(\hat{\alpha}) = \frac{1}{4\widehat{\alpha}}\int_0^{\infty} \mathrm{d}y y^2 e^{-y - y^2/4\widehat{\alpha}} \tag{4.31}$$

The first solution of this equation appear at $\widehat{\varphi} = 6.26 = \widehat{\varphi}_{th}$ that is conjectured to be the J-point in infinite dimensions. The Kauzmann and Glass close packing points can be computed following the lines that we gave in the previous section. It turns out that [145]

$$\widehat{\varphi}_K, \widehat{\varphi}_{GCP} \sim \log d \qquad d \to \infty \,. \tag{4.32}$$

The phase diagram in the $(m, \widehat{\varphi})$ plane is summarized by fig. 4.5 . Moreover let us note that at the 1RSB level we can show that $\widehat{A}^* \sim m^*$ so that the cage radius vanishes with the inverse of the pressure $\widehat{A} \sim 1/p$.

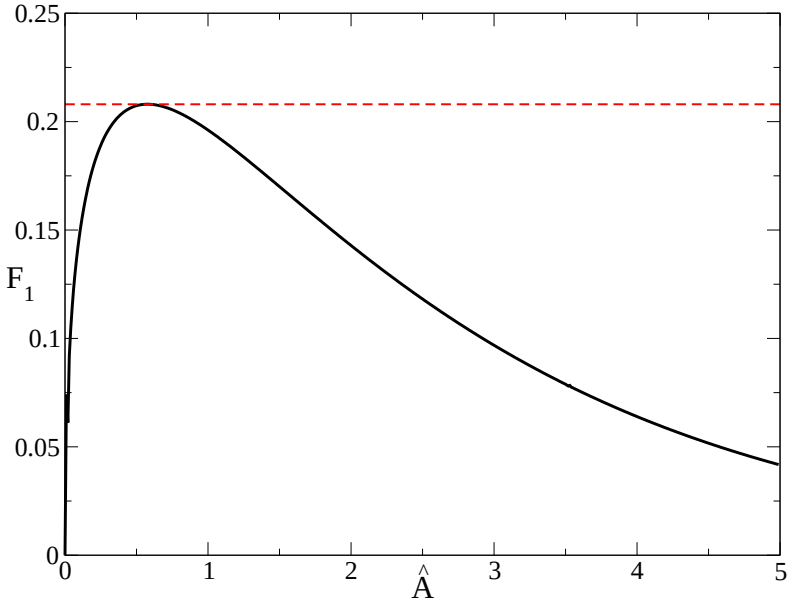

Figure 4.4. The shape of $\mathcal{F}_1(\widehat{A})$. The plot is taken from [145].

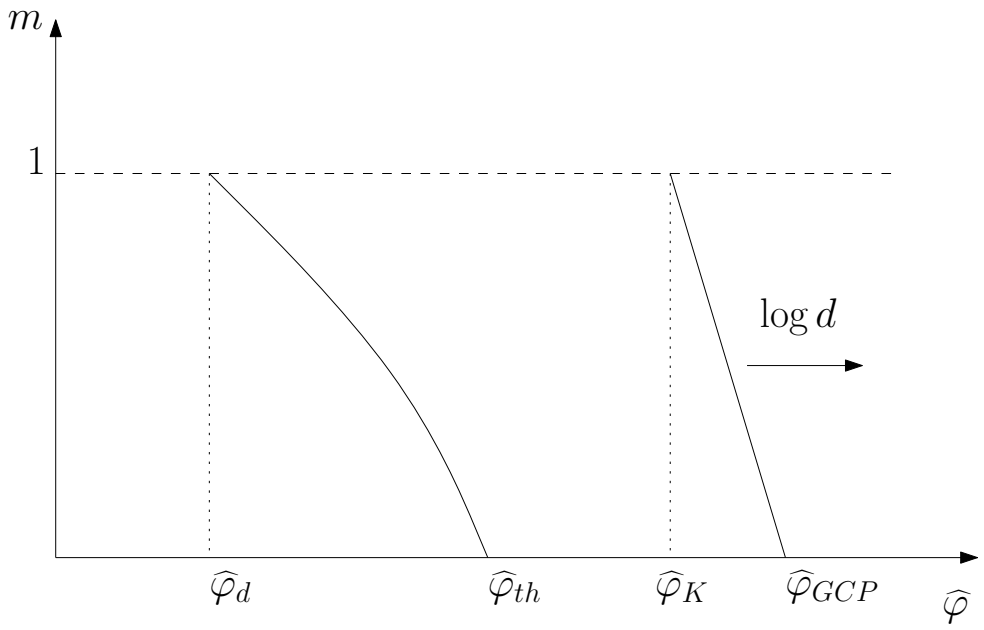

Figure 4.5. The phase diagram as expected from a 1RSB calculation in infinite dimensions. We can recognize the dynamical reduced packing fraction at which the ergodicity breaking appear and the threshold density that is the the density reached by the infinite pressure limit of threshold states. At the Kauzmann density the states that dominate the Boltzmann measure are the ones with highest internal entropy. If we take the infinite pressure limit we obtain the jammed packing with highest density. The jamming point for these states is at $\widehat{\varphi}_{GCP}$. Note that we have identified the infinite pressure limit of the phase diagram with the $m = 0$ line.

4.4 Inconsistencies of the 1RSB solution

The 1RSB predictions for many physical quantities have been compared with numerical data both in the glass phase and at the jamming transition. Despite the overall agreement the solution is inconsistent for some reasons, especially for what concern the jamming physics at high pressure. In fact

- The 1RSB solution predicts the existence of amorphous jammed packings for reduced packing fractions in the whole interval $[6.26, \log d]$. However it happens that the packings with reduced packing fraction of order one are hyperstatic while only the packings with packing fraction of order $\log d$ are isostatic. The role of isostaticity is fundamental here [116]. We say that a packing is isostatic if the average number of force contacts of a sphere is $2d$ while the packing is hyperstatic or hypostatic if the average number of contacts is greater or fewer then $2d$. We expect that jammed packings are isostatic. The reason is the following. A isostatic packing is a packing that is mechanically stable with the smallest number of force contacts. When we produce a jammed packing we compress the system up to the jamming point. During the compression the system goes from one hypostatic configuration to another. At the jamming point it becomes isostatic because it must become mechanically stable. In this way we see that hyperstatic packings cannot be consistent with the dynamical protocols used to obtain such packings.

- In the glass phase, the exact relation between the pressure p and the contact value $y(\varphi)$ of the pair correlation, $p = 1 + 2^{d-1}\varphi y(\varphi)$ [89], is violated. In particular, it is found that when $\varphi \to \varphi_j$ where φ_j is the jamming point, then $p \sim d\,\varphi_j/(\varphi_j - \varphi)$, consistently with numerical results, while

$$y(\varphi) = \frac{d}{2^{d-1}(\varphi_j - \varphi)} \times \frac{1}{1 - 2^{1-d}\, d/\varphi_j} \,, \tag{4.33}$$

  where the first term is the one that is consistent with the scaling of the pressure. Hence, the correct relation between p and $y(\varphi)$ is recovered only if $2^{1-d}\, d/\varphi_j = 2/\widehat{\varphi}_j \ll 1$ when $d \to \infty$, which again suggests that the 1RSB solution is inconsistent when $\widehat{\varphi}$ is of order 1 and might be stable only when $\widehat{\varphi} \gg 1$.

- At the 1RSB level, the mean square displacement can be computed simply and it is given by

$$\Delta = \langle |u_a - u_b|^2 \rangle = 2\alpha_{aa} - 2\alpha_{a\neq b} = 2\widehat{A} \tag{4.34}$$

  This means that when the jamming point is approached the mean square displacement goes to zero with the inverse of the pressure $\Delta \sim p^{-1}$ while in numerical simulation it is found that it vanishes as $\Delta \sim p^{-3/2}$. This exponent controls all the other exponents that characterize the criticality at the jamming transition and to reconcile this prediction with the numerical evidence is extremely important for the theory.

- Other exponents that characterize the structure at jamming, for instance the famous (almost) square-root singularity in the pair correlation function [138,

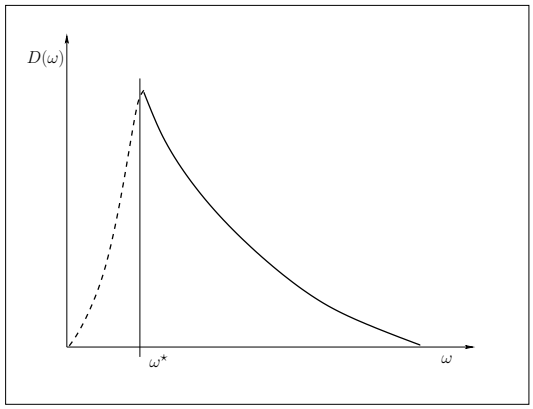

Figure 4.6. A schematic picture of the vibrational spectrum $D(\omega)$ close to jamming. The frequency ω^* goes to zero as the pressure diverges. Below ω^* we expect to find acoustic modes. Surprisingly, other soft modes are present and they does not look like as plane waves. The plot is taken from [110].

62, 156, 41], are not reproduced by the 1RSB solution, at least at the Gaussian level so we expect that a more refined calculation will be able to reconcile this.

The combination of these arguments suggest to search for an instability of the 1RSB solution at least when the packing fraction is very large.

4.5 Stability of the 1RSB phase diagram: the Gardner transition

The stability of the 1RSB solution towards further replica symmetry breaking solution can be carried on within the standard framework of replica theory. However here we have many technical difficulties that must be solved and in this section we will show how to treat these problems. In particular we will start the computation by discussing the general structure of the stability matrix of the replicated entropy around the 1RSB solution and we will give the general expressions for the eigenvalues of this matrix. Then we will compute separately two contributions to the stability matrix, namely the entropic term and the interaction term and finally we will compute the replicon eigenvalue that is the one responsible for the instability of the 1RSB solution. However before entering in the explicit calculation of the stability matrix of the 1RSB solution we want to underline the physical motivations to search for an instability of the 1RSB solution. We have seen that the 1RSB solution suffers of some inconsistencies. However it has been recently put forward that the idea that jammed packings are marginally stable from a mechanical point of view [179, 27, 116]. In particular this marginality becomes evident if one looks directly at the vibrational spectrum $D(\omega)$ at densities that are slightly below the jamming point [25, 26]. This has the general shape represented in Fig. 4.6.

The spectrum can be divided into two parts. In the first one there are the high frequency mode above the frequency ω^* that goes to zero as the pressure goes to infinity. Moreover for $0 < \omega < \omega^*$ there are the acoustic modes which exists at finite pressures. However if we look at the softer modes we can discover that they do not

look like plane waves so that we can think that acoustic modes are not the only soft modes present but other kind of soft modes are there [179, 25, 26, 112, 180, 119]. The Gardner transition provides a simple explanation and physical interpretation for these soft modes even if we are not able now to associate directly the Garnder transition with this marginality. Consider the squared displacements $\widehat{\Delta}_i(t,t') = |x_i(t) - x_i(t')|^2$, where i labels the N particles of system, and its average over particles $\widehat{\Delta}(t,t') = N^{-1}\sum_{i=1}^{N}\widehat{\Delta}_i(t,t')$. In the following we will assume that the system has been prepared by some rapid compression at time $t = 0$, in such a way that if $t > t' > 0$ and t' is large enough, the system is stuck into a glass state. The mean square displacement is given by the average of the squared displacement over the dynamical process,

$$\Delta(t,t') = \langle\widehat{\Delta}(t,t')\rangle = \frac{1}{N}\sum_{i=1}^{N}\langle|x_i(t) - x_i(t')|^2\rangle \tag{4.35}$$

and the variance of the squared displacement defines the so-called four-point susceptibility

$$\begin{aligned}\chi_4(t,t') &= N\left[\left\langle\widehat{\Delta}(t,t')^2\right\rangle - \left\langle\widehat{\Delta}(t,t')\right\rangle^2\right] \\ &= \frac{1}{N}\sum_{ij}\Big[\langle|x_i(t) - x_i(t')|^2|x_j(t) - x_j(t')|^2\rangle \\ &\quad -\langle|x_i(t) - x_i(t')|^2\rangle\langle|x_j(t) - x_j(t')|^2\rangle\Big]\end{aligned} \tag{4.36}$$

In what follows we neglect the presence of rattlers, namely of spheres that are not blocked but that can move inside the cage formed by surrounding blocked spheres. The effect of rattlers can be take into account and this has been done in [91].

The "cage size" is defined by the limit

$$\Delta^2(\infty) = \lim_{t-t'\to\infty}\lim_{t'\to\infty}\Delta(t,t') \tag{4.37}$$

where '∞' stands for times t, t' that are large as the lifetime of the state. Then we introduce a scaled cage size with the help of the pressure P of the system

$$\Delta_\infty = P^2\Delta^2(\infty) \propto \int_0^\infty d\omega\,\frac{D(\omega)}{\omega^2}\,; \tag{4.38}$$

the last relation has been obtained in [27, 91]. Because for ω close to zero $D(\omega) \sim \omega^{d-1}$ then the integral is convergent for any dimension greater than two. However when the pressure diverges, it happens that $\omega^* \to 0$ so that the integral behaves as $\int_{\omega^*}^\infty d\omega\,\frac{D(\omega)}{\omega^2} \sim \frac{D(\omega^*)}{\omega^*}$. If we look to the infinite time behavior of the susceptibility we obtain

$$\chi_4(\infty) = \lim_{t-t'\to\infty}\lim_{t'\to\infty}\chi_4(t,t') \sim \int_0^\infty d\omega\,\frac{D(\omega)}{\omega^4}\,. \tag{4.39}$$

However we expect that if the Gardner transition happens at finite pressure (this is true also for the metastable states, see the discussion below) the four point susceptibility will diverge for all the pressures greater than the Gardner one. This reflects the fact that if the Gardner transition is towards a fullRSB scheme, it is well

known that the fullRSB solution will be always marginally stable [132] and because of the fact that the χ_4 contains the replicon eigenvalue of the solution, it will be always divergent in the fullRSB phase. On the other hand, we may look at this from the point of view of normal modes: we split (4.39) in a contribution above, and one below ω^*:

$$\chi_4(\infty) = \int_0^{\omega^*} d\omega \, \frac{D(\omega)}{\omega^4} + \frac{D(\omega^*)}{(\omega^*)^3} \tag{4.40}$$

Even in three dimensions the integral is divergent due to acoustic modes. However the effect of the acoustic modes is seen only on very large timescales $t - t' \gg 1/\omega^*$ so that it is possible to give a definition of four point susceptibility the one for which $t - t' \sim 1/\omega^*$. In our large dimensional case the effect of acoustic modes is highly suppressed but we think that the integral will be still divergent due to other soft modes that are connected to the fullRSB physics. It is tempting to identify these modes with the ones observed in [179, 25, 26, 112, 180, 119] but here we are not able to establish a deeper and more convincent connection. The consequences of the Gardner transition could be detected also at the dynamical level. Even if this is a static calculation and the dynamics has not been solved yet, we can argue what will be the resulting dynamics from the structure of the states emerging form the fullRSB solution.

4.5.1 The general structure of the stability matrix

The matrix $\hat{\alpha}$ is constrained to have the sum of the elements of every column and every row equal to zero because of translational invariance. This means that we can take as independent entries the elements above the diagonal of the matrix, provided that the matrix is symmetric and the diagonal is fixed by this constraint. In this way we denote with $\delta/\delta\alpha_{a<b}$ the derivative taken with respect of the element α_{ab} with $a < b$ because this element is assumed to be the only independent one. This means that its variation induces a variation of the element α_{ba} and of the diagonal elements α_{aa} and α_{bb}.

Given this, we can define the stability matrix in the following way

$$\begin{aligned} M_{a\neq b,c\neq d} &= \frac{2\widehat{A}^2}{d} \left. \frac{\delta^2 s[\hat{\alpha}]}{\delta\alpha_{a<b}\delta\alpha_{c<d}} \right|_{\hat{\alpha}^{1\mathrm{RSB}}} \\ &= M_1 \left(\frac{\delta_{ac}\delta_{bd} + \delta_{ad}\delta_{bc}}{2} \right) + M_2 \left(\frac{\delta_{ac} + \delta_{ad} + \delta_{bc} + \delta_{bd}}{4} \right) + M_3 \, . \end{aligned} \tag{4.41}$$

The replica structure is a direct consequence of the structure of the 1RSB parametrization of the single molecule density. The matrix M is defined only for $a < b$ and $c < d$. However it is convenient to define it also for $a > b$ and $c > d$ so that we can assume that it is symmetric (hence the notation $M_{a\neq b,c\neq d}$). The prefactor $2\widehat{A}^2/d$ is chosen for later convenience and is positive, so that it does not affect the sign of the eigenvalues of the stability matrix. The 1RSB stability matrix has three eigenvalues whose expressions are

$$\begin{aligned} \lambda_R &= M_1 \, , \\ \lambda_L &= M_1 + (m-1)(M_2 + mM_3) \, , \\ \lambda_A &= M_1 + \frac{1}{2}(m-2)M_2 \, . \end{aligned} \tag{4.42}$$

We define the "entropic" and the "interaction" terms

$$\begin{aligned} M^{(I)}_{a\neq b;c\neq d} &= \left.\frac{\delta^2 \mathcal{F}[\hat{v}]}{\delta v_{a<b}\delta v_{c<d}}\right|_{\hat{v}=2\hat{\alpha}^{\rm 1RSB}} \\ M^{(E)}_{a\neq b;c\neq d} &= \left.\frac{\delta^2}{\delta\alpha_{a<b}\delta\alpha_{c<d}}\log\det(\hat{\alpha}^{m,m})\right|_{\hat{\alpha}=\hat{\alpha}^{\rm 1RSB}} \end{aligned} \tag{4.43}$$

so that we have

$$M_i = \widehat{A}^2 M_i^{(E)} - 4\widehat{\varphi}\,\widehat{A}^2 M_i^{(I)} \ . \tag{4.44}$$

The entropic and interaction terms will be computed separately because we need different techniques in order to do the calculations.

4.5.2 The entropic term

First of all it is convenient to introduce a shorthand notation $\hat{\beta} = \hat{\alpha}^{m,m}$. Moreover we use indices $i, j, k, \cdots$ for β to highlight that they run from 1 to $m-1$ because $\hat{\beta}$ is a $m-1 \times m-1$ matrix. The 1RSB ansatz $\beta_{ij}^{\rm 1RSB} = \widehat{A}(\delta_{ij} - 1/m)$ has the same form of $\hat{\alpha}$ but on the reduced $(m-1)\times(m-1)$ space. A simple algebraic computation shows that

$$(\hat{\beta}^{\rm 1RSB})^{-1}_{ij} = \frac{1}{\widehat{A}}(\delta_{ij}+1) \ . \tag{4.45}$$

and that

$$\frac{\delta\beta_{ij}}{\delta\alpha_{a<b}} = \delta_{ia}\delta_{jb} + \delta_{ib}\delta_{ja} - \delta_{ij}(\delta_{ia}+\delta_{ib}) \ . \tag{4.46}$$

Moreover using the standard result

$$\frac{\delta\log\det(\hat{\beta})}{\delta\beta_{ij}} = \beta^{-1}_{ji} \tag{4.47}$$

we obtain that

$$\frac{\delta}{\delta\alpha_{a<b}}\log\det(\hat{\beta}) = \sum_{ij}\beta^{-1}_{ji}\frac{\delta\beta_{ij}}{\delta\alpha_{a<b}} = {\rm Tr}\left[\hat{\beta}^{-1}\frac{\delta\hat{\beta}}{\delta\alpha_{a<b}}\right] \ . \tag{4.48}$$

and, from the fact that $\hat{\beta}\hat{\beta}^{-1} = I$ where I is the identity matrix, we can write

$$0 = \frac{\delta}{\delta\alpha_{c<d}}(\hat{\beta}\hat{\beta}^{-1}) \quad \Rightarrow \quad \frac{\delta\hat{\beta}^{-1}}{\delta\alpha_{c<d}} = -\hat{\beta}^{-1}\frac{\delta\hat{\beta}}{\delta\alpha_{c<d}}\hat{\beta}^{-1} \ . \tag{4.49}$$

It follows that the entropic part of the stability matrix is given by

$$\begin{aligned} M^{(E)}_{a<b;c<d} &= \left.\frac{\delta^2}{\delta\alpha_{a<b}\delta\alpha_{c<d}}\log\det(\hat{\beta})\right|_{\hat{\beta}=\hat{\beta}^{\rm 1RSB}} = -{\rm Tr}\left[\hat{\beta}^{-1}\frac{\delta\hat{\beta}}{\delta\alpha_{a<b}}\hat{\beta}^{-1}\frac{\delta\hat{\beta}}{\delta\alpha_{c<d}}\right]_{\hat{\beta}=\hat{\beta}^{\rm 1RSB}} \\ &= -\frac{1}{\widehat{A}^2}\left[2\left(\delta_{ac}\delta_{bd}+\delta_{ad}\delta_{bc}\right)+\left(\delta_{ac}+\delta_{ad}+\delta_{bc}+\delta_{bd}\right)\right] \end{aligned} \tag{4.50}$$

from which it follows that

$$\begin{aligned} M_1^{(E)} &= M_2^{(E)} = -\frac{4}{\widehat{A}^2} \ , \\ M_3^{(E)} &= 0 \ . \end{aligned} \tag{4.51}$$

4.5.3 The interaction term

The interaction part of the stability matrix can be computed by expanding the quantity $\mathcal{F}$ around the 1RSB solution. This can be done starting directly from (4.22). In this way the interaction part of the stability matrix is given by:

$$\begin{aligned} M^{(I)}_{a<b;c<d} &= \frac{\delta^2 \mathcal{F}}{\delta \upsilon_{a<b} \delta \upsilon_{c<d}} [\hat{v}^{\mathrm{1RSB}}] \Big|_{\hat{v}^{1RSB}=2\hat{\alpha}^{1RSB}} \\ &= \lim_{n\to 0} \sum_{n_1,\ldots,n_m;\sum_a^m n_a=n} \frac{n!}{n_1!\ldots n_m!} f(n_a,n_b) f(n_c,n_d) \exp\left[-\widehat{A} + \widehat{A}\sum_{a=1}^{m} \frac{n_a^2}{n^2}\right] \end{aligned} \tag{4.52}$$

where f is given by:

$$f(n_a,n_b) = \frac{n_a}{2n} + \frac{n_b}{2n} - \frac{n_a^2}{2n^2} - \frac{n_b^2}{2n^2} + \frac{n_a n_b}{n^2}\,. \tag{4.53}$$

We introduce now the following notation

$$\langle O \rangle = \lim_{n\to 0} \sum_{n_1,\ldots,n_m;\sum_a^m n_a=n} \frac{n!}{n_1!\ldots n_m!} O \exp\left[-\widehat{A} + \widehat{A}\sum_{a=1}^{m} \frac{n_a^2}{n^2}\right] \tag{4.54}$$

so that the stability matrix can be written as

$$\begin{aligned} M^{(I)}_{a<b;c<d} = &\frac{1}{4}\left(\langle\frac{n_a n_c}{n^2}\rangle + \langle\frac{n_a n_d}{n^2}\rangle + \langle\frac{n_b n_c}{n^2}\rangle + \langle\frac{n_b n_d}{n^2}\rangle\right) \\ &- \frac{1}{4}\left(\langle\frac{n_a^2 n_c}{n^3}\rangle + \langle\frac{n_a^2 n_d}{n^3}\rangle + \langle\frac{n_b^2 n_c}{n^3}\rangle + \langle\frac{n_b^2 n_d}{n^3}\rangle\right. \\ &+ \langle\frac{n_a n_c^2}{n^3}\rangle + \langle\frac{n_a n_d^2}{n^3}\rangle + \langle\frac{n_b n_c^2}{n^3}\rangle + \langle\frac{n_b n_d^2}{n^3}\rangle \\ &\left.-2\langle\frac{n_a n_c n_d}{n^3}\rangle - 2\langle\frac{n_b n_c n_d}{n^3}\rangle - 2\langle\frac{n_c n_a n_b}{n^3}\rangle - 2\langle\frac{n_d n_a n_b}{n^3}\rangle\right) \\ &+ \frac{1}{4}\left(\langle\frac{n_a^2 n_c^2}{n^4}\rangle + \langle\frac{n_a^2 n_d^2}{n^4}\rangle + \langle\frac{n_b^2 n_c^2}{n^4}\rangle + \langle\frac{n_b^2 n_d^2}{n^4}\rangle\right. \\ &- 2\langle\frac{n_a^2 n_c n_d}{n^4}\rangle - 2\langle\frac{n_b^2 n_c n_d}{n^4}\rangle - 2\langle\frac{n_c^2 n_a n_b}{n^4}\rangle \\ &\left.-2\langle\frac{n_d^2 n_a n_b}{n^4}\rangle + 4\langle\frac{n_a n_b n_c n_d}{n^4}\rangle\right)\,. \end{aligned} \tag{4.55}$$

Note that the expression above is not so simple and systematic as it seems at the first sight. The real difficulty is that we need to perform the sum that appears in Eq. 4.54 when monomials of $\{n_a\}$ are present and then we have to evaluate the sum in the limit $n \to 0$.

Monomials of n

In the section above we have seen that the computation of the interaction part of the stability matrix can be reduced to the calculation of averages of monomials of

$\{n_a\}$. A simple way to treat the averages and to overcome the difficulties related to the sum and the multinomial factors, is to introduce a set of Gaussian integrals in such a way that we can do the sum in a simpler way. The advantage in doing this is that the averages will be expressed in terms of special functions that can be computed numerically. Let us see how this procedure can be put in a formal way. A general term that must be evaluated is the following

$$\begin{aligned}
&\left\langle \frac{n_{a_1}}{n}\cdots\frac{n_{a_k}}{n}\right\rangle = \lim_{n\to 0}\frac{1}{n^k}\sum_{n_1,\ldots,n_m;\sum_a^m n_a=n}\frac{n!}{n_1!\ldots n_m!}\,n_{a_1}\cdots n_{a_k}\\
&\times\exp\left[-\widehat{A}+\widehat{A}\sum_{a=1}^m\frac{n_a^2}{n^2}\right] = e^{-\widehat{A}}\lim_{n\to 0}\int\left(\prod_a\frac{\mathrm{d}\lambda_a}{\sqrt{2\pi}}\right)e^{-\sum_{a=1}^m\frac{\lambda_a^2}{2}}\\
&\times\sum_{n_1,\ldots,n_m;\sum_a^m n_a=n}\frac{n!}{n_1!\ldots n_m!}\frac{n_{a_1}\cdots n_{a_k}}{n^k}\exp\left[-\sqrt{2\widehat{A}}\sum_{a=1}^m\frac{n_a\lambda_a}{n}\right]\\
&=\frac{(-1)^k e^{-\widehat{A}}}{(2\widehat{A})^{k/2}}\lim_{n\to 0}\int\left(\prod_a\frac{\mathrm{d}\lambda_a}{\sqrt{2\pi}}\right)e^{-\sum_{a=1}^m\frac{\lambda_a^2}{2}}\\
&\times\sum_{n_1,\ldots,n_m;\sum_a^m n_a=n}\frac{n!}{n_1!\ldots n_m!}\frac{\partial^k}{\partial\lambda_{a_1}\cdots\partial\lambda_{a_k}}\exp\left[-\sqrt{2\widehat{A}}\sum_{a=1}^m\frac{n_a\lambda_a}{n}\right]\\
&=\frac{e^{-\widehat{A}}}{(2\widehat{A})^{k/2}}\int\left(\prod_a\frac{\mathrm{d}\lambda_a}{\sqrt{2\pi}}\right)\left(\frac{\partial^k}{\partial\lambda_{a_1}\cdots\partial\lambda_{a_k}}e^{-\sum_{a=1}^m\frac{\lambda_a^2}{2}}\right)\exp\left[-\sqrt{2\widehat{A}}\min_a\lambda_a\right]\\
&=\frac{1}{(2\widehat{A})^{k/2}}\int\left(\prod_a\frac{\mathrm{d}\lambda_a}{\sqrt{2\pi}}\right)\left(e^{\sum_{a=1}^m\frac{\lambda_a^2}{2}}\frac{\partial^k}{\partial\lambda_{a_1}\cdots\partial\lambda_{a_k}}e^{-\sum_{a=1}^m\frac{\lambda_a^2}{2}}\right)\\
&\times\exp\left[-\frac{1}{2}\sum_{a=1}^m\left(\lambda_a+\sqrt{2\widehat{A}}\,\delta_{a,\min}\right)^2\right]\\
&=\frac{1}{(2\widehat{A})^{k/2}}\left\langle e^{\sum_{a=1}^m\frac{\lambda_a^2}{2}}\frac{\partial^k}{\partial\lambda_{a_1}\cdots\partial\lambda_{a_k}}e^{-\sum_{a=1}^m\frac{\lambda_a^2}{2}}\right\rangle
\end{aligned}\tag{4.56}$$

where we have introduced a new definition of average that now is given by

$$\langle O\rangle = \int\left(\prod_a\frac{\mathrm{d}\lambda_a}{\sqrt{2\pi}}\right)O\exp\left[-\frac{1}{2}\sum_{a=1}^m\left(\lambda_a+\sqrt{2\widehat{A}}\,\delta_{a,\min}\right)^2\right]\tag{4.57}$$

The important point here is that the polynomial factors in the $\{n_a\}$ will be translated in this way in polynomials of $\{\lambda_a\}$. Because of the fact that the measure that defines the average is replica symmetric over $\{\lambda_a\}$, we need to compute the following particular objects:

$$\begin{aligned}
B_{ab} &= \left\langle\frac{n_a n_b}{n^2}\right\rangle = \frac{1}{2\widehat{A}}\left\langle-\delta_{ab}+\lambda_a\lambda_b\right\rangle\\
T_{abc} &= \left\langle\frac{n_a n_b n_c}{n^3}\right\rangle = \frac{1}{(2\widehat{A})^{3/2}}\left\langle\delta_{bc}\lambda_a+\delta_{ac}\lambda_b+\delta_{ab}\lambda_c-\lambda_a\lambda_b\lambda_c\right\rangle\\
\Delta_{abcd} &= \left\langle\frac{n_a n_b n_c n_d}{n^4}\right\rangle = \frac{1}{(2\widehat{A})^2}\langle\delta_{ab}\delta_{cd}+\delta_{bc}\delta_{ad}+\delta_{ac}\delta_{cd}-\delta_{ab}\lambda_c\lambda_d\\
&\quad-\delta_{bc}\lambda_a\lambda_d-\delta_{ac}\lambda_b\lambda_d-\delta_{cd}\lambda_a\lambda_b-\delta_{bd}\lambda_a\lambda_c-\delta_{ad}\lambda_b\lambda_c+\lambda_a\lambda_b\lambda_c\lambda_d\rangle
\end{aligned}\tag{4.58}$$

so that the interaction part of the stability matrix will be given finally by

$$\begin{aligned} M^{(I)}_{a<b;c<d} = & \frac{1}{4}\left(B_{ac}+B_{ad}+B_{bc}+B_{bd}\right) \\ & -\frac{1}{4}\left(T_{aac}+T_{aad}+T_{bbc}+T_{bbd}+T_{acc}+T_{add}+T_{bcc}+T_{bdd}\right. \\ & \left.-2T_{acd}-2T_{bcd}-2T_{abc}-2T_{abd}\right) \\ & +\frac{1}{4}\left(\Delta_{aacc}+\Delta_{aadd}+\Delta_{bbcc}+\Delta_{bbdd}\right. \\ & \left.-2\Delta_{aacd}-2\Delta_{bbcd}-2\Delta_{ccab}-2\Delta_{abdd}+4\Delta_{abcd}\right)\ . \end{aligned} \tag{4.59}$$

Monomials of λ

In the end the evaluation of the elements of the stability matrix has been reduced to the evaluation of the averages of polynomials of $\{\lambda_a\}$. These averages can be computed on the same line of reasoning of Eq. (4.23) and it will be convenient to define one more average over λ

$$\langle f(\lambda)\rangle = \int_{-\infty}^{\infty} \frac{\mathrm{d}\lambda}{\sqrt{2\pi}} e^{-\frac{1}{2}\left(\lambda+\sqrt{2\widehat{A}}\right)^2} f(\lambda) \tag{4.60}$$

With this new definition of average we have

$$\begin{aligned} \langle 1\rangle =& \mathcal{F}[\hat{v}^{\mathrm{1RSB}}] = \left\langle m\,\Theta_0(\lambda)^{m-1}\right\rangle \\ \left\langle \lambda_1^k\right\rangle =& \left\langle \lambda^k\,\Theta_0(\lambda)^{m-1} + (m-1)\,\Theta_k(\lambda)\Theta_0(\lambda)^{m-2}\right\rangle \\ \left\langle \lambda_1^k\lambda_2^l\right\rangle =& \left\langle \lambda^k\Theta_l(\lambda)\Theta_0(\lambda)^{m-2} + \lambda^l\Theta_k(\lambda)\Theta_0(\lambda)^{m-2}\right. \\ & \left.+(m-2)\Theta_k(\lambda)\Theta_l(\lambda)\Theta_0(\lambda)^{m-3}\right\rangle \\ \left\langle \lambda_1^k\lambda_2^l\lambda_3^n\right\rangle =& \langle \lambda^k\Theta_l(\lambda)\Theta_n(\lambda)\Theta_0(\lambda)^{m-3} + \lambda^l\Theta_k(\lambda)\Theta_n(\lambda)\Theta_0(\lambda)^{m-3} \\ & + \lambda^n\Theta_k(\lambda)\Theta_l(\lambda)\Theta_0(\lambda)^{m-3} \\ & + (m-3)\Theta_k(\lambda)\Theta_l(\lambda)\Theta_n(\lambda)\Theta_0(\lambda)^{m-4}\rangle \\ \left\langle \lambda_1^k\lambda_2^l\lambda_3^n\lambda_4^p\right\rangle =& \langle \lambda^k\Theta_l(\lambda)\Theta_n(\lambda)\Theta_p(\lambda)\Theta_0(\lambda)^{m-4} + \lambda^l\Theta_k(\lambda)\Theta_n(\lambda)\Theta_p(\lambda)\Theta_0(\lambda)^{m-4} \\ & + \lambda^n\Theta_k(\lambda)\Theta_l(\lambda)\Theta_p(\lambda)\Theta_0(\lambda)^{m-4} + \lambda^p\Theta_k(\lambda)\Theta_l(\lambda)\Theta_n(\lambda)\Theta_0(\lambda)^{m-4} \\ & + (m-4)\Theta_k(\lambda)\Theta_l(\lambda)\Theta_n(\lambda)\Theta_p(\lambda)\Theta_0(\lambda)^{m-5}\rangle \end{aligned} \tag{4.61}$$

and so on.

The structure of the stability matrix

Because of the fact that in this real replica calculation the 1RSB ansatz corresponds to a replica symmetric parametrization for the single molecule density, the stability

matrix has only three independent matrix elements that are

$$
\begin{aligned}
M^{(I)}_{12;12} &= \frac{1}{2}(B_{11}+B_{12}) + (T_{112}-T_{111}) + \frac{1}{4}(2\Delta_{1111}+6\Delta_{1122}-8\Delta_{1112}) \ , \\
M^{(I)}_{12;13} &= \frac{1}{4}(B_{11}+3B_{12}) - \frac{1}{2}(T_{111}+T_{112}-2T_{123}) + \frac{1}{4}(\Delta_{1111}+3\Delta_{1122}-4\Delta_{1112}) \ , \\
M^{(I)}_{12;34} &= B_{12} - 2(T_{112}-T_{123}) + (\Delta_{1122}-2\Delta_{1123}+\Delta_{1234}) \ .
\end{aligned}
\tag{4.62}
$$

However we can enlighten the replica structure of the stability matrix by writing it in the following form

$$
M^{(I)}_{a<b;c<d} = M^{(I)}_1 \frac{\delta_{ac}\delta_{bd}+\delta_{ad}\delta_{bc}}{2} + M^{(I)}_2 \frac{\delta_{ac}+\delta_{ad}+\delta_{bc}+\delta_{bd}}{4} + M^{(I)}_3 \tag{4.63}
$$

and the relation of this expression with the independent matrix elements is given by

$$
\begin{aligned}
M^{(I)}_1 &= 2M^{(I)}_{12;12} - 4M^{(I)}_{12;13} + 2M^{(I)}_{12;34} = 2\Delta_{1122} - 4\Delta_{1123} + 2\Delta_{1234} \\
M^{(I)}_2 &= 4M^{(I)}_{12;13} - 4M^{(I)}_{12;34} = B_{11} - B_{12} - 2T_{111} + 6T_{112} - 4T_{123} \\
&\quad + \Delta_{1111} - 4\Delta_{1112} - \Delta_{1122} + 8\Delta_{1123} - 4\Delta_{1234} \\
M^{(I)}_3 &= M^{(I)}_{12;34} = B_{12} - 2T_{112} + 2T_{123}) + \Delta_{1122} - 2\Delta_{1123} + \Delta_{1234}
\end{aligned}
\tag{4.64}
$$

The equations we have just derived and Eqs. (4.58) and (4.61), represent the complete expression of the interaction part of the stability matrix.

4.5.4 The replicon eigenvalue

In replica calculations, the eigenvalue that is responsible for the instability of the 1RSB solution towards further replica symmetry broken solutions is the replicon that is given by $\lambda_R = M_1 = \widehat{A}^2 M^{(E)}_1 - 4\widehat{\varphi}\,\widehat{A}^2 M^{(I)}_1$. We can use the results we have derived on the matrix elements of the stability matrix to compute directly this eigenvalue. By simplifying the algebra we finally end up with the following expression

$$
\begin{aligned}
\lambda_R &= -4 - 2\widehat{\varphi}\,\Lambda_m(\widehat{A}) \\
\Lambda_m(\widehat{A}) &= \Big\langle \Theta_0(\lambda)^{m-5}[\Theta_1(\lambda)^2 - \lambda\Theta_1(\lambda)\Theta_0(\lambda)] \\
&\quad \times[(2-2\lambda^2)\Theta_0(\lambda)^2 + (m-4)\Theta_1(\lambda)^2 + (6-m)\lambda\Theta_0(\lambda)\Theta_1(\lambda)]\Big\rangle \\
&= \left\langle \Theta_0(\lambda)^{m-1}\left[\left(\frac{\Theta_1(\lambda)}{\Theta_0(\lambda)}\right)^2 - \lambda\frac{\Theta_1(\lambda)}{\Theta_0(\lambda)}\right]\right. \\
&\quad \left.\times\left[(2-2\lambda^2) + (m-4)\left(\frac{\Theta_1(\lambda)}{\Theta_0(\lambda)}\right)^2 + (6-m)\lambda\frac{\Theta_1(\lambda)}{\Theta_0(\lambda)}\right]\right\rangle
\end{aligned}
\tag{4.65}
$$

The value of the replicon eigenvalue can be computed numerically on the 1RSB solution. In fact, given a point in the $(m,\widehat{\varphi})$ plane where a 1RSB solution is present, we can compute the value of $\widehat{A}$ that satisfies Eq. 4.28, and then we can compute

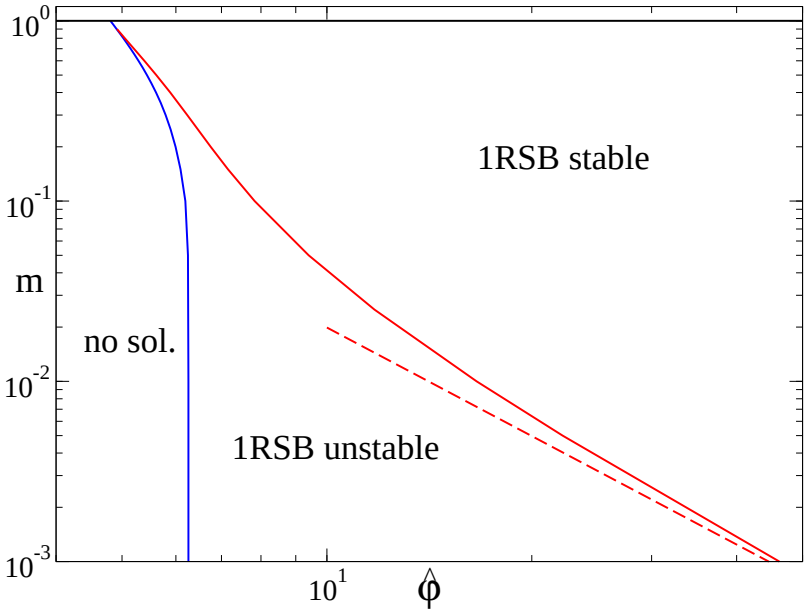

Figure 4.7. The stability diagram of 1RSB solution in the $(m, \widehat{\varphi})$ plane. Above the blue line a 1RSB solution is present but this solution is unstable up to the red line that is the line $m_G(\widehat{\varphi})$. The red dashed line is the asymptotic fit of the instability line that shows that the asymptotic behavior of the red line is $\widehat{\varphi}_G(m) \sim m^{-1/2}$. Picture taken from [110]

the averages that appear in Eq. 4.65. In this way we can find the line where $\lambda_R = 0$ and the 1RSB solution becomes unstable towards further replica symmetry breaking schemes. The instability line in the $(m, \widehat{\varphi})$ plane, which corresponds to the line $\widehat{\varphi}_G(m)$ on which the replicon vanishes, is reported in Fig. 4.7.

From the numerical computation of the instability line we see that $\widehat{\varphi}_G(m) \sim m^{-1/2}$ for $m \to 0$. To confirm this we must compute the asymptotic behaviour of the function $\Lambda(m, \widehat{A})$ when both m and $\widehat{A}$ are small that is the high density region. A simple way to do this is to use Eq. 4.28 to write everything as a function of $\widehat{\varphi}$ instead of $\widehat{A}$. In this way the equation for the instability line becomes

$$2\mathcal{F}_m(\widehat{A}) = -\Lambda_m(\widehat{A}) \,. \tag{4.66}$$

This equation gives the value of $\widehat{A}_G(m)$ and by using Eq. 4.28 we can obtain again $\widehat{\varphi}_G(m)$.

The first thing that we have to do is to examine the asymptotic behavior of all the different terms for $\lambda \to \infty$. We have

$$\begin{aligned}
&\Theta_0(\lambda) \sim \frac{e^{-\frac{1}{2}\lambda^2}}{\sqrt{2\pi}\lambda}\left(1 - \frac{1}{\lambda^2} + \frac{3}{\lambda^4} - \frac{15}{\lambda^6} + \cdots\right) \,, \\
&\left(\frac{\Theta_1(\lambda)}{\Theta_0(\lambda)}\right)^2 - \lambda\frac{\Theta_1(\lambda)}{\Theta_0(\lambda)} \sim 1 - \frac{1}{\lambda^2} + \frac{6}{\lambda^4} - \frac{50}{\lambda^6} + \cdots \,, \\
&(2 - 2\lambda^2) + (m-4)\left(\frac{\Theta_1(\lambda)}{\Theta_0(\lambda)}\right)^2 + (6-m)\lambda\frac{\Theta_1(\lambda)}{\Theta_0(\lambda)} \\
&\sim m - \frac{m}{\lambda^2} + \frac{6m-4}{\lambda^4} + \frac{52 - 50m}{\lambda^6} + \cdots \,.
\end{aligned} \tag{4.67}$$

We define here

$$\mathcal{L}(\lambda) = \left[\left(\frac{\Theta_1(\lambda)}{\Theta_0(\lambda)}\right)^2 - \lambda\frac{\Theta_1(\lambda)}{\Theta_0(\lambda)}\right]\left[2 - 2\lambda^2 + (m-4)\left(\frac{\Theta_1(\lambda)}{\Theta_0(\lambda)}\right)^2 + (6-m)\lambda\frac{\Theta_1(\lambda)}{\Theta_0(\lambda)}\right] ,$$
$$\mathcal{L}(\lambda) \sim m - \frac{2m}{\lambda^2} + \frac{13m-4}{\lambda^4} + \frac{56-112m}{\lambda^6} + \cdots . \tag{4.68}$$

In order to see what happens for large value of $\widehat{\varphi}$ we expand Eq. (4.66) for small $\widehat{A}$. Moreover we have that $\mathcal{G}_m(\widehat{A}) = 1 - m\left\langle \Theta_0(\lambda)^{m-1}\right\rangle$ so that

$$\begin{aligned}
\mathcal{G}_m(\widehat{A}) &= G_1(m)\sqrt{\widehat{A}} + G_2(m)\widehat{A} + \cdots , \\
\mathcal{F}_m(\widehat{A}) &= \frac{G_1(m)}{1-m}\frac{1}{2}\sqrt{\widehat{A}} + \frac{G_2(m)}{1-m}\widehat{A} + \cdots , \\
G_1(m) &= -m\int \frac{\mathrm{d}\lambda}{\sqrt{2\pi}} e^{-\lambda^2/2}\Theta_0(\lambda)^{m-1}(-\lambda\sqrt{2}) , \\
G_2(m) &= -m\int \frac{\mathrm{d}\lambda}{\sqrt{2\pi}} e^{-\lambda^2/2}\Theta_0(\lambda)^{m-1}(\lambda^2-1) ,
\end{aligned} \tag{4.69}$$

and similarly

$$\begin{aligned}
\Lambda_m(\widehat{A}) &= L_1(m)\sqrt{\widehat{A}} + L_2(m)\widehat{A} + \cdots , \\
L_1(m) &= \int \frac{\mathrm{d}\lambda}{\sqrt{2\pi}} e^{-\lambda^2/2}\Theta_0(\lambda)^{m-1}\mathcal{L}(\lambda)(-\lambda\sqrt{2}) , \\
L_2(m) &= \int \frac{\mathrm{d}\lambda}{\sqrt{2\pi}} e^{-\lambda^2/2}\Theta_0(\lambda)^{m-1}\mathcal{L}(\lambda)(\lambda^2-1) .
\end{aligned} \tag{4.70}$$

The fact that the horrible integral corresponding to $\Lambda_m(\widehat{A}=0)$ is exactly 0 can be proven by a series of integrations by parts.

It follows that Eq. (4.66) in the high density region becomes

$$0 = \sqrt{\widehat{A}}\Delta_1(m) + \widehat{A}\Delta_2(m) + \cdots \quad \Rightarrow \quad \sqrt{\widehat{A}_G} = -\frac{\Delta_1(m)}{\Delta_2(m)} + \cdots , \tag{4.71}$$

where

$$\begin{aligned}
\Delta_1(m) &= \frac{G_1(m)}{1-m} + L_1(m) , \\
\Delta_2(m) &= 2\frac{G_2(m)}{1-m} + L_2(m) .
\end{aligned} \tag{4.72}$$

The asymptotic behaviors of the integrals in the above expressions for small m can be different, and they depend on the way in which the integrand for large λ behaves when m goes to zero. In fact, we can see that if the integrand decays faster than $1/\lambda$, the integral is convergent for $m \to 0$. In the opposite case, the integral is divergent with a divergence that is dominated by the large λ behavior: in this case one has to analyze all the possibly divergent parts to determine the behavior of the integral at $m \to 0$.

Let us take the term $\Delta_1(m)$. The large λ contribution to the integral is given by

$$\Delta_1(m) \sim \int \frac{\mathrm{d}\lambda}{\sqrt{2\pi}} e^{-m\lambda^2/2} (\sqrt{2\pi}\lambda)^{1-m} (-\lambda\sqrt{2}) \left[-m^2 - \frac{2m}{\lambda^2} - \frac{4}{\lambda^4} + \cdots \right] . \quad (4.73)$$

The first two terms give contributions that are not divergent when $m \to 0$, hence they are subleading with respect to the $1/\lambda^4$ term that gives a finite contribution. It follows that $\Delta_1(m)$ has a finite limit for $m \to 0$ that is given by

$$\begin{aligned} \Delta_1(0) = \int \frac{\mathrm{d}\lambda}{\sqrt{2\pi}} e^{-\lambda^2/2} \Theta_0(\lambda)^{-1} \left[\left(\frac{\Theta_1(\lambda)}{\Theta_0(\lambda)} \right)^2 - \lambda \frac{\Theta_1(\lambda)}{\Theta_0(\lambda)} \right] \\ \times \left[2 - 2\lambda^2 - 4 \left(\frac{\Theta_1(\lambda)}{\Theta_0(\lambda)} \right)^2 + 6\lambda \frac{\Theta_1(\lambda)}{\Theta_0(\lambda)} \right] (-\lambda\sqrt{2}) \approx 1.6 \end{aligned} \quad (4.74)$$

To investigate the leading large λ behavior of the integrand of $\Delta_2(m)$ we change variable of integration to $y = \sqrt{m}\lambda$ so that we have

$$\begin{aligned} \Delta_2(m) &\sim \int \frac{\mathrm{d}\lambda}{\sqrt{2\pi}} e^{-m\lambda^2/2} (\sqrt{2\pi}\lambda)^{1-m} (\lambda^2 - 1) \left[-m + \cdots \right] \\ &= -\frac{1}{m} \int_0^\infty \mathrm{d}y \, e^{-y^2/2} \, y^3 = -\frac{2}{m} . \end{aligned} \quad (4.75)$$

We conclude that $\sqrt{\widehat{A}_G} \approx 0.8m$. Finally, we can show similarly that for small m

$$\begin{aligned} G_1(m) &\sim -m \int \frac{\mathrm{d}\lambda}{\sqrt{2\pi}} e^{-m\lambda^2/2} (\sqrt{2\pi}\lambda)^{1-m} (-\lambda\sqrt{2}) \\ &= \sqrt{\frac{2}{m}} \int_0^\infty \mathrm{d}y \, e^{-y^2/2} y^2 \sim \sqrt{\frac{\pi}{m}} , \end{aligned} \quad (4.76)$$

hence

$$\widehat{\varphi}_G \sim \frac{1}{\frac{G_1(m)}{1-m} \frac{1}{2} \sqrt{\widehat{A}_G}} \sim \sqrt{\frac{4m}{\pi \widehat{A}_G}} \approx \sqrt{\frac{4}{\pi}} \frac{1}{0.8\sqrt{m}} \approx 1.41 m^{-1/2} . \quad (4.77)$$

This result is consistent with the numerical calculation of $\widehat{A}_G$ and $\widehat{\varphi}_G$.

4.6 Computation of the dynamical exponents from the cubic expansion

In this section we will compute the mode-coupling exponent parameter by expanding the replicated entropy to the third order around the 1RSB solution at the dynamical point. The strategy that we will use is exactly the same that we used above to compute the stability matrix but it will be adapted to compute the cubic terms of the expansion of the replicated entropy.

Let us define, following the same notation as for the second order terms (hence for $a \neq b$, $c \neq d$, $e \neq f$ which we omit from now on)

$$W_{ab,cd,ef} = \frac{\delta^3 s[\hat{\alpha}]}{\delta\alpha_{a<b} \delta\alpha_{c<d} \delta\alpha_{e<f}} . \quad (4.78)$$

Around the replica symmetric solution the two coefficients w_1 and w_2 can be written in the following form [169]

$$\begin{aligned} w_1 &= W_{ab,bc,ca} - 3W_{ab,ac,bd} + 3W_{ac,bc,de} - W_{ab,cd,ef} \ , \\ w_2 &= \frac{1}{2}W_{ab,ab,ab} - 3W_{ab,ab,ac} + \frac{3}{2}W_{ab,ab,cd} + 3W_{ab,ac,bd} + 2W_{ab,ac,ad} - 6W_{ac,bc,de} \\ &\quad + 2W_{ab,cd,ef} \ , \end{aligned} \tag{4.79}$$

and as we have seen in the previous sections we have that $\lambda_{\mathrm{MCT}} = \frac{w_2}{w_1}$. We divide the computation of the cubic terms above into the interaction and entropic part

$$\begin{aligned} W^{(I)}_{ab,cd,ef} &= \left. \frac{\delta^3 \mathcal{F}[\hat{v}]}{\delta v_{a<b} \delta v_{c<d} \delta v_{e<f}} \right|_{\hat{v}=2\hat{\alpha}^{\mathrm{1RSB}}} \\ W^{(E)}_{ab,cd,ef} &= \left. \frac{\delta^3}{\delta \alpha_{a<b} \delta \alpha_{c<d} \delta \alpha_{e<f}} \log\det(\hat{\alpha}^{m,m}) \right|_{\hat{\alpha}=\hat{\alpha}^{\mathrm{1RSB}}} \end{aligned} \tag{4.80}$$

In this way we have

$$W_{ab,cd,ef} = W^{(E)}_{ab,cd,ef} - 8\widehat{\varphi}\, W^{(I)}_{ab,cd,ef} \ . \tag{4.81}$$

4.6.1 The entropic term

The entropic term can be computed on the same lines of Sec. 4.5.2 and we obtain

$$\begin{aligned} W^{(E)}_{ab,cd,ef} &= \mathrm{Tr}\left[\hat{\beta}^{-1} \frac{\delta \hat{\beta}}{\delta \alpha_{a<b}} \hat{\beta}^{-1} \frac{\delta \hat{\beta}}{\delta \alpha_{c<d}} \hat{\beta}^{-1} \frac{\delta \hat{\beta}}{\delta \alpha_{e<f}} \right]_{\hat{\beta}=\hat{\beta}^{\mathrm{1RSB}}} \\ &\quad + \mathrm{Tr}\left[\hat{\beta}^{-1} \frac{\delta \hat{\beta}}{\delta \alpha_{a<b}} \hat{\beta}^{-1} \frac{\delta \hat{\beta}}{\delta \alpha_{e<f}} \hat{\beta}^{-1} \frac{\delta \hat{\beta}}{\delta \alpha_{c<d}} \right]_{\hat{\beta}=\hat{\beta}^{\mathrm{1RSB}}} \end{aligned} \tag{4.82}$$

Using Eq. (4.79), the results of Sec. 4.5.2 and performing the traces we obtain

$$\begin{aligned} w^{(E)}_1 &= \frac{2}{\widehat{A}^3} \ , \\ w^{(E)}_2 &= 0 \ . \end{aligned} \tag{4.83}$$

4.6.2 The interaction term

The interaction term is given by

$$W^{(I)}_{ab,cd,ef} = \left. \frac{\delta^3 \mathcal{F}[\hat{v}]}{\delta v_{a<b} \delta v_{c<d} \delta v_{e<f}} \right|_{\hat{v}=2\hat{\alpha}^{\mathrm{1RSB}}} = \langle f(n_a, n_b) f(n_c, n_d) f(n_e, n_f) \rangle \ . \tag{4.84}$$

By expanding the products of f and simplifying many monomials using the symmetries (for example we have that $\left\langle n_a^3 n_d n_f^2 \right\rangle = \langle n_a^3 n_b^2 n_c \rangle$), we obtain

$$\begin{aligned} w_1^{(I)} &= \left\langle \frac{n_a^2 n_b^2 n_c^2 - 3 n_a^2 n_b^2 n_c n_d + 3 n_a^2 n_b n_c n_d n_e - n_a n_b n_c n_d n_e n_f}{n^6} \right\rangle , \\ w_2^{(I)} &= \left\langle \frac{(1/2) n_a^3 n_b^3 - 3 n_a^3 n_b^2 n_c + 2 n_a^3 n_b n_c n_d + (9/2) n_a^2 n_b^2 n_c n_d}{n^6} \right\rangle \\ &\quad + \left\langle \frac{2 n_a n_b n_c n_d n_e n_f - 6 n_a^2 n_b n_c n_d n_e}{n^6} \right\rangle \end{aligned} \tag{4.85}$$

As before, we convert the average over n into an average over λ, using Eq. (4.56). Performing the derivatives and exploiting again the symmetries to simplify the result we obtain

$$\begin{aligned} w_1^{(I)} =& \frac{1}{(2\widehat{A})^3} \Big\langle -1 + 3\lambda_1^2 - 3\lambda_1\lambda_2 - 3\lambda_1^2\lambda_2^2 + 6\lambda_1^2\lambda_2\lambda_3 + \lambda_1^2\lambda_2^2\lambda_3^2 - 3\lambda_1\lambda_2\lambda_3\lambda_4 \\ & -3\lambda_1^2\lambda_2^2\lambda_3\lambda_4 + 3\lambda_1^2\lambda_2\lambda_3\lambda_4\lambda_5 - \lambda_1\lambda_2\lambda_3\lambda_4\lambda_5\lambda_6 \Big\rangle , \\ w_2^{(I)} =& \frac{1}{(2\widehat{A})^3} \Big\langle \frac{1}{2}\lambda_1^3\lambda_2^3 - 3\lambda_1^3\lambda_2^2\lambda_3 + 2\lambda_1^3\lambda_2\lambda_3\lambda_4 + \frac{9}{2}\lambda_1^2\lambda_2^2\lambda_3\lambda_4 \\ & -6\lambda_1^2\lambda_2\lambda_3\lambda_4\lambda_5 + 2\lambda_1\lambda_2\lambda_3\lambda_4\lambda_5\lambda_6 \Big\rangle . \end{aligned} \tag{4.86}$$

By using Eq. (4.61), we can compute explicitly all the averages to obtain

$$\begin{aligned} w_1^{(I)} =& -\frac{1}{(2\widehat{A})^3} \Big\langle \Theta_0(\lambda)^{m-7} [\Theta_0(\lambda)^2 + \Theta_1(\lambda)^2 - \Theta_0(\lambda)\Theta_2(\lambda)]^2 \\ & \{(m - 3\lambda^2)\Theta_0(\lambda)^2 + (m-6)\Theta_1(\lambda)^2 + \Theta_0(\lambda)[6\lambda\Theta_1(\lambda) - (m-3)\Theta_2(\lambda)]\} \Big\rangle , \\ w_2^{(I)} =& \frac{1}{2(2\widehat{A})^3} \Big\langle \Theta_0(\lambda)^{m-7} [2\Theta_1(\lambda)^3 - 3\Theta_0(\lambda)\Theta_1(\lambda)\Theta_2(\lambda) + \Theta_0(\lambda)^2\Theta_3(\lambda)] \\ & \{2\lambda^3\, \Theta_0(\lambda)^3 + 2(m-6)\Theta_1(\lambda)^3 + 3\Theta_0(\lambda)\Theta_1(\lambda)(4\lambda\Theta_1(\lambda) - (m-4)\Theta_2(\lambda)) \\ & + \Theta_0(\lambda)^2[-6\lambda(\lambda\Theta_1(\lambda) + \Theta_2(\lambda)) + (m-2)\Theta_3(\lambda)]\} \Big\rangle , \end{aligned} \tag{4.87}$$

These two terms can be computed numerically at the dynamical transition point.

4.6.3 Numerical result

Using the results of the previous section we finally have

$$\lambda_{\mathrm{MCT}} = \frac{w_2}{w_1} = \frac{-8\widehat{\varphi} w_2^{(I)}}{2/\widehat{A}^3 - 8\widehat{\varphi} w_1^{(I)}} . \tag{4.88}$$

This quantity must be computed at the dynamical point which means that $m = 1$, $\widehat{\varphi} = \widehat{\varphi}_d = 4.80677$ and $\widehat{A} = \widehat{A}_d = 0.57668$. The numerical result is

$$\lambda_{\mathrm{MCT}} = 0.70698 , \tag{4.89}$$

which implies that the MCT exponents are $a = 0.324016$, $b = 0.629148$ and $\gamma = 2.33786$. The result for γ is roughly consistent with the numerical estimate of Ref. [43].

4.7 Phenomenological extension to finite dimensions

The results that we have obtained in the previous sections are valid only in the limit $d \to \infty$. However we can assume that these results are also an approximation for the finite dimensional physics and we can try to extract some predictions also in the finite d case. To obtain quantitative results in finite d we first we go back to non-rescaled density and we rearrange the replicated entropy as

$$\begin{aligned} s[\hat{\alpha}] =& 1 - \log\rho - 2^{d-1}\varphi + d\log m + \frac{(m-1)d}{2}\log(2\pi e D^2/d^2) + \frac{d}{2}\log\det(\hat{\alpha}^{m,m}) \\ &+ 2^{d-1}\varphi\left[1 - \mathcal{F}\left(2\hat{\alpha}\right)\right] . \end{aligned} \tag{4.90}$$

We now see that $s_{liq} = 1 - \log\rho - 2^{d-1}\varphi$. Moreover, if we compare this with the finite d results obtained in the small cage expansion [145], we have that the interaction term is renormalized by the contact value of the liquid correlation $y_{liq}(\varphi)$. It follows that the entropy can be assumed to be

$$\begin{aligned} s[\hat{\alpha}] =& s_{liq}(\varphi) + d\log m + \frac{(m-1)d}{2}\log(2\pi e D^2/d^2) + \frac{d}{2}\log\det(\hat{\alpha}^{m,m}) \\ &+ 2^{d-1}\varphi y_{liq}(\varphi)\left[1 - \mathcal{F}\left(2\hat{\alpha}\right)\right] . \end{aligned} \tag{4.91}$$

In the 1RSB ansatz we have

$$\begin{aligned} s[\widehat{A}] =& s_{liq}(\varphi) + \frac{d}{2}\log m + \frac{(m-1)d}{2} + \frac{(m-1)d}{2}\log\left(\frac{2\pi D^2\widehat{A}}{d^2}\right) \\ &+ 2^{d-1}\varphi y_{liq}(\varphi)\,\mathcal{G}_m(\widehat{A}) \ , \\ \mathcal{F}_m(\widehat{A}) =& \frac{d}{2^d\varphi y_{liq}(\varphi)} \ , \\ \lambda_R =& -4 - 2\frac{2^d\varphi y_{liq}(\varphi)}{d}\,\Lambda_m(\widehat{A}) \end{aligned} \tag{4.92}$$

that are the same equations of the small cage expansion of Ref. [145] at the leading order in $\widehat{A}$.

If we express the equation for the stability of the 1RSB solution (namely $\lambda_R = 0$) in terms of $\widehat{A}$ and m we see that it is the same as in the limit $d \to \infty$, Eq. (4.66). This means that the result for $\widehat{A}_G(m)$ is valid in any dimension.

A consistency check is that even in $d = 3$ the Gardner transition appears only at very large pressure, so that the approximation m and $\widehat{A}$ is valid. In this way we can use the asymptotic expansions to obtain quantitative results. The procedure is the following:

- For $m \to 0$ we know that $\sqrt{\widehat{A}_G} \approx 0.8m$.

d	φ_G	φ_{GCP}	p_G
3	0.683581	0.683657	26727
4	0.486755	0.486874	16374
5	0.330586	0.330718	12535
6	0.218074	0.218203	10119
7	0.140074	0.140189	8469
8	0.0876190	0.0877137	7407
9	0.0534490	0.0535198	6805
10	0.0318889	0.0319377	6550
11	0.0186760	0.0187075	6548
12	0.0107756	0.0107949	6724
13	0.00614419	0.00615559	7019

Table 4.1. Values of φ_{GCP} [145] and of φ_G and p_G for several dimensions. Note that these values correspond to the *equilibrium* Gardner transition. For out-of-equilibrium states (which are the one produced in all experiments and numerical simulations), we expect that the Gardner instability will happen at lower, possibly much lower, pressures and densities.

- Then we obtain $\varphi_G(m)$ (or better $m_G(\varphi)$) by solving

$$\begin{aligned} &\frac{d}{2^d \varphi y_{liq}(\varphi)} = \mathcal{F}_m(\widehat{A}) \sim \frac{G_1(m)}{1-m}\frac{\sqrt{\widehat{A}_G}}{2} \approx \sqrt{\frac{\pi}{m}}\, 0.4m \approx 0.71\sqrt{m} \\ &\Rightarrow \quad m_G \approx \left(\frac{d}{0.71 \times 2^d \varphi y_{liq}(\varphi)}\right)^2 . \end{aligned} \tag{4.93}$$

- Moreover a result of Ref. [145] is that

$$\begin{aligned} &m^* \sim \mu\,(\varphi_{GCP} - \varphi)\ , \\ &\mu = \frac{1}{d}\left[2^{d-1} y_{liq}(\varphi) - d\frac{y'_{liq}(\varphi)}{y_{liq}(\varphi)} + \frac{1-d}{\varphi}\right]_{\varphi=\varphi_{GCP}} . \end{aligned} \tag{4.94}$$

- The Gardner transition happens when the equilibrium line and the instability line cross that means that φ_G is the solution of $m_G(\varphi) = m^*(\varphi)$. The crossing point can be found numerically once an equation of state for the liquid has been chosen. We use the Carnahan-Starling equation that has been already employed in Ref. [145].

- Finally we can use the result [145]

$$p(\varphi_G) \sim \frac{d\,\varphi_{GCP}}{\varphi_{GCP} - \varphi} \tag{4.95}$$

  to compute the Gardner pressure $p_G = p(\varphi_G)$.

We report the numerical results for the Gardner pressure in Tab. 4.1 for several dimensions. We observe that p_G is non monotonic and we don't have here an explanation for this even if it could also be only an artifact of the crude approximations

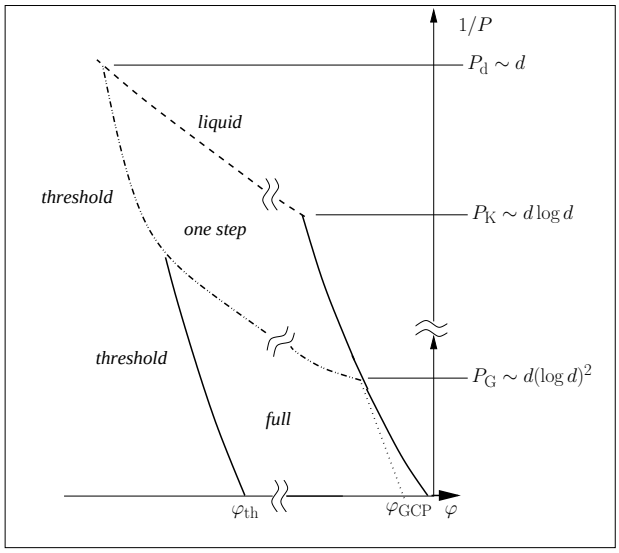

Figure 4.8. A sketch of the resulting phase diagram. Picture taken from [110].

used. Moreover we see that p_G is always much larger than the pressure at the glass transition (we have taken it from Ref. [145, 42]), and the value of p_G corresponds to the Gardner instability of the equilibrium ("ideal") glass that is always inaccessible to real experiments or simulations. *However we expect that a Gardner transition occurs also for all the metastable states that are between* $\widehat{\varphi}_d$ *and* $\widehat{\varphi}_K$. However this kind of phenomenon cannot be investigated with the equilibrium calculation that we have done now but it requires the use of "state following" techniques [182] . Let us now investigate the behavior of $\widehat{\varphi}_{GCP} - \widehat{\varphi}_G$ when $d \to \infty$. Because of the fact that $\widehat{\varphi}_{GCP} \sim \log d$ [145] and $y_{liq} \to 1$ we have that $\mu \sim 2^{d-1}/d$ and the equation for $\widehat{\varphi}_G$ becomes

$$\frac{1}{2}(\widehat{\varphi}_{GCP} - \widehat{\varphi}_G) = \left(\frac{1}{0.71 \times \widehat{\varphi}_G}\right)^2 \sim \left(\frac{1}{0.71 \times \widehat{\varphi}_{GCP}}\right)^2 \sim \left(\frac{1}{0.71 \times \log d}\right)^2 , \quad (4.96)$$

which shows that $\widehat{\varphi}_G$ and $\widehat{\varphi}_{GCP}$ shrinks as $(\log d)^{-2}$ and the Gardner pressure diverges as $p_G \sim d(\log d)^3$, as is sketched in Fig. 4.8. Let us underline that at this level of approximation, it can be easily shown that $\lambda_{\rm MCT}$ does not depend on dimension and the dimensional dependence of $\lambda_{\rm MCT}$ reported in Ref. [43] should be explained by corrections to this approximation that are not treated here.

4.8 Towards the fullRSB computation: general expression for the entropy

Let us consider again the general form of the replicated entropy

$$s[\hat{\alpha}] = 1 - \log \rho + d \log m + \frac{d}{2}(m-1)\log(2\pi e D^2/d^2) + \frac{d}{2}\log\det(\hat{\alpha}^{m,m}) - \frac{d}{2}\widehat{\varphi}\,\mathcal{F}\,(2\hat{\alpha}) \ . \quad (4.97)$$

Again, the matrix $\alpha_{ab} = d\,\langle u_a \cdot u_b \rangle / D^2$ is related to the fluctuations of the replica displacement vectors u_a. Let us define the mean square displacement between two

replicas

$$\Delta_{ab} = \frac{d}{D^2}\left\langle (u_a - u_b)^2 \right\rangle = \alpha_{aa} + \alpha_{bb} - 2\alpha_{ab}\,. \tag{4.98}$$

This encodes the physical content of the theory because it tells what is the size of the cage that particles feel and it is the most important quantity that will be studied in the following.

Let us now rewrite the interaction term in terms of the replica displacements. Using the same techniques of the precious sections we have

$$\mathcal{F}(\hat{v}) = \lim_{n\to 0} \sum_{n_1,\ldots,n_m:\sum_a n_a = n} \frac{n!}{n_1!\ldots n_m!} \exp\left[-\frac{1}{2}\sum_{a=1}^{m} v_{aa}\frac{n_a}{n} + \frac{1}{2}\sum_{a,b}^{m} v_{ab}\frac{n_a n_b}{n^2} \right] \tag{4.99}$$

where we have denoted with $\hat{v} = 2\hat{\alpha}$.

Suppose now that the matrix $\hat{v}$ has a diagonal that is proportional to the identity so that $v_{aa} = v_d$ for all a. This is true if we focus on matrices that have a hierarchical structure like the ones that enters in the kRSB calculations [132]. As a consequence we have that

$$v_{ab} = v_d - \Delta_{ab}\,. \tag{4.100}$$

so that the interaction term can be rewritten as

$$\begin{aligned}\mathcal{F}(\hat{\Delta}) &= \lim_{n\to 0} \sum_{n_1,\ldots,n_m:\sum_a n_a = n} \frac{n!}{n_1!\ldots n_m!} \exp\left[-\frac{v_d}{2} + \frac{1}{2}\sum_{a,b}^{m} (v_d - \Delta_{ab})\frac{n_a n_b}{n^2} \right] \\ &= \lim_{n\to 0} \sum_{n_1,\ldots,n_m:\sum_a n_a = n} \frac{n!}{n_1!\ldots n_m!} \exp\left[-\frac{1}{2}\sum_{a,b}^{m} \Delta_{ab}\frac{n_a n_b}{n^2} \right]\,.\end{aligned} \tag{4.101}$$

The matrix of the replica mean square displacements has a diagonal that must be zero. Therefore we define a modified matrix

$$\Delta^*_{ab} = \Delta_{ab} + \Lambda\delta_{ab} \tag{4.102}$$

in order to obtain a new expression for the interaction term that is given by

$$\mathcal{F}(\hat{\Delta}) = \lim_{n\to 0} \sum_{n_1,\ldots,n_m:\sum_a n_a = n} \frac{n!}{n_1!\ldots n_m!} \exp\left[-\frac{1}{2}\sum_{a,b}^{m} \Delta^*_{ab}\frac{n_a n_b}{n^2} + \frac{\Lambda}{2}\sum_{a=1}^{m}\frac{n_a^2}{n^2} \right]\,. \tag{4.103}$$

We assume that the parameter Λ is positive.

A central identity is the following

$$e^{-\frac{1}{2}\sum_{a,b}^{m}\Delta^*_{ab}\frac{n_a n_b}{n^2}} = e^{-\frac{1}{2}\sum_{a,b=1}^{m}\Delta^*_{ab}\frac{\partial^2}{\partial h_a \partial h_b}} e^{\sum_{a=1}^{m} h_a \frac{n_a}{n}}\Big|_{\{h_a=0\}}\,. \tag{4.104}$$

It allows to rewrite the interaction term in the following form

$$\begin{aligned}\mathcal{F}(\hat{\Delta}) &= \lim_{n\to 0} \sum_{n_1,\ldots,n_m:\sum_a n_a=n} \frac{n!}{n_1!\ldots n_m!} \exp\left[-\frac{1}{2}\sum_{a,b=1}^m \Delta^*_{ab}\frac{\partial^2}{\partial h_a \partial h_b}\right]\times \\ &\quad \times \exp\left[\frac{\Lambda}{2}\sum_{a=1}^m \frac{n_a^2}{n^2} + \sum_{a=1}^m h_a \frac{n_a}{n}\right]\Bigg|_{\{h_a=0\}} \\ &= \lim_{n\to 0} \sum_{n_1,\ldots,n_m:\sum_a n_a=n} \frac{n!}{n_1!\ldots n_m!} \exp\left[-\frac{1}{2}\sum_{a,b=1}^m \Delta^*_{ab}\frac{\partial^2}{\partial h_a \partial h_b}\right]\times \\ &\quad \times \int \left(\prod_{a=1}^m \mathcal{D}\lambda_a\right) \exp\left[-\sqrt{\Lambda}\sum_{a=1}^m \frac{n_a}{n}\lambda_a + \sum_{a=1}^m \frac{n_a}{n}h_a\right]\Bigg|_{\{h_a=0\}} \\ &= \exp\left[-\frac{1}{2}\sum_{a,b=1}^m \Delta^*_{ab}\frac{\partial^2}{\partial h_a \partial h_b}\right] \int \left(\prod_{a=1}^m \mathcal{D}\lambda_a\right) \exp\left[-\min_a\left(\sqrt{\Lambda}\lambda_a - h_a\right)\right]\Bigg|_{\{h_a=0\}}\end{aligned}, \tag{4.105}$$

where we have introduced Gaussian measures $\mathcal{D}\lambda_a$ with unit variance and zero mean.

Let us now think at the variables λ_a as random variables with a Gaussian probability density. This means that the variable $h = \min_a\left(\sqrt{\Lambda}\lambda_a - h_a\right)$ is a random variable whose probability density is given by

$$\mu_{\min}(h) = -\frac{d}{dh}\prod_{a=1}^m \int_{(h+h_a)/\sqrt{\Lambda}}^\infty \mathcal{D}\lambda_a = -\frac{d}{dh}\prod_{a=1}^m \Theta\left(-\frac{h+h_a}{\sqrt{2\Lambda}}\right)\ , \tag{4.106}$$

because the product of integrals is the probability that $\sqrt{\Lambda}\lambda_a - h_a \geq h,\ \forall a$, which is nothing but (one minus) the cumulative distribution of h. Again here $\Theta(z) = (1+\mathrm{erf}(z))/2$ and $\int_h^\infty \mathcal{D}\lambda = \Theta(-h/\sqrt{2})$. It follows that

$$\begin{aligned}&\int \left(\prod_{a=1}^m \mathcal{D}\lambda_a\right) \exp\left[-\min_a\left(\sqrt{\Lambda}\lambda_a - h_a\right)\right] = \int_{-\infty}^\infty \mathrm{d}h\, e^{-h}\, \mu_{\min}(h) \\ &= -\int_{-\infty}^\infty \mathrm{d}h\, e^{-h}\, \frac{d}{dh}\prod_{a=1}^m \Theta\left(-\frac{h+h_a}{\sqrt{2\Lambda}}\right)\end{aligned} \tag{4.107}$$

so that the final expression for the interaction term is given by

$$\begin{aligned}\mathcal{F}(\hat{\Delta}) &= -\exp\left[-\frac{1}{2}\sum_{a,b=1}^m \Delta^*_{ab}\frac{\partial^2}{\partial h_a \partial h_b}\right] \int_{-\infty}^\infty \mathrm{d}h\, e^{-h}\frac{d}{dh}\prod_{a=1}^m \Theta\left(-\frac{h+h_a}{\sqrt{2\Lambda}}\right)\Bigg|_{\{h_a=0\}} \\ &= -\int_{-\infty}^\infty \mathrm{d}h\, e^{-h}\frac{d}{dh}\left\{\exp\left[-\frac{1}{2}\sum_{a,b=1}^m \Delta^*_{ab}\frac{\partial^2}{\partial h_a \partial h_b}\right]\prod_{a=1}^m \Theta\left(-\frac{h_a}{\sqrt{2\Lambda}}\right)\right\}_{\{h_a=h\}} \\ &= \int_{-\infty}^\infty \mathrm{d}h\, e^{h}\frac{d}{dh}\left\{\exp\left[-\frac{1}{2}\sum_{a,b=1}^m \Delta^*_{ab}\frac{\partial^2}{\partial h_a \partial h_b}\right]\prod_{a=1}^m \Theta\left(\frac{h_a}{\sqrt{2\Lambda}}\right)\right\}_{\{h_a=h\}}\end{aligned}, \tag{4.108}$$

where in the last part of the sequence of equality we changed the sign to all the fields and to h.

Let us now define the notation $\gamma_a(z) = e^{-z^2/(2a)}/\sqrt{2\pi a}$; a simple relation that can be proved by expanding in a Taylor series all the exponential functions is

$$\exp\left[\frac{a}{2}\frac{\partial^2}{\partial h^2}\right] f(h) = \int_{-\infty}^{\infty} \frac{\mathrm{d}z}{\sqrt{2\pi a}} e^{-\frac{z^2}{2a}} f\left(h - z\right) = \gamma_a \star f(h) \ , \tag{4.109}$$

where $\gamma_a \star f$ is defined as the convolution between γ_a and f. A simple application of the above identity gives

$$\Theta(h/\sqrt{2a}) = \int_{-\infty}^{\infty} \frac{\mathrm{d}z}{\sqrt{2\pi a}} e^{-\frac{z^2}{2a}} \theta(h - z) = \exp\left[\frac{a}{2}\frac{\partial^2}{\partial h^2}\right] \theta(h) = \gamma_a \star \theta(h) \ . \tag{4.110}$$

By using this we obtain that

$$\begin{aligned} \mathcal{F}(\hat{\Delta}) &= \int_{-\infty}^{\infty} \mathrm{d}h \, e^h \frac{d}{dh} \left\{ \exp\left[-\frac{1}{2} \sum_{a,b=1}^{m} \Delta^*_{ab} \frac{\partial^2}{\partial h_a \partial h_b} \right] \prod_{a=1}^{m} e^{\frac{1}{2}\Lambda \frac{\partial^2}{\partial h_a^2}} \theta(h_a) \right\}_{\{h_a = h\}} \\ &= \int_{-\infty}^{\infty} \mathrm{d}h \, e^h \frac{d}{dh} \left\{ \exp\left[-\frac{1}{2} \sum_{a,b=1}^{m} \Delta_{ab} \frac{\partial^2}{\partial h_a \partial h_b} \right] \prod_{a=1}^{m} \theta(h_a) \right\}_{\{h_a = h\}} \ . \end{aligned} \tag{4.111}$$

Let us underline that the expression we have just derived is quite useful to investigate k-step replica symmetry breaking solution for any value of k and it has been derived under the only assumption that the diagonal elements of $\hat{v}$ are all equal.

4.9 The replicated entropy within the RSB construction

4.9.1 Parametrization of hierarchical matrices

In the section above we have seen how the expression for the replicated entropy can be written conveniently in terms of the matrix of the mean square displacements. Now we will do the calculation of the replicated entropy with the ansatz in which the matrix $\hat{\Delta}$ has a hierarchical parametrization [132]. To begin with, we will recall some generalities about hierarchical matrices that can be found in [132]. Even if the calculation is in spirit very similar to the kind of calculations that are carried on in spin glass physics being the role of $\hat{\Delta}$ played by the overlap matrix q_{ab}, here we remark that an important difference with respect to the spin glass case is that $\sum_b \alpha_{ab} = 0, \ \forall b$ while in spin glasses we do not have any constraint on the matrix elements except on the diagonal that is fixed to one.

The simplest hierarchical matrix is a 1RSB matrix [1] that has been studied in

[1] In the standard notation of [132] this would be called a replica-symmetric matrix, but remember that here we are using the Monasson's real replica scheme [133] where we consider m coupled replicas and treat m as a parameter to select different metastable states. It is a standard convention to denote a RS matrix in the Monasson's scheme as a "1RSB matrix": the reason is that in models with quenched disorder the two schemes are indeed equivalent.

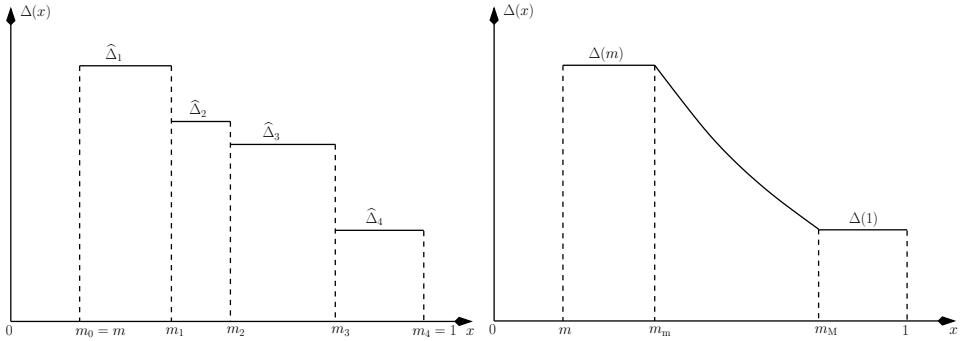

Figure 4.9. (Left) An example of the parametrization of the matrix Δ_{ab} for a 4RSB case. When needed for notational purposes, we use the convention $\widehat{\Delta}_0 \equiv 0$. (Right) The expected form of the function $\Delta(x)$ in the ∞RSB limit.

the sections above and corresponds to the parametrization $\alpha_{ab} = -\widehat{\alpha}_1,\ \forall a \neq b$

$$\alpha_{ab}^{\mathrm{1RSB}} = \widehat{\alpha}_1 \left(m\delta_{ab} - 1\right) \ . \tag{4.112}$$

The next step is to define a 2RSB matrix. The standard construction is that replicas are arranged in m/m_1 groups and the matrix element $\alpha_{ab} = -\widehat{\alpha}_2$ if replicas a and b are in the same group and $\alpha_{ab} = -\widehat{\alpha}_1$ if they are not. If we introduce the notation for which we say that $b \sim a$ when replica b is in the same group of replica a and $b \not\sim a$ if it is not and we define an indicator function $\mathrm{I(e)} = 1$ if the event e is true and $\mathrm{I(e)} = 0$ otherwise, then the parametrization of the 2RSB matrix can be written as follows

$$\alpha_{ab}^{\mathrm{2RSB}} = \delta_{ab}\left[(m_1 - 1)\widehat{\alpha}_2 + (m - m_1)\widehat{\alpha}_1\right] - (1 - \delta_{ab})\left[\widehat{\alpha}_2 \mathrm{I}(b \sim a) + \widehat{\alpha}_1 \mathrm{I}(b \not\sim a)\right] \ . \tag{4.113}$$

This contraction can be iterated at any level of replica symmetry breaking scheme. For example, at the 3RSB level, the groups of m_1 replicas are divided in m_1/m_2 subgroups of replicas, where each group contains m_2 replicas. Here we will not write explicitly the 3RSB parametrization for the overlap matrix $\hat{\alpha}$ even if it could be done using recursively the notation we have just introduced. An important remark is about the diagonal elements. From the construction we have given, it follows that the diagonal elements of the hierarchical matrices are all equal.

At any fixed level k of replica symmetry breaking, the corresponding hierarchical matrices form a closed algebra. Moreover, if we study the analytic continuation to $m < 1$, a generic hierarchical matrix $\hat{Q}$ can be parametrized by its diagonal element q_d and a single function $q(x)$ in the following way. We define $m_0 = m$ and $m_k = 1$; for integer values of $m > 1$ we have $m_k \equiv 1 < m_{k-1} < m_{k-2} < \cdots < m_1 < m_0 \equiv m$. When $m < 1$ then the correct prescription is to reverse the inequalities [132] so that $1 > m_{k-1} > m_{k-2} > \cdots > m_1 > m > 0$. The function $q(x)$ is defined as a piecewise constant function in $x \in [0, 1]$ which takes in the interval $x \in [m_{i-1}, m_i]$ the value of the elements q_i in the corresponding sub-block (with $i = 1 \cdots k$), and $q(x) = 0$ for $x \in [0, m_0]$. We write this parametrization as $\hat{Q} \leftrightarrow \{q_d, q(x)\}$. This means that in our case the matrices $\hat{\alpha}$ are parametrized with $\hat{\alpha} \leftrightarrow \{\alpha_d, -\alpha(x)\}$ where $\alpha(x)$ is a piecewise constant function given by the $\widehat{\alpha}_i$ in each block. The diagonal value for

the matrix elements is fixed by $\sum_b \alpha_{ab} = 0$ so that

$$\alpha_d = (m_{k-1} - 1)\widehat{\alpha}_k + (m_{k-2} - m_{k-1})\widehat{\alpha}_{k-1} + \ldots + (m - m_1)\widehat{\alpha}_1 = -\int_m^1 \mathrm{d}x\, \alpha(x) \ . \tag{4.114}$$

Having defined the matrix $\hat{\alpha}$, we can infer the expression for the matrix $\Delta_{ab} = 2\alpha_{aa} - 2\alpha_{ab}$ which is therefore parametrized by $\hat{\Delta} \leftrightarrow \{0, \Delta(x)\}$ where

$$\Delta(x) = 2\alpha_d + 2\alpha(x) = -2\int_m^1 \mathrm{d}y\, \alpha(y) + 2\alpha(x) \ . \tag{4.115}$$

If we integrate this relation we have $\int_m^1 \mathrm{d}x\, \alpha(x) = \frac{1}{2m}\int_m^1 \mathrm{d}x\, \Delta(x)$ so that

$$\alpha(x) = \frac{1}{2}\Delta(x) + \frac{1}{2m}\int_m^1 \mathrm{d}y\, \Delta(y) \ . \tag{4.116}$$

Note that within this parametrization the functions $\alpha(x)$ and $\Delta(x)$ are positive. Clearly this must be true for $\Delta(x)$ that has a direct physical interpretation and by using Eq. (4.116) we see that this must be true also for $\alpha(x)$. Let us note also that $\Delta(x)$ have to be a decreasing function of x in contrast to the spin glass case in which the overlap profile is an increasing function [132]. The reason for this is that larger values of x corresponds to inner blocks of the matrix Δ_{ab}, hence to replicas that are "closer" to each other in the usual interpretation, and therefore must have smaller value of Δ. In Fig. 4.9 we show an example of a possible profile for $\Delta(x)$.

Of course, this construction is valid for all values of the number of replica symmetry breakings k and in particular it is valid in the case in which such number goes to infinity. Practically, this means that the profile $\Delta(x)$ is no more a piecewise constant function but it acquires a continuous part. The scheme in which the number of breakings of the replica symmetry is infinite is called full replica symmetry breaking scheme. In spin glasses it has been shown and proved that this construction gives the correct free energy for the Sherrington-Kirkpatrick model [132] and it is deeply related to the hierarchical structure of states in which the Boltzmann measure splits when the spin glass transition point is crossed.

4.9.2 Hierarchical matrices: their algebra and the entropic term

General expression of the entropic term

We now focus on the computation of the entropic term. The problem is how to compute $\log\det\hat{\alpha}^{(m,m)}$ for a general hierarchical matrix. This can be solved using some known results on the algebra of hierarchical matrices that we are going to recall now. Let us consider a generic hierarchical matrix q_{ab} that is parametrized by its diagonal elements all equal to q_d and by the function $q(x)$. In our case the matrices we consider are $m \times m$ matrices $\hat{Q}_m$ and we take $m < 1$. In order to simplify the calculation we embed these matrices in $n \times n$ dimensional matrices $\hat{Q}_n$ with $n \to 0$ that are constructed by putting the matrix $\hat{Q}_m$ on the diagonal and by setting the outermost diagonal elements to zero. This means that $q(x)$ is defined in $x \in [0, 1]$ and $q(x) = 0$ for $x \in [0, m]$. Adopting this strategy we can use the results on the algebra of hierarchical matrices in the limit $n \to 0$ [126].

We introduce the notation

$$[q](x) = xq(x) - \int_0^x \mathrm{d}y\, q(y) \ , \qquad \langle q \rangle = \int_0^1 \mathrm{d}x\, q(x) \ , \tag{4.117}$$

so that we can recall one of the most important results for the determinant [126, Eq.(AII.11)]

$$\lim_{n\to 0} \frac{1}{n} \log\det \hat{Q}_n = \log(q_d - \langle q \rangle) + \frac{q(0)}{q_d - \langle q \rangle} - \int_0^1 \frac{\mathrm{d}y}{y^2} \log\left(\frac{q_d - \langle q \rangle - [q](y)}{q_d - \langle q \rangle} \right) \ , \tag{4.118}$$

and for the diagonal element of the inverse [126, Eq.(AII.7)]

$$q_d^{-1} = \frac{1}{q_d - \langle q \rangle} \left(1 - \int_0^1 \frac{\mathrm{d}y}{y^2} \frac{[q](y)}{q_d - \langle q \rangle - [q](y)} - \frac{q(0)}{q_d - \langle q \rangle} \right) \ . \tag{4.119}$$

In our case we have that the elements in the outermost blocks vanish so that $q(0) = 0$. Moreover $q(x) = [q](x) = 0$ for $x < m$ and finally $\det \hat{Q}_n = (\det \hat{Q}_m)^{n/m}$, hence $\log\det \hat{Q}_m = (m/n) \log\det \hat{Q}_n$, and the diagonal element of the inverse of $\hat{Q}_n$ and $\hat{Q}_m$ are identical. In this way, in the $m \times m$ space we have

$$\begin{aligned}
\log\det \hat{Q}_m &= m \log(q_d - \langle q \rangle) - m \int_m^1 \frac{\mathrm{d}y}{y^2} \log\left(\frac{q_d - \langle q \rangle - [q](y)}{q_d - \langle q \rangle} \right) \\
&= \log(q_d - \langle q \rangle) - m \int_m^1 \frac{\mathrm{d}y}{y^2} \log\left(q_d - \langle q \rangle - [q](y) \right) \ , \\
q_d^{-1} &= \frac{1}{q_d - \langle q \rangle} \left(1 - \int_m^1 \frac{\mathrm{d}y}{y^2} \frac{[q](y)}{q_d - \langle q \rangle - [q](y)} \right) \ , \\
[q](x) &= xq(x) - \int_m^x \mathrm{d}y\, q(y) \ , \\
\langle q \rangle &= \int_m^1 \mathrm{d}x\, q(x) \ .
\end{aligned} \tag{4.120}$$

We must now compute $\log\det \hat{\alpha}^{(m,m)}$. To do this, we introduce a matrix $\hat{\beta}$ which is "regularized" in such a way that $\sum_b \beta_{ab} = \varepsilon$, and $\hat{\alpha} = \lim_{\varepsilon\to 0} \hat{\beta}$. An example is

$$\hat{\beta} \leftrightarrow \{\beta_d, \beta(x)\} = \{\alpha_d, -\alpha(x) + \varepsilon\delta(x - x_0)\} \ , \tag{4.121}$$

for any $x_0 \in [m, 1]$. By construction, the matrix $\hat{\beta}$ is invertible so that we can use again $\det \hat{\beta}^{(m,m)} = (\hat{\beta}^{-1})_{mm} \det \hat{\beta}$. Then, using Eq. (4.120) we get

$$\begin{aligned}
&\log\det \hat{\alpha}^{(m,m)} = \lim_{\varepsilon\to 0} \left\{ \log\det \hat{\beta} + \log(\hat{\beta}^{-1})_{mm} \right\} = \lim_{\varepsilon\to 0} \left\{ \log\det \hat{\beta} + \log \beta_d^{-1} \right\} \\
&= \lim_{\varepsilon\to 0} \left\{ -m \int_m^1 \frac{\mathrm{d}y}{y^2} \log\left(\beta_d - \langle \beta \rangle - [\beta](y) \right) + \log\left(1 - \int_m^1 \frac{\mathrm{d}y}{y^2} \frac{[\beta](y)}{\beta_d - \langle \beta \rangle - [\beta](y)} \right) \right\} \ .
\end{aligned} \tag{4.122}$$

Let us underline that for $\varepsilon \to 0$ we have $\langle \beta \rangle = -\int_m^1 \alpha(x) = \alpha_d = \beta_d$. The singular terms cancel and we obtain a finite result

$$\begin{aligned}
\log\det \hat{\alpha}^{(m,m)} &= -m \int_m^1 \frac{\mathrm{d}y}{y^2} \log\left([\alpha](y) \right) + \log\left(1 + \int_m^1 \frac{\mathrm{d}y}{y^2} \right) \\
&= -\log m - m \int_m^1 \frac{\mathrm{d}y}{y^2} \log\left([\alpha](y) \right) \ .
\end{aligned} \tag{4.123}$$

We can rephrase the above expression in terms of $\Delta(x)$ by using Eq. (4.116). We have that

$$-m\int_m^1 \frac{\mathrm{d}y}{y^2}\log\left([\alpha](y)\right) = -(m-1)\log 2 - m\int_m^1 \frac{\mathrm{d}y}{y^2}\log\left[y\Delta(y)+\int_y^1 \mathrm{d}z\Delta(z)\right] , \tag{4.124}$$

so that

$$\log\det\hat{\alpha}^{(m,m)} = -\log m - (m-1)\log 2 - m\int_m^1 \frac{\mathrm{d}y}{y^2}\log\left[y\Delta(y)+\int_y^1 \mathrm{d}z\Delta(z)\right] . \tag{4.125}$$

This concludes the calculation of the entropic part of the replicated entropy. Let us underline that this expression is valid both in the fullRSB case and in the kRSB case for a finite value of k. This is because we can always obtain a finite kRSB result from a fullRSB result by choosing the function $\Delta(x)$ to be piecewise constant. To show how we can do this, let us see how it works in the 1RSB and 2RSB case.

1RSB and 2RSB results

When specialized to the 1RSB case Eq. (4.112), which corresponds to $\alpha(x) = \widehat{\alpha}_1$ and $\Delta(x) = \widehat{\Delta}_1 = 2m\widehat{\alpha}_1$, we get

$$\log\det\hat{\alpha}^{(m,m)}_{\mathrm{1RSB}} = -\log m + (m-1)\log(m\widehat{\alpha}_1) = -\log m + (m-1)\log(\widehat{\Delta}_1/2) , \tag{4.126}$$

which reproduces the results of the previous sections. The 2RSB solution is parametrized by a step function

$$\alpha(x) = \begin{cases} \widehat{\alpha}_1 & m \le x < m_1 \\ \widehat{\alpha}_2 & m_1 \le x \le 1 \end{cases} \qquad [\alpha](x) = \begin{cases} m\widehat{\alpha}_1 & m \le x < m_1 \\ m_1\widehat{\alpha}_2 + (m-m_1)\widehat{\alpha}_1 & m_1 \le x \le 1 \end{cases} \tag{4.127}$$

and therefore

$$\begin{aligned} \log\det\hat{\alpha}^{(m,m)}_{\mathrm{2RSB}} = &-\log m + \left(\frac{m}{m_1}-1\right)\log(m\widehat{\alpha}_1) \\ &+ \left(m-\frac{m}{m_1}\right)\log\left(m_1\widehat{\alpha}_2 + (m-m_1)\widehat{\alpha}_1\right) . \end{aligned} \tag{4.128}$$

Using the relations

$$\begin{aligned} \widehat{\Delta}_2 &= 2m_1\widehat{\alpha}_2 + 2\left(m-m_1\right)\widehat{\alpha}_1 , \\ \widehat{\Delta}_1 &= \widehat{\Delta}_2 + 2(\widehat{\alpha}_1 - \widehat{\alpha}_2) , \end{aligned} \tag{4.129}$$

or directly Eq. (4.125), we have

$$\begin{aligned} \log\det\hat{\alpha}^{(m,m)}_{\mathrm{2RSB}} = &-\log m - (m-1)\log 2 + \left(\frac{m}{m_1}-1\right)\log[m_1\widehat{\Delta}_1 + (1-m_1)\widehat{\Delta}_2] \\ &+ \left(m-\frac{m}{m_1}\right)\log\widehat{\Delta}_2 . \end{aligned} \tag{4.130}$$

kRSB result

Writing explicitly the kRSB expression requires the introduction of a function

$$G(x) = x\Delta(x) + \int_x^1 dz\Delta(z) \ . \tag{4.131}$$

In fact, if $\Delta(x)$ is a kRSB piecewise constant function, it is easy to check that $G(x)$ has the same structure, with

$$\widehat{G}_i = m_i\widehat{\Delta}_i + \sum_{j=i+1}^{k}(m_j - m_{j-1})\widehat{\Delta}_j \ . \tag{4.132}$$

Note that $\dot{G}(x) = x\dot{\Delta}(x)$, and $G(1) = \Delta(1)$, therefore from $G(x)$ one can reconstruct $\Delta(x)$ as

$$\Delta(x) = G(1) - \int_x^1 \mathrm{d}z\dot{G}(z)/z = \frac{G(x)}{x} - \int_x^1 \frac{\mathrm{d}z}{z^2}G(z) \ , \tag{4.133}$$

or for a kRSB function

$$\widehat{\Delta}_i = \frac{\widehat{G}_i}{m_i} + \sum_{j=i+1}^{k}\left(\frac{1}{m_j} - \frac{1}{m_{j-1}}\right)\widehat{G}_j \ . \tag{4.134}$$

Then, from Eq. (4.125), we have

$$\begin{aligned}\log\det\hat{\alpha}^{(m,m)} &= -\log m - m\int_m^1 \frac{\mathrm{d}y}{y^2}\log\left[G(y)/2\right] \\ &= -\log m + \sum_{i=1}^{k}\left(\frac{m}{m_i} - \frac{m}{m_{i-1}}\right)\log(\widehat{G}_i/2)\end{aligned} \tag{4.135}$$

From this result it is easy to check that we can reobtain the 1RSB and 2RSB expressions.

4.9.3 The computation of the interaction term

We now focus on the interaction term.

kRSB derivation

Let us start from Eq. 4.111. We need to compute

$$g(m,h) = \left\{\exp\left[-\frac{1}{2}\sum_{a,b=1}^{m}\Delta_{ab}\frac{\partial^2}{\partial h_a\partial h_b}\right]\prod_{a=1}^{m}\theta\left(h_a\right)\right\}_{\{h_a=h\}} \ . \tag{4.136}$$

The general trick here is to take the derivative with respect to the external fields in a hierarchic way [64]. We define the matrix $I_{ab}^{m_i}$, which has elements equal to 1 in blocks of size m_i around the diagonal, and zero otherwise. This means that this

matrix is parametrized by a function $I^{m_i}(x) = 1$ for $m_i \leq x \leq 1$ and zero otherwise. With the notation of Fig. 4.9, and noting that $I_{ab}^{m_k=1} = \delta_{ab}$ we can see that

$$\Delta_{ab} = \sum_{i=1}^{k} \widehat{\Delta}_i (I_{ab}^{m_{i-1}} - I_{ab}^{m_i}) = \sum_{i=0}^{k-1} (\widehat{\Delta}_{i+1} - \widehat{\Delta}_i) I_{ab}^{m_i} - \widehat{\Delta}_k \delta_{ab} \ . \tag{4.137}$$

Let us insert this expression in Eq. (4.136); we obtain a sequence of differential operators that act on the products of the theta functions. Each operator is the sum of partial derivatives inside a given block. It is easy to see that a sequence of operations of this kind can be written in a recursive way. Firstly, if we consider the term containing $\widehat{\Delta}_k$ we obtain, recalling Eq. (4.109):

$$g(1,h) = \exp\left[\frac{\widehat{\Delta}_k}{2}\frac{\partial^2}{\partial h^2}\right]\theta(h) = \gamma_{\widehat{\Delta}_k} \star \theta(h) = \Theta\left(\frac{h}{\sqrt{2\widehat{\Delta}_k}}\right) \ . \tag{4.138}$$

Then, the action of each of the terms $i = k-1, \cdots, 0$ can be seen as a recursion of the following form

$$g(m_i,h) = \exp\left[\frac{\widehat{\Delta}_i - \widehat{\Delta}_{i+1}}{2}\frac{\partial^2}{\partial h^2}\right] g(m_{i+1},h)^{\frac{m_i}{m_{i+1}}} = \gamma_{\widehat{\Delta}_i - \widehat{\Delta}_{i+1}} \star g(m_{i+1},h)^{\frac{m_i}{m_{i+1}}} \ . \tag{4.139}$$

The last iteration is given by

$$g(m,h) = \gamma_{-\widehat{\Delta}_1} \star g(m_1,h)^{\frac{m}{m_1}} \ . \tag{4.140}$$

This recursive procedure is an easy way to compute both $g(m,h)$ for any k, and, according to Eq. (4.111), the function $\mathcal{F}(\Delta)$. Let us make a remark about the last iteration. It can be seen that it could be problematic because of the fact that the Gaussian kernel γ_a has a negative parameter $a = -\widehat{\Delta}_1$ and therefore cannot be represented as in Eq. (4.109). However this is not a problem because with an integration by parts

$$\begin{aligned}\mathcal{F}(\Delta) &= \int_{-\infty}^{\infty} \mathrm{d}h\, e^h \frac{d}{dh} g(m,h) = \int_{-\infty}^{\infty} \mathrm{d}h\, e^h e^{-\frac{\widehat{\Delta}_1}{2}\frac{\partial^2}{\partial h^2}} \frac{d}{dh} g(m_1,h)^{\frac{m}{m_1}} \\ &= \int_{-\infty}^{\infty} \mathrm{d}h \left[e^{-\frac{\widehat{\Delta}_1}{2}\frac{\partial^2}{\partial h^2}} e^h\right] \frac{d}{dh} g(m_1,h)^{\frac{m}{m_1}} = e^{-\frac{\widehat{\Delta}_1}{2}} \int_{-\infty}^{\infty} \mathrm{d}h\, e^h \frac{d}{dh} g(m_1,h)^{\frac{m}{m_1}} \ ,\end{aligned} \tag{4.141}$$

and we have assumed that the boundary terms vanish because all the derivatives of the function $\frac{d}{dh} g(m_1,h)^{\frac{m}{m_1}}$ vanish for $h \to \infty$. This assumption is justified because $g(m_i,h)$ behaves similarly to a $\Theta(h)$ function for large h. This can be seen directly from the recursive equations (4.138) and (4.139). If we assume again that $1 - g(m_1,h)^{\frac{m}{m_1}}$ decays at $h \to -\infty$ faster than a simple exponential, we can assume again to be able to do another integration by parts so that we have

$$\mathcal{F}(\Delta) = e^{-\frac{\widehat{\Delta}_1}{2}} \int_{-\infty}^{\infty} \mathrm{d}h\, e^h \frac{d}{dh} g(m_1,h)^{\frac{m}{m_1}} = e^{-\frac{\widehat{\Delta}_1}{2}} \int_{-\infty}^{\infty} \mathrm{d}h\, e^h \left\{1 - g(m_1,h)^{\frac{m}{m_1}}\right\} \ . \tag{4.142}$$

1RSB and 2RSB approximations for the interaction term

Let us use the expressions that we have just derived to obtain the expression for the replicated entropy at finite level of RSB. At the 1RSB level, using Eq. (4.138), we have

$$\mathcal{F}_{\rm 1RSB}(\Delta) = e^{-\frac{\widehat{\Delta}_1}{2}} \int_{-\infty}^{\infty} {\rm d}h\, e^h \left\{ 1 - [\gamma_{\widehat{\Delta}_1} \star \theta(h)]^m \right\} \ , \tag{4.143}$$

at the 2RSB level

$$\begin{aligned} g(m_1,h)^{\frac{m}{m_1}} &= \left[\gamma_{\widehat{\Delta}_1 - \widehat{\Delta}_2} \star g(1,h)^{m_1} \right]^{\frac{m}{m_1}} = \left[\gamma_{\widehat{\Delta}_1 - \widehat{\Delta}_2} \star \left(\gamma_{\widehat{\Delta}_2} \star \theta(h) \right)^{m_1} \right]^{\frac{m}{m_1}} \ , \\ \mathcal{F}_{\rm 2RSB}(\Delta) &= e^{-\frac{\widehat{\Delta}_1}{2}} \int_{-\infty}^{\infty} {\rm d}h\, e^h \left\{ 1 - \left[\gamma_{\widehat{\Delta}_1 - \widehat{\Delta}_2} \star \left(\gamma_{\widehat{\Delta}_2} \star \theta(h) \right)^{m_1} \right]^{\frac{m}{m_1}} \right\} \ , \end{aligned} \tag{4.144}$$

and so on. At the 1RSB level, have reproduced the results of the previous sections.

The fullRSB limit

It is very easy to obtain the continuum limit for the equations we have derived. In fact in this case we can write $m_i = x - dx$, $m_{i+1} = x$, and $\widehat{\Delta}_i - \widehat{\Delta}_{i+1} = -\dot{\Delta}(x)dx$ where we have denoted with the dot the derivative with respect to x. This means that Eq. (4.139) becomes in the region where $\Delta(x)$ can be considered a continuous function

$$g(x - {\rm d}x, h) = \exp\left[-{\rm d}x \frac{\dot{\Delta}(x)}{2} \frac{\partial^2}{\partial h^2} \right] g(x,h)^{\frac{x-{\rm d}x}{x}} \tag{4.145}$$

and then, by expanding in powers of dx, we get the Parisi equation

$$\frac{\partial g(x,h)}{\partial x} = \frac{1}{2}\dot{\Delta}(x) \frac{\partial^2 g(x,h)}{\partial h^2} + \frac{1}{x} g(x,h) \log g(x,h) \tag{4.146}$$

that must be solved with the initial condition (4.138). An important remark is that this partial differential equation is well defined because $\dot{\Delta}(x) \leq 0$. The equation we just derived must be integrated from $x = 1$ to $x = m_1$. By doing this we obtain $g(m_1, h)$ that can be put inside Eq. (4.142) in order to get finally $\mathcal{F}(\Delta)$. If we introduce

$$f(x,h) = \frac{1}{x} \log g(x,h) \tag{4.147}$$

then we can rewrite the Parisi equation as

$$\frac{\partial f(x,h)}{\partial x} = \frac{1}{2}\dot{\Delta}(x) \left[\frac{\partial^2 f(x,h)}{\partial h^2} + x \left(\frac{\partial f(x,h)}{\partial h} \right)^2 \right] \tag{4.148}$$

that must be solved with initial condition

$$f(1,h) = \log \Theta \left[\frac{h}{\sqrt{2\Delta(1)}} \right] \ . \tag{4.149}$$

This result is remarkable. In fact we have obtained the same equations that solve the Sherrington-Kirkpatrick model [132, 64] which is at the basis of the spin-glass physics. The only difference with respect to this model is in the initial condition for the fullRSB equations.

4.9.4 Summary: 1RSB, 2RSB, kRSB and fullRSB results

Here we want to summarize the results just obtained. At any level of replica symmetry breaking we have

$$s = 1 - \log\rho + \frac{d}{2} m \log m + \frac{d}{2}(m-1)\log(\pi e D^2/d^2) + \frac{d}{2}\mathcal{S} \ , \tag{4.150}$$

where $\mathcal{S} = \log\det(\hat{\alpha}^{m,m}) - \widehat{\varphi}\,\mathcal{F}\,(2\hat{\alpha})$ contains the non-trivial dependence on $\hat{\alpha}$.

The 1RSB can be obtained by using Eqs. (4.126), (4.143) and (4.142)

$$\mathcal{S}_{\rm 1RSB} = (m-1)\log(\widehat{\Delta}_1/m) - \widehat{\varphi}\, e^{-\widehat{\Delta}_1/2} \int_{-\infty}^{\infty} {\rm d}h\, e^h \{1 - [\gamma_{\widehat{\Delta}_1} \star \theta(h)]^m\} \tag{4.151}$$

and this coincides with the results of the previous sections.

Using Eqs. (4.130), (4.144) and (4.142) we have at the 2RSB level,

$$\begin{aligned}\mathcal{S}_{\rm 2RSB} = &\left(\frac{m}{m_1} - 1\right)\log[(m_1\widehat{\Delta}_1 + (1-m_1)\widehat{\Delta}_2)/m] + \left(m - \frac{m}{m_1}\right)\log(\widehat{\Delta}_2/m) \\ &- \widehat{\varphi} e^{-\frac{\widehat{\Delta}_1}{2}} \int_{-\infty}^{\infty} {\rm d}h\, e^h \left[1 - \left[\gamma_{\widehat{\Delta}_1-\widehat{\Delta}_2} \star \left(\gamma_{\widehat{\Delta}_2} \star \theta(h)\right)^{m_1}\right]^{m/m_1}\right] .\end{aligned} \tag{4.152}$$

For any kRSB level, with k finite, by employing Eq. (4.135), (4.142), (4.138), (4.139), (4.140) we obtain:

$$\begin{aligned}\mathcal{S}_{\rm kRSB} &= \sum_{i=1}^{k}\left(\frac{m}{m_i} - \frac{m}{m_{i-1}}\right)\log(\widehat{G}_i/m) - \widehat{\varphi}\, e^{-\widehat{\Delta}_1/2}\int_{-\infty}^{\infty}{\rm d}h\, e^h \left\{1 - g(m_1,h)^{\frac{m}{m_1}}\right\} \ , \\ \widehat{G}_i &= m_i\widehat{\Delta}_i + \sum_{j=i+1}^{k}(m_j - m_{j-1})\widehat{\Delta}_j \ , \\ g(1,h) &= \gamma_{\widehat{\Delta}_k} \star \theta(h) \ , \\ g(m_i,h) &= \gamma_{\widehat{\Delta}_i - \widehat{\Delta}_{i+1}} \star g(m_{i+1},h)^{\frac{m_i}{m_{i+1}}} \ , \qquad i = 1\cdots k-1 \ .\end{aligned} \tag{4.153}$$

In the end we can summarize the fullRSB expression that can be obtained from Eqs. (4.125), (4.142), (4.147), (4.148), (4.149):

$$\begin{aligned}\mathcal{S}_{\infty\rm RSB} &= -m\int_m^1 \frac{{\rm d}y}{y^2}\log\left[\frac{y\Delta(y)}{m} + \int_y^1 {\rm d}z\frac{\Delta(z)}{m}\right] \\ &\quad - \widehat{\varphi}\, e^{-\Delta(m)/2}\int_{-\infty}^{\infty}{\rm d}h\, e^h[1 - e^{mf(m,h)}] \ , \\ \frac{\partial f(x,h)}{\partial x} &= \frac{1}{2}\dot{\Delta}(x)\left[\frac{\partial^2 f(x,h)}{\partial h^2} + x\left(\frac{\partial f(x,h)}{\partial h}\right)^2\right] \ , \\ f(1,h) &= \log\Theta\left[\frac{h}{\sqrt{2\Delta(1)}}\right] .\end{aligned} \tag{4.154}$$

4.10 Variational equations

In the previous sections we have obtained the expression of the replicated entropy for any desired replica symmetry scheme. The replicated entropy is in this way a function of the function $\Delta(x)$. We must now optimize over this function in order to obtain the saddle point value for the entropy. This is a very complicated task to do but we will solve the problem in two ways.

4.10.1 Derivation from the kRSB solution

We start from the kRSB expression for the replicated entropy at fixed and finite k. Let us take Eq. (4.136) and (4.142). Without taking into account that the matrix Δ_{ab} is symmetric and for $a \neq b$, we can write

$$\begin{aligned}\frac{dg(m,h)}{d\Delta_{ab}} &= \left\{ \exp\left[-\frac{1}{2}\sum_{c,d=1}^{m} \Delta_{cd} \frac{\partial^2}{\partial h_c \partial h_d} \right] \left(-\frac{1}{2}\frac{\partial^2}{\partial h_a \partial h_b} \right) \prod_{f=1}^{m} \theta\left(h_f\right) \right\}_{\{h_a=h\}} \\ &= -\frac{1}{2} \left\{ \exp\left[-\frac{1}{2}\sum_{c,d=1}^{m} \Delta_{cd} \frac{\partial^2}{\partial h_c \partial h_d} \right] \delta(h_a)\delta(h_b) \prod_{f\neq a,b}^{1,m} \theta(h_f) \right\}_{\{h_a=h\}}\end{aligned} \tag{4.155}$$

Note that there are $m(m_{\ell-1} - m_\ell)$ elements in the block $\ell = 1 \cdots k$ and they all give the same contribution, therefore

$$\begin{aligned}\frac{dg(m,h)}{d\widehat{\Delta}_\ell} = &-\frac{m(m_{\ell-1}-m_\ell)}{2} \times \\ &\times \left\{ \exp\left[-\frac{1}{2}\sum_{c,d=1}^{m} \Delta_{cd} \frac{\partial^2}{\partial h_c \partial h_d} \right] \delta(h_a)\delta(h_b) \prod_{f\neq a,b}^{1,m} \theta(h_f) \right\}_{\{h_a=h\}} .\end{aligned} \tag{4.156}$$

We will use again the recursive approach of [64]. The main difference here is that at the beginning of the recursion, there are two special blocks that contains a delta instead of a theta function. After some iterations of the recursive procedure the two special blocks are merged. If the two replicas ab are in the ℓ-th block, then we have

$$\begin{aligned} N_\ell(1,h) &= \gamma_{\widehat{\Delta}_k} \star \delta(h) = \frac{e^{-h^2/(2\widehat{\Delta}_k)}}{\sqrt{2\pi\widehat{\Delta}_k}} \\ N_\ell(m_i,h) &= \gamma_{\widehat{\Delta}_i - \widehat{\Delta}_{i+1}} \star \left[N_\ell(m_{i+1},h) g(m_{i+1},h)^{m_i/m_{i+1}-1} \right] \qquad i = k-1, \cdots, \ell \\ N_\ell(m_{\ell-1},h) &= \gamma_{\widehat{\Delta}_{\ell-1} - \widehat{\Delta}_\ell} \star \left[N_\ell(m_\ell,h)^2 g(m_\ell,h)^{m_{\ell-1}/m_\ell-2} \right] \\ N_\ell(m_i,h) &= \gamma_{\widehat{\Delta}_i - \widehat{\Delta}_{i+1}} \star \left[N_\ell(m_{i+1},h) g(m_{i+1},h)^{m_i/m_{i+1}-1} \right] \qquad i = \ell-2, \cdots, 0 \\ \frac{dg(m,h)}{d\widehat{\Delta}_\ell} &= -\frac{m(m_{\ell-1}-m_\ell)}{2} N_\ell(m,h) . \end{aligned} \tag{4.157}$$

These equations are valid for all $\ell = k, \cdots, 1$. We define now

$$f(m_i, h) = \frac{1}{m_i} \log g(m_i, h) \ . \tag{4.158}$$

For $i > \ell$, namely just before the two special blocks are merged, we have

$$g'(m_i, h) = m_i N_\ell(m_i, h) \qquad \Leftrightarrow \qquad f'(m_i, h) = N_\ell(m_i, h)/g(m_i, h) \ . \tag{4.159}$$

where the primes are the derivative with respect to h. This gives a great simplification because we do not need N_ℓ for $i \geq \ell$ anymore.

Eqs. (4.157) can be rewritten as

$$\begin{aligned} N_\ell(m_{\ell-1}, h) &= \gamma_{\widehat{\Delta}_{\ell-1} - \widehat{\Delta}_\ell} \star [f'(m_\ell, h)^2 g(m_\ell, h)^{m_{\ell-1}/m_\ell}] \\ N_\ell(m_i, h) &= \gamma_{\widehat{\Delta}_i - \widehat{\Delta}_{i+1}} \star [N_\ell(m_{i+1}, h) g(m_{i+1}, h)^{m_i/m_{i+1}-1}] \qquad i = \ell - 2, \cdots, 0 \\ \frac{dg(m,h)}{d\widehat{\Delta}_\ell} &= -\frac{m(m_{\ell-1} - m_\ell)}{2} N_\ell(m, h) \end{aligned} \tag{4.160}$$

Let us define now the operators Γ_ℓ

$$\begin{aligned} \Gamma_1 \star t(h) &= g(m_1, h)^{\frac{m}{m_1}} t(h) \ , \\ \Gamma_i \star t(h) &= \Gamma_{i-1} \star \left[\frac{1}{g(m_{i-1}, h)} \gamma_{\widehat{\Delta}_{i-1} - \widehat{\Delta}_i} \star g(m_i, h)^{\frac{m_{i-1}}{m_i}} t(h) \right] \qquad i = 2, \cdots, k \ . \end{aligned} \tag{4.161}$$

where $t(h)$ is only a test function. We have

$$N_\ell(m, h) = \gamma_{-\widehat{\Delta}_1} \star \Gamma_\ell \star f'(m_\ell, h)^2 \ . \tag{4.162}$$

The replicated entropy can be rewritten in the following form

$$\mathcal{S}_{\text{kRSB}} = \sum_{i=1}^{k} \left(\frac{m}{m_i} - \frac{m}{m_{i-1}} \right) \log(\widehat{G}_i/m) - \widehat{\varphi} \int_{-\infty}^{\infty} \mathrm{d}h \, e^h \frac{d}{dh} g(m, h) \ . \tag{4.163}$$

The next step is to compute the derivative with respect to $\widehat{G}_i$. This can be done if we use Eq. (4.134)

$$\begin{aligned} &\left(\frac{1}{m_i} - \frac{1}{m_{i-1}} \right) \frac{m}{\widehat{G}_i} = \widehat{\varphi} \int_{-\infty}^{\infty} \mathrm{d}h \, e^h \frac{d}{dh} \sum_{j=1}^{k} \frac{dg(m,h)}{d\widehat{\Delta}_j} \frac{d\widehat{\Delta}_j}{d\widehat{G}_i} \\ &= \widehat{\varphi} \int_{-\infty}^{\infty} \mathrm{d}h \, e^h \frac{d}{dh} \left\{ \frac{1}{m_i} \frac{dg(m,h)}{d\widehat{\Delta}_i} + \sum_{j=1}^{i-1} \frac{dg(m,h)}{d\widehat{\Delta}_j} \left(\frac{1}{m_i} - \frac{1}{m_{i-1}} \right) \right\} \\ &= \frac{m\widehat{\varphi}}{2} \int_{-\infty}^{\infty} \mathrm{d}h \, e^h \frac{d}{dh} \left\{ \frac{1}{m_i} (m_i - m_{i-1}) N_i(m, h) \right. \\ &\left. + \sum_{j=1}^{i-1} (m_j - m_{j-1}) N_j(m, h) \left(\frac{1}{m_i} - \frac{1}{m_{i-1}} \right) \right\} \ . \end{aligned} \tag{4.164}$$

A simple observation shows that from Eq. (4.157) we can see that $N_i(m,h)$ behaves like a Gaussian for $h \to \pm\infty$ and we can integrate by parts. The last expression becomes

$$\begin{aligned}
\frac{1}{\widehat{G}_i} &= -\frac{\widehat{\varphi}}{2}\int_{-\infty}^{\infty} \mathrm{d}h\, e^h \frac{d}{dh}\left\{ m_{i-1}N_i(m,h) - \sum_{j=1}^{i-1}(m_j - m_{j-1})N_j(m,h)\right\} \\
&= -\frac{\widehat{\varphi}}{2}\int_{-\infty}^{\infty} \mathrm{d}h\, e^h \gamma_{-\widehat{\Delta}_1} \star \frac{d}{dh}\left\{ m_{i-1}\Gamma_i \star f'(m_i,h)^2 - \sum_{j=1}^{i-1}(m_j - m_{j-1})\Gamma_j \star f'(m_j,h)^2\right\} \\
&= -\frac{\widehat{\varphi}}{2}e^{-\widehat{\Delta}_1/2}\int_{-\infty}^{\infty} \mathrm{d}h\, e^h \frac{d}{dh}\left\{ m_{i-1}\Gamma_i \star f'(m_i,h)^2 - \sum_{j=1}^{i-1}(m_j - m_{j-1})\Gamma_j \star f'(m_j,h)^2\right\} \\
&= \frac{\widehat{\varphi}}{2}e^{-\widehat{\Delta}_1/2}\int_{-\infty}^{\infty} \mathrm{d}h\, e^h \left\{ m_{i-1}\Gamma_i \star f'(m_i,h)^2 - \sum_{j=1}^{i-1}(m_j - m_{j-1})\Gamma_j \star f'(m_j,h)^2\right\} ,
\end{aligned} \tag{4.165}$$

where we have used the same trick as in Eq. (4.141). Finally we obtain

$$\int_{-\infty}^{\infty} \mathrm{d}h\, e^h\, \Gamma_i \star f'(m_i,h)^2 = \int_{-\infty}^{\infty} \mathrm{d}h P(m_i,h) f'(m_i,h)^2 , \tag{4.166}$$

provided that the function $P(m_i,h)$ satisfies the equations:

$$P(m_1,h) = e^h\, g(m_1,h)^{\frac{m}{m_1}} , \tag{4.167}$$

$$P(m_i,h) = \int dz \frac{P(m_{i-1},z)}{g(m_{i-1},z)} \gamma_{\widehat{\Delta}_{i-1}-\widehat{\Delta}_i}(h-z) g(m_i,h)^{\frac{m_{i-1}}{m_i}} \tag{4.168}$$

$$i = 2, \cdots, k . \tag{4.169}$$

The final result is

$$\begin{aligned}
\frac{1}{\widehat{G}_i} = \frac{\widehat{\varphi}}{2}e^{-\widehat{\Delta}_1/2}\int_{-\infty}^{\infty} \mathrm{d}h\, \Big[& m_{i-1}P(m_i,h)f'(m_i,h)^2 \\
& - \sum_{j=1}^{i-1}(m_j - m_{j-1})P(m_j,h)f'(m_j,h)^2\Big] .
\end{aligned} \tag{4.170}$$

Let us now summarize what we have obtained. Eqs. (4.170), (4.167)-(4.168), (4.138)-(4.139), (4.134) are a complete set of equations for $\widehat{G}_i$, or equivalently for $\widehat{\Delta}_i$ and it can be solved in an iterative scheme. A simple procedure to solve it is as follows. We start from a guess for $\widehat{\Delta}_i$; then we can first solve the recurrence (4.138)-(4.139) and then the recurrence (4.167)-(4.168). By using Eq. (4.170), this gives us a new $\widehat{G}_i$ that can be translated into the new values for $\widehat{\Delta}_i$ using Eq. (4.134). This gives a new starting point for the iteration. This protocol gives us a numerical route to solve the saddle point equations for any kRSB ansatz with k finite. In the next section we want to see that we can obtain a set of saddle point equations directly working in the fullRSB scheme. The two sets of variational equation are shown to coincide in the continuum limit.

4.10.2 Derivation from the full RSB solution

The variational equations can be obtained directly without going through the finite kRSB equations of the section above. The way we can do this is by introducing Lagrange multipliers that can enforce the Parisi equation [159]. Once we have obtained the new variational equations we will show that they are the same as those computed in the section above when the continuum limit is taken.

Adding Lagrange multipliers

The first step is to introduce Lagrange multipliers. This is forced by the fact that the replicated entropy is written in terms of the function $g(x,h)$ or, equivalently, of the function $f(x,h)$, that must satisfy the Parisi equation (4.148). We can introduce two Lagrange multipliers: the first one, $P(x,h)$ is the one needed to enforce the Parisi equation while the second one, $P(1,h)$ is the one needed to enforce its initial condition. We go back to the fullRSB expression for the replicated entropy given in Eq. (4.154) (we neglect constant terms that do not play any role for the saddle point) and we add to it the two Lagrange multipliers. We always indicate with a prime the derivative with respect to h and with a dot the derivative with respect to x. Using Eqs. (4.133), (4.131) with $\Delta(m) = \frac{G(m)}{m} - \int_m^1 \frac{\mathrm{d}z}{z^2} G(z)$, we have to impose stationarity of the function

$$\begin{aligned}
\mathcal{S}_{\infty\mathrm{RSB}} &= -m \int_m^1 \frac{\mathrm{d}x}{x^2} \log[G(x)/m] - \widehat{\varphi}\, e^{-\frac{\Delta(m)}{2}} \int_{-\infty}^{\infty} \mathrm{d}h\, e^h [1 - e^{mf(m,h)}] \\
&+ m\widehat{\varphi}\, e^{-\frac{\Delta(m)}{2}} \int_{-\infty}^{\infty} \mathrm{d}h \int_m^1 \mathrm{d}x\, P(x,h) \left\{ \dot{f}(x,h) - \frac{1}{2} \frac{\dot{G}(x)}{x} \left[f''(x,h) + x f'(x,h)^2 \right] \right\} \\
&- m\widehat{\varphi}\, e^{-\frac{\Delta(m)}{2}} \int_{-\infty}^{\infty} \mathrm{d}h\, P(1,h) \left\{ f(1,h) - \log \Theta\left(\frac{h}{\sqrt{2G(1)}} \right) \right\}
\end{aligned} \tag{4.171}$$

over $\Delta(x)$, $f(x,h)$, $P(x,h)$, $f(m,h)$ and $P(1,h)$. The first two saddle point equations can be obtained by taking the variation with respect to $P(x,h)$ and $f(x,h)$

$$\dot{f}(x,h) = \frac{1}{2} \frac{\dot{G}(x)}{x} \left[f''(x,h) + x f'(x,h)^2 \right] , \tag{4.172}$$

$$\dot{P}(x,h) = -\frac{1}{2} \frac{\dot{G}(x)}{x} \left[P''(x,h) - 2x (P(x,h) f'(x,h))' \right] . \tag{4.173}$$

By varying with respect $P(1,h)$ and $f(m,h)$ we obtain

$$f(1,h) = \log \Theta\left(\frac{h}{\sqrt{2G(1)}} \right) , \tag{4.174}$$

$$P(m,h) = e^{mf(m,h)+h} . \tag{4.175}$$

Finally, optimizing over $G(x)$ (for $x \neq 1$ and $x \neq m$) we obtain

$$\begin{aligned}\frac{m}{G(x)} &= -\frac{m\widehat{\varphi}}{2}e^{-\frac{\Delta(m)}{2}}\int_{-\infty}^{\infty}\mathrm{d}hP(x,h)f''(x,h) - \frac{\widehat{\varphi}}{2}e^{-\frac{\Delta(m)}{2}}\int_{-\infty}^{\infty}\mathrm{d}h\,e^h[1-e^{mf(m,h)}] \\ &= -\frac{m\widehat{\varphi}}{2}e^{-\frac{\Delta(m)}{2}}\int_{-\infty}^{\infty}\mathrm{d}hP(x,h)f''(x,h) - \frac{\widehat{\varphi}}{2}e^{-\frac{\Delta(m)}{2}}\int_{-\infty}^{\infty}\mathrm{d}h\,e^h e^{mf(m,h)}mf'(m,h) \\ &= -\frac{m\widehat{\varphi}}{2}e^{-\frac{\Delta(m)}{2}}\left\{\int_{-\infty}^{\infty}\mathrm{d}hP(x,h)f''(x,h) + \int_{-\infty}^{\infty}\mathrm{d}h\,P(m,h)f'(m,h)\right\}\,,\end{aligned}$$

that can be rewritten as

$$\frac{1}{G(x)} = -\frac{\widehat{\varphi}}{2}e^{-\frac{\Delta(m)}{2}}\int_{-\infty}^{\infty}\mathrm{d}h[P(x,h)f''(x,h) + P(m,h)f'(m,h)]\,. \tag{4.176}$$

Eqs. (4.172)-(4.176) can be in principle solved according to the following numerical protocol:

- start with a guess for the function $G(x)$;
- solve Eq. (4.172) with boundary condition (4.174) to obtain $f(x,h)$;
- solve Eq. (4.173) with boundary condition (4.175) to get $P(x,h)$;
- obtain a new $G(x)$ from Eq. (4.176)

The fullRSB limit of the kRSB variational equations

To show that the equations we have just obtained coincide with the ones we have derived for finite kRSB we need to take the continuum limit of the latter. To do this we will follow the same lines of section 4.9.3. It has been already shown that in this limit the recurrence equations for $g(x,h)$, Eqs. (4.138) and (4.139), become the Parisi equation (4.172) with boundary condition (4.174). Moreover, the boundary condition for $P(x,h)$ in the discrete, Eq. (4.167), is clearly equivalent to the one in the continuum, Eq. (4.175). It is very simple, following again the lines of section 4.9.3, to show that Eq. (4.168) becomes Eq. (4.173) when the continuum limit is taken. The only point that must be proved is to derive Eq. (4.176).

Let us start from Eq. (4.170) . In the continuum it becomes

$$\frac{1}{G(x)} = \frac{\widehat{\varphi}}{2}e^{-\frac{\Delta(m)}{2}}\int_{-\infty}^{\infty}\mathrm{d}h\left\{xP(x,h)f'(x,h)^2 - \int_m^x dzP(z,h)f'(z,h)^2\right\}\,. \tag{4.177}$$

We will show now that Eq. (4.176) and Eq. (4.177) are indeed the same. This is equivalent to prove that

$$\begin{aligned}\int_{-\infty}^{\infty}\mathrm{d}h[P(x,h)f''(x,h) + P(m,h)f'(m,h)] = -\int_{-\infty}^{\infty}\mathrm{d}h\,\Big\{xP(x,h)f'(x,h)^2 \\ -\int_m^x dzP(z,h)f'(z,h)^2\Big\}\,.\end{aligned} \tag{4.178}$$

The proof of the equality (4.178) is given with the following strategy. We first prove that the equality is true at $x = m$. Then we prove that the first derivative

with respect to x of the two sides of the equality are the same. Let us define also the following notation. We say that $a(x,h) \sim b(x,h)$ if $\int_{-\infty}^{\infty} \mathrm{d}h a(x,h) = \int_{-\infty}^{\infty} \mathrm{d}h b(x,h)$ If we integrate by parts and if we note that from the initial condition (4.175) it follows that $P'(m,h) = [1 + mf'(m,h)]P(m,h)$, we obtain

$$\begin{aligned} P(m,h)f''(m,h) + P(m,h)f'(m,h) &\sim f'(m,h)[P(m,h) - P'(m,h)] \\ &\sim -mP(m,h)f'(m,h)^2 \end{aligned} \tag{4.179}$$

that shows that Eq. (4.178) is true at $x = m$. Let us compute now the derivative with respect to x of the arguments of the integrals in Eq. (4.178). Using Eqs. (4.172) and (4.173), we have that

$$\dot{P}f''+P\dot{f}'' \sim \dot{P}f''+P''\dot{f} \sim \frac{1}{2}\frac{\dot{G}}{x}\left[\left(2x(Pf')' - P''\right)f'' + P''\left(f'' + xf'^2\right)\right] \sim \dot{G}P(f'')^2 \,, \tag{4.180}$$

and

$$x\dot{P}f'^2 + 2xPf'\dot{f}' \sim \frac{1}{2}\dot{G}\left[\left(2x(Pf')' - P''\right)f'^2 + 2Pf'\left(f''' + 2xf'f''\right)\right] \sim -\dot{G}P(f'')^2 \,. \tag{4.181}$$

This proves that the derivatives of the two sides of Eq. (4.178) with respect to x coincide and therefore completes the proof of Eq. (4.178), and of the equivalence of Eq. (4.176) and Eq. (4.177). We have therefore derived the set of fullRSB equations Eqs. (4.172)-(4.176) in two independent way.

4.11 Perturbative 2RSB solution around the Gardner line

4.11.1 Development around the 1RSB solution

In the previous sections we have been able to derive the expression for the entropy for any replica symmetry breaking scheme. Here we want to address the following problem. In the $(m, \widehat{\varphi})$ plane, we know that the 1RSB solution is unstable along the instability line that we computed before. However we can think that further replica symmetry breaking schemes (and we think that the fullRSB scheme will be the correct one) can cure the instability. Moreover we know that in the unstable region but very close to the instability line, the replicon is close to zero. In this situation we can think that we can produce a 2RSB solution perturbatively around the 1RSB one when we are very close to the instability line.

To do this let us take the 2RSB entropy. We compute it for a hierarchical matrix of the form

$$\alpha_{ab} = \alpha_{ab}^{1RSB} + \delta q_{ab} \tag{4.182}$$

where

$$\delta q_{ab} = \delta\alpha_0(1-\delta_{ab})\left(\frac{m-m_1}{1-m_1}\mathrm{I}(a \prec b) + \mathrm{I}(a \not\prec b)\right) \tag{4.183}$$

The matrix δq_{ab} is a matrix that is in the replicon subspace [169] namely it is in the eigenspace corresponding to the replicon eigenvalue. Temesvari, Pimentel and De Dominicis [169] have shown that the cubic terms of the expansion of the 2RSB

entropy around the 1RSB solution are eight but if the perturbation matrix δq is in the replicon subspace, only the two terms proportional to w_1 and w_2 survive. This means that we have

$$\begin{aligned} S[\hat{\alpha}_{1RSB}+\hat{\delta q}] &= S[\alpha_{1RSB}]+\frac{1}{2}\lambda_R(m)\sum_{a\neq b}\delta q_{ab}^2+\frac{1}{6}\left[w_1(m)\mathrm{Tr}\delta q^3+w_2(m)\sum_{a\neq b}\delta q_{ab}^3\right] \\ &= S[\alpha_{1RSB}]+\frac{1}{2}\hat{\lambda}_R(m,m_1)\delta\alpha_0^2+\frac{1}{6}W[w_1(m),w_2(m),m,m_1]\delta\alpha_0^3\,. \end{aligned} \tag{4.184}$$

where $\lambda_R(m)$ is the replicon eigenvalue. Every coefficient in the above expression depends also on the density $\widehat{\varphi}$ but we have not indicated this dependance.

The relation between the replicon eigenvalue $\lambda_R(m)$ and $\hat{\lambda}_R(m,m_1)$ is given by

$$\hat{\lambda}_R(m,m1)=\frac{m(1-m)(m-m_1)}{1-m_1}\lambda_R(m)\,. \tag{4.185}$$

We want to exploit now the relation between W and w_1 and w_2. Note that $w_1(m)$ and $w_2(m)$ depend only on m and not on m_1 as a consequence of the fact that the starting point of the expansion is a completely replica symmetric solution that does not depend on m_1. To write the cubic terms in terms of $\delta\alpha_0$ let us define the matrix

$$\begin{aligned} r_{ab} &= (1-\delta_{ab})\left(\frac{m-m_1}{1-m_1}\mathrm{I}(a\prec b)+\mathrm{I}(a\not\prec b)\right)= \\ &= \frac{1-m}{m_1-1}\mathbf{1}_{m_1}+\mathbf{1}_m+\frac{m-m_1}{m_1-1}\mathbf{1} \end{aligned} \tag{4.186}$$

where $\mathbf{1}_{m_1}$ is a matrix that has the entries equal to 1 only inside the diagonal blocks of size m_1 while $\mathbf{1}_m$ is a matrix that is full of 1 and $\mathbf{1}$ is the identity. By using the relations

$$\begin{aligned} &\mathbf{1}_{m_1}^2=m_1\mathbf{1}_{m_1} \qquad \mathbf{1}_m^2=m\mathbf{1}_m \\ &\mathbf{1}_m\mathbf{1}_{m_1}=\mathbf{1}_{m_1}\mathbf{1}_m=m_1\mathbf{1}_m \end{aligned} \tag{4.187}$$

one can obtain that

$$\begin{aligned} \mathrm{tr}r^3 &= \frac{m(m_1-m)(m-1)}{(m_1-1)^2}\left(mm_1+m_1-2m\right) \\ \sum_{a\neq b}r_{ab}^3 &= \frac{m(m_1-m)(m-1)}{(m_1-1)^2}(1+m-2m_1) \end{aligned} \tag{4.188}$$

and finally that

$$\begin{aligned} W[w_1,w_2,m,m_1] =& \frac{m(m_1-m)(m-1)}{(m_1-1)^2}\left[w_1(m)\left(mm_1+m_1-2m\right)\right. \\ &\left.+w_2(m)(1+m-2m_1)\right]\,. \end{aligned} \tag{4.189}$$

Suppose that we want to see if there is a 2RSB solution that appears in the $(m,\widehat{\varphi})$ plane where we know that the 1RSB solution is unstable. Because the instability is in the replicon subspace we search for a non trivial stationary point solution for the

expression (4.184). The trivial 1RSB solution $\delta\alpha_0 = 0$ can always be found but we have shown that is unstable in a given region of the $(m, \widehat{\varphi})$ plane so that we want to find another solution. To do this we first optimize over $\delta\alpha_0$ and then we optimize over the breaking point m_1. The saddle point equation for $\delta\alpha_0$ gives

$$\delta\alpha_0 = -\frac{2\hat{\lambda}_R}{W} \,. \tag{4.190}$$

The entropy as a function of m_1 is given by plugging the above expression in (4.184) and it gives

$$S[\alpha_{1RSB} + \delta q] = S[\alpha_{1RSB}] - \frac{1}{3}\frac{\hat{\lambda}_R^3(m, m_1)}{W^2(m, m_1)} \,. \tag{4.191}$$

At this point we can search for the extremum in m_1 and we obtain that the breaking point is

$$m_1 = \frac{w_2(m)}{w_1(m)} = \lambda(m) \tag{4.192}$$

However, as it is usual in replica computations, we have to require that when $m < 1$ then the saddle point solution for the breaking point should satisfy

$$m < m_1 < 1 \,. \tag{4.193}$$

This implies that the a 2RSB solution exists only if

$$m \leq \frac{w_2(m)}{w_1(m)} \equiv \lambda(m) \tag{4.194}$$

Let us precise how to compute $\lambda(m)$. We have seen that in the $(m, \widehat{\varphi})$ plane there exists an instability line that separates the stable 1RSB saddle point from the unstable one. In the unstable region we want to find if there exist a 2RSB solution. To do this, we have developed the entropy around the 1RSB solution on the critical instability line. It follows that all the quantities $\hat{\lambda}_R(m)$, $w_1(m)$ and $w_2(m)$ are computed on the critical line. The condition (4.194) tells us that there exist a point in the $(m, \widehat{\varphi})$ plane where

$$m^* = \lambda(m^*) \tag{4.195}$$

so that below this point a 2RSB solution is possible. However the relation between the breaking point and $\lambda(m)$ is valid only when we are close enough to the instability line so that it is valid only asymptotically. If we are at a finite distance, the breaking point m_1 can decrease when decreasing m up to a point where it becomes equal to the value of m. If we decrease further m the breaking point become less then m and the first condition in (4.193) is violated so that below the point where $m = m_1$ the 2RSB solution no longer exists [151]. This condition defines a line in the $(m, \widehat{\varphi})$ plane that together with the instability line describes a region where a 2RSB solution can be obtained. The point where $\lambda(m)$ becomes equal to m and a 2RSB solution appears can be computed using the expression for $w_1(m)$ and $w_2(m)$ that we computed in the previous sections. The numerical solution of the equation (4.195) gives

$$m^* \simeq 0.414 \implies \widehat{\varphi}^* = 5.84 \,. \tag{4.196}$$

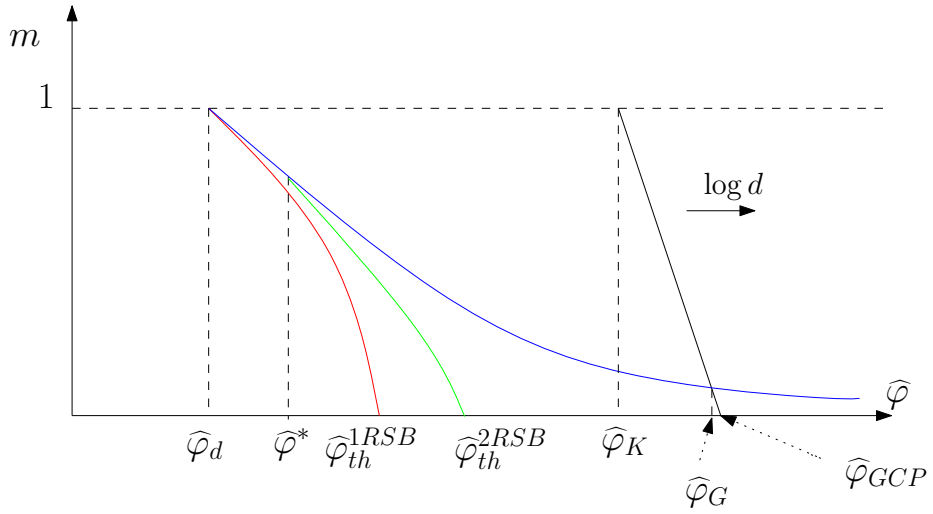

Figure 4.10. 2RSB phase diagram in the $m - \hat{\varphi}$ plane.

In the end, the phase diagram that we obtain is the one represented in Fig. 4.10. Below the red line, no saddle point glassy solution exists while above it there exists a 1RSB glassy solution that is stable only above the blue line. The blue line is the instability line where the replicon eigenvalue is zero when computed around the 1RSB solution. Between the red and the blue line, the 1RSB solution is unstable and we have looked to the 2RSB solution. The point where the 2RSB solution can appear is the $(\hat{\varphi}^*, m^*)$ point that is where $\lambda(m) = m$. The green line is defined by the condition such that $m_1^{SP} = m$ where m_1^{SP} is the saddle point value for the 2RSB breaking parameter. It follows that if there exist a 2RSB solution that is stable, it should be in between the green and the red line.

4.11.2 The large density behavior of $\lambda(m)$

In this section we want to perform an asymptotic computation to see the behavior of $\lambda(m)$ for $m \to 0$ on the Gardner line. The importance of this computation is related to the fact that we know that below the instability line we have to do a fullRSB computation in order to obtain consistent results. Moreover we have showed that in the 2RSB ansatz the value of the breaking point m_1 coincides with the value of $\lambda(m)$ computed in the instability line. Actually this is true also if we perform a fullRSB calculation and we are very close to the transition point that is where we have the instability line [30]. It follows that the computation of λ gives us a precise estimate of the behavior of the breaking point in the fullRSB ansatz. Here we want to address the problem in how to compute the properties the behavior of $\lambda(m)$ in the limit $m \to 0$ that is relevant for the jamming.

Let us first recall the expression for $\lambda(m)$:

$$\lambda(m) = \frac{-\hat{w}_2^{(I)}(\widehat{A}_G(m), m)}{\frac{2}{\widehat{\varphi}_G(m)} - \hat{w}_1^{(I)}(\widehat{A}_G(m), m)} \tag{4.197}$$

where $\widehat{\varphi}_G(m)$ and $\widehat{A}_G(m)$ are respectively the instability reduced packing fraction

and the instability line for the 1RSB cage radius. Moreover we have defined

$$\begin{aligned}
\hat{w}_1^{(I)}(A_G(m),m) &= -\left\langle \Theta_0^{m-1}(\lambda)\left[1+\frac{\Theta_1^2(\lambda)}{\Theta_0^2(\lambda)}-\frac{\Theta_2(\lambda)}{\Theta_0(\lambda)}\right]^2\right. \\
&\left.\times\left[(m-3\lambda^2)+(m-6)\frac{\Theta_1^2(\lambda)}{\Theta_0^2(\lambda)}+6\lambda\frac{\Theta_1(\lambda)}{\Theta_0(\lambda)}-(m-3)\frac{\Theta_2(\lambda)}{\Theta_0(\lambda)}\right]\right\rangle_{A_G(m)} \\
\hat{w}_2^{(I)}(A_G(m),m) &= \frac{1}{2}\left\langle \Theta_0^{m-1}(\lambda)\left[2\left(\frac{\Theta_1(\lambda)}{\Theta_0(\lambda)}\right)^3-3\frac{\Theta_1(\lambda)\Theta_2(\lambda)}{\Theta_0^2(\lambda)}+\frac{\Theta_3(\lambda)}{\Theta_0(\lambda)}\right]\right. \\
&\times\left[2\lambda^3+2(m-6)\left(\frac{\Theta_1(\lambda)}{\Theta_0(\lambda)}\right)^3 3\frac{\Theta_1(\lambda)}{\Theta_0(\lambda)}\left[4\lambda\frac{\Theta_1(\lambda)}{\Theta_0(\lambda)}-(m-4)\frac{\Theta_2(\lambda)}{\Theta_0(\lambda)}\right]\right. \\
&\left.\left.-6\lambda\left(\lambda\frac{\Theta_1(\lambda)}{\Theta_0(\lambda)}+\frac{\Theta_2(\lambda)}{\Theta_0(\lambda)}\right)+(m-2)\frac{\Theta_3(\lambda)}{\Theta_0(\lambda)}\right]\right\rangle_{A_G(m)}
\end{aligned} \tag{4.198}$$

where we have denoted as usual

$$\langle O(x)\rangle_A = \int_{-\infty}^{\infty}\frac{\mathrm{d}x}{\sqrt{2\pi}}O(x)e^{-\frac{1}{2}\left(x+\sqrt{2A}\right)^2} \tag{4.199}$$

Moreover let us recall that at the instability line we have that

$$\widehat{\varphi}_G(m) = \frac{1}{\mathcal{F}_m(A_G(m))} \tag{4.200}$$

where $A_G(m)$ satisfies the equation

$$2\mathcal{F}_m(A_G(m)) = -\Lambda_m(A_G(m)) \tag{4.201}$$

and

$$\begin{aligned}
\Lambda_m(A_G(m)) &= \langle\mathcal{L}(\lambda,m)\rangle_{A_G(m)} \\
\mathcal{L}(\lambda,m) &= \Theta_0^{m-1}(\lambda)\left[\left(\frac{\Theta_1(\lambda)}{\Theta_0(\lambda)}\right)^2-\lambda\frac{\Theta_1(\lambda)}{\Theta_0(\lambda)}\right] \\
&\times\left[2-2\lambda^2+(m-4)\left(\frac{\Theta_1(\lambda)}{\Theta_0(\lambda)}\right)^2+(6-m)\lambda\frac{\Theta_1(\lambda)}{\Theta_0(\lambda)}\right]
\end{aligned} \tag{4.202}$$

It follows that the expression for λ can be put in the form

$$\lambda(m) = \frac{\hat{w}_2^{(I)}(\widehat{A}_G(m),m)}{\Lambda_m(A_G(m))+\hat{w}_1^{(I)}(\widehat{A}_G(m),m)} \tag{4.203}$$

Let us now recall that in the limit $m\to 0$, $\sqrt{A_G(m)}\simeq 0.8m$. This implies that we can hope to expand both the numerator and the denominator in powers of $\sqrt{A_G}$.

$$\begin{aligned}
\hat{w}_2^{(I)}(A_G(m),m) &= w_2^{(0)}(m)+\sqrt{A_G(m)}w_2^{(1)}(m)+A_G(m)w_2^{(2)}(m)+\dots \\
\hat{w}_1^{(I)}(A_G(m),m) &= w_1^{(0)}(m)+\sqrt{A_G(m)}w_1^{(1)}(m)+A_G(m)w_2^{(1)}(m)+\dots \\
\Lambda_m(A_G(m)) &= \Lambda_m^{(0)}(m)+\sqrt{A_G(m)}\Lambda_m^{(1)}(m)+A_G(m)\Lambda_m^{(1)}(m)+\dots
\end{aligned} \tag{4.204}$$

Let us begin with the numerator. With very good numerical accuracy we have that $w_2^{(0)}(m) = 0$. Let us look at the first order term that can be written as

$$w_2^{(1)}(m) = \frac{1}{2}\int_{-\infty}^{\infty} \frac{\mathrm{d}\lambda}{\sqrt{2\pi}} e^{-\lambda^2/2}(-\lambda\sqrt{2})\Theta_0^{m-1}(\lambda)\Gamma_2(\lambda, m) \tag{4.205}$$

where

$$\Gamma_2(\lambda, m) = \left[2\left(\frac{\Theta_1(\lambda)}{\Theta_0(\lambda)}\right)^3 - 3\frac{\Theta_1(\lambda)\Theta_2(\lambda)}{\Theta_0^2(\lambda)} + \frac{\Theta_3(\lambda)}{\Theta_0(\lambda)}\right]\left[2\lambda^3 + 2(m-6)\left(\frac{\Theta_1(\lambda)}{\Theta_0(\lambda)}\right)^3 + \right.$$
$$\left. +3\frac{\Theta_1(\lambda)}{\Theta_0(\lambda)}\left[4\lambda\frac{\Theta_1(\lambda)}{\Theta_0(\lambda)} - (m-4)\frac{\Theta_2(\lambda)}{\Theta_0(\lambda)}\right] - 6\lambda\left(\lambda\frac{\Theta_1(\lambda)}{\Theta_0(\lambda)} + \frac{\Theta_2(\lambda)}{\Theta_0(\lambda)}\right) + (m-2)\frac{\Theta_3(\lambda)}{\Theta_0(\lambda)}\right] \tag{4.206}$$

As usual the behavior of the integral depends on how the function inside behaves as $\lambda \to \infty$ for small m. We have two possibilities: the integral decays as λ^α with $\alpha > 1$ and in that case it is convergent; in the other case, we have a divergent contribution that has to be studied looking at the limit $m \to 0$. To see which of the two behaviors happens we develop asymptotically the integrand

$$e^{-\lambda^2/2}(-\lambda\sqrt{2})\Theta_0^{m-1}(\lambda)\Gamma_2(\lambda, m) \sim e^{-m\lambda^2/2}(-\lambda\sqrt{2})(\lambda\sqrt{2\pi})^{1-m}\times$$
$$\times\left(\frac{2m}{\lambda^6} - \frac{12(4m-1)}{\lambda^8} + \dots\right) \tag{4.207}$$

from which it follows that the integral is finite at $m = 0$ and it is given by

$$\int_{-\infty}^{\infty} \frac{\mathrm{d}\lambda}{\sqrt{2\pi}} e^{-\lambda^2/2}(-\lambda\sqrt{2})\Theta_0^{-1}(\lambda)\Gamma_2(\lambda, 0) \simeq -0.134 \tag{4.208}$$

Let us now consider the denominator. Also in this case the zeroth order term is zero with very good numerical accuracy. In an analogous way we define

$$\Gamma_1(\lambda, m) = \left[1 + \frac{\Theta_1^2(\lambda)}{\Theta_0^2(\lambda)} - \frac{\Theta_2(\lambda)}{\Theta_0(\lambda)}\right]^2$$
$$\times\left[(m - 3\lambda^2) + (m-6)\frac{\Theta_1^2(\lambda)}{\Theta_0^2(\lambda)} + 6\lambda\frac{\Theta_1(\lambda)}{\Theta_0(\lambda)} - (m-3)\frac{\Theta_2(\lambda)}{\Theta_0(\lambda)}\right] \tag{4.209}$$

and then we look at the asymptotic expansion of the integral that defines the first order term of the denominator

$$\int \frac{\mathrm{d}\lambda}{\sqrt{2\pi}}(-\lambda\sqrt{2})e^{-\lambda^2/2}\Theta_0^{m-1}(\lambda)\left[\mathcal{L}(\lambda, m) + \Gamma_1(\lambda, m)\right]$$
$$\sim \int \frac{\mathrm{d}\lambda}{\sqrt{2\pi}} e^{-m\lambda^2/2}(\lambda\sqrt{2\pi})^{1-m}(-\lambda\sqrt{2})\left[\frac{m}{\lambda^2} + \frac{2-8m}{\lambda^4} + \dots\right] \tag{4.210}$$

from which it follows that also in this case the integral is finite at $m \to 0$ and it is given by

$$\int \frac{\mathrm{d}\lambda}{\sqrt{2\pi}} e^{-\lambda^2/2}(-\lambda\sqrt{2})\Theta_0^{m-1}(\lambda)\left[\mathcal{L}(\lambda, m) + \Gamma_1(\lambda, m)\right] \simeq -1.067 \tag{4.211}$$

In the end we get

$$\lim_{m\to 0} \lambda(m) = 0.124\,. \tag{4.212}$$

4.12 The 2RSB solution in the jamming limit

In this section we want to study the infinite pressure limit of the 2RSB replicated entropy. This limit can be taken into account by simply looking at the limit $m \to 0$. This has been investigated in full details at the 1RSB level [145, 118]: in this case the parameter $\widehat{\gamma}_1 = 2\widehat{\alpha}_1$ remains finite, in such a way that the mean square displacement in the glass, $\widehat{\Delta}_1 = m\widehat{\gamma}_1$ vanishes proportionally to m, $\widehat{\Delta}_1 \sim m \sim 1/p$.

Here we will see what happens at the 2RSB level.

4.12.1 2RSB equations at $m = 0$

To start the calculation it is convenient to first define $\widehat{\gamma}_i = \widehat{G}_i/m$. Then, at the 2RSB level we can express $\widehat{\gamma}_2$ and m_1 as function of

$$\begin{aligned} \eta &= 1 - \frac{\widehat{\gamma}_2}{\widehat{\gamma}_1} \,, \\ \nu &= \frac{m}{m_1} = \frac{1}{y_1} \,. \end{aligned} \tag{4.213}$$

All the other parameters that enters in the 2RSB calculation can be reconstructed as follows

$$\begin{aligned} m_1 &= m/\nu \,, \\ \widehat{\gamma}_2 &= \widehat{\gamma}_1(1-\eta) \,, \\ \widehat{\Delta}_1 &= m\widehat{\gamma}_1(1-\eta) + \widehat{\gamma}_1\eta\nu \,, \\ \widehat{\Delta}_2 &= m\widehat{\gamma}_1(1-\eta) \,. \end{aligned} \tag{4.214}$$

Moreover, the physical constraint $\widehat{\Delta}_1 \geq \widehat{\Delta}_2 \geq 0$, forces $\eta \in [0,1]$, while from the condition $1 \geq m_1 \geq m$ we have that $\nu \in [m,1]$. In terms of these new variables, the replicated 2RSB entrapy is given by

$$\begin{aligned} s_{\text{2RSB}} &= 1 - \log\rho + \frac{d}{2} m \log m + \frac{d}{2}(m-1)\log(\pi e D^2/d^2) \\ &\quad + \frac{d}{2}\Big\{ (m-1)\log\widehat{\gamma}_1 + (m-\nu)\log(1-\eta) - \widehat{\varphi}\sqrt{\nu\eta\widehat{\gamma}_1}\, e^{-\widehat{\gamma}_1[m(1-\eta)+\eta\nu]/2} \times \\ &\quad \times \int_{-\infty}^{\infty} dx\, e^{x\sqrt{\nu\eta\widehat{\gamma}_1}} \left[1 - (I_2^m(x))^\nu\right] \Big\} \\ I_2^m(x) &= \int_{-\infty}^{\infty} \mathcal{D}z\, \Theta^{m/\nu}\left[\sqrt{\frac{\nu}{m}\frac{\eta}{1-\eta}}\frac{x-z}{\sqrt{2}}\right] \end{aligned} \tag{4.215}$$

We will soon use the above expression to compute numerically the saddle point values for $\widehat{\gamma}_1$, η, ν. However we will first look at the limit of Eq. (4.215) when $m \to 0$. We want to show that the 2RSB entropy has a finite limit when $\widehat{\gamma}_1, \eta, \nu$ are fixed (i.e. they do not scale with m). This means that in this limit both $\eta, \nu \in [0,1]$ and $\widehat{\Delta}_2 \to 0$ while $\widehat{\Delta}_1$ remains finite.

The limit $m \to 0$ of Eq. (4.215) is simple. Let us look at the function $I_2^m(x)$. If we use the following simple formula

$$\lim_{\mu\to 0} \Theta\left(\frac{z}{\sqrt{\mu}}\right)^{\mu} = e^{-z^2\theta(-z)} \,, \tag{4.216}$$

we obtain

$$\begin{aligned} I_2(x) &= \lim_{m\to 0} I_2^m(x) = \int_{-\infty}^{\infty} \mathcal{D}z \exp\left[-\frac{\eta}{2(1-\eta)}(x-z)^2\,\theta(z-x)\right] \\ &= \Theta\left(\frac{x}{\sqrt{2}}\right) + e^{-\frac{\eta}{2}x^2}\sqrt{1-\eta}\,\Theta\left(-\sqrt{\frac{1-\eta}{2}}x\right) , \end{aligned} \tag{4.217}$$

and finally

$$\begin{aligned} s_{\text{2RSB}} &= 1 - \log\rho - \frac{d}{2}\log(\pi e D^2/d^2) \\ &\quad + \frac{d}{2}\left\{-\log\widehat{\gamma}_1 - \nu\log(1-\eta) - \widehat{\varphi}\sqrt{\eta\nu\widehat{\gamma}_1}e^{-\widehat{\gamma}_1\eta\nu/2}\int dx\, e^{x\sqrt{\eta\nu\widehat{\gamma}_1}}\left[1 - I_2(x)^\nu\right]\right\} \\ I_2(x) &= \Theta\left(\frac{x}{\sqrt{2}}\right) + e^{-\frac{\eta}{2}x^2}\sqrt{1-\eta}\,\Theta\left(-\sqrt{\frac{1-\eta}{2}}x\right) . \end{aligned} \tag{4.218}$$

This proves that a smooth limit for the 2RSB entropy is achieved when $m \to 0$ and $\widehat{\gamma}_1$, η, ν remain finite. This has the important consequence that the mean square displacement *inside a glass*, $\widehat{\Delta}_2$, vanishes at jamming, as it should, but the mean square displacement $\widehat{\Delta}_1$ *between different sub-glasses inside a meta-glass remains finite*. This means that sub-glasses inside a meta-glass are distinct at the microscopic level. We conclude by noting that m_1 vanishes linearly with m because ν remains finite.

4.12.2 Asymptotic analysis at jamming for high density

In this section we want to discuss the the perturbative expansion around the infinite density limit of the solution of the saddle point equations for the 2RSB entropy. This will allows us to check the eventual numerical solution of the same equations. Let us start with the observation that in the 1RSB case $\widehat{\gamma}_1 \sim \widehat{\varphi}^{-2}$ so that we must recover the same scaling also at the 2RSB level. Moreover a crucial result is that on the Gardner line (namely the 1RSB instability line) we showed that $m_1 = \lambda(m) \to 0.124$ and that $m \sim 1.98\widehat{\varphi}^{-2}$. This means that $\nu = m/m_1 \sim 15.97\widehat{\varphi}^{-2}$. We therefore seek for a small $\widehat{\gamma}_1$ and small ν expansion of Eq. (4.218). Because both $\widehat{\gamma}_1$ and ν are of the same order of magnitude, we use $1/\widehat{\varphi}$ as the small expansion parameter and write $\widehat{\gamma}_1, \nu \sim \mathcal{O}(2)$ to indicate that these quantities are of order 2 in $1/\widehat{\varphi}$, and similarly for other quantities. If we come back to the 2RSB expression of the entropy and we neglect trivial constant factors that are useless for the saddle point, we see that we must optimize the following function

$$\mathcal{S} = -\nu\log(1-\eta) - \log\widehat{\gamma}_1 - \widehat{\varphi}\mathcal{I} , \tag{4.219}$$

where the integral $\mathcal{I}$ is given by

$$\mathcal{I} = \sqrt{\widehat{\gamma}_1\eta\nu}\int_{-\infty}^{\infty} dx\, e^{x\sqrt{\widehat{\gamma}_1\eta\nu} - \widehat{\gamma}_1\eta\nu/2}\left[1 - I_2(x)^\nu\right] \tag{4.220}$$

If ν is small we can separate this integral in two pieces

$$\begin{aligned}
\mathcal{I} &= \mathcal{I}^{(a)} + \mathcal{I}^{(n)} \\
\mathcal{I}^{(n)} &= \sqrt{\widehat{\gamma}_1\eta\nu}\int_{-\infty}^{\infty} dx\, e^{x\sqrt{\widehat{\gamma}_1\eta\nu}-\widehat{\gamma}_1\eta\nu/2}\,[\theta(-x)e^{-\frac{\eta}{2}x^2\nu}\sqrt{1-\eta}^{\nu}+\theta(x)-I_2(x)^{\nu}] \\
&= \sqrt{\widehat{\gamma}_1\eta\nu}e^{-\widehat{\gamma}_1\eta\nu/2}\int_0^{\infty} dx\,\Big[e^{x\sqrt{\widehat{\gamma}_1\eta\nu}}(1-I_2(x)^{\nu}) \\
&+e^{-x\sqrt{\widehat{\gamma}_1\eta\nu}}(e^{-\frac{\eta}{2}x^2\nu}\sqrt{1-\eta}^{\nu}-I_2(-x)^{\nu})\Big] \\
\mathcal{I}^{(a)} &= \sqrt{\widehat{\gamma}_1\eta\nu}\int_{-\infty}^{0} dx\, e^{x\sqrt{\widehat{\gamma}_1\eta\nu}-\widehat{\gamma}_1\eta\nu/2}\,[1-e^{-\frac{\eta}{2}x^2\nu}\sqrt{1-\eta}^{\nu}] \\
&= \sqrt{\widehat{\gamma}_1\eta}\int_{-\infty}^{0} dy\, e^{y\sqrt{\widehat{\gamma}_1\eta}-\widehat{\gamma}_1\eta\nu/2}\,[1-e^{-\frac{\eta}{2}y^2}\sqrt{1-\eta}^{\nu}] \\
&= e^{-\widehat{\gamma}_1\eta\nu/2}[1-e^{\widehat{\gamma}_1/2}\sqrt{\pi\widehat{\gamma}_1/2}(1-\eta)^{\nu/2}(1-\mathrm{erf}(\sqrt{\widehat{\gamma}_1/2}))]
\end{aligned} \tag{4.221}$$

The advantage in doing this is the $\mathcal{I}^{(a)}$ can be easy expanded in a power series of ν and $\widehat{\gamma}_1$ while $\mathcal{I}^{(n)}$ decays as a Gaussian at large value of $|x|$ and can be expanded in powers of ν too.

The expansion of $\mathcal{I}^{(n)}$ is given by

$$\begin{aligned}
\mathcal{I}^{(n)} &= e^{-\widehat{\gamma}_1\eta\nu/2}\int_0^{\infty} dx\sum_{l=0}^{\infty}\frac{x^l}{l!}(\widehat{\gamma}_1\eta\nu)^{(l+1)/2}\times \\
&\times\sum_{k=1}^{\infty}\frac{\nu^k}{k!}\left\{-\log I_2(x)^k+(-1)^l\left[\left(\frac{1}{2}\log(1-\eta)-\frac{\eta}{2}x^2\right)^k-\log I_2(-x)^k\right]\right\} \\
&= e^{-\widehat{\gamma}_1\eta\nu/2}\sum_{l=0}^{\infty}\sum_{k=1}^{\infty}\frac{1}{l!k!}(\widehat{\gamma}_1\eta\nu)^{(l+1)/2}\nu^k\mathcal{I}_{l,k}(\eta)\ , \\
\mathcal{I}_{l,k}(\eta) &= \int_0^{\infty} dx\, x^l\left\{-\log I_2(x)^k+(-1)^l\left[\left(\frac{1}{2}\log(1-\eta)-\frac{\eta}{2}x^2\right)^k-\log I_2(-x)^k\right]\right\}
\end{aligned} \tag{4.222}$$

We note that all the functions $\mathcal{I}_{l,k}(\eta)$ are defined by well convergent integrals and we can differentiate them. We now consider the following power series expansion

$$\begin{aligned}
\widehat{\gamma}_1 &= \sum_{k=2}^{\infty}\widehat{\gamma}_{1,k}\widehat{\varphi}^{-k}\ , \\
\nu &= \sum_{k=2}^{\infty}\nu_k\widehat{\varphi}^{-k}\ , \\
\eta &= \sum_{k=0}^{\infty}\eta_k\widehat{\varphi}^{-k}\ .
\end{aligned} \tag{4.223}$$

If we perform a systematic expansion of the entropy as a function of $1/\widehat{\varphi}$ we can obtain order after order in $1/\widehat{\varphi}$ the coefficients $\widehat{\gamma}_{1,k}$, ν_k, η_k. Here we show how to do just for the lowest orders.

The lowest order is given by

$$\begin{aligned}\mathcal{I}^{(n)} &= \nu^{3/2}\sqrt{\widehat{\gamma}_1\eta}\,\mathcal{I}_{0,1}(\eta) + \mathcal{O}(6)\ ,\\ \mathcal{I}_{0,1}(\eta) &= \int_0^\infty dx\left[-\log I_2(x) + \frac{1}{2}\log(1-\eta) - \frac{\eta}{2}x^2\ - \log I_2(-x)\right]\ .\end{aligned} \tag{4.224}$$

and

$$\begin{aligned}\mathcal{I}^{(a)} &= -\sqrt{\pi\widehat{\gamma}_1/2} + \widehat{\gamma}_1 - \sqrt{\pi(\widehat{\gamma}_1/2)^3} - \frac{1}{2}\sqrt{\frac{\pi\widehat{\gamma}_1}{2}}\nu\log(1-\eta)\\ &\quad + \frac{1}{3}\widehat{\gamma}_1^2 + \frac{1}{2}\widehat{\gamma}_1\nu(\log(1-\eta)-\eta) + \mathcal{O}(5)\ .\end{aligned} \tag{4.225}$$

Putting together the two contribution in the entropy we get

$$\begin{aligned}S &= -\log\widehat{\gamma}_1 + \widehat{\varphi}\sqrt{\pi\widehat{\gamma}_1/2} - \widehat{\varphi}\widehat{\gamma}_1\\ &\quad - \nu\log(1-\eta) + \widehat{\varphi}\sqrt{\pi(\widehat{\gamma}_1/2)^3} + \frac{1}{2}\widehat{\varphi}\sqrt{\frac{\pi\widehat{\gamma}_1}{2}}\nu\log(1-\eta)\\ &\quad - \widehat{\varphi}\left(\frac{1}{3}\widehat{\gamma}_1^2 + \frac{1}{2}\widehat{\gamma}_1\nu(\log(1-\eta)-\eta) + \nu^{3/2}\sqrt{\widehat{\gamma}_1\eta}\,\mathcal{I}_{0,1}(\eta)\right) + \mathcal{O}(4)\end{aligned} \tag{4.226}$$

We will now optimize Eq. (4.226) order by order. We have now to optimize Eq. (4.226) order by order. At the leading order the equation for $\widehat{\gamma}_1$ which coincides with the one that can be found within a 1RSB optimization:

$$-\frac{2}{\widehat{\gamma}_1} + \frac{1}{2}\widehat{\varphi}\sqrt{\frac{2\pi}{\widehat{\gamma}_1}} = 0 \quad \Rightarrow \quad \widehat{\gamma}_1 = \frac{8}{\pi}\widehat{\varphi}^{-2} + \mathcal{O}(3) \quad \Rightarrow \quad \widehat{\gamma}_{1,2} = \frac{8}{\pi}\ . \tag{4.227}$$

This means that at the next order we must search for a solution of the form $\widehat{\gamma}_1 = \frac{8}{\pi}\widehat{\varphi}^{-2} + \widehat{\gamma}_{1,3}\widehat{\varphi}^{-3} + \mathcal{O}(4)$. If we put this in Eq. (4.226) and we expand we get

$$S = \text{const.} + \left(-\widehat{\gamma}_{1,3} + \frac{\pi^2}{256}\widehat{\gamma}_{1,3}^2\right)\widehat{\varphi}^{-2} + \mathcal{O}(3) \tag{4.228}$$

that can be used to obtain $\widehat{\gamma}_{1,3} = 128/\pi^2$. The last step is to look for $\widehat{\gamma}_1 = \frac{8}{\pi}\widehat{\varphi}^{-2} + (128/\pi^2)\widehat{\varphi}^{-3} + \widehat{\gamma}_{1,4}\widehat{\varphi}^{-4} + \mathcal{O}(5)$ and $\nu = \nu_2\widehat{\varphi}^{-2} + \mathcal{O}(3)$. We insert these expansions in Eq. (4.226), we expand again and we obtain

$$S = \text{const.} - \frac{2}{3\pi}\left(-6\nu_2(\eta + \log(1-\eta)) + 3\sqrt{2\pi\eta}\nu_2^{3/2}h(\eta)\right)\widehat{\varphi}^{-3} + \mathcal{O}(4) \tag{4.229}$$

By optimizing numerically this function we get $\nu_2 = 5.4226$ and $\eta_0 = 0.6752$. Collecting these results we can write the first terms if the 2RSB solution at $m = 0$ in the limit $\widehat{\varphi} \to \infty$

$$\begin{aligned}\widehat{\gamma}_1 &= \frac{8}{\pi}\widehat{\varphi}^{-2} + (128/\pi^2)\widehat{\varphi}^{-3} + \mathcal{O}(4)\ ,\\ \nu &= 5.4226\widehat{\varphi}^{-2} + \mathcal{O}(3)\ ,\\ \eta &= 0.6752 + \mathcal{O}(1)\ ,\end{aligned} \tag{4.230}$$

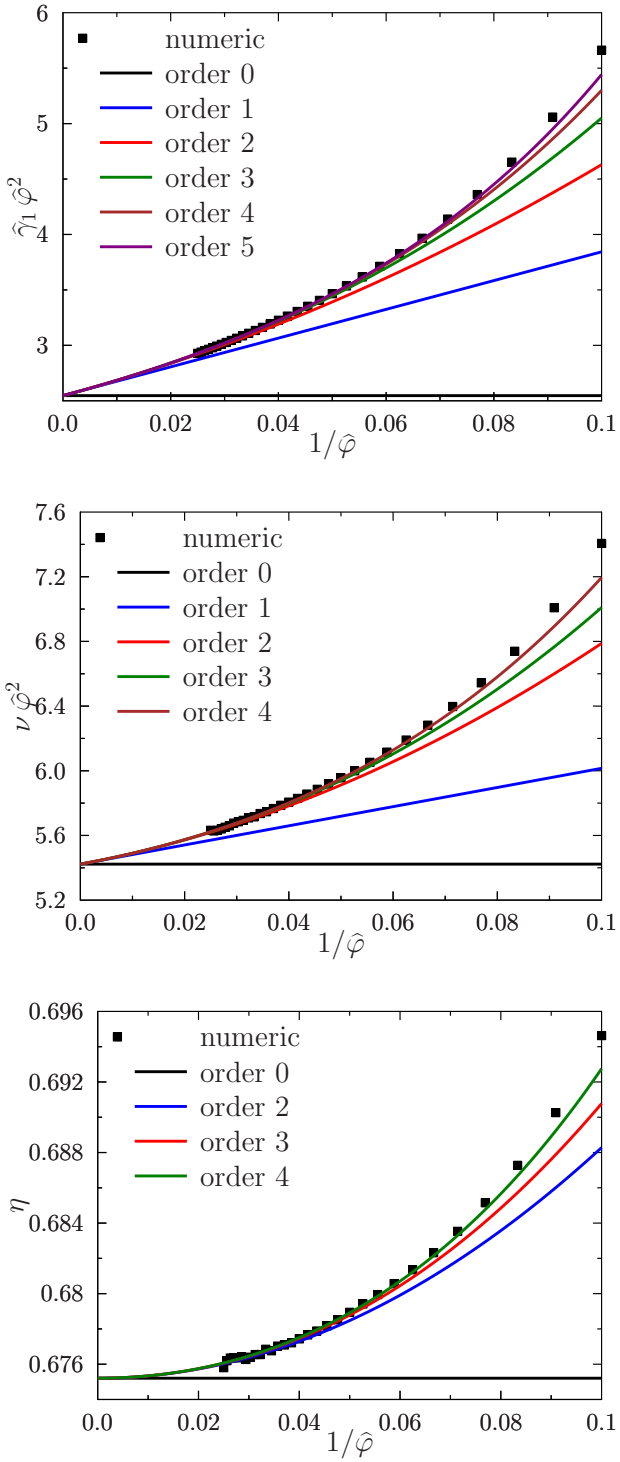

Figure 4.11. We show the comparison between the numerical optimization (black points) of the 2RSB entropy and the analytic large density asymptotic expansion at different orders (full lines) of the saddle point solution. We see the convergence of the analytical computation to the numerical estimation of the saddle point value of $\hat{\gamma}_1$, ν and η.

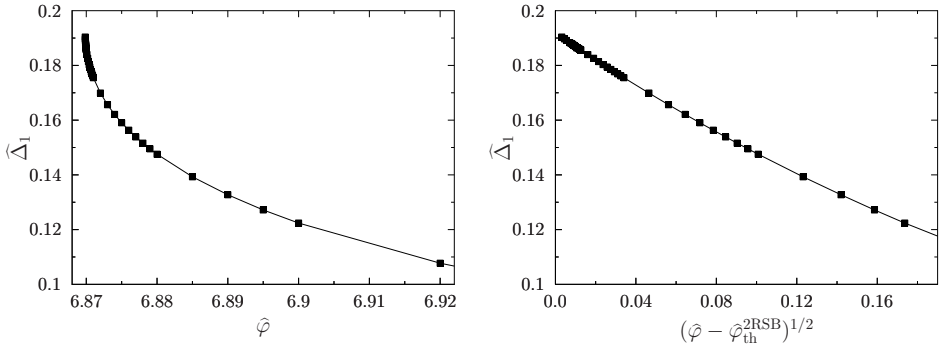

Figure 4.12. The inter-state overlap $\widehat{\Delta}_1 = \widehat{\gamma}_1\eta\nu$ of the 2RSB solution at $m = 0$ as a function of $\widehat{\varphi}$. The square root behavior can be easily seen, and the threshold point can be located to $\widehat{\varphi}_{\rm th}^{\rm 2RSB} = 6.86984$.

and

$$s[\hat{\alpha}_{2RSB}] = s[\hat{\alpha}_{1RSB}] - \frac{d}{2}\,1.03416\,\widehat{\varphi}^{-3} + \mathcal{O}(4)\ . \tag{4.231}$$

We can produce higher orders in the perturbative expansion by just iterating this calculation. We will not report them here. The Fig. 4.11 summarize our findings both for the analytical asymptotic expansion of the saddle point solution at different orders and the numerical optimization of the 2RSB entropy (4.218) at $m = 0$. The analytical calculation has been done up to order 11 in density which allows to obtain $\widehat{\gamma}_1$ to order $\widehat{\varphi}^{-7}$, ν to order $\widehat{\varphi}^{-6}$ and η to order $\widehat{\varphi}^{-4}$. The two results are in perfect agreement.

4.13 The new 2RSB threshold

We can use the numerical optimization for the 2RSB replicated entropy to obtain the 2RSB value of $\widehat{\varphi}_{th}^{2RSB}$. It is defined as the point on the $m = 0$ line at which the 2RSB solution disappears. The behavior of α_1, η and ν near $\widehat{\varphi}_{th}^{2RSB}$ are reported in Fig. 4.13. Moreover in Fig. 4.12 we report the behavior of $\widehat{\Delta}_1$ close to the threshold. From these plots we extract that the new value of the new 2RSB threshold is $\widehat{\varphi}_{th}^{2RSB} \simeq 6.86984$. Moreover we see that the typical square root behavior is verified

$$\begin{aligned}
\alpha_1(\widehat{\varphi}) &= \alpha_1^* + \sqrt{\widehat{\varphi} - \widehat{\varphi}_{th}^{2RSB}}\,\alpha_1^{(1)} + \dots \\
\eta(\widehat{\varphi}) &= \eta^* + \sqrt{\widehat{\varphi} - \widehat{\varphi}_{th}^{2RSB}}\,\eta^{(1)} + \dots \\
\nu(\widehat{\varphi}) &= \nu^* + \sqrt{\widehat{\varphi} - \widehat{\varphi}_{th}^{2RSB}}\,\nu^{(1)} + \dots
\end{aligned} \tag{4.232}$$

In this way let us take the saddle point equation on the line $m = 0$

$$\begin{aligned}
0 &= \frac{\partial s_{2RSB}[\alpha_1,\eta,\nu]}{\partial\alpha_1} \\
0 &= \frac{\partial s_{2RSB}[\alpha_1,\eta,\nu]}{\partial\eta} \\
0 &= \frac{\partial s_{2RSB}[\alpha_1,\eta,\nu]}{\partial\nu}\ ;
\end{aligned} \tag{4.233}$$

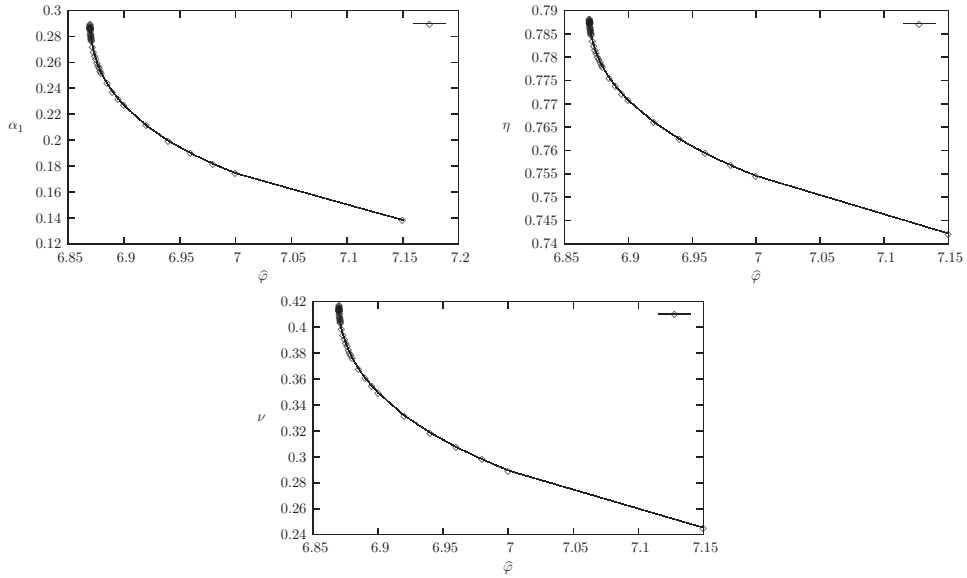

Figure 4.13. The square root behavior of the saddle point value of α_1, η and ν close to $\widehat{\varphi}_{th}^{2RSB}$

as in the 1RSB case we take the derivative with respect to the control parameter $\widehat{\varphi}$ to obtain

$$0 = \begin{bmatrix} \frac{\partial^2 s_{2RSB}[\alpha_1,\eta,\nu]}{\partial \alpha_1^2} & \frac{\partial^2 s_{2RSB}[\alpha_1,\eta,\nu]}{\partial \alpha_1 \partial \eta} & \frac{\partial^2 s_{2RSB}[\alpha_1,\eta,\nu]}{\partial \alpha_1 \partial \nu} \\ \frac{\partial^2 s_{2RSB}[\alpha_1,\eta,\nu]}{\partial \alpha_1 \partial \eta} & \frac{\partial^2 s_{2RSB}[\alpha_1,\eta,\nu]}{\partial \eta^2} & \frac{\partial^2 s_{2RSB}[\alpha_1,\eta,\nu]}{\partial \eta \partial \nu} \\ \frac{\partial^2 s_{2RSB}[\alpha_1,\eta,\nu]}{\partial \alpha_1 \partial nu} & \frac{\partial^2 s_{2RSB}[\alpha_1,\eta,\nu]}{\partial \nu \partial \eta} & \frac{\partial^2 s_{2RSB}[\alpha_1,\eta,\nu]}{\partial \nu^2} \end{bmatrix} \begin{bmatrix} \frac{\partial \alpha_1}{\partial \widehat{\varphi}} \\ \frac{\partial \eta}{\partial \widehat{\varphi}} \\ \frac{\partial \nu}{\partial \widehat{\varphi}} \end{bmatrix} + \begin{bmatrix} \frac{\partial^2 s_{2RSB}[\alpha_1,\eta,\nu]}{\partial \alpha_1 \partial \widehat{\varphi}} \\ \frac{\partial^2 s_{2RSB}[\alpha_1,\eta,\nu]}{\partial \eta \partial \widehat{\varphi}} \\ \frac{\partial^2 s_{2RSB}[\alpha_1,\eta,\nu]}{\partial \nu \partial \widehat{\varphi}} \end{bmatrix} \tag{4.234}$$

and we have again that at the 2RSB threshold $\widehat{\varphi}_{th}^{2RSB}$ we must have that

$$\det \begin{bmatrix} \frac{\partial^2 s_{2RSB}[\alpha_1,\eta,\nu]}{\partial \alpha_1^2} & \frac{\partial^2 s_{2RSB}[\alpha_1,\eta,\nu]}{\partial \alpha_1 \partial \eta} & \frac{\partial^2 s_{2RSB}[\alpha_1,\eta,\nu]}{\partial \alpha_1 \partial \nu} \\ \frac{\partial^2 s_{2RSB}[\alpha_1,\eta,\nu]}{\partial \alpha_1 \partial \eta} & \frac{\partial^2 s_{2RSB}[\alpha_1,\eta,\nu]}{\partial \eta^2} & \frac{\partial^2 s_{2RSB}[\alpha_1,\eta,\nu]}{\partial \eta \partial \nu} \\ \frac{\partial^2 s_{2RSB}[\alpha_1,\eta,\nu]}{\partial \alpha_1 \partial nu} & \frac{\partial^2 s_{2RSB}[\alpha_1,\eta,\nu]}{\partial \nu \partial \eta} & \frac{\partial^2 s_{2RSB}[\alpha_1,\eta,\nu]}{\partial \nu^2} \end{bmatrix} = 0 \tag{4.235}$$

that is the vanishing of the longitudinal eigenvalue at the 2RSB level.

4.14 Numerical solution of the fullRSB equation

In the previous sections we derived a set of variational equations to study the fullRSB solution. The purpose of this section is to review the iterative equation that has been solved to obtain the numerical solution of such equations. Let us start again from the variational equations at fixed kRSB.

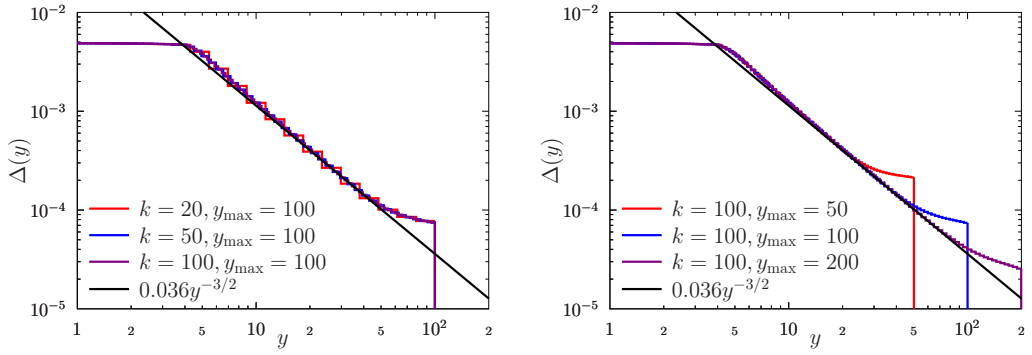

Figure 4.14. The numerical findings for the function $\Delta(y)$ at $m = 0$ and $\widehat{\varphi} = 10$ as can be obtained by solving numerically Eq. 4.240. On the left we plot the results for fixed $y_{\max} = 100$ and $k = 20, 50, 100$, which show that the fullRSB limit is approached smoothly. On the right we plot the results for fixed $k = 100$ and $y_{\max} = 50, 100, 200$, which show that for large $y_{\max}$ the cutoff at large y disappears and the power law regime seems to be reached. However note that the power low scaling is valid for one decade which means that is not very robust. The power law fit is done with $\Delta(y) \sim 0.036 y^{-\sigma}$ that implies that $\Delta_{EA} \sim m^{-\sigma}$ with $\sigma \sim 3/2$. However let us underline that this result is not definitive and must be considered as preliminary. Further numerical investigation must be done in order to see what happens for larger values of y.

These are

$$
\begin{aligned}
\mathcal{S}_{\rm kRSB} &= \sum_{i=1}^{k} \left(\frac{m}{m_i} - \frac{m}{m_{i-1}} \right) \log(\widehat{G}_i/m) - \widehat{\varphi}\, e^{-\widehat{\Delta}_1/2} \int_{-\infty}^{\infty} {\rm d}h\, e^h \left\{ 1 - e^{m f(m_1,h)} \right\} \ , \\
\widehat{\Delta}_i &= \frac{\widehat{G}_i}{m_i} + \sum_{j=i+1}^{k} \left(\frac{1}{m_j} - \frac{1}{m_{j-1}} \right) \widehat{G}_j \ , \\
f(1,h) &= \log \gamma_{\widehat{\Delta}_k} \star \theta(h) = \log \Theta \left(\frac{h}{\sqrt{2\widehat{\Delta}_k}} \right) \ , \\
f(m_i,h) &= \frac{1}{m_i} \log \left[\gamma_{\widehat{\Delta}_i - \widehat{\Delta}_{i+1}} \star e^{m_i f(m_{i+1},h)} \right] \ , \qquad i = 1 \cdots k-1 \ , \\
P(m_1,h) &= e^h\, e^{m f(m_1,h)} \ , \\
P(m_i,h) &= \int dz P(m_{i-1},z) e^{-m_{i-1} f(m_{i-1},z)} \gamma_{\widehat{\Delta}_{i-1} - \widehat{\Delta}_i}(h-z) e^{m_{i-1} f(m_i,h)} \quad i = 2, \cdots, k \ , \\
\frac{1}{\widehat{G}_i} &= \frac{\widehat{\varphi}}{2} e^{-\widehat{\Delta}_1/2} \int_{-\infty}^{\infty} {\rm d}h \, \Big\{ m_{i-1} P(m_i,h) f'(m_i,h)^2 \\
&\quad - \sum_{j=1}^{i-1} (m_j - m_{j-1}) P(m_j,h) f'(m_j,h)^2 \Big\} \ .
\end{aligned}
\tag{4.236}
$$

Our purpose is to solve these equation in the jamming limit $m \to 0$. To do this we rewrite the equations above by using some scaled variables that remain finite in the $m \to 0$ limit. First of all we introduce $y_i = m_i/m$ (remember that $y_0 = 1$ and that $y_k = 1/m$ diverges with m at jamming and plays here the same role

that usually is played by the temperature in the SK model). Moreover we define $\widehat{f}(y_i,h) = mf(m_i,h)$ and $\widehat{\gamma}_i = \widehat{G}_i/m$ from which it follows that $\widehat{\Delta}_k = m\widehat{\gamma}_k$ while all the other $\widehat{\Delta}_i$ remain finite for $m \to 0$. It is also convenient to introduce $\widehat{P}(y_i,h) = e^{-\widehat{\Delta}_1/2}e^{-h}P(y_i,h)$ Moreover it is simple to show that $\widehat{\Delta}_i - \widehat{\Delta}_{i+1} = (\widehat{\gamma}_i - \widehat{\gamma}_{i+1})/y_i$. The variational equations can be rewritten in terms of these new variables

$$
\begin{aligned}
\mathcal{S}_{\rm kRSB} &= \sum_{i=1}^{k}\left(\frac{1}{y_i}-\frac{1}{y_{i-1}}\right)\log\widehat{\gamma}_i - \widehat{\varphi}\,e^{-\widehat{\Delta}_1/2}\int_{-\infty}^{\infty}{\rm d}h\,e^h\left\{1-e^{\widehat{f}(y_1,h)}\right\}\ ,\\
\widehat{\Delta}_i &= \frac{\widehat{\gamma}_i}{y_i} + \sum_{j=i+1}^{k}\left(\frac{1}{y_j}-\frac{1}{y_{j-1}}\right)\widehat{\gamma}_j\ ,\\
\widehat{f}(1/m,h) &= m\log\Theta\left(\frac{h}{\sqrt{2m\widehat{\gamma}_k}}\right)\ ,\\
\widehat{f}(y_i,h) &= \frac{1}{y_i}\log\left[\gamma_{(\widehat{\gamma}_i-\widehat{\gamma}_{i+1})/y_i}\star e^{y_i\widehat{f}(y_{i+1},h)}\right]\ , \qquad i=1\cdots k-1\ ,\\
\widehat{P}(y_1,h) &= e^{-\widehat{\Delta}_1/2}e^{\widehat{f}(y_1,h)}\ ,\\
\widehat{P}(y_i,h) &= \int dz\,e^{z-h}\,\widehat{P}(y_{i-1},z)e^{-y_{i-1}\widehat{f}(y_{i-1},z)}\times\\
&\quad\times\gamma_{(\widehat{\gamma}_{i-1}-\widehat{\gamma}_i)/y_{i-1}}(h-z)e^{y_{i-1}\widehat{f}(y_i,h)} \qquad i=2,\cdots,k\ ,\\
\widehat{\kappa}_i &= \frac{\widehat{\varphi}}{2}\int_{-\infty}^{\infty}{\rm d}h\,e^h\,\widehat{P}(y_i,h)\widehat{f}'(y_i,h)^2\ ,\\
\frac{1}{\widehat{\gamma}_i} &= y_{i-1}\widehat{\kappa}_i - \sum_{j=1}^{i-1}(y_j-y_{j-1})\widehat{\kappa}_j\ .
\end{aligned}
$$

We would now want to investigate the asymptotic behavior of the functions that appear above for $h \to \pm\infty$. Let us consider the function $\widehat{f}(y_i,h)$. By using the initial condition we have that $\widehat{f}(1/m, h\to\infty) = 0$ and $\widehat{f}(1/m, h\to-\infty) \sim -h^2/(2\widehat{\gamma}_k)$. If we put this asymptotic behaviors in the evolution equation for $\widehat{f}(y_i,h)$ we can show that

$$
\begin{aligned}
\widehat{f}(y_i, h\to-\infty) &\sim -h^2/(2\widehat{\gamma}_i)\ ,\\
\widehat{f}(y_i, h\to\infty) &= 0\ .
\end{aligned}
\tag{4.237}
$$

It follows that $\widehat{P}(y_1, h\to-\infty) = 0$ while $\widehat{P}(y_1, h\to\infty) = e^{-\widehat{\Delta}_1/2}$. This means that if we look at the recurrence equation for $\widehat{P}(y_i,h)$ we can see that

$$
\begin{aligned}
\widehat{P}(y_i, h\to-\infty) &= 0\ ,\\
\widehat{P}(y_i, h\to\infty) &= e^{-\widehat{\Delta}_i/2}\ .
\end{aligned}
\tag{4.238}
$$

Let us now consider the change of variables

$$
\widehat{f}(y_i,h) = -\frac{h^2\theta(-h)}{2\widehat{\gamma}_i} + \widehat{j}(y_i,h)\ . \tag{4.239}
$$

The final version of the variational equations is then

$$
\begin{aligned}
\mathcal{S}_{\rm kRSB} &= \sum_{i=1}^{k}\left(\frac{1}{y_i}-\frac{1}{y_{i-1}}\right)\log\widehat{\gamma}_i - \widehat{\varphi}\,e^{-\widehat{\Delta}_1/2}\int_{-\infty}^{\infty}\mathrm{d}h\,e^{h}\left\{1-e^{-\frac{h^2\theta(-h)}{2\widehat{\gamma}_1}+\widehat{j}(y_1,h)}\right\}\,,\\
\widehat{\Delta}_i &= \frac{\widehat{\gamma}_i}{y_i}+\sum_{j=i+1}^{k}\left(\frac{1}{y_j}-\frac{1}{y_{j-1}}\right)\widehat{\gamma}_j\,,\\
\widehat{j}(1/m,h) &= m\log\Theta\left(\frac{h}{\sqrt{2m\widehat{\gamma}_k}}\right)+\frac{h^2\theta(-h)}{2\widehat{\gamma}_k}\,,\\
\widehat{j}(y_i,h) &= \frac{1}{y_i}\log\left[\int_{-\infty}^{\infty}dz\,K_{\widehat{\gamma}_i,\widehat{\gamma}_{i+1},y_i}(h,z)\,e^{y_i\widehat{j}(y_{i+1},z)}\right]\,,\qquad i=1\cdots k-1\,,\\
\widehat{P}(y_1,h) &= e^{-\widehat{\Delta}_1/2-\frac{h^2\theta(-h)}{2\widehat{\gamma}_1}+\widehat{j}(y_1,h)}\,,\\
\widehat{P}(y_i,h) &= \int dz\,K_{\widehat{\gamma}_{i-1},\widehat{\gamma}_i,y_{i-1}}(z,h)\,\widehat{P}(y_{i-1},z)\,e^{z-h}\times\\
&\quad\times e^{-y_{i-1}\widehat{j}(y_{i-1},z)+y_{i-1}\widehat{j}(y_i,h)}\qquad i=2,\cdots,k\,,\\
\widehat{\kappa}_i &= \frac{\widehat{\varphi}}{2}\int_{-\infty}^{\infty}\mathrm{d}h\,e^{h}\,\widehat{P}(y_i,h)\left(-\frac{h\theta(-h)}{\widehat{\gamma}_i}+\widehat{j}'(y_i,h)\right)^2\,,\\
\frac{1}{\widehat{\gamma}_i} &= y_{i-1}\widehat{\kappa}_i-\sum_{j=1}^{i-1}(y_j-y_{j-1})\widehat{\kappa}_j\,.
\end{aligned}
\tag{4.240}
$$

where the kernel

$$
K_{\widehat{\gamma},\widehat{\gamma}',y}(h,z)=\frac{\exp\left[-\frac{y}{2}\left(\frac{(z-h)^2}{\widehat{\gamma}-\widehat{\gamma}'}-\frac{h^2\theta(-h)}{\widehat{\gamma}}+\frac{z^2\theta(-z)}{\widehat{\gamma}'}\right)\right]}{\sqrt{2\pi(\widehat{\gamma}-\widehat{\gamma}')/y}}
\tag{4.241}
$$

is *not* a symmetric function of h and z, nor a function of $h-z$. However, the advantage of this formulation is that the kernel K is an almost Gaussian function which is well behaved, and all the other functions that appear in the integrals are smooth. An important fact is that Eqs. (4.240) have a smooth limit when $m\to 0$. In fact we can first set $1/y_k=m$, $\widehat{\Delta}_k=0$. Then, by using Eq. 4.216 we can show that $j(y_k,h)=0$. Remarkably all the other equations coincides with the case $m>0$.

It is very easy to take the continuum limit of the equations above. It is given by

$$
\begin{aligned}
\mathcal{S}_{\infty\mathrm{RSB}} &= -\int_1^{1/m} \frac{\mathrm{d}y}{y^2} \log\left[\gamma(y)\right] - \widehat{\varphi}\, e^{-\Delta(1)/2} \int_{-\infty}^{\infty} \mathrm{d}h\, e^h [1 - e^{-\frac{h^2\theta(-h)}{2\gamma(1)} + \widehat{j}(1,h)}] \;, \\
\Delta(y) &= \frac{\gamma(y)}{y} - \int_y^{1/m} \frac{dz}{z^2}\gamma(z) \;, \qquad \Leftrightarrow \qquad \gamma(y) = y\Delta(y) + \int_y^{1/m} \mathrm{d}z \Delta(z) \;, \\
\widehat{j}(1/m,h) &= m \log \Theta\left(\frac{h}{\sqrt{2m\gamma(1/m)}}\right) + \frac{h^2\theta(-h)}{2\gamma(1/m)} \;, \\
\frac{\partial \widehat{j}(y,h)}{\partial y} &= \frac{1}{2}\frac{\dot{\gamma}(y)}{y}\left[-\frac{\theta(-h)}{\gamma(y)} + \frac{\partial^2 \widehat{j}(y,h)}{\partial h^2} - 2y\frac{h\theta(-h)}{\gamma(y)}\frac{\partial \widehat{j}(y,h)}{\partial h} + y\left(\frac{\partial \widehat{j}(y,h)}{\partial h}\right)^2\right] \;, \\
\widehat{P}(1,h) &= e^{-\Delta(1)/2 - \frac{h^2\theta(-h)}{2\gamma(1)} + \widehat{j}(1,h)} \;, \\
\frac{\partial \widehat{P}(y,h)}{\partial y} &= -\frac{1}{2}\frac{\dot{\gamma}(y)}{y} e^{-h}\left\{\frac{\partial^2[e^h \widehat{P}(y,h)]}{\partial h^2}\right. \\
&\qquad \left. -2y\frac{\partial}{\partial h}\left[e^h \widehat{P}(y,h)\left(-\frac{h\theta(-h)}{\gamma(y)} + \frac{\partial \widehat{j}(y,h)}{\partial h}\right)\right]\right\} \;, \\
\kappa(y) &= \frac{\widehat{\varphi}}{2}\int_{-\infty}^{\infty} \mathrm{d}h\, e^h\, \widehat{P}(y,h)\left(-\frac{h\theta(-h)}{\gamma(y)} + \widehat{j}'(y,h)\right)^2 \;, \\
\frac{1}{\gamma(y)} &= y\kappa(y) - \int_1^y dz \kappa(z) \;.
\end{aligned}
\tag{4.242}
$$

Let us come back to the iterative equations. They can be solved at $m = 0$ iteratively for any value of the breaking number k by simply setting the initial condition $\hat{j}(\infty, h) = 0$. Moreover we need to introduce a cutoff in y that we call $y_{\max}$ that acts effectively as a finite m. In order to study the fullRSB limit and the jamming limit we need to make both k and $y_{\max}$ as large as possible. We fix the density to $\widehat{\varphi} = 10$, which is a value large enough that we are sure to be above the fullRSB threshold. We report in Fig. 4.14 the numerical finding for the function $\Delta(x)$ obtained for different values of the number of replica symmetry breaking schemes k and for different values of the cutoff $y_{\max}$. From the plots we can see that we can reach the continuum limit in which both k and $y_{\max}$ diverges. Moreover we see that as the cutoff $y_{\max}$ is increased, the curves approach a limiting solution that can be fitted with a power law behavior $\Delta(y) \sim y^{-\sigma}$ with $\sigma \sim 3/2$. However let us note that the power law behavior is seen only on one decade of y and it is not clear if we are already in the asymptotic regime or not. In fact if we plot $\gamma(y)$ instead of $\Delta(y)$ (see Fig.4.15) we can see that at very large values of y the power law exponent cannot be estimated with high precision due to the fact that it is very difficult to disentangle the effect of the finite cutoff $y_{\max}$ with the true asymptotic behavior. Note that if we fit the curves for $\Delta(y)$ with $\Delta(y) \sim y^{-\sigma}$ then $\gamma(y) \sim y^{-\sigma+1}$.

The physical implication of this analysis can be understood as follows. In the sections above we have discussed that taking $m \to 0$ is equivalent to take the jamming limit being $m \sim 1/p$. Moreover we have argued that a finite small m is equivalent to a finite large cutoff $y_{\max} \sim m^{-1} \sim p$. The Debye-Waller factor $\widehat{\Delta}_{EA}$ is then inferred from the power law as $\widehat{\Delta}_{EA} \sim \Delta(y \sim 1/m) \sim m^{\sigma} \sim p^{-\sigma}$.

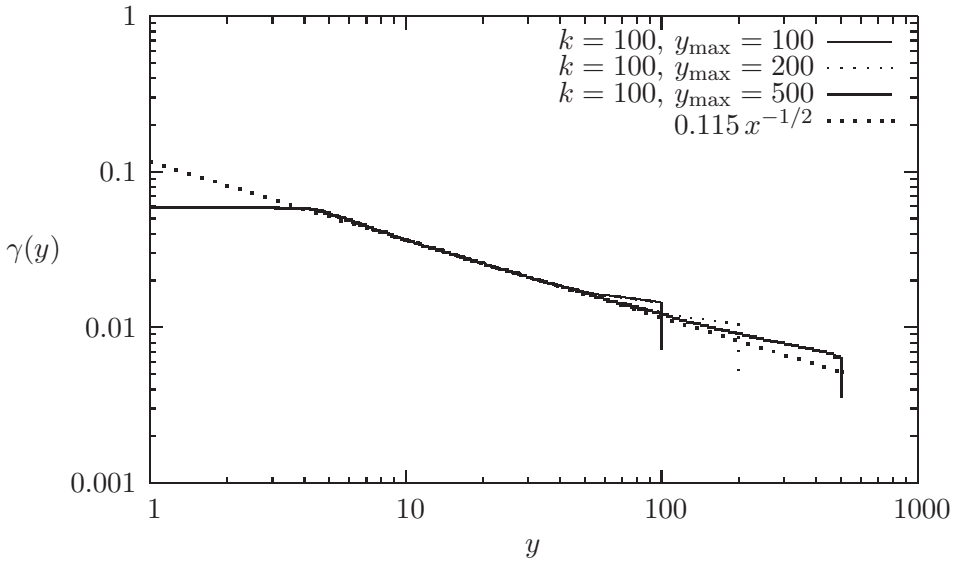

Figure 4.15. The plot of $\gamma(y)$ for different values of $y_{\max}$. Here we can see that for large values of y, the asymptotic behavior of $\gamma(y)$ deviates from the guessed asymptotic behavior derived from $\sigma = 3/2$. It is not clear if this is an effect of the cutoff $y_{\max}$ or the power law regime in which $\sigma = 3/2$ is a preasymptotic regime that will be followed by a power law with $\sigma \leq 3/2$. To understand this we must improve the numerical solution of the equations and then we should try to extract the asymptotic behavior analytically.

Our numerical findings seems to point towards a value of σ close to $\sigma \sim 3/2$ and consistent with alternative analytical arguments and numerical observations [91, 26]. However we remark that the actual value of σ cannot be obtained with very high precision but a more accurate numerical analysis is needed. Moreover let us underline that the argument above is not rigorous. In fact we are estimating the behavior of $\widehat{\Delta}_{EA}$ for finite m with the solution at $m = 0$ (but with a finite cutoff). In order to check the results above we should solve the fullRSB equations at m finite and the we should look directly to the behavior of $\widehat{\Delta}_{EA}$ with m. In fact at finite m the profile of $\Delta(x)$ will probably contain two flat pieces, one at $y > 1$ and the other one at $y < 1/m$. The size of these two pieces is controlled by two breaking points and it is important to see what is the behavior of them as a function of m. This means that our argument on the scaling of $\widehat{\Delta}_{EA}$ with the pressure may be wrong once the correct solution at finite small m is taken into account; this means that it must be considered only as a preliminary argument that will justify future research in this direction.

4.15 Conclusion and Perspectives

In this chapter we have studied the theory of hard spheres in the limit of large space dimension. Our analysis has clarified the characterization of the phase diagram. In particular, the first important point that has emerged is that the 1RSB solution is unstable in a certain region of the phase diagram. The instability affects deeply the jamming region, that is the one in which $m \to 0$, and is responsible for a Gardner

transition of the equilibrium glass at very high density.

However we expect that all the metastable states undergo to a Gardner transition but the calculation we have done is not sufficient to study this more detailed situation. In particular if we want to obtain the Gardner point for the non-equilibrium states, we need to perform a state following calculation and this is one of the possible future work that must be done. Let us also underline that hard spheres are prototypes for simple liquids and glasses so that we can expect that the Gardner transition can be be a general phenomenon in glass physics.

Moreover, in characterizing the phase diagram we have seen that it is possible in the unstable region, to search for replica symmetry breaking solutions that go beyond the simplest 1RSB ansatz. We started this approach by looking at the 2RSB solution and we have seen that there exist a point on the instability line, above which a 2RSB (and possibly a fullRSB) solution does exist. Moreover, at the 2RSB level we have computed the details of the jamming limit and we have obtained the new value of the threshold reduced packing fraction at which the first jammed states appear. The value of this new threshold point is actually slightly above the one that can be obtained in the 1RSB scheme. Moreover we have looked at the general case in which we search for a fullRSB solution. We have performed a fullRSB calculation of the replicated entropy and we have derived the Parisi equation for the hard sphere model. We have solved numerically these equations and we have shown that the scaling of the Debye-Waller factor with the pressure seems to be consistent with $\widehat{\Delta}_{EA} \sim p^{-\sigma}$ where σ is close to $\sigma \sim 3/2$. However the numerical analysis is very preliminary and a more detailed study of the fullRSB equation is required in order to establish this results on more solid grounds.

Let us also note that an important consideration is that here the picture that comes from the Gardner instability tells us that the phenomenology of a glass with this kind of behavior is reacher than the one that comes form the understanding of the spherical p-spin model. The meaning of the fullRSB phase is the following. The 1RSB calculation tells us that the entropy landscape is built by a very large number of 1RSB metastable glassy states that are described by well formed minima in the same landscape. However at some packing fraction the bottom of these minima breaks in a manner that is similar to what happens in the Sherrington-Kirkpatrick model. The final picture in the fullRSB phase is the one in which the old 1RSB states become metabasins of fullRSB states. The complexity curve in the unstable phase (that has not been given here) does not tell us the number of metastable states, but the number of metabasins of states.

The main work to do now is first to improve the numerical solution of the fullRSB equations in other to explore more decades in y in the plot of $\Delta(y)$. This is important to confirm or not our preliminary results on the scaling of the Debye-Waller factor with the pressure. Moreover we have solved numerically the equation in the $m \to 0$ limit but with a cutoff at large y. It is important to solve numerically the fullRSB equations at finite but small m in order to check that the results we have obtained are not changed and that our argument for the scaling of the Debye-Waller factor is correct. Finally an analytical derivation of the behavior of $\Delta(y)$ as y diverges (namely the exponent σ) from the fullRSB equations is mandatory in order to confirm the numerical findings. This could be done by following the same strategy of [140] in which the zero temperature scaling solution of the Sherrington-

Kirkpatrick model has been discussed. This is important for two reasons. First of all we need to understand better the behavior of the fullRSB solution. Moreover, once definitive results on that are established, we can try to extract all the physical consequences on the jamming physics of hard spheres.

Chapter 5

Mode-coupling dynamics for a quasi continuous transition

In this chapter we study the mode-coupling dynamics in a situation in which the dynamical transition is slightly discontinuous, actually in the limit in which it is becoming continuous. The prototypical (mean field) dynamical glass transition, at the mode-coupling level, is the one in which one sees the characteristic two steps relaxation with an infinite plateau appearing at the transition point.

However there is the limiting case in which the height of the plateau is shrinking to the infinite time limit of the correlation function so that the transition becomes continuous. This kind of situation is the standard one for spin glass models that undergo to a fullRSB transition [132]. In the framework of MCT, Götze and Sjogren [86] have studied a model where the transition can be tuned smoothly from a discontinuous to a continuous one. In the MCT jargon, the point in which the transition becomes continuous is called an A_3 singularity, according to the Arnol'd's classification.

The discontinuous/continuous crossover can be found in many different situations. For example this behavior appears in spin glass models in a magnetic field, kinetic models on random graphs [155, 154], liquids in porous media [106, 107, 33]. In [86] this problem has been addressed in MCT and a series of results has been produced especially for the characterization of the β-relaxation dynamics. However a complete description of the α regime is lacking even if some first results have been obtained in [87, 160]. In this chapter we will give a complete characterization of the dynamics in this regime and we will found its universal form. The content of this chapter follows strictly [75].

Note that apparently this chapter has not so much in common with the rest of the thesis. The original motivation for this study is however linked to the study of dynamical fluctuations. In fact we have seen in the introductory chapter that the perturbative series for the dynamical susceptibilities is difficult to resum leading to a difficult estimation of dynamical four point functions in the long time α regime. However we can hope that there are some lucky cases in which exact non perturbative results can be obtained. We tried to see if the particular situation of having a quasi-continuous transition could be of any help in this job. We have found that in this kind of dynamical transition, the calculations are easier for the case of the

dynamical correlation functions but it remains open the question if we can gain something also in the calculation of the four point correlation functions.

5.1 Mode-coupling theory near a continuous transition

In this section we discuss the schematic treatment of MCT close to an A_3 singularity. Let us introduce a dynamical correlation function $C(t)$. This can be the dynamical autocorrelation function in spin-glass models, or the normalized dynamical structure factor computed on the peak of the static structure factor for structural glasses. The most general schematic MCT equation for $C(t)$ can be written in the following way

$$\frac{dC(t)}{dt} = -TC(t) + \frac{1}{T}(1 - C(t))\hat{M}[C(t)] - \frac{1}{T}\int_0^t \mathrm{d}u \, \frac{\mathrm{d}C(u)}{\mathrm{d}u} \left(\hat{M}[C(t-u)] - \hat{M}[C(t)]\right) , \tag{5.1}$$

and we have defined the memory kernel $\hat{M}[C(t)]$. The latter quantity depends on the control parameter that drives the transition, and on the details of the system. For example, we have seen in the previous chapter the standard example of the p-spin spherical model where $\hat{M}[q] = pq^{p-1}/2$. We want to analyze the above equations when we approach the dynamical point (provided of course that the details of the potential are such that a dynamical transition exists) in the long time regime where $C(t)$ escapes from the plateau. We will suppose that $C(0) = 1$ and this will not restrict our analysis.

This general equation is suitable for the study of many kinds of transitions and the relevant object for this is the memory kernel. By fine tuning the parameters that build $\hat{M}[C(t)]$ we can have a discontinuous or a continuuous dynamical transition. Standard examples for the explicit form of the memory kernel are the schematic F_{12} and F_{13} models [86] that are specified respectively by $\hat{M}(q) = \hat{v}_1 q + \hat{v}_2 q^2$ and $\hat{M}(q) = \hat{v}_1 q + \hat{v}_3 q^3$. The infinite time limit of the correlation function at the dynamical point must satisfy the following equation

$$q = (1 - q)M[q]. \tag{5.2}$$

where, for convenience we have denoted $M[q] = \hat{M}[q]/T^2$. In the standard liquid-glass transition, Eq. 5.2 admits always the trivial solution $q = 0$ but at the dynamical point it develops a non-trivial glassy solution with $q > 0$. Moreover the same equation could be obtained from replica theory by analyzing the Franz-Parisi potential and by looking at the equation for the non trivial saddle, or by analyzing the value at which the real replica potential of the Monasson method admits a non-trivial saddle point solution. A maximum theorem of MCT [84] states that if more then one non trivial glassy solution exist, the infinite time limit of the dynamical correlation function at the dynamical point is given by the largest solution, provided that it is in between 0 and 1. The different kind of dynamical transitions are connected on the way in which the non trivial glassy solutions develop. They will be reviewed in the next section.

5.1.1 Mode-coupling equations near an A_2 singularity

The standard two-steps relaxation is described by the so called A_2 singularity. The typical behavior of the solutions of Eq. 5.2 is that it admits a trivial solution q_0

everywhere in the space of the control parameters, but at the dynamical point, for example, in lowering the temperature at T_d, a non trivial solution with $q = q_1 > q_0$ appears. The dynamical correlation function is such that it decays to the trivial solution q_0 if $T > T_d$ and it remains stuck at $q_1 > q_0$ at T_d. The F_{13} is the prototype for this kind of behavior. If the transition is such that q_0 is finite, we call it a glass-glass transition, otherwise if $q_0 = 0$ the transition is liquid-glass. The discussion above implies that the solution $q = q_1$ is a solution of Eq. 5.2 with double multiplicity so that it satisfies also

$$1 = \frac{d}{dq}(1-q)M[q]|_{q=q_1} \tag{5.3}$$

In the replica method, this equation is exactly the marginal stability condition that ensure that the non-trivial stationary point of the Franz-Parisi potential is also a saddle. To prove the statement above we can first notice that physically we must require $\mathrm{d}C/\mathrm{d}t \leq 0$ so that

$$-TC(t) + \frac{1}{T}(1-C(t))\hat{M}[C(t)] \leq 0 \tag{5.4}$$

If we want that a glassy solution appears we must have that the function on the left hand side of the previous equation, when considered as a function of $C(t)$, must have a maximum between zero and one. The inequality is always satisfied in the liquid phase but at the dynamical point the height of the maximum of this function touches zero and the inequality is no more satisfied. The system remains stuck in the metastable glassy state [39]. Moreover from this analysis it follows that the value of the maximum is the one at which the correlation function converges at large times so that we have the Eq. 5.3.

The description of the dynamics in the A_2 case can be done by dividing the problem in the study of the β regime where there is the relaxation of $C(t)$ up to q_1 and in the α regime where it finally decays to q_0. In the β regime we can characterize the dynamics by doing an expansion of the MCT equation in $C(t) = q_1 + \delta C(t)$ and by looking at a power law behavior for $\delta C(t)$ on the same lines of Sec. 3.5, see also [83]. In the α region the dynamical correlation function $C(t)$ satisfies the "time-temperature superposition principle", namely it has a scaling form

$$C(t) \approx \mathbf{C}(t/\tau_\alpha) \tag{5.5}$$

where $\tau_\alpha(T) \sim |\sigma|^{-\gamma}$ is the relaxation time that of course is a function of the distance from the critical point. At the mode-coupling level it is possible to prove that

$$\gamma = \frac{1}{2a} + \frac{1}{2b} \ . \tag{5.6}$$

The function $\mathbf{C}(u)$ is the scaling function independent on the temperature and can be computed by setting to zero the derivative term in Eq. 5.1

$$0 = -TC(t) + \frac{1}{T}(1-C(t))\hat{M}[C(t)] - \frac{1}{T}\int_0^t \mathrm{d}u \, \frac{\mathrm{d}C(u)}{\mathrm{d}u}\left(\hat{M}[C(t-u)] - \hat{M}[C(t)]\right) \ , \tag{5.7}$$

The fact that in the α regime the derivative term is subdominant is not always true. In particular we have discussed that the mode-coupling equation that describe the dynamics of the $p = 2$ spherical model are of the same form of Eq. 5.1 but to study the long time regime we cannot neglect the derivative term. However we have also said that from the static solution of this model, we know that the dynamical transition does not coincide with the appearance of an exponential number of metastable states and in the end this model is not glassy.

5.1.2 Mode-coupling equations near an A_3 singularity

In the previous section we have introduced the A_2 singularity. However it may happen that q_1 collapses on q_0. This endpoint of the A_2 singularity is called an A_3 singularity. In this case the general structure of the Eq. 5.2 can be studied by expanding it around some finite value q_c and it turns out that the coefficients of the constant, linear and quadratic terms are small when expressed in terms of the control parameters. If we apply a shift to q_c by following [86] so that the quadratic part vanishes, we obtain the following equation

$$0 = \xi + \eta\delta q - \mu\delta q^3 \,. \tag{5.8}$$

The quantities ξ and η and μ can be expressed in terms of the derivative of the memory kernel. While ξ and η vanish at the transition point, μ remains finite.

If we look at the solutions of Eq. 5.8 in the plane (η, ξ) we have

- The solution $\delta q = 0$ is the only solution on the line $(\xi = 0, \eta < 0)$.
- Going counter-clockwise, on the critical line $\xi = -2\eta(\eta/3\mu)^{1/2}$ two solutions appear discontinuously so that this line is of classical A_2 singularities so that the dynamics is described by what is written in the previous section.
- Going again counter-clockwise, another critical line is encountered where $\xi = 2\eta(\eta/3\mu)^{1/2}$ and $\eta > 0$.

It follows that near the A_3 singularity δq is small so that if $q_c > 0$ the critical line describes a glass-glass transition. Only in the case where $q_c = 0$, as it happens in the F_{12} model, we have a liquid-glass transition. As said before, it has been shown in [86] that at the critical point we have $\xi = \eta = 0$ and that $C(t)$ displays logarithmic decay

$$C(t) = \frac{\rho^2}{\ln^2 t} \tag{5.9}$$

where $\rho^2 = 4\pi^2/(6\mu)$.

If we are not exactly at the critical point so that ξ and η are not exactly zero, the times, over which we can appreciate this fact can be computed directly from Eq. 5.8

$$t_\xi \propto \exp[\rho(\mu/|\xi|)^{1/6}] \tag{5.10}$$

$$t_\eta \propto \exp[\rho(\mu/|\eta|)^{1/4}] \,. \tag{5.11}$$

On this time scale we have

$$C(t) = \rho^2 p(\ln(t/t_1)) \tag{5.12}$$

and t_1 cannot be fixed because the equation that determines it is scale invariant and $p(y)$ is the solution of [85]

$$p' = -(4p^3 - g_2 p - g_3)^{1/2} \tag{5.13}$$

and we have introduced $g_2 \equiv 4\eta/(\mu\rho^4)$ and $g_3 \equiv 4\xi/\mu(\rho^6)$. A complete characterization of the dynamics in this case in the α regime is still lacking at the purpose of this chapter is to discuss it. In [87] this problem was studied by producing a series expansion in $\ln^k t$ beyond the leading order that gave $\ln t$ and on the line $(\eta = 0, \xi < 0)$. In what will follows we will analyze what happens on the critical line $\xi = -2\eta(\eta/3\mu)^{1/2}$.

5.1.3 α-relaxation near weakly discontinuous transitions

The regime we want to study is such that we are close to an A_2 singularity in the control parameter space (so that we can discuss the α regime) but this transition is also very close to the end point of the critical line so that it is close to an A_3 singularity where q_1 is very close to q_0. For small $q_1 - q_0$ the exponent parameter

$$\lambda = \frac{\hat{M}''(q_1)}{2(\hat{M}'(q_1))^{3/2}}\,, \tag{5.14}$$

is close to one and both the exponents a and b are close to zero. In particular we have at leading order

$$a = b = \sqrt{\frac{6}{\pi^2}(1-\lambda)} \sim \sqrt{q_1 - q_0} \tag{5.15}$$

This means that a natural way to parametrize the distance from the A_3 endpoint is given by the actual value of b and $q_1 - q_0$ will be a vanishing function of b when $b \to 0$.

In [85] it has been underlined that $\mathbf{C}(t)$ can be expanded in power series of t^b at small times and the coefficients of the expansion can be computed recursively. Unfortunately this expansion is not convergent. However we can solve exactly the MCT equation in the α regime in the limit $b \to 0$. Let us suppose that

$$\lim_{\substack{b\to 0;\ t\to\infty \\ y=(t/\tau_\alpha)^b}} (\mathbf{C}(t,b) - q_0)/(q_1 - q_0) = G(y)\,, \tag{5.16}$$

where $G(y)$ is a well behaved function. Eq. 5.7 can be rewritten as

$$C(t) = M[C(t)](1 - C(t)) - \int_0^t \mathrm{d}u\, \frac{\mathrm{d}C(u)}{\mathrm{d}u}\,(M[C(t-u)] - M[C(t)])\ . \tag{5.17}$$

and let us consider the various terms that appear in the above equation in the limit $b \to 0$.

The memory kernel can be expanded as

$$\begin{aligned} M[C(t-u)] - M[C(t)] &\simeq M'[C(t)](C(t-u) - C(t)) \\ &\simeq byM'(q_1)(q_1 - q_0)\frac{\mathrm{d}G(y)}{\mathrm{d}y}\ln\left(1 - \frac{u}{t}\right) \end{aligned} \tag{5.18}$$

Moreover we have

$$C'(u) = \simeq \frac{b}{u} y (q_1 - q_0) \frac{\mathrm{d}G(y)}{\mathrm{d}y}. \tag{5.19}$$

Because we are close to the A_2 transition point we have that $N(C) = -C + (1 - C)M(C)$ must have a single root in $C = q_0$ and a double root in $C = q_1$ at the dynamical transition point. Because we are also close to the A_3 singularities we can take advantage from the fact that $q_1 - q_0$ is small and we can develop $N(C) = -A(C - q_0)(q_1 - C)^2$ where $A = \frac{M'(q_1)(1-\lambda)}{q_1 - q_0}$. In the end, the leading order of the MCT equation can be written as

$$0 = M'(q_1)(q_1 - q_0)^2 [(1-\lambda)G(1-G)^2 - (b\,y)^2 \left[G'(y)\right]^2 \int_0^1 \frac{\mathrm{d}u}{u} \ln(1-u)\,. \tag{5.20}$$

Because $1 - \lambda = b^2 \int_0^1 \frac{\mathrm{d}u}{u} \ln(1-u) = b^2 \frac{\pi^2}{6}$ we finally obtain

$$G(1-G)^2 = y^2 \left[G'(y)\right]^2. \tag{5.21}$$

that can be also rewritten as

$$\frac{dG}{\sqrt{G}(1-G)} = -\frac{dy}{y}\,. \tag{5.22}$$

The above equation admits the solution

$$G(y) = \left(\frac{1 - y/y_0}{1 + y/y_0}\right)^2 . \tag{5.23}$$

Due to the scale invariance of the equation in the α regime, the value y_0 cannot be determined from this analysis but can be fixed only by the matching with the β region. Here for convenience we choose $y_0 = 1$. An important point is that the function $G(y)$ starts from one to become zero at $y = y_0$. This is a consequence of the fact that we have taken the limit $b \to 0$. If we are at finite (but small) b we will have that in the final part of the α relaxation, for $y > y_0$, the correlation will decay as $C(y) \sim e^{-A(y/y_0)^{1/b}}$. It is clear that this term is exponentially small as $b \to 0$ and it corresponds to the final exponential relaxation $C(t) \sim e^{-At/t_0}$ where $t_0 = y_0^{1/b}$. In Fig. 5.1 we consider the F_{12} model where $M[C] = \left[(2\lambda - 1)C + C^2\right]/\lambda^2$ and we compare our analytic computation with the Padé approximants for the series expansion of the solution of Eq. 5.7 for small value of b. The line on the bottom is the scaling function $\left(\frac{1-y}{1+y}\right)^2$. Let us underline that even if this result has been obtained for the F_{12} model where $q_c = 0$ this holds also in the case in which we have a glass-glass transition described by the F_{13} model.

5.1.4 The aging regime

The analysis that has been shown up to here can be generalized to the aging regime. If we consider a generalized p-spin spherical model and we put in evidence the

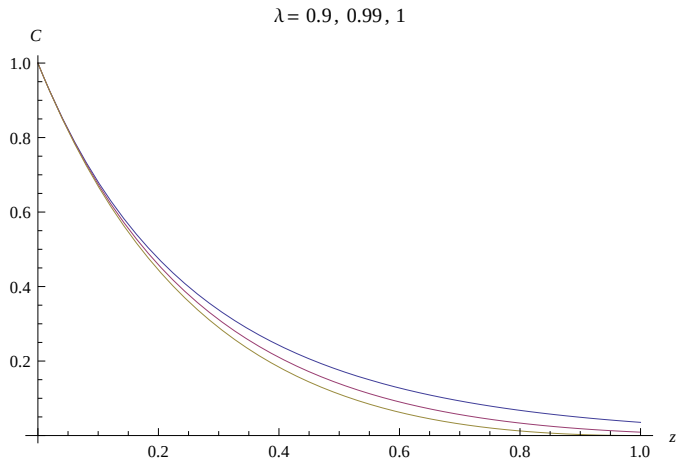

Figure 5.1. Scaling function $G(y)$. From top to bottom $\lambda = 0.9,\ 0.99,\ 1$. The plot is taken from [75].

temperature, the structure of the dynamical equation is similar to the equilibrium case and one has

$$\begin{aligned} 0 = &-TC(t,t') + \beta[q_1 f'(q_1)(1-x) - q_0 f'(q_0)x]C(t,t') \\ &+\beta f'(C(t,t'))(1-q_1) - \beta f'(q_1)(1-x)C(t,t') \\ &-\beta x q_0 f'(q_0) + \beta x f'(C(t,t'))(q_1 - C(t,t')) \\ &-\beta x \int_{t'}^{t} ds\, \frac{\partial C(t',s)}{\partial s}[f'(C(t,s)) - f'(C(t,t'))] \ . \end{aligned} \tag{5.24}$$

Here $f'(c)$ is nothing but the memory kernel of the previous sections. In the equation appears explicitly the fluctuation-dissipation ratio x that is fixed from the marginal stability condition that states that the function

$$\begin{aligned} K(C) = &-TC + \beta[q_1 f'(q_1)(1-x) - q_0 f'(q_0)x]C + \\ &\beta f'(C)(1-q_1) - \beta f'(q_1)(1-x)C - \beta x q_0 f'(q_0) - \beta x f'(C)(q_1 - C) \end{aligned} \tag{5.25}$$

must have a double root in $C = q_1$.

From [51, 52] we know that the above equation is reparametrization invariant and admits a scaling solution of the form $C(t,t') = \mathbf{C}(g(t) - g(t'))$ where $g(t)$ is undetermined. If we make an expansion

$$\mathbf{C}(u) = q_1 + (u)^b \ , \tag{5.26}$$

then we can see that [23]

$$\lambda = \frac{T}{2}\frac{f'''(q_1)}{f''(q_1)^{\frac{3}{2}}} = x\frac{\Gamma(1+b)^2}{\Gamma(1+2b)}. \tag{5.27}$$

As in the equilibrium case we have that if $q_1 - q_0$ is small we can make an expansion $K(C) = A(C - q_0)(q_1 - C)^2)$. The reason is that everything must go as in the equilibrium case because if we think in terms of the off-equilibrium potential it

must have a saddle in $C = q_1$ so that q_1 is a double root of $K(C)$. We suppose that $\mathbf{C}$ is an analytic function of $y = (g(t) - g(t'))^b$: if, for large t, $g''(t)/g'(t)^2 << 1$ then $y = \left(\frac{t-t'}{\tau_{t'}}\right)^b$. We can then define the scaling function

$$G(y) = \lim_{\substack{b\to 0,\ t,t'\to\infty \\ y=(g(t)-g(t'))^b}} \frac{C(t,t') - q_0}{q_1 - q_0} \tag{5.28}$$

and we can do exactly the same analysis as before and verify that $G(y)$ has the same form of the equilibrium case.

5.2 Phenomenological approach to fluctuations

We can use the analysis that we have done in the sections above to study the dynamical fluctuations in the α regime. Let us recall the susceptibilities we introduced in chapter 2

$$\begin{aligned} \chi_{th}(t) &= [\langle C(t)^2\rangle] - [\langle C(t)\rangle^2]\,, \\ \chi_{het}(t) &= [\langle C(t)\rangle^2] - [\langle C(t)\rangle]^2\,, \\ \chi_4 &= [\langle C(t)^2\rangle] - [\langle C(t)\rangle]^2 = \chi_{th} + \chi_{het} \end{aligned} \tag{5.29}$$

Moreover a remarkable result proposed in [14] is that

$$\chi_{th}(t) \propto \frac{\partial C(t)}{\partial T}. \tag{5.30}$$

we know that the divergence of χ_{het} is double the one of χ_{th} in the β regime [74]. Actually this double divergence can be described by a field theory in a random field. The random field encodes the effect of the fluctuations of the initial condition on the dynamics and in particular the effective way to describe them is just by consider a random temperature heterogeneous in space. Although these considerations are valid in the β regime we can try to extend them in the α regime using the time-temperature superposition principle. By having in mind all this we can write

$$\begin{aligned} N\chi_{th}(t) &= \frac{\partial \mathbf{C}(t/\tau(T))}{\partial T}\,, \\ N\chi_{het}(t) &= [\delta T^2]\chi_{th}(t)^2\,. \end{aligned} \tag{5.31}$$

The first one of these equations has been proved in [14] and we remark that it can be proven at the Gaussian level [74]. Using the relation $\tau(T) \sim (T - T_d)^{-\frac{1}{2a}+\frac{1}{2b}}$ and the explicit expression for the correlation function that we derived before we have finally

$$\begin{aligned} \chi_{th}(t) &= 2\frac{1}{T-T_d}(q_1 - q_0)zG'(z) = 2\frac{1}{T-T_d}(q_1 - q_0)\sqrt{G}(1-G)\,, \\ \chi_{het}(t) &= 4[\delta T^2]\frac{1}{(T-T_d)^2}(q_1 - q_0)^2 G(1-G)^2\,. \end{aligned} \tag{5.32}$$

5.3 Conclusions

In this chapter we have analyzed a schematic mode-coupling equation that describes a slightly discontinuous glassy behavior. In general, mode-coupling theory is used to describe the discontinuous aspect of glassy dynamics, namely the appearance of a finite plateau in the dynamical correlation function. This general picture is directly related to the 1RSB static interpretation of glassy dynamics. Here we have analyzed a different picture in which the glass transition can take place. In fact we have seen that there are cases in which the vitrification is described by a plateau in the dynamical correlation function whose height is close asymptotically to zero with respect the long time limit of the dynamical correlation function itself. In particular such a situation can be present both in transitions from liquid to glass and also in glass to glass transitions. We have seen that the quasi-continuous character of the dynamical transition can be used to simplify the MCT equation in the long time regime where they are reparametrization invariant. In this way we have been able to compute the asymptotic solution of the equations. Using this result we tried to investigate the dynamical fluctuations. However we would like to have a full analytical derivation for the behavior of the four point functions. We hope that the quasi-continuum limit will help in simplifying also the full derivation of the fluctuations of the dynamical correlation function and we leave this for future work.

Chapter 6

Conclusions and Perspectives

In this thesis we have discussed several problems and aspects of the physics of glassy systems. The theoretical approach we have discussed is the one provided by the replica theory. We have started with the study of the dynamical fluctuations in the β regime and we have seen how they can be described using a static formalism. This has had the great advantage that we have been able to give a tentative systematic approach to the dynamical glass transition of structural glasses on the standard lines of critical phenomena. In fact by using the potential method we were able to give a Landau expansion of the free energy that can be used to obtain first a Gaussian prediction for the fluctuations of the order parameter and for the critical exponents, and, second, a systematic loop expansion that here has been used to obtain a Ginzburg Criterion. The latter result is very important in practice because it tells where the mean field calculations give reliable predictions and where they fail.

All these results have been derived by analyzing the structure of the soft modes of the Gaussian term of the Landau expansion around the transition point coming from the glass phase. This has been done previously in schematic spin-glass models but in this thesis we have analyzed the structural glass case that is complicated by the presence of the spatial structure of the order parameter. Actually this dependance is the one that is needed in order to define the dynamical correlation length. All the theory we have introduced and discussed is only partially studied. In fact a natural continuation of this chapter would be a systematic analysis of the field theory derived and of the corrections to the Gaussian predictions that here have not been analyzed. As a side product of the analysis of the critical fluctuations we have been able to compute within replica theory, and for the structural glass case, the mode-coupling exponent parameter λ that controls the behavior of the dynamical correlation function in the β regime. This result is quite important because it allows to compare the replica theory prediction with the mode-coupling one. All the results have been derived in the most general setting but to obtain quantitative predictions we needed an approximation for the free energy and we have chosen the hypernetted chain approximation that is the simplest one. Let us underline again that what we have studied is only valid for the fluctuations of the dynamical correlation function in the β regime, namely for times that are such that the correlation function is very close to its plateau value. What happens in the α regime cannot be obtained in this

framework.

This was the first motivation for the study of a new quasi-static approach to the mode-coupling dynamics in the α regime. This is what has been called the Boltzmann Pseudodynamics construction for the long time glassy dynamics. In fact, the important advantage of the replica approach to the theory of fluctuations is that it is a static framework and many static techniques and approximations can be used. In the α regime, we did not have a static prescription to describe the dynamics so that in principle we had to solve the full dynamical equations for the four point dynamical correlation function.

The Pseudodynamics approach solves this problem because it provides a static construction for the whole α relaxation. It is based on the idea that in the long time regime, the dynamics is described by a random walk from one metastable state to another, being each metastable state explored in an ergodic way. Because of this quasi equilibrium idea at the basis of the long time description of glassy dynamics, it is clear that a static construction is possible in principle. The actual realization of all this is in a generalization of the Franz-Parisi potential. We have presented this approach in two cases: the cornerstone case of the p-spin spherical model where everything is known so that we can compare it with known results, and the hypernetted chain approximation to the dynamical transition in structural glasses. In the last case we have seen that the results we have obtained for both the equilibrium regime and the aging one, follow closely the theoretical description provided by the p-spin spherical model. However all this approach, as the one for the theory of fluctuations, is 1RSB in nature. This is not the most general case where fullRSB effects could be important. An analysis of this most general case would be a natural continuation for this work. Moreover we have studied the theory only to derive the dynamical equations for the order parameter in the α regime but we have not studied how we can derive the fluctuations in this regime. In fact, having a static prescription to study the whole dynamics for the α relaxation, it would be natural to study the quadratic fluctuations around the saddle point trajectory. The actual technical work to do is to take the generalized Franz-Parisi potential and to study the quadratic fluctuations around the saddle point. This is a very difficult task because the replica structure of the saddle point is really complicated so that the "mass" matrix of the correspondent Landau expansion is difficult to diagonalize. However we hope that in the future this problem will be solved.

The third part of this work was motivated by the fact that the quantitative prediction for the mode-coupling exponent parameter λ obtained in the hypernetted chain approximation did not agree with the experimental value that is usually found. In this way we tried to see if there were a simpler setting where exact calculations were reliable and we analyzed the theory of mono disperse hard spheres in high dimensions. The large dimension limit is a true mean field limit where we can obtain exact results. As for the structural glass case, in order to obtain the exponent parameter we need an accurate analysis of the soft modes that appear at the glass transition. This means that in replica calculation we need to see where the 1RSB solution is stable and where is its instability line. By doing this we have analyzed the stability of the 1RSB phase diagram of hard spheres in high dimensions and we have found that an instability line is present and it is responsible for a Gardner transition at high density towards further replica symmetry breaking schemes. This means

that we cannot neglect fullRSB effects at high density. However the interesting point is that we have seen that the instability part of the phase diagram is in the region that controls the jamming physics. In order to study fullRSB effects we tried to compute firstly a perturbative 2RSB solution around the instability line that was able to predict the point above which fullRSB solution can be present. Then we performed a 2RSB calculation for the replicated entropy that was used to obtain the new predictions for the jamming limit so that we calculated a new 2RSB threshold. In the end we have obtained the fullRSB equations and we have discovered that they are very close to the one that describes the physics of the Sherrington-Kirkpartick model. We have solved them numerically an we have found that the numerical data are consistent with a power law scaling of the Debye-Waller factor $\widehat{\Delta}_{EA} \sim p^{-\sigma}$ with the exponent close to $\sigma \sim 3/2$. However in order to confirm this result we must work out all the finite size analysis and moreover we need to solve the equations at $m > 0$. The last step is essential in order to prove our argument for which the cutoff y_{max} plays the role a finite m. The last step is to compute analytically the exponent σ directly from the fullRSB equations. This could be done following the same line of [140]. Once precise numerical and analytical results on the fullRSB equations are established we can start to explore all the features and predictions of the fullRSB physics.

A point that we have not discussed in this thesis is what happens to metastable states. We have seen that a Gardner transition for the equilibrium state is present in the phase diagram but we know that it is present also in the metastable states. In order to detect the Gardner transition for metastable states one should perform a following state calculation. What can happen is that this computation can be done using a 1RSB ansatz up to the point where the Gardner instability appears and then a fullRSB ansatz is required. Another possible point to study is to try to mix the Pseudodynamics calculation in the case of the hard sphere model in high dimensions. At the first sight, this is a very complicated task to do because the pseudodynamic ansatz for the matrix of the mean square displacement is difficult to handle if we put it in the expression for the replicated entropy. However this calculation would be very welcome because first of all how to solve the dynamics for this kind of systems is unknown and moreover because we can appreciate fullRSB effects.

The final part of this work is devoted to the study of the dynamical mode-coupling equations that describe a slightly discontinuous transition. In general, mode coupling theory describes the dynamical relaxation as a two step process with the dynamical correlation function developing a finite plateau. This is important in the cases where discontinuous transitions take place and is related to the 1RSB static description of the glass transition. In this thesis we have addressed a different possibility for vitrification. We have analyzed the situation in which the value of the correlation function at the plateau is asymptotically close to the infinite time limit of the dynamical correlation itself. This means that we are in a situation in which the transition becomes continuous. This situation can appear both in liquid to glass transition and in glass to glass transitions. We have analyzed in great detail the dynamical equation in the reparametrization invariant regime and we have discovered that they become very simple in the continuum limit. This has allowed us to solve them both at equilibrium and in the off-equilibrium case.

Based on this result, a preliminary analysis of the dynamical fluctuations in the long time regime has been done. The main point that must be discussed is about the possibility to derive analytically the fluctuations in the long time regime by making use of the simple form of the MCT equations in the continuum limit.

We leave for future work all the points discussed above.

Appendix A

Double Counting Problem on the φ^4 theory

The following appendix strictly follows [68].

We consider the φ^4 theory defined by the action in Eq. (2.11). The generating functional is defined is given by Eq. (2.10) and at the mean field level we have $\Gamma_{\mathrm{MF}}[\phi] = S[\phi]$. If we include one loop corrections, we get the following expression:

$$\Gamma_{\mathrm{1L}}[\phi] = \Gamma_{\mathrm{MF}}[\phi] + \frac{1}{2}\mathrm{Tr}\log K \ , \tag{A.1}$$

where K is the operator defined by

$$K(x,y) = \delta(x-y)(m_0^2 - \nabla^2 + \frac{g}{2}\phi^2(x)) \ . \tag{A.2}$$

We isolate a free operator $K_0(x,y) = \delta(x-y)(m_0^2 - \nabla^2)$ and define an operator $(\phi^2)(x,y) = \phi^2(x)\delta(x-y)$; we can rewrite the kernel K operator in this way

$$K = K_0 \otimes [1 + \frac{g}{2}K_0^{-1} \otimes \phi^2] \ , \tag{A.3}$$

where $\otimes$ is the operator (integral) product. Moreover we have

$$K_0^{-1}(x,y) = \int \frac{\mathrm{d}p}{(2\pi)^D}\frac{e^{ip(x-y)}}{p^2+m_0^2} \, . \tag{A.4}$$

This means that

$$\Gamma_{\mathrm{1L}}[\phi] = \Gamma_{\mathrm{MF}}[\phi] + \frac{1}{2}\mathrm{Tr}\log\left[1 + \frac{g}{2}K_0^{-1} \otimes \phi^2\right] + \frac{1}{2}\mathrm{Tr}\log K_0 \ . \tag{A.5}$$

The last term is ϕ-independent which means that it can be neglected for our purposes. In fact we want to see what happens if we compute the two point function at order g using Γ_{1L} as an action instead of using the bare action S. We want the two point function at order g; this means that we need to perform a Taylor expansion of the extra term $\mathrm{Tr}\log[1 + (g/2)K_0^{-1} \otimes \phi^2]$ which is given by

$$\mathrm{Tr}\log\left[1 + \frac{g}{2}K_0^{-1} \otimes \phi^2\right] = \mathrm{Tr}\left[\frac{g}{2}K_0^{-1} \otimes \phi^2\right] + O(g^2) = \frac{g}{2}D_1(m_0^2)\int \mathrm{d}x\phi^2(x) + O(g^2) \tag{A.6}$$

where

$$D_1(m_0^2) = \int \frac{\mathrm{d}p}{(2\pi)^D} \frac{1}{p^2 + m_0^2} \tag{A.7}$$

We now use $\Gamma_{1\mathrm{L}}$ as the bare action, $S_{1\mathrm{L}}[\varphi] = \Gamma_{1\mathrm{L}}[\varphi]$ and compute the two point function. The diagrammatic rules are the standard ones for the φ^4 theory [141]:

$G(p) =$ 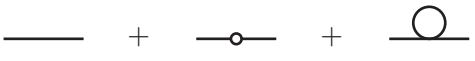 (A.8)

where the second diagram is the one originated by the term in Eq. (A.6). Remarkably enough, the second diagram has exactly the same expression as the last one. This is the nothing but the double counting problem.

We can now compute the Ginzburg Criterion starting by $S_{1\mathrm{L}}[\varphi] = \Gamma_{1\mathrm{L}}[\varphi]$. Let us consider the action at order g given by

$$S_{1\mathrm{L}}[\varphi] = \frac{1}{2} \int \mathrm{d}x \varphi(x) \left[-\nabla^2 + m_0^2 + \frac{g}{2} D_1(m_0^2) \right] \varphi(x) + \frac{g}{4!} \int \mathrm{d}x \varphi^4(x) \ . \tag{A.9}$$

It must be underlined at this point that the only difference with respect to the bare action $S[\varphi]$ is a change in the bare mass, $m_0 \to m_0^2 + \frac{g}{2} D_1(m_0^2)$. However, a result of Section 2.2.4 is that the final expression of the Ginzburg criterion must be expressed in terms of the renormalized mass only, and is therefore not affected by a change of the bare mass. It follows that whatever microscopic action we use – provided it can be developed in powers of φ^2 at small φ, which is the crucial assumption of mean field theory – will give the same results for the Ginzburg criterion. In this sense the Ginzburg criterion can be thought as a check *a posteriori* of this assumption.

Appendix B

Computation of the Jacobian $J(\hat{q})$

This appendix strictly follows [110]. The Jacobian $J(\hat{q})$ we want to compute is defined by the following relation

$$J(\hat{q}) = m^d \prod_{a=1}^{m} \delta \left[\sum_{b=1}^{m} q_{ab} \right] \int \mathrm{d}^d u_1 \dots \mathrm{d}^d u_{m-1} \prod_{a \leq b}^{1,m-1} \delta \left(q_{ab} - u_a \cdot u_b \right) \tag{B.1}$$

We introduce now some notations. Let us define a $d \times (m-1)$ matrix U whose first column contains the components of the d-dimensional vector u_1, the second column contain the components of u_2 and the $m-1$ column contains the components of u_{m-1}. We introduce also the $m \times m$ matrix $\hat{q}$ and its reduced version which is the matrix $\hat{q}^{(m,m)}$ that can be obtained from $\hat{q}$ by deleting the last column and the last row. We consider the integral that appears in the expression (B.1):

$$\int \mathrm{d}^d u_1 \dots \mathrm{d}^d u_{m-1} \prod_{a \leq b}^{1,m-1} \delta \left(q_{ab} - u_a \cdot u_b \right) = \int \mathrm{d}U \delta \left[\hat{q}^{(m,m)} - U^T U \right] \ , \tag{B.2}$$

where the measure of the last integral is a flat one over the entries of the matrix U. In order to compute this we start from the simplest case in which the matrix $\hat{q}^{(m,m)}$ has a diagonal structure

$$\hat{q}^{(m,m)} \equiv \hat{q}_D \ , \qquad (\hat{q}_D)_{ab} = q_{aa} \delta_{ab} \ . \tag{B.3}$$

This implies

$$\int \mathrm{d}U \delta \left[\hat{q}^{(m,m)} - U^T U \right] = \int \mathrm{d}^d u_1 \dots \mathrm{d}^d u_{m-1} \prod_{a=1}^{m-1} \delta \left(q_{aa} - |u_a|^2 \right) \prod_{a<b}^{(1,m-1} \delta (u_a \cdot u_b) \ . \tag{B.4}$$

The second Dirac delta function constraints the vectors u to be all orthogonal. The first Dirac delta is a constraint on the length of these vectors. If we change integration variables to polar coordinates, the previous expression can be rewritten

as

$$\begin{aligned}&\int \mathrm{d}^d\hat{u}_1 \dots \mathrm{d}^d\hat{u}_{m-1} \int_0^\infty \mathrm{d}u_1 u_1^{d-1} \dots \int_0^\infty \mathrm{d}u_{m-1} u_{m-1}^{d-1} \times \\ &\times \prod_{a=1}^{m-1} \delta\left(q_{aa} - u_a^2\right) \prod_{a<b}^{1,m-1} \delta(u_a u_b \hat{u}_a \cdot \hat{u}_b)\end{aligned} \tag{B.5}$$

where we have indicated with $\mathrm{d}^d\hat{u}$ the angular integration in d dimensions and with $\hat{u}_a$ the unit vector parallel to u_a. If we manipulate a little bit the Dirac deltas we can rewrite the previous expression in the following way

$$\begin{aligned}&2^{1-m} \int \mathrm{d}^d\hat{u}_1 \dots \mathrm{d}^d\hat{u}_{m-1} \int_0^\infty \mathrm{d}u_1 u_1^{d-1} \dots \int_0^\infty \mathrm{d}u_{m-1} u_{m-1}^{d-1} \times \\ &\times \left(\prod_{a=1}^{m-1} \frac{1}{\sqrt{q_{aa}}} \delta\left(\sqrt{q_{aa}} - u_a\right)\right) \left(\prod_{a<b}^{1,m-1} \frac{1}{\sqrt{q_{aa} q_{bb}}}\right) \prod_{a<b}^{1,m-1} \delta(\hat{u}_a \cdot \hat{u}_b) = \\ &= C_{m,d} \prod_{a=1}^{m-1} q_{aa}^{(d-m)/2} = C_{m,d} \left[\det \hat{q}^{(m,m)}\right]^{(d-m)/2} ,\end{aligned} \tag{B.6}$$

where we have defined

$$C_{m,d} = 2^{1-m} \int \mathrm{d}^d\hat{u}_1 \dots \mathrm{d}^d\hat{u}_{m-1} \prod_{a<b}^{1,m-1} \delta(\hat{u}_a \cdot \hat{u}_b) . \tag{B.7}$$

Let us understand how to compute the last expression. The integral that defines $C_{m,d}$ is very simple. The Dirac deltas force the unit vectors $\hat{u}$ to be all orthogonal. This means that we have to compute only the phase space accessible to them. This can be done iteratively. If we have only one unit free vector, it will have a phase space available given by the solid angle in d dimensions which is Ω_d. Then we can think to add a second unit vector. Once the position of the first has been chosen, then the volume accessible to the second one will be Ω_{d-1} due to the orthogonal constraint. Going on by iteration we have

$$C_{m,d} = 2^{1-m} \Omega_d \Omega_{d-1} \dots \Omega_{d-m+2}. \tag{B.8}$$

Let us now generalize this construction to a general non-diagonal matrix $\hat{q}^{(m,m)}$. Because $\hat{q}^{(m,m)}$ is symmetric we can diagonalize it and we can write it as

$$\hat{q}^{(m,m)} = \Lambda^{-1} \hat{q}_D \Lambda , \qquad \det \Lambda = 1 , \qquad \det \hat{q}_D = \det \hat{q}^{(m,m)} , \qquad \Lambda^T = \Lambda^{-1} . \tag{B.9}$$

We have that

$$\begin{aligned}\int \mathrm{d}U \delta\left[\hat{q}^{(m,m)} - U^T U\right] &= \int \mathrm{d}U \delta\left[\Lambda^{-1} \hat{q}_D \Lambda - U^T U\right] = \\ &= \int \mathrm{d}U \delta\left[\hat{q}_D - \Lambda U^T U \Lambda^{-1}\right] .\end{aligned} \tag{B.10}$$

We can now change integration variables

$$U' = U \Lambda^{-1} , \tag{B.11}$$

whose Jacobian is one due to the orthogonality property of the matrix Λ. The previous expression assumes the following form

$$\int \mathrm{d}U \delta \left[\hat{q}_D - \Lambda U^T U \Lambda^{-1} \right] = \int \mathrm{d}U \delta \left[\hat{q}_D - U^T U \right] \ , \tag{B.12}$$

that is exactly the same as the one that we have discussed above. It follows that

$$J(\hat{q}) = m^d C_{m,d} \prod_{a=1}^{m} \delta \left[\sum_{b=1}^{m} q_{ab} \right] \left[\det \hat{q}^{(m,m)} \right]^{(d-m)/2} \ , \tag{B.13}$$

which is the analytical result that was deeply used in Ref. [111].

Appendix C

Stability of the 1RSB solution via the 2RSB calculation

We can use the expression for the entropy with a 2RSB ansatz to compute the stability of the 1RSB solution. The strategy is based on the fact that we know that the eigenvector of the stability matrix that has a vanishing eigenvalue is the replicon one. Let us take the entropy at the 1RSB level. We want to study the stability of it so that we have to study how the entropy behaves when we do a perturbation of the 1RSB solution. In the end we need to study $S[\alpha_{1RSB} + \delta q]$ form small δq. If we want to study the replicon perturbation we have to set also

$$\sum_{b=1,\ b\neq a}^{m} \delta q_{ab} = 0\,. \tag{C.1}$$

At this point let us expand the 2RSB replicated entropy around the 1RSB solution with a perturbation along the replicon eigenmode.

$$S[\alpha_{1RSB} + \delta q] = S[\alpha_{1RSB}] + \frac{1}{2}\lambda_R(\hat{A}, m, \hat{\varphi}) \sum_{a\neq b} \delta q_{ab}^2 + \dots \tag{C.2}$$

How can we take advantage of the knowledge of the 2RSB entropy? We can construct a 2RSB matrix that is of the form $\alpha_{2RSB} = \alpha_{1RSB} + \delta q$ with a special form of δq that has a non vanishing projection on the replicon subspace. In particular we can choose

$$\delta q_{ab} = (1 - \delta_{ab}) \left(\frac{m - m_1}{1 - m_1} \delta\alpha_0 \mathrm{I}(a \prec b) + \delta\alpha_0 \mathrm{I}(a \not\prec b) \right) \tag{C.3}$$

Note that eq. (C.1) is satisfied for this choice. It follows that

$$S[\alpha_{1RSB} + \delta q] = S[\alpha_{1RSB}] + \frac{1}{2} \left[\lim_{\alpha_1 \to \alpha_0 = -\hat{A}/m} \hat{D}^2 S[\alpha_{1RSB}] \right] \delta\alpha_0^2 \tag{C.4}$$

so that it follows that

$$\lambda_R(\hat{A}, m, \hat{\varphi}) = \left[\lim_{\alpha_1 \to \alpha_0 = -\hat{A}/m} \hat{D}^2 S[\alpha_{2RSB}] \right] \left[\frac{m_1 - 1}{m(m - m_1)(m - 1)} \right] \tag{C.5}$$

where we have introduced the differential operator (which satisfy trivially the Leibnitz rule)

$$\hat{D} = \frac{\partial}{\partial \alpha_0} + \frac{m - m_1}{1 - m_1} \frac{\partial}{\partial \alpha_1} \,. \tag{C.6}$$

We see from the form of the 2RSB entropy that to compute the replicon eigenvalue from Eq. C.5 we need to compute the derivatives of the entropy. To do this, we separately compute the derivative of the entropic and the interaction term.

C.1 The interaction part of the replicon eigenvalue

We want to compute

$$\lambda_R^I(\hat{A}, m, \hat{\varphi}) = -\frac{\hat{\varphi}}{2} \left[\frac{m_1 - 1}{m(m - m_1)(m - 1)} \right] \lim_{\alpha_1 \to \alpha_0 = -\hat{A}/m} \hat{D}^2 \mathcal{F}[\alpha_{2RSB}] \tag{C.7}$$

Let us rewrite the expression for the interaction part of the entropy in a more concise form

$$\begin{aligned} \mathcal{F}[\alpha_{2RSB}] =& m \int_{-\infty}^{\infty} \frac{\mathrm{d}\lambda \mathrm{d}\omega}{2\pi} e^{-(\omega^2+\lambda^2)/2} \Theta^{m_1 - 1} \left[g(\alpha_1, \alpha_0, \lambda) \right] \\ & \times \left[\int_{-\infty}^{\infty} \frac{\mathrm{d}\hat{\omega}}{\sqrt{2\pi}} e^{-\hat{\omega}^2/2} \Theta^{m_1} \left[f(\alpha_1, \alpha_0, \lambda, \omega, \hat{\omega}) \right] \right]^{(m - m_1)/m_1} \end{aligned} \tag{C.8}$$

where we have defined two functions

$$\begin{aligned} g(\alpha_1, \alpha_0, \lambda) &= \frac{1}{\sqrt{2}} \left(\sqrt{-2m_1\alpha_1 - 2(m - m_1)\alpha_0} - \lambda \right) \\ f(\alpha_1, \alpha_0, \lambda, \omega, \hat{\omega}) &= \frac{1}{\sqrt{2}} \left(\sqrt{-2m_1\alpha_1 - 2(m - m_1)\alpha_0} - \lambda \right. \\ & \left. - \sqrt{\frac{\alpha_0 - \alpha_1}{m_1\alpha_1 + (m - m_1)\alpha_0}} \left[\omega - \hat{\omega} - \sqrt{2\alpha_1 - 2\alpha_0} \right] \right] \,. \end{aligned} \tag{C.9}$$

Let us take the derivative. We obtain

$$\begin{aligned} \hat{D}^2 \mathcal{F}[\alpha_{2RSB}] &= m \int_{-\infty}^{\infty} \frac{\mathrm{d}\omega \mathrm{d}\lambda}{2\pi} e^{-(\omega^2+\lambda)^2/2} \left\{ \left[\left((m_1 - 1) \left(\hat{D}^2 g \right) \Theta'(g) \right. \right. \right. \\ &+ (m_1 - 1) \left(\hat{D} g \right)^2 \Theta''(g) \Big) \Theta^{m_1 - 2}(g) + (m_1 - 1)(m_1 - 2) \left(\hat{D} g \right)^2 \left(\Theta'(g) \right)^2 \Theta^{m_1 - 3}(g) \Big] \\ &\times \left[\int_{-\infty}^{\infty} \frac{\mathrm{d}\hat{\omega}}{2\pi} e^{-\hat{\omega}^2/2} \Theta^{m_1}(f) \right]^{(m - m_1)/m_1} \Bigg\} + \\ &+ m \int_{-\infty}^{\infty} \frac{\mathrm{d}\lambda}{\sqrt{2\pi}} e^{-\lambda^2/2} \left\{ 2(m_1 - 1) \left(\hat{D} g \right) \Theta'(g) \Theta^{m_1 - 2}(g) \right. \\ &\times \left[\hat{D} \int_{-\infty}^{\infty} \frac{\mathrm{d}\omega}{\sqrt{2\pi}} e^{-\omega^2/2} \left[\int_{-\infty}^{\infty} \frac{\mathrm{d}\hat{\omega}}{2\pi} e^{-\hat{\omega}^2/2} \Theta^{m_1}(f) \right]^{\frac{m}{m_1} - 1} \right] \\ &\left. + \Theta^{m_1 - 1}(g) \left[\hat{D}^2 \int_{-\infty}^{\infty} \frac{\mathrm{d}\omega}{\sqrt{2\pi}} e^{-\omega^2/2} \left[\int_{-\infty}^{\infty} \frac{\mathrm{d}\hat{\omega}}{2\pi} e^{-\hat{\omega}^2/2} \Theta^{m_1}(f) \right]^{\frac{m}{m_1} - 1} \right] \right\} \end{aligned} \tag{C.10}$$

where we have defined

$$\Theta'(x) = \frac{\mathrm{d}\Theta(x)}{\mathrm{d}x} \tag{C.11}$$

and an analogous notation for Θ'' and so on. At this point one should take the limit $\alpha_1 \to \alpha_0$. However one can argue that taking this limit is trivial for the first three terms of the expression above while it is very tricky in the case of the last three terms. The reason is that the derivative of the function f with respect to α_0 (and, of course, with respect to α_1) contains a term which is divergent like $(\alpha_0 - \alpha_1)^{-1/2}$. However one soon realizes that this divergent term is proportional to $\omega - \hat{\omega}$ so that it's integral is zero in the limit $\alpha_1 \to \alpha_0$. This means that we cannot take in a naive way the derivative under the integral sign but we should perform the integral before taking the derivative. Let us define the following quantities

$$\begin{aligned} R[\alpha_1, \alpha_0, \lambda] &= \frac{\sqrt{-2m_1\alpha_1 - 2(m-m_1)\alpha_0} - \lambda}{\sqrt{2}} + \sqrt{\frac{-(\alpha_0-\alpha_1)^2}{m_1\alpha_1 + (m-m_1)\alpha_0}} \\ h(\alpha_1, \alpha_0) &= \sqrt{2}\sqrt{m_1\alpha_1 + (m-m_1)\alpha_0} \end{aligned} \tag{C.12}$$

In order to compute the derivative we expand with a Taylor series the integrals. For the first derivative we get

$$\begin{aligned}
&\lim_{\alpha_1\to\alpha_0} \hat{D} \int_{-\infty}^{\infty} \frac{\mathrm{d}\omega}{\sqrt{2\pi}} e^{-\omega^2/2} \left[\int_{-\infty}^{\infty} \frac{\mathrm{d}\hat{\omega}}{2\pi} e^{-\hat{\omega}^2/2} \Theta^{m_1}(f)\right]^{\frac{m}{m_1}-1} = \lim_{\alpha_1\to\alpha_0} \hat{D} \int_{-\infty}^{\infty} \frac{\mathrm{d}\omega}{\sqrt{2\pi}} e^{-\omega^2/2} \cdot \\
&\cdot \left[\int_{-\infty}^{\infty} \frac{\mathrm{d}\hat{\omega}}{2\pi} e^{-\hat{\omega}^2/2} \Theta^{m_1}\left[R[\alpha_1,\alpha_0,\lambda] - \frac{\sqrt{\alpha_0-\alpha_1}}{h(\alpha_1,\alpha_0)}(\omega-\hat{\omega})\right]\right]^{\frac{m}{m_1}-1} = \\
&= \lim_{\alpha_1\to\alpha_0} \hat{D} \int_{-\infty}^{\infty} \frac{\mathrm{d}\omega}{\sqrt{2\pi}} e^{-\omega^2/2} \left[\int_{-\infty}^{\infty} \frac{\mathrm{d}\hat{\omega}}{2\pi} e^{-\hat{\omega}^2/2} \left[\Theta_0[R[\alpha_1,\alpha_0,\lambda]]\right.\right. \\
&- \Theta_1[R[\alpha_1,\alpha_0,\lambda]] \frac{\sqrt{\alpha_0-\alpha_1}}{h(\alpha_1,\alpha_0)}(\omega-\hat{\omega}) + \frac{1}{2}\Theta_2[R[\alpha_1,\alpha_0,\lambda]] \frac{\alpha_0-\alpha_1}{h^2(\alpha_1,\alpha_0)}(\omega-\hat{\omega})^2 \\
&\left.\left. -\frac{1}{6}\Theta_3[R[\alpha_1,\alpha_0,\lambda]] \frac{(\sqrt{\alpha_0-\alpha_1})^3}{h^3(\alpha_1,\alpha_0)}(\omega-\hat{\omega})^3 + \frac{1}{24}\Theta_4[R[\alpha_1,\alpha_0,\lambda]] \frac{(\alpha_0-\alpha_1)^2}{h^4(\alpha_1,\alpha_0)}(\omega-\hat{\omega})^4\right]\right]^{\frac{m}{m_1}-1} \\
&= \lim_{\alpha_1\to\alpha_0} \hat{D} \int_{-\infty}^{\infty} \frac{\mathrm{d}\omega}{\sqrt{2\pi}} e^{-\omega^2/2} \left[\left[\Theta^{m-m_1}[R[\alpha_1,\alpha_0,\lambda]] + \frac{m-m_1}{m_1}\Theta^{m-2m_1}[R[\alpha_1,\alpha_0,\lambda]] \cdot\right.\right. \\
&\cdot \int_{-\infty}^{\infty} \frac{\mathrm{d}\hat{\omega}}{2\pi} e^{-\hat{\omega}^2/2} \left(-\Theta_1[R[\alpha_1,\alpha_0,\lambda]] \frac{\sqrt{\alpha_0-\alpha_1}}{h(\alpha_1,\alpha_0)}(\omega-\hat{\omega}) + \frac{1}{2}\Theta_2[R[\alpha_1,\alpha_0,\lambda]] \frac{\alpha_0-\alpha_1}{h^2(\alpha_1,\alpha_0)}(\omega-\hat{\omega})^2\right. \\
&\left. -\frac{1}{6}\Theta_3[R[\alpha_1,\alpha_0,\lambda]] \frac{(\sqrt{\alpha_0-\alpha_1})^3}{h^3(\alpha_1,\alpha_0)}(\omega-\hat{\omega})^3 + \frac{1}{24}\Theta_4[R[\alpha_1,\alpha_0,\lambda]] \frac{(\alpha_0-\alpha_1)^2}{h^4(\alpha_1,\alpha_0)}(\omega-\hat{\omega})^4\right) + \\
&+ \frac{1}{2}\frac{(m-m_1)(m-2m_1)}{m_1^2}\Theta^{m-3m_1}[R[\alpha_1,\alpha_0,\lambda]] \int_{-\infty}^{\infty} \frac{\mathrm{d}\omega_1 \mathrm{d}\omega_2}{\sqrt{2\pi}} e^{-(\omega_1^2+\omega_2^2)/2} \Theta_1^2[R[\alpha_1,\alpha_0,\lambda]] \cdot \\
&\left.\left. \cdot \frac{\alpha_0-\alpha_1}{h^2(\alpha_1,\alpha_0)}(\omega-\omega_1)(\omega-\omega_2) + \ldots\right]\right] = (m-m_1)\Theta^{m-m_1-1}[\zeta(\alpha_0)]\Theta'[\zeta(\alpha_0)]R_1(\alpha_0) \\
&+ \frac{m-m_1}{m_1}\Theta^{m-2m_1}[\zeta(\alpha_0)]\Theta_2[\zeta(\alpha_0)] \frac{m-1}{(m_1-1)h^2(\alpha_0,\alpha_0)} + \\
&+ \frac{1}{2}\frac{(m-m_1)(m-2m_1)}{m_1^2}\Theta^{m-3m_1}[\zeta(\alpha_0)]\Theta_1^2[\zeta(\alpha_0)] \frac{m-1}{(m_1-1)h^2(\alpha_0,\alpha_0)}
\end{aligned}$$

where we have defined the following quantities

$$\begin{aligned}
\zeta(\alpha_0) &= \frac{1}{\sqrt{2}}\left(\sqrt{-2m\alpha_0} - \lambda\right) \\
\Theta_n(x) &= \frac{\mathrm{d}^n}{\mathrm{d}x^n}\left[\Theta^{m_1}[x]\right] \\
\lim_{\alpha_1\to\alpha_0} \hat{D}g(\alpha_1,\alpha_0,\lambda) &= \frac{1}{2}\frac{m-m_1}{m_1-1}\frac{1}{\sqrt{-m\alpha_0}} := g_1(\alpha_0) \\
\lim_{\alpha_1\to\alpha_0} \hat{D}^2 g(\alpha_1,\alpha_0,\lambda) &= -\frac{1}{4}\left[\frac{m-m_1}{m_1-1}\right]^2 \frac{1}{\left(\sqrt{-m\alpha_0}\right)^3} := g_2(\alpha_0) \\
\lim_{\alpha_1\to\alpha_0^+} \hat{D}R[\alpha_1,\alpha_0] &= \frac{2-m-m_1}{2\sqrt{-m\alpha_0}(m_1-1)} := R_1(\alpha_0) \\
\lim_{\alpha_1\to\alpha_0^+} \hat{D}^2 R[\alpha_1,\alpha_0] &= \frac{(3m+m_1-4)(m-m_1)}{4(m_1-1)^2\left(\sqrt{-m\alpha_0}\right)^3} := R_2(\alpha_0)
\end{aligned}$$

Note that in the last two relations we used the physical fact that $\alpha_1 \to \alpha_0^+$ because if we had taken the limit in the other direction we would have an opposite sign in the final result. This physical requirement is signaled by the fact that we know that at the 1RSB saddle point α_0 is negative because it is $-\hat{A}/m$ so that if we want that all the square roots be definite we must have $\alpha_1 > \alpha_0$ that is also the usual fact that happens in spin glass theory where the αs corresponds to the overlaps and they are organized in an ultra metric structure. The second derivative is a little bit more complicated but it can be computed on the same lines. By defining

$$\mathcal{D}x = \frac{\mathrm{d}x}{\sqrt{2\pi}} e^{-x^2/2}$$

we have

$$\begin{aligned}
\lim_{\alpha_1\to\alpha_0} \hat{D}^2 \int_{-\infty}^{\infty} \frac{\mathrm{d}\omega}{\sqrt{2\pi}} e^{-\omega^2/2} \left[\int_{-\infty}^{\infty} \frac{\mathrm{d}\hat{\omega}}{\sqrt{2\pi}} e^{-\hat{\omega}^2/2} \Theta^{m_1}(f)\right]^{\frac{m}{m_1}-1} &= \lim_{\alpha_1\to\alpha_0} \hat{D}^2 \int_{-\infty}^{\infty} \frac{\mathrm{d}\omega}{\sqrt{2\pi}} e^{-\omega^2/2}. \\
= \cdot \left[\int_{-\infty}^{\infty} \frac{\mathrm{d}\hat{\omega}}{\sqrt{2\pi}} e^{-\hat{\omega}^2/2} \Theta^{m_1}\left[R[\alpha_1,\alpha_0,\lambda] - \frac{\sqrt{\alpha_0-\alpha_1}}{h(\alpha_1,\alpha_0)}(\omega-\hat{\omega})\right]\right]^{\frac{m}{m_1}-1} &= \\
= \lim_{\alpha_1\to\alpha_0} \hat{D}^2 \int_{-\infty}^{\infty} \frac{\mathrm{d}\omega}{\sqrt{2\pi}} e^{-\omega^2/2} \left[\int_{-\infty}^{\infty} \frac{\mathrm{d}\hat{\omega}}{\sqrt{2\pi}} e^{-\hat{\omega}^2/2} \left[\Theta_0[R[\alpha_1,\alpha_0,\lambda]]\right.\right. & \\
-\Theta_1[R[\alpha_1,\alpha_0,\lambda]]\frac{\sqrt{\alpha_0-\alpha_1}}{h(\alpha_1,\alpha_0)}(\omega-\hat{\omega}) + \frac{1}{2}\Theta_2[R[\alpha_1,\alpha_0,\lambda]]\frac{\alpha_0-\alpha_1}{h^2(\alpha_1,\alpha_0)}(\omega-\hat{\omega})^2 & \\
-\frac{1}{6}\Theta_3[R[\alpha_1,\alpha_0,\lambda]]\frac{\left(\sqrt{\alpha_0-\alpha_1}\right)^3}{h^3(\alpha_1,\alpha_0)}(\omega-\hat{\omega})^3 & \\
\left.\left.+\frac{1}{24}\Theta_4[R[\alpha_1,\alpha_0,\lambda]]\frac{(\alpha_0-\alpha_1)^2}{h^4(\alpha_1,\alpha_0)}(\omega-\hat{\omega})^4\right]\right]^{\frac{m}{m_1}-1} &=
\end{aligned}$$

$$= \lim_{\alpha_1 \to \alpha_0} \hat{D}^2 \int_{-\infty}^{\infty} \mathcal{D}\omega \left[\Theta^{m-m_1}[R[\alpha_1,\alpha_0,\lambda]] + \frac{m-m_1}{m_1} \Theta^{m-2m_1}[R[\alpha_1,\alpha_0,\lambda]] \cdot \right.$$

$$\cdot \int_{-\infty}^{\infty} \mathcal{D}\hat{\omega} \left(-\Theta_1[R[\alpha_1,\alpha_0,\lambda]] \frac{\sqrt{\alpha_0-\alpha_1}}{h(\alpha_1,\alpha_0)} (\omega-\hat{\omega}) + \frac{1}{2}\Theta_2[R[\alpha_1,\alpha_0,\lambda]] \frac{\alpha_0-\alpha_1}{h^2(\alpha_1,\alpha_0)} (\omega-\hat{\omega})^2 - \right.$$

$$\left. - \frac{1}{6}\Theta_3[R[\alpha_1,\alpha_0,\lambda]] \frac{(\sqrt{\alpha_0-\alpha_1})^3}{h^3(\alpha_1,\alpha_0)} (\omega-\hat{\omega})^3 + \frac{1}{24}\Theta_4[R[\alpha_1,\alpha_0,\lambda]] \frac{(\alpha_0-\alpha_1)^2}{h^4(\alpha_1,\alpha_0)} (\omega-\hat{\omega})^4 \right) +$$

$$+ \frac{1}{2} \frac{(m-m_1)(m-2m_1)}{m_1^2} \Theta^{m-3m_1}[R[\alpha_1,\alpha_0,\lambda]] \cdot$$

$$\cdot \int_{-\infty}^{\infty} \mathcal{D}\omega_1 \mathcal{D}\omega_2 \left(\Theta_1^2[R[\alpha_1,\alpha_0,\lambda]] \frac{\alpha_0-\alpha_1}{h^2(\alpha_1,\alpha_0)} (\omega-\omega_1)(\omega-\omega_2) + \right.$$

$$+ \frac{1}{3}\Theta_1[R[\alpha_1,\alpha_0,\lambda]]\Theta_3[R[\alpha_1,\alpha_0,\lambda]] \frac{(\alpha_0-\alpha_1)^2}{h^4(\alpha_1,\alpha_0)} (\omega-\omega_1)(\omega-\omega_2)^3 +$$

$$\left. + \frac{1}{4}\Theta_2^2[R[\alpha_1,\alpha_0,\lambda]] \frac{(\alpha_0-\alpha_1)^2}{h^4(\alpha_1,\alpha_0)} (\omega-\omega_1)^2(\omega-\omega_2)^2 \right) +$$

$$+ \frac{1}{6} \frac{(m-m_1)(m-2m_1)(m-3m_1)}{m_1^3} \Theta^{m_1-4m_1}[R[\alpha_1,\alpha_0,\lambda]] \int_{-\infty}^{\infty} \mathcal{D}\omega_1 \mathcal{D}\omega_2 \mathcal{D}\omega_3 \cdot$$

$$\cdot \left(\frac{3}{2}\Theta_1^2[R[\alpha_1,\alpha_0,\lambda]]\Theta_2[R[\alpha_1,\alpha_0,\lambda]] \frac{(\alpha_0-\alpha_1)^2}{h^4(\alpha_1,\alpha_0)} (\omega-\omega_1)^2(\omega-\omega_2)(\omega-\omega_3) \right) +$$

$$+ \frac{1}{24} \frac{(m-m_1)(m-2m_1)(m-3m_1)(m-4m_1)}{m_1^4} \Theta^{m-5m_1}[R[\alpha_1,\alpha_0,\lambda]] \cdot$$

$$\left. \cdot \int_{-\infty}^{\infty} \mathcal{D}\omega_1 \mathcal{D}\omega_2 \mathcal{D}\omega_3 \mathcal{D}\omega_4 \Theta_1^4[R[\alpha_1,\alpha_0,\lambda]] \frac{(\alpha_0-\alpha_1)^2}{h^4(\alpha_1,\alpha_0)} (\omega-\omega_1)\dots(\omega-\omega_4) \right] =$$

$$= (m-m_1) R_2(\alpha_0) \Theta'[\zeta(\alpha_0)] \Theta^{m-m_1-1}[\zeta(\alpha_0)] + (m-m_1) R_1^2(\alpha_0) \Theta''[\zeta(\alpha_0)] \cdot$$

$$\cdot \Theta^{m-m_1-1}[\zeta(\alpha_0)] + (m-m_1)(m-m_1-1) R_1^2(\alpha_0) \left(\Theta'[\zeta(\alpha_0)]\right)^2 \Theta^{m-m_1-2}[\zeta(\alpha_0)] +$$

$$+ 2\frac{m-m_1}{m_1} \frac{m-1}{m_1-1} \left[(m-2m_1)\Theta'[\zeta(\alpha_0)]\Theta^{m-2m_1-1}[\zeta(\alpha_0)] R_1(\alpha_0) \frac{\Theta_2[\zeta(\alpha_0)]}{h^2(\alpha_0,\alpha_0)} + \right.$$

$$\left. + \Theta^{m-2m_1}[\zeta(\alpha_0)]\Theta_3[\zeta(\alpha_0)] \frac{R_1(\alpha_0)}{h^2(\alpha_0,\alpha_0)} - 2\Theta^{m-2m_1}[\zeta(\alpha_0)]\Theta_2[\zeta(\alpha_0)] \frac{\hat{D}h}{h^3(\alpha_0,\alpha_0)} \right] +$$

$$+ \frac{m-m_1}{m_1} \Theta^{m-2m_1}[\zeta(\alpha_0)]\Theta_4[\zeta(\alpha_0)] \frac{1}{h^4(\alpha_0,\alpha_0)} \frac{(m-1)^2}{(m_1-1)^2} +$$

$$+ \frac{(m-m_1)(m-2m_1)}{m_1^2} \left[\frac{(m-3m_1)\Theta^{m-3m_1-1}[\zeta(\alpha_0)]\Theta'[\zeta(\alpha_0)] R_1(\alpha_0)\Theta_1^2[\zeta(\alpha_0)]}{h^2(\alpha_0,\alpha_0)} + \right.$$

$$\left. + 2\Theta^{m-3m_1}[\zeta(\alpha_0)]\Theta_1[\zeta(\alpha_0)]\Theta_2[\zeta(\alpha_0)] \frac{R_1(\alpha_0)}{h^2} - 2\Theta^{m-3m_1}[\zeta(\alpha_0)]\Theta_1^2[\zeta(\alpha_0)] \frac{\hat{D}h}{h^3(\alpha_0,\alpha_0)} \right] \cdot$$

$$\cdot \frac{m-1}{m_1-1} + 2\frac{(m-m_1)(m-2m_1)}{m_1^2} \frac{\Theta^{m-3m_1}[\zeta(\alpha_0)]\Theta_1[\zeta(\alpha_0)]\Theta_3[\zeta(\alpha_0)](m-1)^2}{(m_1-1)^2 h^4(\alpha_0,\alpha_0)} +$$

$$+ \frac{3}{2} \frac{(m-m_1)(m-2m_1)}{m_1^2} \Theta^{m-3m_1}[\zeta(\alpha_0)]\Theta_2^2[\zeta(\alpha_0)] \frac{(m-1)^2}{(m_1-1)^2 h^4(\alpha_0,\alpha_0)} +$$

$$+ 2\frac{(m-m_1)(m-2m_1)(m-3m_1)}{m_1^3} \frac{\Theta^{m-4m_1}[\zeta(\alpha_0)]\Theta_1^2[\zeta(\alpha_0)]\Theta_2[\zeta(\alpha_0)](m-1)^2}{(m_1-1)^2 h^4(\alpha_0,\alpha_0)} +$$

$$+ \frac{1}{4} \frac{(m-m_1)(m-2m_1)(m-3m_1)(m-4m_1)}{m_1^4} \frac{\Theta^{m-5m_1}[\zeta(\alpha_0)]\Theta_1^4[\zeta(\alpha_0)](m-1)^2}{(m_1-1)^2 h^4(\alpha_0,\alpha_0)}$$

At this point let us split the interaction part of the replicon eigenvalue into three terms

$$\lambda_R^I = \left[\frac{m_1-1}{m(m-m_1)(m-1)}\right](\Delta_1+\Delta_2+\Delta_3) \tag{C.13}$$

where

$$\Delta_1 = -\frac{m\hat{\varphi}}{2}\int_{-\infty}^{\infty}\frac{\mathrm{d}\lambda}{\sqrt{2\pi}}e^{-\lambda^2/2}\Big[\Big((m_1-1)g_2(\alpha_0)\Theta'(\zeta)+(m_1-1)g_1^2(\alpha_0)\Theta''(\zeta)\Big)\cdot \\ \cdot\Theta^{m-2}(\zeta)+(m_1-1)(m_1-2)g_1^2(\zeta)\left(\Theta'(\zeta)\right)^2\Theta^{m-3}(\zeta)\Big]$$

$$\Delta_2 = -\frac{m\hat{\varphi}}{2}\int_{-\infty}^{\infty}\frac{\mathrm{d}\lambda}{\sqrt{2\pi}}e^{-\lambda^2/2}\left[2(m_1-1)g_1(\alpha_0)\Theta'[\zeta]\right]\cdot \\ \cdot\Big((m-m_1)\Theta^{m-3}[\zeta]\Theta'[\zeta]R_1(\alpha_0)+(m-m_1)\Big(\Theta''[\zeta]\Theta^{m-3}[\zeta]+ \\ +(m_1-1)(\Theta'[\zeta])^2\Theta^{m-4}\Big)\frac{m-1}{(m_1-1)h^2(\alpha_0,\alpha_0)} \\ +\frac{1}{2}(m-m_1)(m-2m_1)(\Theta'[\zeta])^2\Theta^{m-4}[\zeta]\frac{m-1}{(m_1-1)h^2(\alpha_0,\alpha_0)}\Big)$$

$$\Delta_3 = -\frac{m\hat{\varphi}}{2}\int_{-\infty}^{\infty}\frac{\mathrm{d}\lambda}{\sqrt{2\pi}}e^{-\lambda^2/2}\Big[(m-m_1)R_2(\alpha_0)\Theta'[\zeta]\Theta^{m-2}[\zeta]+ \\ +(m-m_1)R_1^2(\alpha_0)\Theta''[\zeta]\Theta^{m-2}[\zeta]+ \\ +(m-m_1)(m-m_1-1)R_1^2(\alpha_0)(\Theta'[\zeta])^2\Theta^{m-3}[\zeta]+$$

$$+2(m-m_1)\Big((m-2m_1)\Theta'[\zeta]\frac{R_1(\alpha_0)}{h^2(\alpha_0,\alpha_0)}\Big(\Theta''[\zeta]\Theta^{m-3}[\zeta]+(m_1-1)(\Theta'[\zeta])^2\Theta^{m-4}[\zeta]\Big)+$$

$$+\Big(3(m_1-1)\Theta'[\zeta]\Theta''[\zeta]\Theta^{m-3}[\zeta]+\Theta'''[\zeta]\Theta^{m-2}[\zeta]+(m_1-1)(m_1-2)(\Theta'[\zeta])^3\Theta^{m-4}[\zeta]\Big)\cdot$$

$$\cdot\frac{R_1(\alpha_0)}{h^2(\alpha_0,\alpha_0)}-2\Big(\Theta''[\zeta]\Theta^{m-2}[\zeta]+(m_1-1)(\Theta'[\zeta])^2\Theta^{m-3}[\zeta]\Big)\frac{\hat{D}h}{h^3(\alpha_0,\alpha_0)}\Big)\frac{m-1}{m_1-1}+$$

$$+(m-m_1)\Big(\Theta''''[\zeta]\Theta^{m-2}[\zeta]+4(m_1-1)\Theta'''[\zeta]\Theta'[z]\Theta^{m-3}[\zeta]+3(m_1-1)(\Theta''[\zeta])^2\Theta^{m-3}[\zeta]$$

$$+6(m_1-1)(m_1-2)\Theta''[\zeta](\Theta'[\zeta])^2\Theta^{m-4}[\zeta]+(m_1-1)(m_1-2)(m_1-3)(\Theta'[\zeta])^4\Theta^{m-5}[\zeta]\Big)\cdot$$

$$\cdot\frac{(m-1)^2}{(m_1-1)^2h^4(\alpha_0,\alpha_0)}+\frac{(m-m_1)(m-2m_1)(m-1)}{m_1-1}\Big[\frac{(m-3m_1)(\Theta'[\zeta])^3\Theta^{m-4}R_1(\alpha_0)}{h^2(\alpha_0,\alpha_0)}+$$

$$+2\Theta'[\zeta]\Big(\Theta''[\zeta]\Theta^{m-3}[\zeta]+(m_1-1)(\Theta'[\zeta])^2\Theta^{m-4}[\zeta]\Big)\frac{R_1(\alpha_0)}{h^2(\alpha_0,\alpha_0)}-\frac{2(\Theta'[\zeta])^2\Theta^{m-3}[\zeta]\hat{D}h}{h^3(\alpha_0,\alpha_0)}\Big]$$

$$+\frac{2(m-m_1)(m-2m_1)(m-1)^2}{(m_1-1)^2h^4(\alpha_0,\alpha_0)}\Theta'[\zeta]\Big(\Theta'''[\zeta]\Theta^{m-3}[\zeta]+3(m_1-1)\Theta''[\zeta]\Theta'[\zeta]\Theta^{m-4}[\zeta]+$$

$$+(m_1-1)(m_1-2)(\Theta'[\zeta])^3\Theta^{m-5}[\zeta]\Big)+$$

$$+\frac{3(m-m_1)(m-2m_1)\Big(\Theta''[\zeta]\Theta^{(m-3)/2}[\zeta]+(m_1-1)(\Theta'[\zeta])^2\Theta^{(m-5)/2}\Big)^2(m-1)^2}{2(m_1-1)^2h^4(\alpha_0,\alpha_0)}+$$

$$+2(m-m_1)(m-2m_1)(m-3m_1)(\Theta'[\zeta])^2\left(\Theta''[\zeta]\Theta^{m-4}+(m_1-1)(\Theta'[\zeta])^2\Theta^{m-5}[\zeta]\right)\cdot$$
$$\cdot\frac{(m-1)^2}{(m_1-1)^2h^4(\alpha_0,\alpha_0)}+$$
$$+\frac{1}{4}(m-m_1)(m-2m_1)(m-3m_1)(m-4m_1)(\Theta'[\zeta])^4\Theta^{m-5}[\zeta]\frac{(m-1)^2}{(m_1-1)^2h^4(\alpha_0,\alpha_0)}\Bigg]$$

This concludes the calculation of the interaction part of the replicon eigenvalue.

C.2 The entropic part of the replicon eigenvalue

Let us now compute the entropic contribution to the replicon eigenvalue. This is simply given by

$$\lambda_R^E=\left[\frac{m_1-1}{m(m-m_1)(m-1)}\right]\lim_{\alpha_1\to\alpha_0}\frac{1}{2}\hat{D}^2\left[\ln\left[-\frac{\left[-(m_1-1)\alpha_1-(m-m_1)\alpha_0\right]^m}{m^2\alpha_0}\cdot\right.\right.$$
$$\left.\left.\cdot\left[\frac{m\alpha_0}{(m_1-1)\alpha_1+(m-m_1)\alpha_0}\right]^{m/m_1}\left[1+\frac{\alpha_1}{(m_1-1)\alpha_1+(m-m_1)\alpha_0}\right]^{m(m_1-1)/m_1}\right]\right]$$
$$=-\left[\frac{m_1-1}{m(m-m_1)(m-1)}\right]\frac{m(m-1)(m-m_1)}{2(-m\alpha_0)^2(m_1-1)}=-\frac{1}{2(-m\alpha_0)^2}=-\frac{1}{2\hat{A}^2} \tag{C.14}$$

By putting together this result with the one of the previous section and by doing some algebra, we can recover the replicon eigenvalue we have computed using the perturbative expansion around the 1RSB entropy.

Appendix D

Riassunto

In questo lavoro di tesi abbiamo studiato numerosi aspetti della teoria dei sistemi disordinati. In particolare, abbiamo studiato approfonditamente i sistemi vetrosi. La descrizione dettagliata di questi sistemi rappresenta un problema ancora aperto nella fisica della materia condensata. Infatti ancora non esiste una teoria univoca e ben stabilita per la comprensione delle caratteristiche fisiche di tali sistemi. I sistemi vetrosi sono molto comuni in natura. Generalmente un liquido diventa un solido cristallino quando la temperatura diventa più bassa della temperatura critica. Tuttavia per molte sostanze liquide è possibile sottoraffreddare il sistema al di sotto della temperatura di fusione prevenendo così la formazione del cristallo. Il liquido entra così in una fase metastabile sottoraffreddata dove mostra particolari ed interessanti proprietà. Una prima osservazione è che ad un certo punto la viscosità del liquido aumenta in maniera esponenziale al diminuire della temperatura. Questo significa che la dinamica del sistema rallenta enormemente. La temperatura della transizione vetrosa è definita come la temperatura alla quale la viscosità diventa pari a 10^{13} Poise. Un sistema con una tale viscosità non può più essere considerato un liquido (anche se sottoraffreddato) ma è un solido amorfo, un vetro. Un problema fondamentale è che il vetro ha tutte le caratteristiche

strutturali del liquido da cui proviene. Infatti se si osserva la struttura nella quale sono arrangiate le molecole, allora si può vedere che non ci sono molte differenze tra le configurazioni tipiche della fase vetrosa e quelle della fase liquida.

La transizione vetrosa può essere descritta facilmente osservando la dinamica del sistema nella fase sottoraffreddata quando la temperatura viene abbassata. Una delle caratteristiche principali dei sistemi vetrosi è che quando la temperatura è molto vicina a quella di transizione, la dinamica avviene su due scale di tempo. Questo può essere osservato se si guarda direttamente il mean square displacement che è definito come il quadrato della distanza media tra la posizione di una particella all'istante di tempo t e la sua posizione iniziale. Questa quantità è una funzione crescente del tempo t. Per piccoli valori di t si è in un regime balistico dove ogni particella non ha avuto il tempo di sentire la presenza delle altre. Ne segue che in tale regime il mean square displacement cresce proporzionalmente a t^2. Per tempi molto grandi invece, ci aspettiamo che prevalga la diffusione delle particelle e quindi il mean square displacement crescerà come t. Quando ci avviciniamo alla transizione vetrosa, questi due regimi sono separtati dalla comparsa di un plateau nel mean square displacement la cui lunghezza aumenta al diminuire della temperatura. L'interpretazione fisica è la seguente. Proviamo a seguire il movimento di una singola particella. A tempi corti, ci aspettiamo che essa non senta l'effetto delle altre particelle e segua una traiettoria di moto libero. Non appena il tempo aumenta, ad un certo punto tale particella comincerà a sentire l'effetto "gabbia" formato dalle altre particelle intorno. Se queste ultime possono riarrangiarsi cooperativamente, la particella che stiamo seguendo riuscirà ad uscire dalla gabbia formata dalle altre, altrimenti rimarrà intrappolata in essa. Alla transizione vetrosa, il riarrangiamento collettivo delle particelle è bloccato e ogni particella rimane intrappolata nella gabbia formata dalle particelle intorno ad

essa. Questa descrizione dà una interpretazione chiara della formazione del plateau nel mean square displacement.

Un altro fenomeno che possiamo osservare nei liquidi sottoraffreddati vicini alla transizione vetrosa è quello delle eterogeneità dinamiche. Se osserviamo la mobilità delle particelle possiamo accorgerci che ci sono alcune particelle con una mobilità molto elevata e altre particelle pressochè immobili. Inoltre è cruciale osservare che le particelle mobili sono organizzate in cluster la cui taglia cresce non appena la temperatura descresce verso quella della transizione vetrosa. L'ultimo decennio ha visto degli enormi progressi nello studio delle eterogeneità dinamiche e del loro ruolo per la comprensione della transizione vetrosa.

Tutta questa fenomenologia può essere spiegata all'interno di molti quadri teorici. In questa tesi abbiamo studiato tali problemi all'interno della teoria delle repliche. Tale approccio ha origine nella trattazione teorica dei modelli di vetri di spin che stanno ai vetri strutturali così come il modello di Ising sta ai materiali ferromagnetici. La teoria delle repliche è stata sviluppata per risolvere analiticamente alcuni modelli di campo medio per i vetri di spin la cui dinamica è molto vicina qualitativamente alla dinamica lenta tipica dei vetri strutturali vicino alla transizione vetrosa. La lezione che si può ricavare dalla soluzione dei modelli di campo medio è che quando la temperatura si avvicina al punto di transizione, il paesaggio di energia libera diventa molto corrugato e sviluppa un numero molto grande di minimi locali. Il numero di tali minimi è esponenzialmente grande nella taglia del sistema e la funzione che controlla tale numero è chiamata complessità o entropia configurazionale. Tali minimi non sono nient'altro che gli stati metastabili nei quali la dinamica del sistema rimane intrappolata quando siamo vicini alla transizione.

All'interno di questo formalismo abbiamo analizzato la teoria delle fluttuazioni intorno alla soluzione di campo medio per i vetri strutturali. L'idea

principale è quella di fare un parallelo tra la transizione ferromagnetica del modello di Ising e i la transizione vetrosa nei vetri strutturali. Per fare ciò, il primo oggetto da definire è un parametro d'ordine per le due transizioni. Nel caso del modello di Ising il parametro d'ordine corretto è la magnetizzazione media del sistema che è pari a zero se la temperatura è più grande della temperatura critica e diversa da zero sotto la temperatura critica. Nel caso della transizione vetrosa invece non è molto chiaro quale sia il parametro d'ordine corretto. Infatti abbiamo visto che le configurazioni del liquido e del vetro sono molto simili e non c'è nessuna differenza qualitativa tra le due. In generale quando siamo in una situazione di questo tipo, possiamo risolvere il problema confrontando due configurazioni. Supponiamo di fare ciò nel caso della transizione ferromagnetica. Se siamo sotto la temperatura critica, due configurazioni del sistema avranno in media la stessa magnetizzazione e saranno quindi piuttosto simili. Il grado di somiglianza tra due configurazioni è rappresentato dall'overlap tra esse. Nei vetri diciamo che se l'overlap medio tra due configurazioni è diverso da zero allora siamo in una fase vetrosa altrimenti siamo nella fase liquida.

A livello dinamico, possiamo identificare l'overlap nel seguente modo. Supponiamo di prendere una configurazione di un sistema ben equilibrato ad una certa temperatura. Se facciamo evolvere la dinamica a partire da tale configurazione, possiamo monitorare la somiglianza della configurazione del sistema con quella iniziale al variare del tempo. Questo ci dà una funzione di correlazione dinamica del sistema. Ad alte temperature ci aspettiamo che a grandi tempi, tale funzione di correlazione vada a zero. Tuttavia quando la temperatura viene abbassata verso quella alla quale avviene la transizione vetrosa, tale funzione di correlazione sviluppa un plateau ad un valore strettamente diverso da zero la cui lunghezza aumenta non appena la temperatura scende verso quella critica. Il valore della funzione di correlazione dinamica al plateau

non è nient'altro che l'overalp del sistema. Nei modelli di campo medio, la lunghezza del plateau diverge alla transizione vetrosa mentre sappiamo bene che in dimensione infinita, tale plateau ha una lunghezza finita a causa dei fenomeni di nucleazione. La presenza del plateau divide il rilassamento della funzione di correlazione in due regimi temporali. Il primo è il regime β che riguarda tutto il rilassamento della funzione di correlazione dinamica fino al plateau; il secondo è il regime α che riguarda il rilassamento a partire dal plateau. Il fatto che la funzione di correlazione si blocchi al valore di plateau è indicativo del fatto che la configurazione che evolve nel tempo non è in grado di allontanarsi da quella iniziale. Questo vuol dire che il sistema è intrappolato in uno dei tanti stati metastabili che si formano alla transizione vetrosa.

Una volta definito il corretto parametro d'ordine per la transizione vetrosa, possiamo studiare le sue fluttuazioni. Avendo stabilito il collegamento tra l'overlap e la dinamica, quello che possiamo fare è studiare quali sono le fluttuazioni della funzione di correlazione dinamica per tempi che sono tali per cui essa è al suo valore di plateau. Tale studio può essere effettuato utilizzando la teoria delle repliche. In questa tesi è stata derivata una teoria di campo effettiva per tali fluttuazioni. Questa è stata studiata a livello Gaussiano e ne sono stati dati gli esponenti critici predetti. Inoltre, attraverso un conto perturbativo, è stato dato un numero di Ginzburg per la transizione vetrosa che dà due informazioni importanti: la prima è la dimensione critica superiore; la seconda ci dice invece quanto dobbiamo essere vicini alla temperatura di transizione per poter apprezzare gli effetti non mean field nel caso in cui la dimensione fosse inferiore a quella critica superiore. Inoltre attraverso lo stesso tipo di analisi è stata data l'espressione per l'exponent parameter che nella teoria di mode-coupling è il parametro che controlla gli esponenti con cui la funzione di correlazione dinamica arriva e riparte dal plateau. Tale calcolo è estremamente rilevante dato il fatto che è di cruciale importanza mettere in

relazione diverse teorie della transizione vetrosa. La teoria di mode-coupling si basa su un approccio completamente dinamico e fenomenologico e usualmente si rivolge allo studio di osservabili fisiche puramente dinamiche. La teoria delle repliche invece è un approccio statico che si focalizza sullo studio del paesaggio di energia libera. Ne segue che è difficile mettere in relazione le due teorie visto che le osservabili che si calcolano in entrambi i casi sono spesso diverse. In questa tesi abbiamo calcolato l'exponent parameter dalla teoria delle repliche e possiamo metterlo in relazione con i calcoli della teoria di mode coupling.

E' fondamentale notare che la teoria delle fluttuazioni così derivata è valida nell'ultimo tratto della regione β per la dinamica, cioè lì dove la funzione di correlazione è al suo valore di plateau. Possiamo chiederci se è possibile derivare qualche stima delle fluttuazioni in tutta la regione in cui la funzione di correlazione decade dal plateau. Questo problema può essere studiato puramente in dinamica ma è estremamente difficile. D'altro canto ci piacerebbe avere una descrizione statica anche per la dinamica a lunghi tempi. L'osservazione cruciale è che ci aspettiamo che la dinamica in questo regime sia un processo di quasi-equilibrio in cui il sistema rilassa da uno stato metastabile all'altro avendoli esplorati ciascuno in maniera quasi ergodica. E' possibile formalizzare questa intuizione fisica attraverso una costruzione quasi statica per la dinamica a lunghi tempi. Tale costruzione si chiama pseudodinamica di Boltzmann ed è stata recentemente introdotta da Franz e Parisi nel contesto dei vetri di spin. In tale costruzione si ha una catena di sistemi ognuno vincolato ad avere un overlap fissato con il sistema che lo precede. Se si studia l'energia libera dell'ultimo sistema della catena, si può ottenere una generalizzazione del potenziale di Franz-Parisi. Nei modelli di vetri di spin in campo medio, è stato osservato che tale formalismo riproduce la dinamica di Langevin a lunghi tempi nel limite in cui la lunghezza della catena diventa infinita. In questo la-

voro di tesi, abbiamo applicato tale costruzione ai vetri strutturali. Abbiamo fatto ciò nell'approssimazione più semplice che disponiamo per descrivere la transizione vetrosa che è l'approssimazione Hypernetted Chain replicata. In questo schema siamo riusciti a dare una versione dinamica delle equazioni di Ornstein-Zernike e siamo riusciti ad ottenere un set di equazioni dinamiche chiuse. Il primo risultato è che tali equazioni sono estremamente simili alle equazioni di mode-coupling. Inoltre abbiamo studiato sia la dinamica di equilibrio che quella di fuori equilibrio ed abbiamo calcolato di nuovo l'exponent parameter ed il fluctuation-dissipation ratio della dinamica di ageing. Il risultato per l'exponent paramenter coincide con quello ottenuto nello studio delle fluttuazioni dinamiche mentre il fluctuation-dissipation ratio è fissato dalla condizione di stabilità marginale che seleziona gli stati di threshold della dinamica. Gli stati di threshold sono gli stati metastabili più alti in energia libera e con più alta entropia configurazionale. Ne segue che a questo livello la pseudodinamica dà lo stesso quadro teorico ottenuto nei modelli di campo medio dei vetri di spin.

La terza parte della tesi ha riguardato lo studio degli stati amorfi di sfere dure in dimensione infinita. La motivazione originale per tale studio è stata il fatto che in approssimazione Hypernetted Chain, la stima dell'exponent parameter non era molto accurata per cui è stato abbastanza naturale cercare una approssimazione quantitativamente migliore in cui ottenere dei risultati numerici che meglio riproducono le osservazioni sperimentali e numeriche. Le sfere dure in dimensione infinita forniscono un framework perfetto per tale tipo di analisi. Infatti il limite di dimensione infinita non è nient'altro che un'approssimazione di campo medio nella quale sperabilmente possiamo ottenere dei risultati esatti. Recentemente, una teoria per le sfere dure in dimensione infinita è stata fornita in un lavoro di Kurchan, Parisi e Zamponi. In tale lavoro viene mostrato che l'approssimazione gaussiana per la densità

di molecole fornisce i risultati corretti per l'entropia libera del sistema. In tale quadro è possibile usare la teoria delle repliche per stimare il diagramma di fase delle sfere dure. In particolare è possibile studiare il diagramma di fase che si può ottenere in approssimazione 1RSB (one-step-replica-symmetry-breaking).

Per calcolare l'exponent parameter in questo framework è cruciale studiare la stabilità della soluzione 1RSB. In questo lavoro di tesi abbiamo effettuato tale analisi ed abbiamo scoperto che la teoria delle repliche per le sfere dure in dimensione infinita predice una linea di instabilità della soluzione 1RSB che a grandi valori della densità e di pressione è responsabile di una transizione di Gardner. La transizione di Gardner è stata scoperta nel caso dei modelli di campo medio per i vetri di spin. Nel contesto analizzato in questa tesi ha un significato estremamente interessante. Infatti il diagramma di fase a livello 1RSB descrive il comportamento del sistema quando appaiono a livello di campo medio un numero esponenziale di stati metastabili. Tuttavia tali stati sono stabili nel senso stretto del termine e cioè sono dei veri minimi dell'energia libera. Quando il sistema va incontro alla transizione di Gardner, tali minimi non sono più completamente stabili ma diventano solo marginalmente stabili. In particolare, i vecchi minimi della soluzione 1RSB diventano bacini di stati marginalmente stabili. Per descrivere correttamente questa situazione occorre rilassare l'approssimazione 1RSB e cercare una soluzione nello schema che prende il nome di fullRSB. Tale schema è stato introdotto per risolvere alcuni modelli di campo medio di vetri di spin.

Uno dei risultati dell'analisi della stabilità del diagramma di fase 1RSB è il fatto che la parte instabile di tale diagramma si ha nella regione ad alte pressioni. Questo vuol dire che i risultati 1RSB non predicono correttamente il comportamento del sistema al jamming. Che la soluzione 1RSB non fosse corretta in questa situazione era già noto poichè essa risulta inconsistente con molte evidenze numeriche e sperimentali. La scoperta che tale soluzione

è instabile apre la via allo studio della fisica del jamming con tecniche ed approssimazioni più raffinate che sperabilmente possono riconciliare la teoria delle repliche con i dati sperimentali e numerici. Contemporaneamente a questo risultato abbiamo ottenuto una nuova stima per l'exponent parameter della teoria di mode-coupling ed abbiamo trovato un risultato numerico che sembra essere consistente con i risultati sperimentali.

Una volta stabilito che la soluzione 1RSB è instabile al jamming, abbiamo provato a vedere se soluzioni con un numero più elevato di rotture di simmetria delle repliche possono dare risultati migliori. Il primo passo è stato quello di cercare una soluzione 2RSB (two-steps-replica-symmetry-breaking). I risultati di questa analisi sono stati molteplici. Il primo di essi è stato l'individuazione del punto preciso all'interno del diagramma di fase oltre il quale è possibile avere una soluzione 2RSB e (quindi anche fullRSB). Questo è estremamente importante perchè restringe la regione del diagramma di fase in cui cercare soluzioni con ulteriori rotture di simmetria delle repliche. Successivamente siamo riusciti a derivare l'espressione per l'entropia libera a livello 2RSB ed abbiamo utilizzato tale risultato per ottenere delle predizioni alla fisica del jamming in approssimazione 2RSB. In questo contesto abbiamo derivato il valore della densità di threshold 2RSB. La denistà di threshold rappresenta la densità più bassa alla quale si hanno i primi packing amorfi. Un risultato interessante è che il nuovo valore della densità di threshold è leggermente più alto di quello che si può ottenere in approssimazione 1RSB. Inoltre abbiamo scritto un programma per risolvere numericamente le equazioni 2RSB. Questo ci ha permesso di capire come si comporta la soluzione a grandi densità e i risultati numerici sono stati confrontati con una espansione asintotica per la soluzione delle equazioni 2RSB.

Una volta analizzata la soluzione 2RSB abbiamo tentato di risolvere il problema in approssimazione fullRSB. Questo ci ha permesso di derivare la

cosiddetta equazione di Parisi per i sistemi di sfere dure in dimensione infinita. Un risultato molto sorprendente è che le equazioni derivate sono estremamente simili a quelle che possono essere ricavate nel caso dei modelli di campo medio per i vetri di spin. Questa osservazione è assoultamente rilevante perchè permette di capire la fisica del jamming attraverso i risultati ottenuti nel caso dei sistemi disordinati con disordine quenched. Una volta derivate le equazioni fullRSB abbiamo utilizzato un codice che fosse in grado di risolverle numericamente. I risultati numerici ottenuti possono essere utilizzati per derivare una predizione per il comportamento del Debye-Waller factor come funzione della pressione quando ci si avvicina al punto di jamming. Infatti tale quantità ci si aspetta che tendi a zero con la pressione come una legge a potenza $\Delta_{EA} \sim p^{-\sigma}$. I nostri risultati numerici sembrano indicare un valore dell'esponente σ molto vicino a $3/2$ in accordo con quanto previsto in letteratura. Tuttavia una precisa stima numerica ancora non è disponibile. Per confermare o smentire tale predizione in maniera sicura occorre migliorare l'analisi numerica e soprattutto provare a derivare analiticamente una predizione per σ. Lasciamo questi punti per studi futuri.

L'ultima parte della tesi è dedicata allo studio della dinamica di mode-coupling quando la transizione vetrosa diventa continua. Come abbiamo visto di sopra, la funzione di correlazione dinamica, non appena la temperatura scende in prossimità della transizione vetrosa, sviluppa un plateau ad un valore strettamente diverso da zero. Questa situazione non è la più generale possibile. Infatti esitono casi in cui il valore di plateau è molto vicino a zero. In questa situazione abbiamo studiato le equazioni dinamiche a tempi lunghi ed abbiamo visto che esse possono essere risolte esplicitamente per ottenere la forma asintotica della funzione di correlazione. Abbiamo utilizzato infine tale risultato per studiare le fluttuazioni dinamiche nel regime di tempi lunghi.

Le prospettive aperte da questa tesi sono molteplici. Per quanto riguarda il primo lavoro relativo allo studio delle fluttuazioni dinamiche, è fondamentale cercare di capire in che modo andare oltre il livello Gaussiano. Per quanto riguarda invece la pseudodinamica, ci sono ancora molti territori da esplorare. Il primo punto di fonamentale importanza è capire se è possibile studiare la teoria delle fluttuazioni dinamiche con questo tipo di approccio. Questo problema è estremamente interessante perchè lo studio delle fluttuazioni in regime β con la teoria delle repliche ha mostrato che alla transizione dinamica la teoria effettiva che può essere ricavata può essere messa in corrispondenza con un'azione efficace per un campo scalare in un potenziale cubico e sotto l'azione di un campo random Gaussiano. Sarebbe estremamente interessante capire se questa conclusione può essere ritrovata anche nel caso delle fluttuazioni a tempi lunghi. Per quanto riguarda il lavoro sulle sfere dure, a questo punto il vaso di Pandora della fisica fullRSB è completamente aperto e rimane da esplorare quali sono tutte le sue conseguenze. Un punto cruciale è cercare di derivare analiticamente il valore dell'esponente che controlla come va a zero il Debye-Waller factor con la pressione al jamming. Questo potrebbe essere fatto in linea di principio seguendo le stesse linee guida per derivare le soluzioni asintotiche di temperatura nulla per i modelli di campo medio dei vetri di spin. Per quanto riguarda invece il lavoro sulla dinamica nella transizione quasi continua, una possibilità che va investigata ulteriormente è se si può sfruttare la semplicità che emerge quando la transizione diventa continua nel calcolo delle funzioni dinamiche a quattro punti. Una derivazione analitica per le fluttuazioni in questo contesto sarebbe estremamente utile e interessante.

Appendix E

Résumé

Dans cette thèse nous avons étudié de nombreux aspects de la théorie des systèmes désordonnés. En particulier, nous avons étudié les systèmes vitreux. La description détaillée des systèmes désordonnés et vitreux est un problème ouvert en physique de la matière condensée. A ce jour, il n'existe toujours pas de théorie unique et établi permettant de comprendre ces systèmes. Les systémes vitreux sont très commun dans la nature. Généralement un liquide devient un cristal lorsque la température descend en dessous d'une valeur critique. Toutefois, si on peut prévenir la formation de la phase cristalline, le liquide entre dans une phase appelée "supercooled" où des phenomènes interessants apparaissent. Premièremant la viscosité du fluide devient très grande lorsque la temperature décroit : la dynamique du système devient très lente. La température critique de la transition vitreuse est atteinte lorsque la viscosité est de l'ordre de 10^{13} Poise. Pour ces valeurs de la viscosité, le liquide est si visqueux qu'il ne peut plus être considéré comme un liquide mais comme un solide. Si l'on regarde la structure moleculaire du système on decouvre qu'il n'est pas un cristal puisque les atomes ou molécules ne sont pas ordonné dans un réseau cristallin. Cependant, la structure est très similaire a celle d'un liquide mais la dynamique est si lente que le système peut etre consideré comme

un solide. Un tel sytème est appelé un verre.

Une autre chose très intéressante est que la dynamique est divisée sur deux règions de temps. Ceci peut se voir en regardant le "mean square displacement" défini comme suit : on prend une particule dans le système et on regarde au temps t la distance entre sa position et sa position initiale : la moyenne sur toutes les particules définie le "mean square displacement". Si l'on regarde le "mean square displacement" comme une fonction du temps, on se rend compte que la dynamique est carcaterisée par deux échelles de temps. La première règion de temps correspond à la règion sur laquelle la particule vibre dans la "cage" que les autres particules forment autour d'elle. La deuxième règion de temps est définie comme l'échelle sur laquelle la particule parvient à s'échapper de la cage. Ce mouvement peut avoir lieu uniquement après un réarrangement structurel permettant à la particule piegée de se liberer et est donc très difficile à observer. Les deux échelles de temps sont séparées par la formation d'un plateau qui devient de plus en plus long lorsque la température s'approche de la température de la transition vitreuse.

Si l'on s'interesse maintenant à la mobilité des particules, on observe qu'il existe des régions où la mobilité est très grande et d'autres où la mobilité est très petites. La taille de ces régions croit lorsque la température est très proche la température de la transition vitreuse. C'est le phenomène d'heterogeneités dynamique. Dans la dernière décennie, l'etude des heterogeneités dynamique était crucial pour une meilleure compréhension de la dynamique proche de la transition vitreuse. Toute cette phénoménologie peut etre expliquée dans beaucoup de cadres théoriques. Dans cette thèse nous avons choisi l'approche de la théorie des répliques. Cette approche provient des modèles de verres de spin qui sont les prototypes des verres structuraux. Les verres de spins qui sont résolus avec la théorie des répliques, sont des modèles de champ moyen. La leçon que nous pouvons apprendre avec ces modèles est que lorsque nous

nous approchons de la transition vitreuse, le paysage de l'énergie libre devient très irrégulier avec beaucoup de minimums. En particulier, le nombre de minimums avec une certaine énergie libre est egale à l'exponentielle de la taille du système fois une fonction que nous appellons l'entropie configurationnelle où complexité. L'entropie configurationelle peut expliquer la dynamique vitreuse. Afin de relaxer, le système doit explorer tout le paysage d'énergie libre mais si il y a beaucoup d'états metastables, le système peut tomber dans un état metastable et il faut attendre un très long intervalle de temps pour en sortir. Cependant, ce tableau est vrai uniquement au niveau du champ moyen parce qu'en dimension finie, il est prédit que la transition disparaît grâce au le phénomène de nucléation. Les barrières de potentiels entre les états metastables dans le paysage d'énergie libre ne sont plus de l'ordre de la taille du système, mais sont de taille moindre.

Dans le cadre de la théorie de champ moyen pour les verres structuraux nous avons étudié la théorie des fluctuations proche de la transition vitreuse dynamique. Nous avons fait une comparaison avec la théorie des fluctuations dans le cas de la transition ferromagnétique. La première chose que nous avons fait a été d'introduire un paramètre d'ordre. Dans le cas de la transition ferromagnétique, le paramètre d'ordre correct est la magnétisation. Dans le cas de la transition vitreuse il n'est pas clair quel doit etre le paramètre d'ordre correct. En fait, si l'on regarde la structure du système avant et après la transition on peut voir que le système est qualitativement le meme. Dans une telle situation, la chose la plus simple que l'on peut faire est de prendre deux configurations du système et les comparer. Faisons ceci dans le cas de la transition ferromagnétique. Si la température est inferieure à la température critique, la magnetisation n'est pas nulle. Deux configurations du système seront donc très proche parce qu'elles ont la meme magnétisation. On peut faire la meme chose pour le verres avec l'introduction d'une mesure de

similarité entre les configurations. Nous appelons cet objet l'overlap. Si deux configurations ont un overlap different de zero alors elles sont très proches l'une de l'autre. A l'opposé si l'overlap est nul alors les configurations sont très differentes l'une de l'autre. Si l'overlap moyen est différent de zero, alors le système est dans la phase vitreuse mais si l'overlap est exactement zero, le système est dans la phase liquide.

D'un point de vue dynamique, l'overlap entre deux configurations peut etre caracterisé par la corrélation normalisée entre les configurations du système au temps t et au temps zero. Si la configuration au temps zero est choisi à l'équilibre, cette fonction de correlation dynamique présente un plateau lorsque la température est proche de la température de la transition vitreuse. À la transition vitreuse, la longueur du plateau de la fonction de corrélation devient infinie. L'ergodicité est brisée et la mesure de Boltzmann est divisée sur un nombre exponentielle d'états métastables. Le valeur de la fonction de corrélation sur le plateau est l'overlap du système. Nous avons étudié dans cette thèse les fluctuations de la fonction de corrélation dynamique pour des temps sur lesquels la fonction de corrélation est proche de sa valeur de plateau. Nous appelons cette région des temps, le régime β de la dynamique. Elle est connectée avec l'échelle des temps de relaxation dans la cage. Le régime α est défini comme la région des temps pour lesquels la fonction de corrélation débute par le plateau et est connecté avec le rèarrangement structurel du système. L'étude des fluctuations peut etre fait avec le formalisme statique de la théorie de répliques. Nous avons fait cela en introduisant une théorie des champs pour la transition vitreuse à partir du potentiel microscopique entre les particules. Nous avons étudié dans ce cadre les fluctuations au niveau gaussien et nous avons évalués les exposants critiques dans ces approximations. Nous avons aussi étudié la région de validité de la prédiction gaussienne avec l'introduction d'un critère de Ginzburg pour la transition vitreuse. Dans ce

cadre nous avons aussi étudié les exposants dynamiques de la fonctions de corrélation dynamique quand elle s'approche et débute par le plateau. Nous avons donné des prédictions de cette théorie dans l'approximation "Hypernetted Chain". Cette approximation est une approximation standard de la théorie des liquides et nous avons utilisé une extension de ce cadre qui est valide pour un liquide de répliques. Les résultats que nous avons obtenues ne sont valides que dans la région β . Nous voudrions aussi avoir des résultats pour la région α. La chose très difficile dans ce cas est que nous n'avons pas une description statique de la dynamique dans le régime α. La solution à cette question est donnée par une construction introduite par Franz et Parisi dans le cas de les systèmes de verres de spin et appelée Boltzmann Pseudo-dynamics. Cette construction est basée sur l'interprétation suivante de la dynamique vitreuse. Quand la température est proche de la température de transition vitreuse, la relaxation se déroule dans un paysage d'énergie libre avec beaucoup de minimums. Dans la première échelle de temps de relaxation de la fonction de corrélation dynamique, le sytème tombe dans le premier état metastable disponible. Quand il a exploré tout cet état, il sort et il tombe dans un autre état metastable. La chose la plus importante dans ce processus est que chaque état metastable est exploré d'une façon quasi à l'équilibre. Les configurations des états métastables seront donc exploré avec une fréquence proportionnelle à la mesure de Boltzmann conditionnée sur l'état. Une façon de décrire au niveau théorique cette idée est de généraliser la construction du potentiel de Franz et Parisi. Ce potentiel est l'énergie libre d'un système qui est forcé d'avoir un overlap fixé avec un autre système. Si on regarde ce potentiel comme une fonction de l'overlap on peut voir que dans la phase des hautes températures, le potentiel a un minimum global pour l'overlap égal à zero. A la transition vitreuse, on peut voir que le potentiel développe un minimum local à la valeur de l'overlap qui est égal la valeur du plateau de

la fonction de corrélation dynamique. On peut faire une généralisation de cette construction avec l'introduction d'une chaîne de systèmes. Chaque système est forcé d'avoir un overlap fixé avec les configurations du système qui le precède et il fixe l'overlap avec le système qui le suit. Si on regarde l'énergie libre du dernier système de la chaîne, on a une généralisation du potentiel de Franz-Parisi. Cette géneralisation est appelée Boltzmann Pseudodynamics. Nous avons étudié cette construction dans le cas des verres structuraux. Nous sommes parti des équations de Ornstein-Zernike et nous avons obtenu un ensemble d'équations dynamiques. En utilisant l'approximation Hypernetted Chain nous avons obtenu un ensemble complet d'équations qui sont très similaires aux équations de la théorie de mode-coupling. La première chose que nous avons étudié avec ces équations est la dynamique d'équilibre. Nous avons re-obtenu les exposants dynamique de la fonction de corrélation que nous avons calculé dans l'approche de l'étude des fluctuations.

Après, nous avons étudié la dynamique hors équilibre et nous avons obtenu le "fluctuation-dissipation ratio" de la dynamique de vieillissement. Nous avons montré que la valeur du fluctuation-dissipation ratio peut être obtenu par la condition de stabilité marginale pour la dynamique. Ce qui est équivalent à dire que les états les plus importants pour la dynamique de vieillissement sont les états de « threshold » définies comme suit. À la transition vitreuse nous avons dit que la mesure de Bolzmann est divisée en un nombre exponentiel d'états metastables. Ces états sont organisés en fonction de leur énergie libre. Il y a des états d'énergie libre elevée et des états d'énergie libre basse. Les états qui ont l'énergie libre la plus elevée sont appelés les états de threshold. La solution du modèle de champ moyen pour les verres de spins montre que soit la dynamique à l'équilibre soit la dynamique hors équilibre est dominée par les états de threshold. Ici on a trouvé le meme résultat dans le cas de l'étude des verres structuraux.

La troisième partie de la thèse porte sur l'étude des états amorphes des sphères dures en hautes dimensions. Les motivations pour cette étude proviennent du fait que les résultats que nous avons obtenu sur les exposants dynamiques dans l'approximation Hypernetted Chain ne sont pas en accord avec les indications expérimentales et numériques. Nous avons cherché un cadre dans lequel la théorie des répliques marche mieux. La théorie des sphères dures constituait un très bon candidat. L'étude des états amorphes des sphères dures est un problème ouvert en physique de la matière condensée. En particulier, l'étude de la physique reliée à la transition de jamming est devenu un sujet très populaire dans la cadre de la physique statistique. Les sphères dures sont étudiée comme modèles de verres mais ont aussi des applications en informatique et aussi en mathématique. Les algorithmes utilisés pour produire des "jammed packings" de spheres dures font appel à des protocoles dynamiques avec un peu de désordre. Par exemple, on peut faire une simulation de dynamique moléculaire sur les sphères dures et on peut augmenter le dimension des sphères pendant la simulation jusqu'à ce que les sphères se touchent. La dynamique s'arrête alors puisque le système est bloqué dans un arrangement amorphe. Une chose très intéressante est que la densité finale des packings que l'on peut ainsi constuire est indépendante de la condition initiale et aussi de l'algorithme utilisé. La densité finale à laquelle on arrive est appelée random close packing density. Pour étudier les packings que l'on peut construire on doit directement regarder les protocoles mais c'est une chose très difficile à faire. Notre approche consiste à décrire les jammed packings comme la limite de pression infinie des états vitreux métastables. Cette limite peut être analysée dans le cadre de la théorie des répliques où l'on possede le diagramme de phase dans l'approximation 1RSB (one-step replica symmetry breaking).

Pour obtenir les exposants dynamique dans ce cas, nous avons étudié la stabilité du diagramme de phase 1RSB. Nous avons découvert que ce diagramme

de phase possède une région où la solution 1RSB est instable. La solution 1RSB, là où elle est stable, décrit une situation où les états metastables que nous trouvons sont de vrai états. Ce qui signifie qu'ils sont les vrai minimum du paysage d'énergie libre. Là où la solution 1RSB est instable, les minimums de l'énergie libre ne sont plus de vrais minimum mais ont des directions instables. La région où la solution 1RSB est instable est connectée avec la description théorique de la physique de jamming des sphères dures et nous avons montré que l'instabilité 1RSB est responsable d'une transition de phase en haute densité. Cette transition s'appelle la transition de Gardner et a été découverte dans le cas des verres de spin. La solution devient fullRSB lorsque la densité atteint la valeur permettant la transition de Gardner. Les minimums du paysage d'énergie libre sont organisées avec une structure hiérarchique et ne sont pas de vrai minimums parce qu'ils ont toujours des directions marginalement stables. Dans ce cadre nous avons obtenu les exposants dynamiques du mean square displacement à la transition vitreuse. Les résultat que nous avons obtenu sont meilleurs que ceux obtenus dans l'approximation Hypernetted Chain. Nous avons ensuite étudié la région du diagramme de phase où la solution 1RSB est instable. Nous avons cherché une solution 2RSB et nous avons vu qu'il existait un point en densité après lequel on peut avoir une solution 2RSB (et aussi fullRSB). Nous avons étudié le diagramme de phase 2RSB dans la limite de jamming où la pression devient infini. Nous avons obtenu le nouvelle valeur de la densité de threshold. La densité de threshold est définie comme le point où on a les jammed packings à la densité la plus basse. La densité de threshold 2RSB est un peu plus grande que la densité de threshold au niveau 1RSB. Nous avons aussi étudié la solution 2RSB dans le régime des hautes densité où nous avons des prédictions asymptotiques sur le comportement des paramètres de la solution qui sont en bon accord avec la solution numérique des équations de saddle point. Après la solution 2RSB nous avons

cherché à décrire la solution fullRSB. Nous avons écrit les équations fullRSB et nous avons découvert qu'elles sont identiques aux equations que l'on a dans le cas de un modèle de verres de spins qui s'appelle modèle de Sherrington et Kirkpatrick. Ce modèle est très important car il est le premier modèle à avoir été resolu par la théorie de répliques avec une solution fullRSB. Il s'ensuit que la physique de jamming de sphères dures est très proche la physique des modèles de verres de spins dans le cadre du champs moyen. Nous avons aussi étudié la solution numerique des équations fullRSB dans la limite de jamming. Cette solution montre beaucoup des choses intéressantes. La plus importante est le comportement du mean square displacement dans la limite de jamming. En fait, on peut voir comme la valeur du plateau du mean square displacement s'approche de zero quand la pression devient infini. Dans le cadre de la solution 1RSB et 2RSB (et en general dans tout les cadres où nous avons un nombre fini de replica symmetry breaking) le plateau s'approche de zero comme l'inverse de la pression. Si l'on regard les résultats numériques et éxperimentaux, il semble que le plateau s'approche a zero comme la pression à un exposant proche de $-3/2$. Ce qui signifie que la solution avec un nombre fini de replica symmetry breaking n'est pas exact pour la description de la physique du jamming. Mais nous savions déjà cela puisque la solution 1RSB est instable dans le partie du diagramme de phase qui est connecté avec le jamming. Nous avons vu avec la solution numérique des équations fullRSB que la solution d'échelle correct pour le plateau du mean square displacement semble etre décrit par la solution fullRSB. Cela ouvre la voie à l'étude de la physique du jamming avec les méthodes des verres de spins.

La quatrième partie de la thése a porté sur la dynamique de mode-coupling dans le régime où la transition vitreuse devient continue. Nous avons vu que le comportement de la fonction de corrélation dynamique est décrit avec une relaxation sur deux échelles de temps. Les deux échelles sont séparé par un

plateau. Généralement la valeur de la fonction de corrélation au plateau est légerement plus grande que zero. Il y a aussi des situations où la valeur au plateau est très proche de zero ; signifiant que la transition devient continue. Si on regarde les équations de mode-coupling dans un régime où la transition est continue on peut décrire le relaxation analytiquement. En particulier nous aimerions savoir quelle est la forme analytique de la fonction de corrélation dynamique. Nous avons étudié ce problème et nous avons vu qu'il est possible de prédire une forme analytique pour la fonction de corrélation dans le régime α. Nous avons fait cela dans le cas de la dynamique à l'équilibre et aussi dans le cas de la dynamique hors équilibre. Nous avons utilisé les résultats obtenus pour avoir une estimation des fluctuations de la fonction de corrélation dynamique dans le régime α.

Cette thèse ouvre beaucoup de perspectives. La première chose que l'on peut faire est l'étude avec le groupe de renormalisation de la théorie de champs que nous avons obtenu. Une chose qu'il faut souligner est que toute la théorie développée ne prend pas en compte les processus activés. Ces processus sont responsables de la disparition d'une vraie transition dynamique et détruisent le comportement du champ moyen que nous avons décrit ici. Une autre chose que l'on peut faire est d'utiliser le formalisme de la Boltzmann Pseudodynamics pour décrire les fluctuations dynamiques dans le régime du temps long. A cet effet nous devons étudier les petites fluctuations gaussiennes autour de la solution du saddle point pour le potentiel de Franz-Parisi généralisé. En appliquant ce formalisme aux fluctuations dynamiques dans le régime β on montre que la théorie des répliques que l'on obtient peut être mis en correspondance avec une théorie de champ pour un champ scalaire dans un potentiel cubique et en intéraction avec un champ extérieur aléatoire. Cette relation entre le modèle d'Ising en champ aléatoire et la transition vitreuse dynamique a éte mis en lumière avec l'étude de la structure des répliques de l'Hessian du po-

tentiel de Franz-Parisi autour de la solution de saddle point. Si l'on veut généraliser ces études dans le cas de la transition vitreuse en régime α on doit faire la même analyse sur le potentiel de Franz-Parisi généralisé. La dernière chose que l'on peut faire à partir du résultat de cette thèse est de donner une meilleure description de la physique de jamming des sphères dures avec la solution fullRSB que nous avons obtenu. En particulier, on peut faire un extension phénoménologique de notre résultat en dimension fini pour donner des prédictions de la solution fullRSB sur des quantités que l'on peut mesurer en deux ou trois dimensions.

Acknowledgments

During these three years of Ph.D. studies I have had the opportunity to work under the joint supervision of Giorgio Parisi and Silvio Franz. It is a great pleasure to warmly thank them for all the things that they have taught to me and for the constant encouragement and support that they have given to me. Doing this work with them has been a great experience full of so many things to learn. I will never forget the passion and curiosity with which we have discussed many many times about the topics contained in this thesis and beyond. I want also to warmly thank Francesco Zamponi. Most of the work contained here has been deeply supervised also by him. There are really not enough words to thank him for the wonderful physics we have done together and for the hours he spent trying to explain me and share with me so many things. In Paris, I have had the opportunity and the pleasure to work with Jorge Kurchan and I want to thank him for his collaboration to part of the work contained here. In Rome I have had a lot of fruitful discussions with Tommaso Rizzo and Federico Ricci-Tersenghi and it is a pleasure to thank them. This thesis work has been done both at the Department of Physics of the University of Rome "La Sapienza" and at the Laboratoire de Physique Théorique et Modèles Statistiques of the University of Paris-Sud 11; I want to thank both the two institutions. Moreover I want to thank the University Franco-Italienne that has provided part of the financial support through the Vinci program.

Infine vorrei ringraziare mamma per avermi mostrato i suoi appunti in bella calligrafia sulla radioattività naturale e sulla relatività ristretta e papà per avermi spiegato come usare le operazioni aritmetiche elementari. Grazie per questo e per tutto *il resto.*

Bibliography

[1] G. Adam and J. H. Gibbs. On the temperature dependence of cooperative relaxation properties in glass-forming liquids. *The journal of chemical physics*, 43:139, 1965.

[2] S. Alexander. Amorphous solids: their structure, lattice dynamics and elasticity. *Phys. Rep.*, 296:65, 1998.

[3] D. Amit. The ginzburg criterion-rationalized. *Journal of Physics C: Solid State Physics*, 7(18):3369, 1974.

[4] D. Amit and V. Martin-Mayor. *Field theory, the renormalization group, and critical phenomena*, volume 18. World Scientific Singapore, 2005.

[5] C. A. Angell. Spectroscopy simulation and scattering, and the medium range order problem in glass. *Journal of Non-Crystalline Solids*, 73(1):1–17, 1985.

[6] C. A. Angell. Formation of glasses from liquids and biopolymers. *Science*, 267(5206):1924–1935, 1995.

[7] C. A. Angell. Entropy and fragility in supercooling liquids. *National Institute of Standards and Technology, Journal of Research*, 102(2):171–185, 1997.

[8] T. Aste. Variations around disordered close packing. *J. Phys.: Condens. Matter*, 17:S2361–S2390, 2005.

[9] J. L. Barrat, W. Gotze, and A. Latz. The liquid-glass transition of the hard-sphere system. *Journal of Physics: condensed matter*, 1:7163, 1989.

[10] U. Bengtzelius. Dynamics of a lennard-jones system close to the glass transition. *Physical Review A*, 34(6):5059, 1986.

[11] U. Bengtzelius, W. Gotze, and A. Sjolander. Dynamics of supercooled liquids and the glass transition. *Journal of Physics C: Solid State Physics*, 17(33):5915–5934, 1984.

[12] L. Berthier, G. Biroli, J-P Bouchaud, L. Cipelletti, and W. van Saarloos. Dynamical heterogeneities and glasses. Oxford University Press, 2011.

[13] L. Berthier, G. Biroli, J.P. Bouchaud, L. Cipelletti, D. El Masri, D. L'Hôte, F. Ladieu, and M. Pierno. Direct experimental evidence of a growing length scale accompanying the glass transition. *Science*, 310(5755):1797–1800, 2005.

[14] L. Berthier, G. Biroli, J.P. Bouchaud, W. Kob, K. Miyazaki, and D. R. Reichman. Spontaneous and induced dynamic fluctuations in glass formers. I. General results and dependence on ensemble and dynamics. *The Journal of chemical physics*, 126:184503, 2007.

[15] L. Berthier, G. Biroli, J.P. Bouchaud, W. Kob, K. Miyazaki, and DR Reichman. Spontaneous and induced dynamic correlations in glass formers. II. Model calculations and comparison to numerical simulations. *The Journal of chemical physics*, 126:184504, 2007.

[16] Ludovic Berthier. Time and length scales in supercooled liquids. *Phys. Rev. E*, 69:020201, Feb 2004.

[17] K. Binder and W. Kob. *Glassy materials and disordered solids: An introduction to their statistical mechanics*. World Scientific, 2005.

[18] G. Biroli and J.-P. Bouchaud. Diverging length scale and upper critical dimension in the mode-coupling theory of the glass transition. *EPL (Europhysics Letters)*, 67(1):21, 2004.

[19] G. Biroli and J.P. Bouchaud. Critical fluctuations and breakdown of the Stokes-Einstein relation in the mode-coupling theory of glasses. *J. Phys.: Cond. Matt.*, 19:205101, 2007.

[20] G. Biroli and J.P. Bouchaud. The Random First-Order Transition Theory of Glasses: a critical assessment. In P.G.Wolynes and V.Lubchenko, editors, *Structural Glasses and Supercooled Liquids: Theory, Experiment and Applications*. Wiley & Sons, 2012.

[21] G. Biroli, J.P. Bouchaud, A. Cavagna, TS Grigera, and P. Verrocchio. Thermodynamic signature of growing amorphous order in glass-forming liquids. *Nature Physics*, 4(10):771–775, 2008.

[22] G. Biroli, J.P. Bouchaud, K. Miyazaki, and D.R. Reichman. Inhomogeneous mode-coupling theory and growing dynamic length in supercooled liquids. *Physical review letters*, 97(19):195701, 2006.

[23] J.-P. Bouchaud, L. Cugliandolo, J. Kurchan, and M. Mézard. Mode-coupling approximations, glass theory and disordered systems. *Physica A: Statistical Mechanics and its Applications*, 226(3):243–273, 1996.

[24] J.P. Bouchaud and G. Biroli. On the Adam-Gibbs-Kirkpatrick-Thirumalai-Wolynes scenario for the viscosity increase in glasses. *J. Chem. Phys.*, 121:7347, 2004.

[25] C. Brito and M. Wyart. On the rigidity of a hard-sphere glass near random close packing. *Europhysics Letters (EPL)*, 76(1):149–155, 2006.

[26] C. Brito and M. Wyart. Heterogeneous dynamics, marginal stability and soft modes in hard sphere glasses. *Journal of Statistical Mechanics: Theory and Experiment*, 2007(08):L08003, 2007.

[27] C. Brito and M. Wyart. Geometric interpretation of previtrification in hard sphere liquids. *The Journal of Chemical Physics*, 131(2):024504, 2009.

[28] J.M. Caillol. Non-perturbative renormalization group for simple fluids. *Molecular Physics*, 104(12):1931–1950, 2006.

[29] F. Caltagirone, U. Ferrari, L. Leuzzi, G. Parisi, F. Ricci-Tersenghi, and T. Rizzo. Critical slowing down exponents of mode coupling theory. *Phys. Rev. Lett.*, 108:085702, Feb 2012.

[30] F. Caltagirone, U. Ferrari, L. Leuzzi, G. Parisi, and T. Rizzo. Ising mp-spin mean-field model for the structural glass: Continuous versus discontinuous transition. *Physical Review B*, 83(10):104202, 2011.

[31] F. Caltagirone, U. Ferrari, L. Leuzzi, G. Parisi, and T. Rizzo. Critical slowing down exponents in structural glasses: Random orthogonal and related models. *Physical Review B*, 86(6):064204, 2012.

[32] F. Caltagirone, G. Parisi, and T. Rizzo. Dynamical critical exponents for the mean-field potts glass. *Physical Review E*, 85(5):051504, 2012.

[33] C. Cammarota and G. Biroli. Ideal glass transitions by random pinning. *Proceedings of the National Academy of Sciences*, 109(23):8850–8855, 2012.

[34] C. Cammarota and G. Biroli. Random pinning glass transition: Hallmarks, mean-field theory and renormalization group analysis. *The Journal of chemical physics*, 138:12A547, 2013.

[35] C. Cammarota, G. Biroli, M. Tarzia, and G. Tarjus. Renormalization group analysis of the random first-order transition. *Phys. Rev. Lett.*, 106:115705, Mar 2011.

[36] M. Cardenas, S. Franz, and G. Parisi. Glass transition and effective potential in the hypernetted chain approximation. *Journal of Physics A: Mathematical and General*, 31(9):L163–L169, 1998.

[37] John L Cardy. Nonperturbative effects in a scalar supersymmetric theory. *Physics Letters B*, 125(6):470–472, 1983.

[38] John L Cardy. Nonperturbative aspects of supersymmetry in statistical mechanics. *Physica D: Nonlinear Phenomena*, 15(1):123–128, 1985.

[39] T. Castellani and A. Cavagna. Spin glass theory for pedestrians. *Journal of Statistical Mechanics: Theory and Experiment*, 2005:P05012, 2005.

[40] A. Cavagna. Supercooled liquids for pedestrians. *Physics Reports*, 476(4-6):51–124, 2009.

[41] P. Charbonneau, E. Corwin, G. Parisi, and F. Zamponi. Universal microstructure and mechanical stability of jammed packings. *in preparation*, 2012.

[42] P. Charbonneau, A. Ikeda, G. Parisi, and F. Zamponi. Glass transition and random close packing above three dimensions. *Phys. Rev. Lett.*, 107:185702, Oct 2011.

[43] P. Charbonneau, A. Ikeda, G. Parisi, and F. Zamponi. Dimensional study of the caging order parameter at the glass transition. *Proceedings of the National Academy of Sciences*, 109(35):13939–13943, 2012.

[44] P. Charbonneau, A. Ikeda, J. A. van Meel, and K. Miyazaki. Numerical and theoretical study of a monodisperse hard-sphere glass former. *Phys. Rev. E*, 81:040501, Apr 2010.

[45] P. Charbonneau, J. Kurchan, G Parisi, P. Urbani, and F. Zamponi. Exact theory of dense amorphous hard spheres in high dimension iii. the fullrsb solution. *arxiv*, 2013.

[46] J. H. Conway and N. J. A. Sloane. *Sphere Packings, Lattices and Groups*. Spriger-Verlag, New York, 1993.

[47] J. Cornwall, R. Jackiw, and E. Tomboulis. Effective action for composite operators. *Phys. Rev. D*, 10:2428–2445, Oct 1974.

[48] A. Crisanti and H.-J. Sommers. The sphericalp-spin interaction spin glass model: the statics. *Zeitschrift für Physik B Condensed Matter*, 87(3):341–354, 1992.

[49] L. F. Cugliandolo. Dynamics of glassy systems. *arXiv preprint cond-mat/0210312*, 2002.

[50] L. F. Cugliandolo and D. S. Dean. Full dynamical solution for a spherical spin-glass model. *Journal of Physics A: Mathematical and General*, 28(15):4213, 1995.

[51] L. F. Cugliandolo and J. Kurchan. Analytical solution of the off-equilibrium dynamics of a long-range spin-glass model. *Phys. Rev. Lett.*, 71(1):173–176, Jul 1993.

[52] L. F. Cugliandolo and J. Kurchan. Weak ergodicity breaking in mean-field spin-glass models. *Philosophical Magazine B*, 71(4):501–514, 1995.

[53] LF Cugliandolo and J Kurchan. On the out-of-equilibrium relaxation of the sherrington-kirkpatrick model. *Journal of Physics A: Mathematical and General*, 27(17):5749, 1994.

[54] O. Dauchot, G. Marty, and G. Biroli. Dynamical heterogeneity close to the jamming transition in a sheared granular material. *Physical Review Letters*, 95(26):265701, 2005.

[55] C. De Dominicis. Dynamics as a substitute for replicas in systems with quenched random impurities. *Physical Review B*, 18(9):4913, 1978.

[56] C. De Dominicis and I. Giardina. *Random fields and spin glasses*. Cambridge University Press Cambridge, 2006.

[57] C. De Dominicis and P. C. Martin. Stationary entropy principle and renormalization in normal and superfluid systems. II. Diagrammatic formulation. *Journal of Mathematical Physics*, 5(1):31–59, 1964.

[58] C. De Dominicis and L. Peliti. Field-theory renormalization and critical dynamics above t_ {c}: Helium, antiferromagnets, and liquid-gas systems. *Physical Review B*, 18(1):353, 1978.

[59] P. G. Debenedetti and F. H. Stillinger. Supercooled liquids and the glass transition. *Nature*, 410:259, 2001.

[60] B. Delamotte. Introduction to the non-perturbative renormalization group. In Yurij Holovatch, editor, *Order, Disorder And Criticality, Volume 2*. World Scientific, 2007.

[61] C. Donati, S. Franz, S.C. Glotzer, and G. Parisi. Theory of non-linear susceptibility and correlation length in glasses and liquids. *Journal of non-crystalline solids*, 307:215–224, 2002.

[62] A. Donev, S. Torquato, and F. H. Stillinger. Pair correlation function characteristics of nearly jammed disordered and ordered hard-sphere packings. *Physical Review E (Statistical, Nonlinear, and Soft Matter Physics)*, 71(1):011105, 2005.

[63] E. J. Donth. *The glass transition: relaxation dynamics in liquids and disordered materials*. Springer, 2001.

[64] B Duplantier. Comment on parisi's equation for the sk model for spin glasses. *Journal of Physics A: Mathematical and General*, 14(1):283, 1981.

[65] M. D. Ediger. Spatially heterogeneous dynamics in supercooled liquids. *Annual review of physical chemistry*, 51(1):99–128, 2000.

[66] U. Ferrari, L. Leuzzi, G. Parisi, and T. Rizzo. Two-step relaxation next to dynamic arrest in mean-field glasses: Spherical and ising p-spin model. *Phys. Rev. B*, 86:014204, Jul 2012.

[67] S. Franz, H. Jacquin, G. Parisi, P. Urbani, and F. Zamponi. Quantitative field theory of the glass transition. *Proceedings of the National Academy of Sciences*, 109(46):18725–18730, 2012.

[68] S. Franz, H. Jacquin, G. Parisi, P. Urbani, and F. Zamponi. Static replica approach to critical correlations in glassy systems. *The Journal of chemical physics*, 138:12A540, 2013.

[69] S. Franz and G. Parisi. Recipes for metastable states in spin glasses. *Journal de Physique I*, 5(11):1401–1415, 1995.

[70] S. Franz and G. Parisi. Phase diagram of coupled glassy systems: A mean-field study. *Phys. Rev. Lett.*, 79(13):2486–2489, Sep 1997.

[71] S. Franz and G. Parisi. On non-linear susceptibility in supercooled liquids. *Journal of Physics: Condensed Matter*, 12(29):6335, 2000.

[72] S. Franz and G. Parisi. Quasi-equilibrium in glassy dynamics: an algebraic view. *Journal of Statistical Mechanics: Theory and Experiments*, (02):P02003, 2013.

[73] S. Franz, G. Parisi, and F. Ricci-Tersenghi. Glassy critical points and the random field ising model. *Journal of Statistical Mechanics: Theory and Experiment*, 2013(02):L02001, 2013.

[74] S. Franz, G. Parisi, F. Ricci-Tersenghi, and T. Rizzo. Field theory of fluctuations in glasses. *The European Physical Journal E: Soft Matter and Biological Physics*, 34(9):1–17, 2011.

[75] S. Franz, G. Parisi, F. Ricci-Tersenghi, T. Rizzo, and P. Urbani. A note on weakly discontinuous dynamical transitions. *Journal of Chemical Physics*, 138(6):4504, 2013.

[76] S. Franz, G. Parisi, and P. Urbani. Quasi-equilibrium in glassy dynamics: an algebraic view. *arXiv preprint arXiv:1212.4291*, 2012.

[77] G. H Fredrickson and H. C. Andersen. Kinetic ising model of the glass transition. *Physical review letters*, 53(13):1244, 1984.

[78] G. H Fredrickson and H. C. Andersen. Facilitated kinetic ising models and the glass transition. *The Journal of chemical physics*, 83:5822, 1985.

[79] H. L. Frisch, N. Rivier, and D. Wyler. Classical hard-sphere fluid in infinitely many dimensions. *Phys. Rev. Lett.*, 54:2061–2063, May 1985.

[80] G. S. Fulcher. *J. Am. Ceram. Soc*, 8:339, 1923.

[81] J.P. Garrahan, P. Sollich, and C. Toninelli. Kinetically constrained models. In L. Berthier, G. Biroli, J-P Bouchaud, L. Cipelletti, and W. van Saarloos, editors, *Dynamical Heterogeneities and Glasses*. Oxford University Press, 2011.

[82] A. Georges and J. S. Yedidia. How to expand around mean-field theory using high-temperature expansions. *Journal of Physics A: Mathematical and General*, 24:2173, 1991.

[83] W Götze. Properties of the glass instability treated within a mode coupling theory. *Zeitschrift für Physik B Condensed Matter*, 60(2-4):195–203, 1985.

[84] W. Götze. *Complex dynamics of glass-forming liquids: A mode-coupling theory*, volume 143. Oxford University Press, USA, 2009.

[85] W. Götze and L. Sjogren. α-relaxation near the liquid-glass transition. *Journal of Physics C, Solid State Physics*, 20(7):879, 1987.

[86] W. Gotze and L. Sjogren. Logarithmic decay laws in glassy systems. *Journal of Physics: Condensed Matter*, 1(26):4203, 1989.

[87] W. Götze and M. Sperl. Logarithmic relaxation in glass-forming systems. *Phys. Rev. E*, 66:011405, Jul 2002.

[88] TS Grigera, V Martin-Mayor, G Parisi, and P Verrocchio. Asymptotic aging in structural glasses. *Physical Review B*, 70(1):014202, 2004.

[89] J. P. Hansen and I. R. McDonald. *Theory of simple liquids*. Academic Press, London, 1986.

[90] J. P. Hansen and I. R. McDonald. *Theory of simple liquids*. Academic Press, London, 1986.

[91] A. Ikeda, L. Berthier, and G. Biroli. Dynamic criticality at the jamming transition. *J. Chem. Phys.*, 138:12A507, 2013.

[92] A. Ikeda and K. Miyazaki. Glass transition of the monodisperse gaussian core model. *Phys. Rev. Lett.*, 106:015701, Jan 2011.

[93] R. L. Jack, P. Mayer, and P. Sollich. Mappings between reaction–diffusion and kinetically constrained systems: A+ a? a and the fredrickson–andersen model have upper critical dimension dc= 2. *Journal of Statistical Mechanics: Theory and Experiment*, 2006(03):P03006, 2006.

[94] W. Kauzmann. The nature of the glassy state and the behavior of liquids at low temperatures. *Chemical Reviews*, 43(2):219–256, 1948.

[95] W. K. Kegel and A. van Blaaderen. Direct observation of dynamical heterogeneities in colloidal hard-sphere suspensions. *Science*, 287(5451):290–293, 2000.

[96] A. S. Keys, A. R. Abate, S. C. Glotzer, and D. J. Durian. Measurement of growing dynamical length scales and prediction of the jamming transition in a granular material. *Nature physics*, 3(4):260–264, 2007.

[97] T. R. Kirkpatrick and D. Thirumalai. Dynamics of the structural glass transition and the p-spin-interaction spin-glass model. *Phys. Rev. Lett.*, 58(20):2091–2094, May 1987.

[98] T. R. Kirkpatrick and D. Thirumalai. p-spin-interaction spin-glass models: Connections with the structural glass problem. *Phys. Rev. B*, 36:5388–5397, Oct 1987.

[99] T. R. Kirkpatrick and D. Thirumalai. Comparison between dynamical theories and metastable states in regular and glassy mean-field spin models with underlying first-order-like phase transitions. *Phys. Rev. A*, 37:4439–4448, Jun 1988.

[100] T. R. Kirkpatrick and D. Thirumalai. Random solutions from a regular density functional hamiltonian: a static and dynamical theory for the structural glass transition. *Journal of Physics A: Mathematical and General*, 22(5):L149, 1989.

[101] T. R. Kirkpatrick, D. Thirumalai, and P. G. Wolynes. Scaling concepts for the dynamics of viscous liquids near an ideal glassy state. *Phys. Rev. A*, 40(2):1045–1054, Jul 1989.

[102] T. R. Kirkpatrick and P. G. Wolynes. Connections between some kinetic and equilibrium theories of the glass transition. *Phys. Rev. A*, 35(7):3072–3080, Apr 1987.

[103] T. R. Kirkpatrick and P. G. Wolynes. Stable and metastable states in mean-field Potts and structural glasses. *Phys. Rev. B*, 36(16):8552–8564, Dec 1987.

[104] W. Kob. Course 5: Supercooled liquids, the glass transition, and computer simulations. In *Slow relaxations and nonequilibrium dynamics in condensed matter*, pages 199–269. Springer, 2003.

[105] W. Kob, C. Donati, S. J Plimpton, P. Poole, and S. Glotzer. Dynamical heterogeneities in a supercooled lennard-jones liquid. *Physical review letters*, 79(15):2827, 1997.

[106] V. Krakoviack. Liquid-glass transition of a fluid confined in a disordered porous matrix: A mode-coupling theory. *Physical review letters*, 94(6):65703, 2005.

[107] V. Krakoviack. Mode-coupling theory for the slow collective dynamics of fluids adsorbed in disordered porous media. *Physical Review E*, 75(3):031503, 2007.

[108] W. Krauth. *Statistical Mechanics: Algorithms and Computations*. Oxford University Press, USA, 2006.

[109] J. Kurchan. Supersymmetry in spin glass dynamics. *Journal de Physique I*, 2(7):1333–1352, 1992.

[110] J. Kurchan, G. Parisi, P. Urbani, and F. Zamponi. Exact theory of dense amorphous hard spheres in high dimension. ii. the high density regime and the gardner transition. *The Journal of Physical Chemistry B*, 2013.

[111] J. Kurchan, G. Parisi, and F. Zamponi. Exact theory of dense amorphous hard spheres in high dimension. I. The free energy . *J. Stat. Mech*, (3):P10012, 2012.

[112] E. Lerner and I. Procaccia. Locality and nonlocality in elastoplastic responses of amorphous solids. *Physical Review E*, 79(6):066109, 2009.

[113] E Leutheusser. Dynamical model of the liquid-glass transition. *Physical Review A*, 29(5):2765, 1984.

[114] L. Leuzzi and T.M. Nieuwenhuizen. *Thermodynamics of the glassy state*. Taylor & Francis, 2007.

[115] A.J. Liu and S.R. Nagel. *Jamming and Rheology: Constrained Dynamics on Microscopic and Macroscopic Scales*. Taylor & Francis, 2001.

[116] A.J. Liu, S.R. Nagel, W. Van Saarloos, and M. Wyart. The jamming scenario – an introduction and outlook. In L. Berthier, G. Biroli, J-P Bouchaud, L. Cipelletti, and W. van Saarloos, editors, *Dynamical Heterogeneities and Glasses*. Oxford University Press, 2011.

[117] B. D. Lubachevsky and F. H. Stillinger. Geometric properties of random disk packings. *J. Stat. Phys.*, 60:561–583, 1990.

[118] B. Ludovic, H. Jacquin, and F. Zamponi. Microscopic theory of the jamming transition of harmonic spheres. *Phys. Rev. E*, 84:051103, Nov 2011.

[119] M Lisa Manning and Andrea J Liu. Vibrational modes identify soft spots in a sheared disordered packing. *Physical Review Letters*, 107(10):108302, 2011.

[120] M. K Mapes, S. F. Swallen, and M. D. Ediger. Self-diffusion of supercooled o-terphenyl near the glass transition temperature. *The Journal of Physical Chemistry B*, 110(1):507–511, 2006.

[121] R. Mari, F. Krzakala, and J. Kurchan. Jamming versus glass transitions. *Phys. Rev. Lett.*, 103(2):025701, Jul 2009.

[122] R. Mari and J. Kurchan. Dynamical transition of glasses: From exact to approximate. *J. Chem. Phys.*, 135:124504, 2011.

[123] P. C. Martin, E. D. Siggia, and H. A. Rose. Statistical dynamics of classical systems. *Phys. Rev. A*, 8:423–437, Jul 1973.

[124] L. M. Martinez and C. A. Angell. A thermodynamic connection to the fragility of glass-forming liquids. *Nature*, 410(6829):663–667, 2001.

[125] M. Mézard. How to compute the thermodynamics of a glass using a cloned liquid. *Physica A*, 265(3):352–369, 1999.

[126] M. Mézard and G. Parisi. Replica field theory for random manifolds. *Journal de Physique I*, 1(6):809–836, 1991.

[127] M. Mézard and G. Parisi. A tentative replica study of the glass transition. *Journal of Physics A: Mathematical and General*, 29:6515, 1996.

[128] M. Mézard and G. Parisi. A first-principle computation of the thermodynamics of glasses. *The Journal of Chemical Physics*, 111(3):1076–1095, 1999.

[129] M. Mézard and G. Parisi. Thermodynamics of glasses: A first principles computation. *Phys. Rev. Lett.*, 82(4):747–750, Jan 1999.

[130] M. Mézard and G. Parisi. Statistical physics of structural glasses. *Journal of Physics: Condensed Matter*, 12(29):6655–6673, 2000.

[131] M. Mézard and G. Parisi. Glasses and replicas. In P.G.Wolynes and V.Lubchenko, editors, *Structural Glasses and Supercooled Liquids: Theory, Experiment and Applications*. Wiley & Sons, 2012.

[132] M. Mézard, G. Parisi, and M. A. Virasoro. *Spin glass theory and beyond*. World Scientific, Singapore, 1987.

[133] R. Monasson. Structural glass transition and the entropy of the metastable states. *Phys. Rev. Lett.*, 75(15):2847–2850, Oct 1995.

[134] A. Montanari, G. Parisi, and F. Ricci-Tersenghi. Instability of one-step replica-symmetry-broken phase in satisfiability problems. *Journal of Physics A: Mathematical and General*, 37(6):2073, 2004.

[135] A. Montanari and F. Ricci-Tersenghi. On the nature of the low-temperature phase in discontinuous mean-field spin glasses. *The European Physical Journal B-Condensed Matter and Complex Systems*, 33(3):339–346, 2003.

[136] H. Mori. Transport, collective motion, and brownian motion. *Progress of Theoretical Physics*, 33(3):423–455, 1965.

[137] T. Morita and K. Hiroike. A new approach to the theory of classical fluids. III. *Progr. Theor. Phys.*, 25:537, 1961.

[138] C. S. O'Hern, S. A. Langer, A. J. Liu, and S. R. Nagel. Random packings of frictionless particles. *Phys. Rev. Lett.*, 88(7):075507, Jan 2002.

[139] A. C. Pan, J. P. Garrahan, and D. Chandler. Heterogeneity and growing length scales in the dynamics of kinetically constrained lattice gases in two dimensions. *Physical Review E*, 72(4):041106, 2005.

[140] Sergey Pankov. Low-temperature solution of the sherrington-kirkpatrick model. *Physical review letters*, 96(19):197204, 2006.

[141] G. Parisi. *Statistical field theory*. Addison-Wesley, 1988.

[142] G. Parisi. Mean field theory of glasses: Statics and dynamics. In J.-P. Bouchaud, M. Mézard, and J. Dalibard, editors, *Complex Systems*, Les Houches, France, 2007. Elsevier.

[143] G. Parisi and T. Rizzo. Critical dynamics in glassy systems. *Physical Review E*, 87(1):012101, 2013.

[144] G Parisi and N Sourlas. Supersymmetric field theories and stochastic differential equations. *Nuclear Physics B*, 206(2):321–332, 1982.

[145] G. Parisi and F. Zamponi. Mean-field theory of hard sphere glasses and jamming. *Rev. Mod. Phys.*, 82(1):789–845, Mar 2010.

[146] GIORGIO Parisi and NICOLAS Sourlas. Random magnetic fields, supersymmetry, and negative dimensions. *Physical Review Letters*, 43:744–745, 1979.

[147] A. Parola and L. Reatto. Hierarchical reference theory of fluids and the critical point. *Physical Review A*, 31(5):3309, 1985.

[148] R. Richert and C. A. Angell. Dynamics of glass-forming liquids. v. on the link between molecular dynamics and configurational entropy. *The Journal of chemical physics*, 108:9016, 1998.

[149] R. Richert, N. Israeloff, C. Alba-Simionesco, F. Ladieu, and D. L'Hôte. Experimental approaches to heterogeneous dynamics. *Dynamical Heterogeneities in Glasses, Colloids, and Granular Media*, 150:152, 2011.

[150] F. Ritort and P. Sollich. Glassy dynamics of kinetically constrained models. *Advances in Physics*, 52(4):219–342, 2003.

[151] T. Rizzo. Replica symmetry breaking transitions and off-equilibrium dynamics. *arXiv preprint arXiv:1305.2070*, 2013.

[152] T. Rizzo. Towards a theory of the glass crossover. *arXiv preprint arXiv:1307.4303*, 2013.

[153] C. A. Rogers. *Packing and Covering*. Cambridge University Press, Cambridge, 1964.

[154] M. Sellitto. Cooperative heterogeneous facilitation: Multiple glassy states and glass-glass transition. *Physical Review E*, 86(3):030502, 2012.

[155] M. Sellitto, D. De Martino, F. Caccioli, and J. J. Arenzon. Dynamic facilitation picture of a higher-order glass singularity. *Phys. Rev. Lett.*, 105:265704, Dec 2010.

[156] L. E. Silbert, A. J. Liu, and S. R. Nagel. Structural signatures of the unjamming transition at zero temperature. *Physical Review E (Statistical, Nonlinear, and Soft Matter Physics)*, 73(4):041304, 2006.

[157] P. Sollich and M. R. Evans. Glassy time-scale divergence and anomalous coarsening in a kinetically constrained spin chain. *Physical review letters*, 83(16):3238, 1999.

[158] P Sollich and MR Evans. Glassy dynamics in the asymmetrically constrained kinetic ising chain. *Physical Review E*, 68(3):031504, 2003.

[159] H-J Sommers and W. Dupont. Distribution of frozen fields in the mean-field theory of spin glasses. *Journal of Physics C: Solid State Physics*, 17(32):5785, 1984.

[160] M. Sperl. Dynamics in colloidal liquids near a crossing of glass- and gel-transition lines. *Phys. Rev. E*, 69:011401, Jan 2004.

[161] R. S. L. Stein and H. C. Andersen. Scaling analysis of dynamic heterogeneity in a supercooled Lennard-Jones liquid. *Phys. Rev. Lett.*, 101:267802, Dec 2008.

[162] G. Szamel. Divergent four-point dynamic density correlation function of a glassy suspension. *Phys. Rev. Lett.*, 101:205701, Nov 2008.

[163] G. Szamel and E. Flenner. Diverging length scale of the inhomogeneous mode-coupling theory: A numerical investigation. *Physical Review E*, 81(3):031507, 2010.

[164] G. Tamman and W. Hesse. *Z. Anorg. Allg. Chem.*, 156:245, 1926.

[165] G. Tarjus. An overview of the theories of the glass transition. In L. Berthier, G. Biroli, J-P Bouchaud, L. Cipelletti, and W. van Saarloos, editors, *Dynamical Heterogeneities and Glasses*. Oxford University Press, 2011.

[166] G. Tarjus and D. Kivelson. Breakdown of the stokes–einstein relation in supercooled liquids. *The Journal of chemical physics*, 103:3071, 1995.

[167] G Tarjus and M. Tissier. Nonperturbative functional renormalization group for random-field models: The way out of dimensional reduction. *Physical review letters*, 93(26):267008, 2004.

[168] G. Tarjus and M. Tissier. Nonperturbative functional renormalization group for random field models and related disordered systems. i. effective average action formalism. *Physical Review B*, 78(2):024203, 2008.

[169] T. Temesvári, C. De Dominicis, and I. Pimentel. Generic replica symmetric field-theory for short range ising spin glasses. *The European Physical Journal B-Condensed Matter and Complex Systems*, 25(3):361–372, 2002.

[170] D. J. Thouless, P. W. Anderson, and R. G. Palmer. Solution of 'Solvable model of a spin glass'. *Philosophical Magazine*, 35(3):593–601, 1977.

[171] M. Tissier and G. Tarjus. Nonperturbative functional renormalization group for random field models and related disordered systems. ii. results for the random field o (n) model. *Physical Review B*, 78(2):024204, 2008.

[172] M. Tissier and G. Tarjus. Supersymmetry and its spontaneous breaking in the random field ising model. *Physical Review Letters*, 107(4):041601, 2011.

[173] C. Toninelli, M. Wyart, L. Berthier, G. Biroli, and J.-P. Bouchaud. Dynamical susceptibility of glass formers: Contrasting the predictions of theoretical scenarios. *Physical Review E*, 71(4):041505, 2005.

[174] S. Torquato. *Random Heterogeneous Materials: Microstructure and Macroscopic Properties*. Springer-Verlag, New York, 2002.

[175] H. Vogel. *Phys. Z.*, 22:645, 1921.

[176] E. R. Weeks, J. C. Crocker, A. C. Levitt, A. Schofield, and David A Weitz. Three-dimensional direct imaging of structural relaxation near the colloidal glass transition. *Science*, 287(5453):627–631, 2000.

[177] A. Widmer-Cooper, H. Perry, P. Harrowell, and D. R. Reichman. Irreversible reorganization in a supercooled liquid originates from localized soft modes. *Nature Physics*, 4(9):711–715, 2008.

[178] P. G Wolynes and V. Lubchenko. *Structural Glasses and Supercooled Liquids: Theory, Experiment, and Applications*. Wiley. com, 2012.

[179] M. Wyart, L.E. Silbert, S.R. Nagel, and T.A. Witten. Effects of compression on the vibrational modes of marginally jammed solids. *Physical Review E*, 72(5):051306, 2005.

[180] N. Xu, V. Vitelli, A. J. Liu, and S. R. Nagel. Anharmonic and quasi-localized vibrations in jammed solids,Äö modes for mechanical failure. *Europhys. Lett.*, 90(5):56001, 2010.

[181] F. Zamponi. Mean field theory of spin glasses. *arXiv preprint arXiv:1008.4844*, 2010.

[182] L. Zdeborová and F. Krzakala. Generalization of the cavity method for adiabatic evolution of gibbs states. *Physical Review B*, 81(22):224205, 2010.

[183] J. Zinn-Justin. *Quantum field theory and critical phenomena*, volume 142. Clarendon Press Oxford, 2002.

[184] R. Zwanzig. *in Lectures in theoretical physics*. Wiley, New York, 1961.